Chapter 13: Sea Level Change

Coordinating Lead Authors: John A. Church (Australia), Peter U. Clark (USA)

Lead Authors: Anny Cazenave (France), Jonathan Gregory (UK), Svetlana Jevrejeva (UK), Anders Levermann (Germany), Mark Merrifield (USA), Glenn Milne (Canada), R. Steven Nerem (USA), Patrick Nunn (Australia), Antony Payne (UK), W. Tad Pfeffer (USA), Detlef Stammer (Germany), Alakkat Unnikrishnan (India)

Contributing Authors: David Bahr (USA), Jason E. Box (USA), David H. Bromwich (USA), Mark Carson (Germany), William Collins (UK), Xavier Fettweis (Belgium), Piers Forster (UK), Alex Gardner, Peter Good (UK), Rune Grand Graversen (Sweden), Ralf Greve (Japan), Stephen Griffies (USA), Edward Hanna (UK), Mark Hemer (Australia), Regine Hock (USA), Simon J. Holgate (UK), John Hunter (Australia), Philippe Huybrechts (Belgium), Gregory Johnson (USA), Georg Kaser (Austria), Caroline Katzman (Netherlands), Gerhard Krinner (France), Jan Lanaerts (Netherlands), Ben Marzeion (Austria), Kathleen L. McInnes (Australia), Sebastian Mernild (USA), Ruth Mottram (Denmark), Gunnar Myhre (Norway), J.P. Nicholas (USA), Valentina Radic (Canada), Jamie Rae (UK), Jan H. van Angelen (Netherlands), Willem J. van de Berg (Netherlands), Michiel van den Broeke (Netherlands), Masakazu Yoshimori (Japan)

Review Editors: Jean Jouzel (France), Roderik van de Wal (Netherlands), Philip L. Woodworth (UK), Cunde Xiao (China)

Date of Draft: 16 December 2011

Notes: TSU Compiled Version

Table of Contents

Executive Summary

Changes in sea level represent an integration of many aspects of climate change, and thus occur over a broad range of temporal and spatial scales. The primary contributors to sea level change are the expansion of the ocean as it warms and the transfer of water currently stored on land, particularly from glaciers and ice sheets. The amount of sea level change depends on global aspects of the climate system as well as on regional and local phenomena that may strongly modulate the global rise at any given location. In addition to being affected by a rise in mean sea level, coastal and island communities and ecosystems are also impacted by changes in extreme sea level events and surface waves. We consider sea level measured with respect to the surface of the solid Earth which itself may be moving (relative sea level) and sea level relative to the Earth's center of mass.

Past Sea Level Change

Records of past sea level change from both geological data and modern instrumental data provide critical information for placing the current rates of change in the context of natural variability, and for understanding the processes that determine future change. Our assessment of important information on historical sea level relevant to Earth's current climate is:

- During the middle Pliocene about 3 million years ago, CO_2 concentrations were about 350 to 415 ppm, temperatures were about 2°C to 3°C above preindustrial values and sea level was 10 to 30 m above current values. Most of the additional ocean mass came from the Greenland and West Antarctic Ice Sheets, with additional contributions from the East Antarctic Ice Sheet.
- There is high confidence that during the last interglacial (warm) period, global mean sea level (GMSL) was more than 6 m higher than current values, and low confidence that it reached 10 m above current values. The lower value requires glacier melting, thermosteric rise, and contributions from the Greenland and West Antarctic Ice Sheets whereas the higher values also require a contribution from the East Antarctic Ice Sheet. Modelling studies indicate about about half of the Greenland contribution was related to solar insolation and half to surface warming.
- There is high confidence that rates of sea level change during the last interglaciation were 1 to 2.5 m kyr^{-1}. Entering the last two interglacial highstands (when sea level was within 10 m of present values) rates of sea level rise were from 5.6 m kyr^{-1} to 10 m kyr^{-1} (although faster rates may have occurred over shorter periods). These latter periods reflect transitions from glacial to interglacial conditions and only provide upper limits for land-ice loss.
- For the past 2000 years, paleo sea level data provide high confidence for an increase in the late 19th century (1840–1920) from relatively low rates of change during the late Holocene (order tenths of mm a^{-1}) to modern rates of rise (order mm a^{-1}). Long tide-gauge records and reconstructions of global averaged sea level extending back to the 19th century confirm this acceleration.
- Tide gauge and satellite observations indicate that it is virtually certain that global mean sea level has been rising during the 20th century at rates of 1.7 mm a^{-1} over the 20th century and 3.2 mm a^{-1} since 1993.
- Satellite and *in situ* data also show large regional variability around the global mean trend.
- In addition to the mean rise, global mean sea level shows interannual variability mostly related to ENSO-driven changes of the global water cycle and ocean mass.

Contributions to Sea Level Change

In situ and satellite observations of the oceanic and cryospheric contributions of sea level change have led to an improved understanding of historical change. Since the early 1970s:

- It is very likely that the ocean has continued to warm and expand. About 40% of the observed GMSL rise is a result of ocean warming, about 30% since 1993.
- Glaciers have contributed about 35% of the observed GMSL rise and their contribution has increased significantly over recent decades.
- Both the Greenland and Antarctic ice sheets have made only small contributions to GMSL since the early 1970s. However, their rate of contribution has increased rapidly since the early 1990s and it is likely to have been of a similar magnitude to thermosteric sea level rise since 2005.

- The increased storage of water in dams has been partially offset through the depletion of groundwater. The rate of dam building has slowed and groundwater depletion now exceeds the rate of storage in reservoirs.
- The sum of estimated components (ocean thermal expansion, glaciers, ice sheets and land water) is consistent with the observed sea level rise, within uncertainties; the difference in central estimates is about 25% or less over the last 40 years, during the altimetry era (1993–2010), and over the period that Argo measurements have been available (2005–2010).

Our understanding of and ability to model the observed sea level rise has improved.

- General circulation models reproduce the observed variability (principally a result of large volcanic eruptions) and the global mean trend (to an accuracy of better than 20% on average) in thermosteric sea level rise and upper-ocean (<700 m) heat content.
- Recent analyses have demonstrated that it is likely the abyssal (>3000 m) ocean is warming.
- Improved glacier inventory and mass balance data sets, including for marine terminating glaciers, have led to improved estimates of historical glacier contributions. Some glacier models now include glacier hypsometry, allowing glacier projections to reach a new equilibrium in a warmer climate.
- Modelled surface mass balance for Greenland and Antarctica is in agreement with the available limited observations.
- Satellite observations of volume and mass change and ice-sheet motion have revealed significant dynamic changes in the ice sheets. Our current understanding of the causes of increased ice discharge in Greenland and Antarctica is that they have been largely triggered by local changes in ocean circulation and associated heat transport. However, this understanding is incomplete. Any potential link between these local circulation changes and increasing greenhouse gases has not been well explored.
- The sum of the simulated contributions explains the observed sea level rise since the early 1970s and indicates a faster rate of rise since the early 1990s, in agreement with the increase in the observed rate of rise.
- The largest increase in the storage of heat in the climate system over recent decades has been in the oceans and thus sea level rise from ocean warming is a central part of the Earth's response to increasing greenhouse gas concentrations. Independent estimates of radiative forcing of the Earth by greenhouse gases, volcanic and anthropogenic aerosols, the observed heat storage and surface warming combine to give an energy budget for the Earth that is very likely closed, and is consistent with our best estimate of climate sensitivity. Observations of changes in the Earth's energy storage are thus a powerful tool for the detection of climate change as well as a constraint on climate sensitivity and future warming.

Projections for the 21st Century

Under all the RCP scenarios, the time-mean rate of GMSL rise during the 21st century is very likely to exceed the rate observed during 1971–2010. Ocean thermal expansion and glacier melting are likely to make the largest contributions to GMSL rise during the 21st century. Surface melting from Greenland is very likely to make a positive contribution. For the period 2081 to 2100 compared to 1986 to 2005, GMSL rise is likely to lie in the range 0.27–0.50 m for RCP2.6, 0.32–0.56 m for RCP4.5 and RCP6.0, and 0.41–0.71 m for RCP8.5. Although RCP4.5 and RCP6.0 are very similar at the end of the century, RCP4.5 has a greater rate of rise earlier in the century, RCP6.0 later. Under RCP 8.5, the likely range reaches 0.84 m in 2100. Larger values than these ranges cannot be excluded, but the current state of scientific understanding is insufficient for evaluating their probability.

We have medium confidence in these ranges. The agreement of process-based models with observations and physical understanding is a cause for confidence and an advance since the AR4, but two considerations particularly restrict our confidence. First, we do not have high confidence in our ability to model rapid changes in ice-sheet dynamics. At the time of the AR4, there was an insufficient scientific basis for making projections of these effects. In the ranges given here, the central estimate of this contribution is 0.12 m from the two ice sheets combined, and is the main reason why these ranges are higher than those given in the AR4, which did not include such a contribution. Second, semi-empirical models give higher projections than process-based models. This might point to some presently unidentified or underestimated contribution. For RCP4.5, semi-empirical models give central projections in the range 0.73–1.15 m, and similarly for SRES A1B, and their upper bounds extend to about 1.5 m. It is not understood why semi-empirical models project

a higher rate of rise than process-based models and there is no consensus about the reliability of semi-empirical model projections.

Beyond 2100

Longer-term sea level projections depend critically on future emission scenarios.

- Ocean thermosteric sea level rise will continue for centuries to millennia, unless global temperatures decline.
- Surface melting of the Greenland Ice Sheet is projected to increase with increasing surface temperatures and to exceed accumulation for global average temperatures above 3.1 ± 0.8 °C, leading to ongoing decay of the ice sheet. The loss of the ice sheet is not inevitable, however, because it has long time scales and it might re-grow to its original volume or some fraction thereof if global temperatures decline, depending on cumulative greenhouse gas emissions.
- For Antarctica, accumulation is expected to increase for low-emission scenarios but at some, as of yet poorly defined value, surface melting will begin to contribute significantly to sea level rise.
- Confidence in the models capability to project sea level contributions from dynamic ice-sheet changes in Greenland and Antarctica beyond 2100 is low. In Greenland, dynamic mass loss is limited by topographically defined outlets regions, and solid-ice discharge induced from interaction with the ocean is self-limiting as the ice-sheet margin retreats inland from the coast. A significant portion of the Antarctic Ice Sheet is grounded below sea level and is potentially subject to instability leading to self-accelerated ice loss.
- For 2500, the projected sea level rise ranges from 0.03 m to 1.2 m for low-emission scenarios and from 1. 7 to 5.6 m for high-emission scenarios. Models used for these projections lack fundamental processes that can trigger instabilities, suggesting that they may underestimate sea level rise.

The Regional Distribution of Sea Level Change

Regional sea level change will result largely from a combination of ocean dynamical changes and changes in the gravity field and land height associated with contemporary and historical (recent glacial-interglacial transition) mass exchange between land ice and the oceans.

- There is high confidence that over the next few decades, regional sea level changes will be dominated by interannual to decadal sea level variability caused by internal (dynamical) variability of the climate system. This variability will remain important through the 21st century and beyond.
- There is also medium to high confidence that the pattern of long-term trends in sea level associated with ocean dynamics will progressively dominate the regional pattern of sea level change toward the end of the 21st century, at least for the upper end of the projections. However, the confidence in the projected regional pattern remains low.
- There is high confidence that in the 21st century, there will be a significant contribution to regional sea level changes from melting land ice in the form of a dynamical steric response of the ocean and in the form of gravitational, solid Earth, and rotational responses to the varying distribution of water on the Earth.

It is very likely that in the 21st century, these factors together will result in a total regional pattern of sea level change which will deviate significantly from the global mean. However, while the pattern of change remains uncertain, it is very likely that over the majority of the ocean regional sea level rise will be positive.

Extreme Sea Level Events – Surges and Waves

21st century projections of extreme water levels and waves are developing based on depictions of future storminess in a warming climate using both dynamical and statistical approaches. Uncertainties in the projected atmospheric forcing, however, make it difficult to specify regional changes in storm-driven extremes.

It is likely that 21st century projected increases in extreme sea levels will occur as a result of an increase in mean sea level. There is low confidence in changes in the contribution to extreme sea levels by storm surges caused by atmospheric forcing alone. If the expected frequency of flooding of coastal infrastructure is not to increase, the allowance for GMSL rise needs to be greater than the central GMSL rise projections.

Sea and swell waves reflect changes in surface winds and storm patterns, hence it is likely that climate change will have an impact on significant wave heights and other wave properties. Dynamical and statistical techniques for sea and swell wave projections are improving, and ensemble assessments of wave-model projections are beginning to quantify uncertainties. However, wave projections are only as good as the wind fields used to generate them, and significant uncertainties are involved in the specification of future winds, particularly storm winds. For ocean waves, inter-comparison studies are beginning to identify regions of robust change in model ensembles (e.g., wave height increases in the southern ocean). However, uncertainties remain high. Accordingly, there is low confidence in regional wave projections, with medium confidence assigned to wave-field changes associated with the poleward migration of winter storm tracks at mid-latitudes, which in the Southern Ocean is associated with a trend toward a more positive Southern Annular Mode state and more energetic waves.

13.1 Introduction

This chapter provides a synthesis of past and contemporary sea level change at global and regional scales, explains the reasons for that change, and provides projections of sea level change for the 21st century and beyond.

Changes in sea level occur over a broad range of temporal and spatial scales, with the many factors contributing to sea level change making it an integral measure of climate change (Church et al., 2010; Milne et al., 2009). The primary contributors to sea level change are the expansion of the ocean as it warms and the transfer of water currently stored on land, particularly from glaciers and ice sheets (Church et al., 2011b). The largest increase in the storage of heat in the climate system over recent decades has been in the oceans and thus sea level rise from ocean warming is a central part of the Earth's response to increasing greenhouse gas concentrations. Because of their large size, even a modest increase in loss of mass from the Greenland and Antarctic ice sheets has the potential to become the dominant source of future sea level rise. Although glaciers elsewhere have much less mass altogether than the ice sheets, they are relatively more sensitive to climate change and thus also make an important contribution to sea level rise. These factors affect the volume of water stored in the ocean and thus global averaged sea level.

In this chapter, we emphasize that the amount of sea level change depends not only on global aspects of the climate system but also on regional and local phenomena that may strongly modulate the global rise at any given location (Milne et al., 2009). These latter influences are particularly important to local planning efforts, which require knowledge of how local sea level may change relative to the land. We thus discuss the primary factors that cause regional sea level to differ from the global average and how these may change in the future. In addition to being affected by a rise in mean sea level, coastal and island communities and ecosystems are also impacted by changes in extreme sea level events and surface waves. We therefore also address projected changes in surface waves and the consequences of sea level and climate change for extreme sea level events.

The First IPCC Assessment (Warrick; Oerlemans, 1990) laid the groundwork for much of our current understanding of sea level change. This included the recognition that sea level had risen during the 20th century, that the rate of rise had increased compared to the 19th century, that ocean-thermal expansion and the mass loss from glaciers were likely the main contributors to the 20th century rise, that during the 21st century the rate of rise was projected to be faster than during the 20th century, and that sea level would continue to rise well after greenhouse gas emissions were reduced. They also concluded that no major dynamic response of the ice sheets was expected during the 21st century, leaving ocean-thermal expansion and the melting of glaciers as the most likely main contributors to the 21st century rise. The Second Assessment Report (Warrick et al., 1996) came to very similar conclusions.

By the time of the Third Assessment Report (Church et al., 2001), full process models, including coupled atmosphere-ocean general circulation models (AOGCMs) and ice-sheet models, largely replaced energy-balance climate models as the primary techniques supporting the interpretation of the observations and for the projections of sea level. This approach allowed for the first time a focus on the regional distribution of sea level change in addition to the global averaged change. By the time of the Fourth Assessment Report (AR4) (Solomon et al., 2007), there were more robust observations of the variations in the rate of global average sea level rise for the 20th century (rather than just 20th century trends), some understanding of the variability in the rate of rise, and the satellite altimeter record was long enough to reveal the complexity of the time-variable spatial distribution of sea level. Although sea level was addressed in many chapters in the AR4 in recognition of its integration with other aspects of climate change and its interdisciplinary nature, three central issues remained. Firstly, as in all previous Assessments, the observed sea level rise over decades was larger than the sum of the individual contributions estimated from observations or with models (so-called sea level budget problem), although in general the uncertainties were large enough that there was no significant contradiction. Secondly, it was not possible to make confident projections of the regional distribution of sea level rise. Thirdly, there was insufficient understanding of the potential contributions from the ice sheets. In particular, the AR4 recognised that existing ice-sheet models were unable to explain the recent observations of ice-sheet dynamics and that understanding of these effects was too limited to assess their likelihood or to provide a best estimate or an upper bound for their future contributions.

Despite changes in the scenarios between the four Assessments, the projections for 2100 (compared to 1990) for the full range of scenarios were remarkably similar, with a reduction in the upper end in more recent reports that likely reflects the smaller increase in radiative forcing in recent scenarios due to smaller GHG emissions and the inclusion of aerosols: 15 to 110 cm in the FAR, 13 to 94 cm in the SAR, 9 to 88 cm in the TAR, and 18 to about 80 cm or more in AR4 (when extended to 2100 and including an allowance for a dynamic ice-sheet response).

Since the AR4, it is virtually certain that sea level has continued to rise at a rate faster than the 20th century average (Chapter 3) and contributions from glaciers and ice sheets (Chapter 4) have very likely continued to increase. Improved and new observations of the ocean (Chapter 3) and the cryosphere (Chapter 4) and their representation in models have resulted in better understanding of 20th century sea level rise and its components. Here, we bring all aspects of sea level change together, drawing on the published refereed literature, including as summarised in earlier chapters of this Assessment, and by the analysis of model projections. We make extensive use of results from the World Climate Research Programme's Coupled Model Intercomparison Project phase 5 (CMIP5) and their application to estimate contributions of sea level change.

In Section 13.2, we introduce the major causes of sea level change and summarize the models used to understand and project sea level change. The growth and decay of ice sheets are the largest control of sea level over millennial time scales and we discuss their dynamics and their potential to make rapid contributions to future sea level change. Building on Chapters 3 (Oceans) and 5 (Paleoclimate), past sea level changes are summarised in Section 13.3. Section 13.4 discusses our understanding of sea level change over recent decades and underpins understanding for projections of global averaged sea level. We use an ensemble of climate, ice-sheet and glacier models to project contributions to sea level change, including the dynamic response of the ice sheets (Section 13.5) and bring these together to project sea level change for the 21st century and beyond in Section 13.6. We include the use of semi-empirical models developed using historical data to provide an additional approach for projecting 21st century sea level change. We also consider the potential for crossing critical thresholds that could result in large, prolonged responses and essentially irreversible commitments.

In Section 13.7, we present regional relative sea level change for the next several decades and to 2100. We include all aspects of regional sea level change that are a direct result of both past and future climate change, including large-scale land motions and gravitational effects related to climate-related mass redistribution within the Earth system. However, we do not do not address several aspects of local relative sea level change that do not involve climate but which may be important for assessing its impacts. For example, local relative sea level rise resulting from vertical land motion associated with the compaction of sediments or the withdrawal of water or petroleum products is not considered. This issue may be important in densely populated deltaic regions and elsewhere and might combine with climatically induced sea level change to raise the risk for coastal populations in these regions. Extreme sea level events at the coast occur as a result of natural variability in climate, oceans, storm surges and waves. We assess projections of these extreme events for a number of regions based on the current literature (Section 13.8) and provide some general guidance on potential ways to consider these changes. However, we do not provide comprehensive global projections of changes in extreme events. Also, we do not consider tsunamis that result from land movements. Our observations and understanding of sea level change remain incomplete and we synthesize current understanding and identify key uncertainties throughout the chapter and in Section 13.9.

13.2 Components and Models of Sea Level and Land-Ice Change

This section provides background information on our current understanding of the processes that influence past and present sea level changes and projections of future changes. To isolate the contribution of contemporary climate change to sea level changes observed during the 20th century and projected for 21st century and beyond, the relevant processes are separated into those that are influenced by contemporary climate change (Section 13.2.1.1) and those that are not (Section 13.2.1.2). Models used to interpret observations of past sea level changes and project future changes are introduced in Section 13.2.2. A final section (13.2.3) discusses the mechanisms through which land ice can change and thus contribute to sea level change.

The height of the ocean surface at any given location, or sea level, is measured either with respect to the surface of the solid Earth (relative sea level) or the Earth's center of mass (absolute sea level). The former is the more relevant quantity when considering the coastal response to changes in sea level. Relative sea level has been measured using tide gauges during the past few centuries and estimated or reconstructed for longer time spans from geological records (see Section 13.3.1 and Chapter 5). Absolute sea level has been measured over the past two decades using satellite measurements that quantify the height of the ocean surface relative to a geocentric reference such as the reference ellipsoid (Lambeck, 1988).

Any process that causes vertical motion of the ocean surface or ocean floor will result in sea level change. Height changes of the ocean surface can be affected by flow within the atmosphere and oceans, changes in ocean volume and mass, and changes in the Earth's gravity field. The latter is influenced by tides, changes in Earth rotation and mass redistribution which can occur within or between the various components of the Earth System (e.g., solid Earth, atmosphere, hydrosphere, cryosphere). Height changes of the ocean floor are driven by tectonics, isostatic deformation of the solid Earth, erosion/deposition, sediment compaction, body tides and changes in Earth rotation. Note that height changes of the ocean surface and ocean floor are not independent. For example, changes in ocean-floor height can lead to changes in ocean-surface height through perturbations to the gravity field and the volume of the ocean basins. Conversely, height changes of the ocean surface that relate to a redistribution of ocean mass will influence the height of the ocean floor through isostatic adjustment.

13.2.1 Components of Sea Level Change

13.2.1.1 Components Related to Contemporary Climate Change

The processes through which contemporary climate change can influence sea level (Figure 13.1) involve changes in the ocean and atmosphere, ice grounded on land (land ice), the hydrological cycle, erosion/deposition processes, and the climatic responses to volcanic activity.

[INSERT FIGURE 13.1 HERE]
Figure 13.1: Schematic diagram illustrating climate sensitive processes that can influence sea level. Changes in any one of the components or processes shown will result in a sea level change. The term 'ocean properties' refers to ocean temperature, salinity and density, which influence and are dependent on ocean circulation. The term "sedimentary processes" includes erosion, deposition and compaction of sediment.

Atmosphere-ocean momentum transfer (through surface winds) as well as heat and mass (freshwater) exchange result in ocean currents which cause the sea surface to deviate from an equipotential of the Earth's gravity field (defined by the marine geoid; Lambeck, 1988). Heat and water-mass exchange result in changes in the temperature, salinity and density structure of the ocean. Changes in temperature and salinity affect sea level through the associated changes in ocean water volume (thermosteric and halosteric effects, respectively). Note that changes in temperature affect global average ocean volume whereas changes in salinity do not; both temperature and salinity changes can influence regional sea level change (Church et al., 2010). Changes in the density structure influence ocean currents and therefore the topography of the ocean surface supported by this flow. In addition, regional atmospheric pressure anomalies cause sea level to vary through the so-called atmospheric loading (inverted barometer) effect (Wunsch and Stammer, 1997). The exchange of momentum, heat and freshwater at the ocean surface as well as atmospheric loading can cause sea level to vary on a broad range of space and time scales, some of which can be relatively short lived, such as waves and storm surges, while some are sustained over several decades or centuries and may be associated with atmospheric modes of climate variability (Miller; Douglas, 2007) or internal ocean variability (White et al., 2005a).

Water mass exchange between the terrestrial cryosphere, land and the oceans will lead to a change in global mean sea level (GMSL) by the simple addition/subtraction of water mass to/from the ocean basins. However, the local sea level response may deviate from this global mean change through a range of processes. An influx of freshwater changes ocean temperature and salinity and hence changes ocean currents (Yin et al., 2009). The coupled atmosphere-ocean system can also adjust to temperature anomalies associated with surface freshwater anomalies through air-sea feedbacks, which can result in dynamical adjustments of sea level (Okumora et al., 2009; Stammer et al., 2011). Water mass exchange between land and the ocean also

results in an isostatic adjustment of the ocean floor and change in the gravity field as a consequence of isostatic deformation and water mass redistribution (Farrell; Clark, 1976). These changes affect the Earth's inertia tensor and therefore Earth rotation, which produces an additional sea level response (Milne and Mitrovica, 1998).

Erosion and deposition of sediment can result in sea level change directly through changes in ocean-floor height due to the mass transfer itself and indirectly through the associated isostatic response of the solid Earth (Watts 2001). Compaction of sediments can also contribute to local sea level change (Ericson et al., 2006). These changes in turn influence the regional gravity field which causes further sea level change. Although these processes are active regardless of climate change, climate change can influence their rate and spatial distribution and so contribute significantly to local sea level change, particularly over millennial timescales. However, the component of this process related to contemporary climate change has a negligible influence in most areas over century timescales and so will not be considered further in this chapter.

13.2.1.2 Components Not Related to Contemporary Climate Change

There are a number of processes that occur independently of contemporary climate change that have contributed to the sea level changes measured by tide gauges and satellites and hence are important for understanding the observational record (Section 13.4). In addition, some of these processes will continue to contribute significantly to sea level change in the coming decades to centuries and so should be included when attempting to project future sea level changes and their impacts (Sections 13.5, 13.6, 13.7, 13.8). Five processes fall under this category: the isostatic adjustment of the solid Earth to past (as opposed to current) surface mass redistribution; the dynamic response of ice sheets to past climate change; changes in the hydrological cycle associated with non-climate-related anthropogenic activity; tectonic processes; and coastal processes resulting in erosion, deposition and compaction of sediment.

The isostatic response to a redistribution of surface mass includes both an elastic and viscous deformation of the Earth. The elastic component is instantaneous whereas the viscous is a delayed response that can persist for tens of millennia after a given surface loading change. Mass transfer from land ice to oceans during the most recent deglaciation (~20 to ~6 ka) is one process that contributes significantly to present-day viscous isostatic deformation and therefore sea level change in many regions (Lambeck; Nakiboglu 1984). Because this process, known as glacial isostatic adjustment (GIA), contributed to sea level change in the past century, and will continue to contribute in the coming centuries, it must be considered when interpreting paleo-sea level, tide-gauge and satellite records for past and contemporary climate-related signals (Section 13.3) as well as in projections of regional sea level change (Sections 13.7).

Anthropogenic processes that influence the amount of water stored in the ground or on its surface in lakes and reservoirs, or cause changes in land-surface characteristics that influence runoff or evapo-transpiration rates, will perturb the hydrological cycle and potentially cause an observable sea level change (Sahagian 2000). Such processes include water impoundment (dams, reservoirs), irrigation schemes and ground water extraction (Section 13.4). While some of these changes are a response of society to contemporary climate change, they are included in this section because of their anthropogenic nature.

Deformation of the solid Earth due to convective flow of the mantle, or tectonic processes, cause, on average, relatively low rates of sea level change (< O[0.1 mm yr^{-1}] (Moucha et al., 2008), with the exception of earthquakes, which can cause rapid local changes and tsunamis (Broerse et al., 2011). Coastal processes are important in areas that experience high rates of sedimentation or erosion, most notably deltaic regions (Blum and Roberts, 2009; Syvitski et al., 2009; Vaughan and Spouge, 2002). However, they are less important as a source of sea level change in other areas. These tectonic and coastal processes are not considered in this chapter.

13.2.2 Models Used for Sea Level Studies

Several types of models have been used to simulate changes in global mean and regional sea level. These include atmosphere-ocean general circulation models (AOGCMs; Chapter 9) that simulate the dynamical sea level response to a given climate change, models of the cryosphere (glaciers and ice sheets; see Section 13.2.3), and isostatic models that simulate the static sea level response to surface-mass redistribution. More

recently, semi-empirical models have been used to derive an empirical relationship between temperature or radiative forcing and sea level (Section 13.6.1.2). There are also models that predict extreme sea levels due to storm surges and waves (Section 13.8). Some general information on these different model types is given below.

AOGCMs, which have components representing the ocean, atmosphere, land and cryosphere, simulate the dynamic response of sea level to natural variability of the climate system as well as to anthropogenic changes (Vizcaino et al., 2008). Information about past volcanic eruptions or changes in solar radiation is usually used as external forcing to assess natural variability on decadal time scales. Dynamical processes simulated by climate models include climate modes of variability such as ENSO, PDO or NAO and their impact on sea level through changes in ocean circulation and the associated redistribution of water mass properties (heat and freshwater) (White et al., 2005a). Changes in the strength of the Atlantic meridional overturning circulation (AMOC) and its effect on sea level are also represented (Lorbacher et al., 2010; Yin et al., 2009). AOGCMs also simulate the response of the coupled climate system to anthropogenic increases in greenhouse gases and aerosols. Changes in sea level occur as a dynamic ocean response to changed atmospheric circulation and the associated changes in wind stress and air-sea heat and freshwater fluxes (Timmermann et al., 2010).

Isostatic models are used to simulate the static sea level response to past and contemporary changes in surface water and land-ice mass redistribution and atmospheric pressure changes. Application of these models tends to fall into two categories: those that focus on interannual and annual variability driven by contemporary changes in the hydrological cycle and atmospheric loading (Clarke et al., 2005; Tamisiea et al., 2010), and those that consider secular trends associated with past and contemporary changes in the cryosphere and land hydrology (Lambeck et al., 1998; Mitrovica et al., 2001; Peltier 2004; Riva et al., 2010a). These models typically have four components: a model of space-time changes in the surface load of interest (e.g., land ice, terrestrial water storage), a model of the solid Earth to simulate the isostatic response to the surface load, an algorithm to compute the static redistribution of ocean mass (known as the sea level equation), and an algorithm to compute changes in Earth rotation and the sea level changes associated with this feedback mechanism. A number of currently used isostatic models do not include rotational feedback, but this component signal can be significant (Gomez et al., 2010b). The accuracy of the computed sea level response depends largely on the accuracy of the adopted surface load and Earth model components. The viscous properties of the solid Earth are less well known than the elastic properties and so computations of longer term changes (centuries to millennia) have larger uncertainty than those that require only computation of the elastic response.

Knowledge of spatial and temporal changes in the cryosphere is required input to the above process models that calculate the dynamic and static sea level response to changes in land ice. Information on models used to study changes in the cryosphere is provided in Section 13.2.3. A small number of studies have adopted two other approaches to estimate future changes in land ice: one involves considering limits on the rate and area of mass loss through all processes, including dynamic outflow (Pfeffer et al., 2008), and another involves the solicitation of opinion from experts in the field (often termed ‘expert solicitation’; Vaughan and Spouge 2002).

Storm-surge and wave models are usually regional in extent and are forced by MSLP fields and near-surface wind fields obtained from regional and global climate models (Lowe et al., 2010) and large-scale changes in sea level. Storm-surge models are used to assess changes in extreme sea level caused by changes in storminess or GMSL rise.

Semi-empirical models are based on physical relationships connecting sea level to global mean temperature (Grinsted et al., 2010; Rahmstorf 2007a; Vermeer; Rahmstorf 2009) or total radiative forcing (Jevrejeva et al., 2009; 2010). The form of this relationship is motivated by physical considerations, whereas the parameters are determined from empirical data – hence the term “semi-empirical” (Rahmstorf et al., 2011). Although these models do not explicitly simulate the underlying processes, they assume that sea level rise is caused primarily by changes in global ice volume and global ocean heat content in response to changes in global temperature or radiative forcing with a characteristic response time. This response time could be infinite (Rahmstorf, 2007a) or explicitly determined by the model as a probability density function with a

wide range of time scales (Grinsted et al., 2010). Further detail and assessment of these models is provided in Section 13.6.1.2.

Figure 13.2 is a graphic representation of the processes considered and models used to interpret past observations and project future changes in sea level. This figure serves as a useful navigation aid for the different sections of this chapter and sections of other chapters that are relevant to sea level change.

[INSERT FIGURE 13.2 HERE]

Figure 13.2: Schematic representation of key processes that contribute to sea level change and are considered in this report. Colouring of individual boxes indicates the types of models and approaches used in projecting the contribution of each process to future sea level change. The diagram also serves as an index to the sections in this report that are relevant to the assessment of sea level projections via numbers given at the bottom of each box.

13.2.3 Models Used to Project Changes in Ice Sheets and Glaciers

Models used to assess the contribution of terrestrial ice masses to future sea level change can be divided into three groups: ice-sheet surface mass budget (SMB) models; ice-sheet dynamics models; and glacier models. The representation of these ice masses within AOGCMs is not yet at a stage where projections of their changing mass are routinely available. Additional process models, using output from AOGCMs, are therefore required to evaluate the consequences of projected climate change on these ice masses. In each case, very different types of specialist process models are required to make these projections.

A distinction must be drawn between the flux of ice passing through an ice mass and the ice mass' contribution to sea level. For instance, the flux through the Antarctica ice sheet can be measured by the amount of snowfall annually accumulated on its surface (e.g., 5.0–5.8 mm yr^{-1} SLE) (de Berg et al., 2006). However for the Antarctic, the vast majority of this mass flux is balanced by ice outflow to the ocean so that the actual contribution to sea level rise is likely to be a fraction (~5–10% for instance) of the throughput. The balance between the fluxes of ice added and lost takes time scales of thousands of years to be established (Pollard and DeConto, 2009); changes in either flux away from this long-term balance will make a contribution to sea level change.

The overall contribution of an ice mass to sea level involves changes to either its SMB (primarily snow accumulation and the melt and subsequent runoff of snow and ice) or changes in the dynamics of ice flow which affect the outflow to the oceans. Some ice-sheet models incorporate both effects in their projections; however most studies have focussed on either surface SMB or flow dynamics. It is assumed that the overall contribution can be found by summing the contributions calculated independently for these two sources, which is valid if they do not interact significantly. While this may be acceptable for the ice-sheet projections over the next century, it may become an issue on longer time scales when, for example, changes in ice-sheet geometry driven by dynamics may feedback on SMB.

Another general issue faced in projecting the sea level contribution of land-ice is that model projections are generally made in comparison with a base state which is assumed to be a steady state (i.e., not making a significant sea level contribution). This base state is generally assumed to be either the preindustrial period or, because of our scant knowledge of the ice sheets before the advent of satellites, the late 20th century. In reality, even in these base states, the ice sheets are likely to have been contributing to sea level change and this contribution, although difficult to quantify, should be added to their projected contributions.

For both ice-sheet surface mass budget and dynamics, two distinct steps in making a projection of future sea level can be identified. These are the local climate forcing affecting change in the ice sheet, and the response of the ice sheet in terms of mass fluxes. An example would be the ability to project Greenland's changing SMB which relies on both the ability to simulate regional climate change over the ice sheet and the ability to model how regional changes affect processes at the ice-sheet surface (e.g., Rae et al., submitted). Similar issues exist for Antarctica, where simulations of changing mass outflow rely on the ability to simulate regional oceanographic change and models of ice-flow dynamics (Gladstone et al., submitted).

Regional climate models are now the main source of projections of ice-sheet SMB. These models typically operate at finer spatial scales and with a more complete physical representation of climate than AOGCMs.

They require information on the state of the atmosphere and ocean at their lateral boundaries, which are either derived from AOGCM scenario projections or reanalysis data sets. Such models are coupled to sophisticated representations of the mass and energy budgets associated with snow and ice surfaces. A major source of uncertainty lies in the ability of these schemes to adequately represent the process of internal refreezing of melt water within the snowpack.

Mechanisms (see Chapter 4) that could potentially affect changes in ice-sheet dynamics rely on coupling mechanisms with the rest of the climate system that have not traditionally been included in Earth System models. Triggers for grounding line retreat are thought to be linked to the mass balance of ice shelves and in particular the coupling between ocean circulation in sub-ice shelf cavities and the melt rates experienced by these shelves (Holland et al., 2008b). Detailed regional ocean models are available but they are only beginning to be employed as part of predictive global ocean circulation models (Thoma et al., 2008). While the link between ice dynamics and climate forcing is reasonably clear in the case of ice-shelf melt in Antarctica and potential surface melt water effects in Greenland (basal lubrication) and Antarctica (ice-shelf collapse), the exact mechanisms linking climate change to enhanced calving in Greenland are not well understood. This will clearly affect the predictability of this SLR contribution.

Models of ice dynamics have a fairly complete representation of stresses within an ice mass (and therefore its flow), which are needed because the response of an ice mass to changes at its marine boundary is governed by longitudinal stresses (Schoof 2007a). These advanced models, however, require several orders of magnitude more computer time than ice-sheet models such as those used in AR4. In Antarctica, this problem is exacerbated by the need to employ very high spatial resolution (<1 km) to capture the dynamics of grounding-line migration robustly (i.e., so that results do not depend qualitatively on model resolution) (Durand et al., 2009; Goldberg et al., 2009; Morlighem et al., 2010). An alternative approach is to parameterise grounding line physics in a coarser-resolution model (Gladstone et al., 2010a; Pollard and DeConto, 2009; Schoof 2007b) but since grounding line migration is likely to be the primary control of the sea level rise (SLR) contribution of Antarctica, rigorous efforts are needed to validate any such parameterizations. An alternative is to employ models with adaptable spatial resolution (Gladstone et al., 2010b; Goldberg et al., 2009; Schoof, 2007a).

One-dimensional flowline models have been developed to the stage that modelled iceberg calving is in agreement with many observations (e.g, Nick et al., 2009). The success of this modelling approach relies on the ability of the model's computational grid to evolve to continuously track the migrating calving front. Although relatively easy to do in a one-dimensional model, this technique is difficult to incorporate into three-dimensional ice-sheet models which typically employ a computational grid that is fixed in time. Progress is being made in this area (Amundson et al., 2010; Benn et al., 2007; Nick et al., 2010; Pfeffer, 2007) but many challenges remain in basic process understanding and the need to ensure sufficient spatial resolution in models.

The main challenge faced by models attempting to assess sea level change due to glaciers is the very large number of glaciers (the World Glacier Inventory contains more than 120,000; Radic and Hock, 2010) in comparison to the number for which mass budget observations are available (roughly 300; Radic and Hock, 2010). Statistical techniques are used to derive relations between observed mass budgets and climate variables for the small sample of surveyed glaciers, and then these relations are used to upscale to regions of the world. These techniques often include volume-area scaling to estimate glacier volume from their more readily observable areas. Although tidewater glaciers are also likely to be affected by changes in outflow related to calving, the complexity of the associated processes means that most studies limit themselves to assessing the effects of SMB changes.

13.3 Past Sea Level Change

13.3.1 The Geological Record

Records of past sea level change provide critical context for understanding current changes and evaluating projected changes. In addition to establishing a longer term reference for placing current rates of sea level rise in the context of natural variability, these records provide insight into the sensitivity of sea level to past

climate change. Here we summarize the constraints provided by the record of paleo-sea level variations as assessed by Chapter 5.

13.3.1.1 Previous Warm Periods

13.3.1.1.1 The middle Pliocene

Mean global surface temperatures during the middle Pliocene (~3.3–2.9 Ma) are estimated from proxies and GCMs to have been about 2°C to 3°C above pre-industrial, and CO_2 concentrations are estimated to have been higher than pre-industrial values (350–415 ppm) (Chapter 5). There is high confidence that sea level during the middle Pliocene was higher than present, indicating that there was significantly less ice at that time than present, although there is no information on rates of sea level rise. Uncertainties in mantle dynamic processes and regional sea level variability due to GIA (Raymo et al., 2011) result in medium confidence in the most comprehensive estimate of 20 ± 10 m (Miller et al., submitted). Direct geological evidence from the Northern Hemisphere (Maslin et al., 2000) and Antarctica (Naish et al., 2008), together with climate-driven ice-sheet models (Pollard and DeConto, 2009), suggest that most of the variation in middle Pliocene ice volume was associated with the Greenland and West Antarctic ice sheets, with small changes in the East Antarctic Ice Sheet (EAIS).

13.3.1.1.2 The Last Interglaciation

Accounting for tectonic and isostatic factors, emerged shoreline indicators dating from the Last Interglaciation (LIG) provide high confidence that GMSL during the LIG was at least 6 meters higher than present, with some evidence providing low confidence that it reached 10 m (Dutton and Lambeck, submitted; Kopp et al., 2009). During this time of higher sea level, there is very high confidence that CO_2 concentrations were similar to pre-industrial levels and medium confidence that LIG surface temperatures were about 2^{o}C warmer than pre-industrial temperatures (high confidence in high latitudes) (Chapter 5).

There is medium confidence that thermal expansion of the LIG water column was small (0.3 ± 0.4 m in the model results by McKay et al. (2011), leaving high confidence that the primary sources of the +6 m LIG sea level highstand were from glaciers and the Greenland and West Antarctic ice sheets. There is little evidence for how much glaciers retreated during the LIG, but the modern glacier budget provides an upper limit of ~0.6 m sea level equivalent (Radic and Hock, 2010). There is high confidence that Greenland contributed 2 m of sea level (Colville et al., 2011), with low-to-medium confidence that it contributed 4 m (Robinson et al., 2011). Geological and modeling constraints for retreat of the West Antarctic Ice sheet (WAIS) during the LIG are equivocal, but given the constraints from thermosteric, glaciers, and Greenland contributions for ~3–5 m, some contribution is required to explain a LIG GMSL of +6 m, with an additional contribution from the East Antarctic Ice Sheet if GMSL was +10 m.

There is very high confidence that CO_2 concentrations were similar to pre-industrial levels, indicating that warmer LIG surface temperatures were induced by the greater incoming summer solar radiation in the high northern latitudes than at present and associated feedbacks (Chapter 5). Recent modeling results found that ~55% of the increase in Greenland melting during the LIG can be attributed to warmer temperatures, with the remaining 45% caused directly by higher insolation and associated nonlinear feedbacks (van de Berg et al., 2011). This suggests that of the 2–4 m contribution from the Greenland ice sheet to LIG sea level, only ~1–2 m can be attributed to temperature. In contrast, austral summer solar radiation in the Southern Hemisphere was similar during the LIG as present, and the 3–4^{o}C increase in LIG surface temperature over Antarctica (Jouzel et al., 2007) relative to present remained too low to induce any significant loss from surface melting. Modeling studies indicate that LIG mass loss from the Antarctic may have occurred through warming at intermediate depths in the Southern Ocean (Overpeck et al., 2006).

Establishing the duration of the LIG sea level highstand is critical for deriving rates of sea level change during the LIG. Closed system U/Th ages provide medium-to-high confidence that GMSL reached present values about ~129–130 ka and began to fall significantly below present sea level by 116 ka (Dutton and Lambeck, submitted). These contrast with other reconstructions which place the start of the LIG highstand at ~126 ka to 123.5 ka and ending by 119 ka (Lisiecki and Raymo, 2005; Rohling et al., 2008; Thompson and Goldstein, 2005).

There is high confidence that local LIG sea levels experienced a meter-scale fluctuation sometime between 120-126 ka, suggesting substantial sea level variability during warm climates (Hearty et al., 2007; Kopp et al., 2009; Rohling et al., 2008; Thompson and Goldstein, 2005). Kopp et al. (2009) estimated a median value for sea level rise during the LIG of 3.5 m kyr^{-1} (67% range of –4.4 to 7.4 m kyr^{-1}), although the possibility of higher rates on shorter timescales cannot be excluded. However, these rates are based on a LIG duration that is 3–4 kyr shorter than the duration based on closed-system U/Th ages on fossil corals (Dutton and Lambeck, submitted), suggesting the rates may have been ~70% lower. Dutton and Lambeck (submitted) found that well-dated fossil-corals from many sites point to a 1–2 m change in sea level at ~125–126 ka, while geologic constraints from Bermuda (Muhs et al., 2002) exclude sea level changes greater than a few m in 1 or 2 kyr. These observations thus provide medium-to-high confidence that sea level rose 1–2 m at a rate of ~1.0–2.5 m kyr^{-1}.

In summary, there is high confidence that GMSL during the LIG was at least 6 meters higher than today, with limited evidence that it reached +10 m. Of this sea level rise, contributions from thermosteric and glaciers are ≤1 m, and 1–2 m can be attributed to direct melting of Greenland from higher Northern Hemisphere solar insolation, indicating that at least 3–4 m of sea level rise can be attributed to land-ice loss in response to some combination of ocean and surface temperature forcing. There is high confidence that LIG sea level experienced a meter-scale fluctuation sometime between 120–126 ka, with the best-constrained records providing medium-to-high confidence that sea level rose 1–2 m at a rate of ~1.0–2.5 m kyr^{-1}.

13.3.1.2 The Last Two Deglaciations

The last two transitions from full-glacial to interglacial periods provide opportunities for using observations to evaluate models of ice-sheet and sea level response to a warming planet. In each case, sea level continued to rise from its glacial maximum lowstand well after global temperatures had warmed to near-present interglacial levels. One strategy to infer possible future rates of sea level rise in a warm climate is to constrain them to be less than the observed rates as former sea level approached or reached the present value. These intervals of sea level rise represented continued ice-sheet disequilibrium response to deglacial forcings rather than a near-equilibrium response to greenhouse forcing. Thus, they only provide upper limits for land-ice loss and are not complete analogues for future changes.

Kopp et al. (2009) found that GMSL rose to the initial LIG highstand (when sea level was within -10 m) at rates that likely exceeded 5.6 m kyr^{-1} but were unlikely to have exceeded 9.2 m kyr^{-1}. Based on a chronology that places the start of the LIG highstand at ~123.5 ka, Rohling et al. (2008) used a $\delta^{18}O$ record from the Red Sea to establish that rate of rise above present-day (0 m) sea level was 16 ± 8 m kyr^{-1}. Rohling et al. (2008) considered the implications for a LIG duration from 119–128 ka and found that the rate of sea level rise into the LIG was reduced to 8–13 m kyr^{-1}; that rate would be further reduced if the duration of the LIG highstand is ~130 ka to 116 ka as suggested by closed-system U/Th ages on fossil corals (Dutton and Lambeck, submitted; Muhs et al., 2011). During the present interglacial climate, sea level rose at an average rate of ~10 m kyr^{-1} between 12 ka and 6 ka, when it reached near-present levels.

13.3.1.3 The Late Holocene

There is medium-to-high confidence that for the past ~5000 years, GMSL has been close to present sea level but has not been constant. GMSL rose 2–3 m between about 6000 and 3000 years BP (Lambeck et al., 2004; Lambeck et al., 2010). There is low-to-medium confidence that ~50% of this ocean volume increase can be attributed to a Late Holocene ice reduction over Marie Byrd Land, Antarctica (Stone et al., 2003).

Spatial variability in sea level change during the Late Holocene has remained significant because of the residual isostatic response to the last deglaciation (Milne and Mitrovica, 2008). Local sea level records spanning this interval and based on consistent sea level indicators provide medium-to-high confidence that fluctuations in global sea level during this interval have not exceeded ~ ±25 cm on time scales of a few hundred years.

The observational record for the past 2000 years up to pre-industrial times is of the highest precision, and reconstructions from salt marsh records have been validated against regional 20th century tide-gauge

records. The most robust signal captured in the salt-marsh proxy sea level records from both northern and southern hemispheres provides high confidence for an acceleration in the late 19th century that is widely interpreted to mark the transition from relatively low rates of change during the late Holocene (order tenths of mm a^{-1}) to modern rates (order mm a^{-1}), but there is variability in both the magnitude and the timing (1840–1920) of this acceleration (Gehrels et al., 2008; Gehrels et al., 2006; Kemp et al., 2011).

13.3.2 The Instrumental Record (~1700-2010)

The instrumental record of sea level change is mainly comprised of tide-gauge measurements and, since the early 1990s, satellite-based radar altimeter measurements. Six long tide-gauge records located in northwestern Europe extend back to the 1700s. During the 19th and 20th centuries, the number of tide gauge records has increased, but their spatial coverage remains inhomogeneous, with a bias towards the northern hemisphere and almost no data in the open oceans. The data are also inhomogeneous in terms of quality and length. Because tide gauges are also affected by local vertical crustal motions associated with GIA, tectonic deformation, or other phenomena (Section 13.2), vertical crustal motion is a strong limitation for deriving estimates of GMSL trends. Using different strategies, several analyses of good quality historical tide gauge records attempted to construct a 'mean' sea level curve over the 20th century. Some studies only considered a few tens of long (>60 years) tide gauge records from tectonically stable continental and island coasts, and only corrected the data for GIA (Douglas, 2001; Holgate, 2007; Holgate and Woodworth, 2004; Peltier, 2001). Other studies considered a larger set of records of different length from a variety of regions and looked at regional coherency to exclude some tide gauges affected by large local ground motions (Jevrejeva et al., 2006; 2008) or used past sea level reconstruction methods (see Section 13.4.3.2) (Church and White, 2006, 2011; Church et al., 2004). In these cases also, the only vertical land motion corrected used is GIA. In the last few years, the availability of Global Positioning System (GPS) sites near tide gauge sites has allowed one to directly measure, and thus correct for, vertical crustal motion, whatever the causes (Woppelmann et al., 2009).

Tide-gauge data show that sea level was stable or slowly rising until the mid to late-19th century, when it clearly began to rise (Jevrejeva et al., 2008; Mitchum et al., 2010). The mean rate of GMSL rise for the 20th century is estimated as ~1.7 mm yr^{-1} (Church and White, 2006; Church et al., 2011b; Jevrejeva et al., 2006; Jevrejeva et al., 2008). Global mean sea level is also subject to interannual, decadal and multidecadal variability (Woodworth et al., 2009), in addition to shorter term fluctuations not discussed here.

Church and White (2006) detected an acceleration in the rate of sea level rise of 0.013 ± 0.006 mm yr^{-2} since 1870 using their tide-gauge based reconstruction method, a value confirmed by Jevrejeva et al. (2008) from a global mean sea level reconstruction from 1700 to the present. In an update using longer altimeter time series and a larger number of tide gauges, Church and White (2011) estimated a slightly smaller but not significantly different acceleration of 0.009 ± 0.003 mm yr^{-2}. These reconstruction estimates are compatible with the accelerations obtained from individual long tide-gauge records (order of 0.01 mm yr^{-2} between the 19th and 20th centuries), primarily from a small number of stations in northern Europe (Woodworth et al., 2011a; Woodworth et al., 2011b). Only one or two similarly long records are available from the Atlantic and Pacific coasts of North America; these provide similar estimates of acceleration although with large uncertainties. This picture of long term acceleration between the 19th and 20th centuries is confirmed by information from salt marshes in different parts of the world, although suggestive of a more abrupt 'inflexion' at the end of the 19th century than in the tide gauge records (Woodworth et al., 2011a,b; Kemp et al., 2011) (Section 13.3.1.3).

Satellite altimetry began in 1992 with the launch of TOPEX/Poseidon and, for the first time, provided a globally distributed set of precise sea level measurements. The altimeter time series has been continued with the launch of Jason-1 (2001) and Jason-2 (2008), with each mission overlapping the previous mission so that their measurements could be inter-calibrated. These satellites are in identical orbits that repeat every 10 days and cover ±66° latitude. Other satellites like Envisat (2002) have a higher inclination (up to ± 82° latitude) and thus cover part of the Arctic Ocean. While tide gauges measure sea level relative to the land, satellite altimetry measures 'absolute' sea level variations with respect to a fixed reference (classically a reference ellipsoid that coincides with the mean shape of the Earth, defined within a globally realized terrestrial reference frame).

The current 19+-year satellite altimetry time series (Figure 13.3) shows that from 1993–2010, GMSL has risen at a rate of 3.2 ± 0.5 mm yr^{-1}. A correction of ~ –0.3 mm yr^{-1} has been applied to this value to account for the increasing size of the global ocean basins due to GIA (Peltier, 2009). The current 0.5 mm yr^{-1} level of accuracy is derived from assessments of all potential source of errors affecting the altimetry-based estimates of GMSL rise (Ablain et al., 2009) and from tide gauge comparisons (Beckley et al., 2010; Nerem et al., 2010).

[INSERT FIGURE 13.3 HERE]

Figure 13.3: Global mean sea level variations over 1993-2011 computed from an ensemble mean of five different analyses of altimeter data from the TOPEX/Poseidon, Jason-1, and Jason-2 satellite missions (Ablain et al., 2009; Beckley et al., 2010; Church and White, 2011; Leuliette and Scharroo, 2010; Nerem et al., 2010). Annual and semi-annual variations have been removed and 60-day smoothing has been applied. The secular trend is 3.2 mm yr^{-1} after correcting for GIA (0.3 mm yr^{-1}). The gray shading represents 95% certainties based on the standard deviation of the different analyses.

The larger rate of rise since the early 1990s is almost double the 20th century average rate, although apparently not significantly much larger than rates in the 1940s and late 1970s (Church and White, 2011; Holgate and Woodworth, 2004; Jevrejeva et al., 2008; Mitchum et al., 2010; Ray and Douglas, submitted). Merrifield et al. 2009 argued that this recent trend is distinct from decadal variations in earlier periods principally because the increase occurs simultaneously in the tropical and southern hemisphere oceans, which were sparsely observed in the 1940s and 1970s. However, the 20th century tide gauge-based interannual to decadal variability remains uncertain because of data sparseness and heterogeneity, and shows important differences from one curve to another (Church and White, 2011, Jevrejeva et al., 2008).

13.4 Contributions to Global Mean Sea Level Rise During the Instrumental Period

Since AR4, there has been considerable progress in quantifying the two main factors that contribute to GMSL rise (thermosteric rise due to ocean warming and water-mass input from ice and water reservoirs on land) (Section 13.2), largely as a result of various in situ and satellite data sets covering the last several decades. Since 2002, additional information comes from the GRACE satellite gravity mission, from which it is possible to directly measure the ocean-mass component of sea level rise and the land areas responsible for that change.

13.4.1 Thermosteric Contribution

Thermosteric sea level change is estimated from various historical shipboard measurements (ocean station data, expendable bathythermographs (XBTs), etc.) prior to 2000 (Ishii and Kimoto, 2009; Levitus et al., 2009) and additionally by the Argo profiling floats after 2000 (Roemmich et al., 2010) (see Chapter 3). In recent years, systematic depth-varying biases were detected in historical XBT data (Gouretski and Koltermann, 2007; Wijffels et al., 2008). Similarly, instrumental bias has affected the Argo floats (Lyman et al., 2010). After accounting for these instrument bias corrections, time series of thermosteric sea level change since 1955–1960 show that upper ocean warming (above ~700 m) accounts for about 0.4 ± 0.2 mm yr^{-1} to the observed sea level rise (Levitus et al., 2009; Ishii and Kimoto, 2009). Domingues et al. (2008) estimate the thermosteric rate to be 0.5 ± 0.1 mm yr^{-1} since 1960. However, their number is likely a lower bound, due to a lack of data in the Southern Hemisphere and in the deep ocean (below 700 m to 3000 m). Recent studies have estimated the deep-ocean contribution using ship-based data collected under the world Ocean Circulation Experiment (WOCE) and revisit cruises (Johnson and Gruber, 2007; Johnson et al., 2007; Kouketsu et al., 2011; Purkey and Johnson, 2010) and reported significant warming of the global abyssal and deep southern ocean waters. Accounting for the deep-ocean contribution (below 700 m), Church et al. (2011b) estimated the thermal expansion rate to be 0.7 ± 0.2 mm yr^{-1} for 1972–2008, including both deep and abyssal contributions.

For the 1993–2003 decade, IPCC AR4 reported a 1.6 mm yr^{-1} contribution, but this value was based on uncorrected XBT data. Revised estimates accounting for XBT fall-rate errors lead to a slightly lower rate of 1.3 mm yr^{-1} for that particular decade (Levitus et al., 2009; Ishii and Kimoto, 2009).

Argo-based estimates suggest a reduced rate of thermosteric sea level rise since 2003–2004 (Lymann et al., 2010). However, as shown by Llovel et al. (2010a) using different Argo databases over 2004–2009,

considerable scatter was noted between early short-term trend estimates. More recent Argo-based thermal expansion rates using data beyond 2005 (when the Argo coverage was complete) show more coherent results. Over the 2005–2010 time span, von Schuckmann and Le Traon (submitted) report a thermal expansion contribution of 0.75 ± 0.15 mm yr^{-1} for the 0–2000 m ocean layer.

On average, the contribution of ocean warming accounts for ~ 1.0 ± 0.3 mm yr^{-1}, hence about 30% of the observed GMSL rise, for the 1993–2010 period (Cazenave and Llovel, 2010; Church et al., 2011b). The abyssal ocean (below 3000 m) may contribute ~0.1–0.15 mm yr^{-1} to this value (Purkey and Johnson, 2010; Church et al., 2011).

Observations indicate that thermal expansion accounts for ~30% to 40% of the total rate of observed sea level rise. This contribution was 0.7 ± 0.13 mm yr^{-1} between 1971 and 2010 and 1.0 ± 0.3 mm yr^{-1} between 1993 and 2010. Although we note a slight increase in its absolute value between these two periods, its proportion to the observed rate slightly decreased (from 40% to 30%). Over the recent years (2005–2010), thermal expansion accounted for 0.75 ± 0.15 mm yr^{-1}, i.e., 27% of the observed rate of rise.

13.4.2 Glaciers

"Glaciers" are defined here as all glacier ice exclusive of the Greenland and Antarctic ice sheets, but including the peripheral glaciers surrounding the ice sheets. Measurements of the global changes in glacier mass and area, and an ability to predict changes in these quantities, are complicated by a variety of factors, including the uncertainty in accounting for the large number of potentially significant contributors (the total number may be more than 200,000 (Bahr and Dyurgerov, 1999). Because of the large number of glaciers and their wide geographic distribution, only a very limited subset have point measurements, requiring that these measurements be upscaled to a poorly known (and changing) global distribution. Remotely sensed data are also affected by the complexity of managing data acquisition at many widely dispersed locations and, in the particular case of GRACE gravity observations, by the fact that most individual glaciers and glacier complexes are smaller than the spatial resolution of the GRACE system, so glacier mass change signals cannot be easily distinguished from other nearby mass change signals (e.g., adjacent land hydrology). The uncertainties associated with these issues are compounded by the uncertainties intrinsic to cryospheric measurements that affect glaciers and ice sheets equally.

Upscaling programs require both high-quality, consistently operated ground-based data acquisition programs and a global inventory of glaciers (location, size, elevation, hypsometry, aspect, etc.) to upscale ground-based point data to a global estimate. Prior to 2009, the World Glacier Inventory contained only about 10% of estimated total global glacier area (WGMS, 1989); this fraction increases to 23% with the addition of the Eurasian Glacier Inventory (EGI) (Bedford, 1996). Cogley (2009b) created an "Extended Format" Inventory, or WGI-XF, by combining the core WGI, EGI and several other data sources to bring the total inventoried area up to 48% of the estimated global total glacier area. A completion of the global inventory, at least to standards sufficient for purposes of sea level assessments, is currently underway, with the most significant progress thus far being made in Alaska, Arctic Canada, and Arctic Russia. A completed inventory is scheduled for late 2011/early 2012.

Long-term mass balance measurement programs are few in number, are expensive to operate, and obtain their greatest value when maintained consistently for long periods. Ground-based measurement time series exist for 105 glaciers worldwide, but most of these records are short, with time series extending back as far as 1970 only for 31 glaciers (Zemp et al., 2009). Ideally, glaciers are selected to be representative of the overall average behavior of other glaciers in their region; in practice, glaciers have been chosen primarily on the basis of accessibility and only secondarily on the basis of their regional suitability. Consequently, very large or complex branched glaciers, and glaciers in remote or inaccessible locations tend to be underrepresented in the inventory. Marine-terminating (tidewater) glaciers are also typically absent from conventional mass balance studies, an omission that significantly biases many assessments (Cogley, 2009a).

The AR4 estimated the glacier contribution to sea level rise to be 0.77 ± 0.22 mm yr^{-1} SLE over the period 1993–2003 (Lemke et al., 2007). In a synthesis of the same sources used in AR4, Kaser et al. (2006) discussed differences in assessment arising from differences in methods of interpolation among the analyses,

from which they estimated the glacier contribution to sea level rise for the period 2001–2004 to be 0.98 ± 0.19 mm yr^{-1} SLE.

Reported global glacier contributions to sea level rise at the time of AR4 were highly variable for several reasons, including the absence of an adequate global inventory and the fact that some analyses included the peripheral glaciers surrounding the ice sheets while others did not, leading to various authors using widely varying total glacier areas and volumes for upscaling (Dyurgerov et al., 2005; Raper and Braithwaite, 2005). Since the AR4, Radic and Hock (2010) reported an area of 741 ± 68 x10^3 km^2 and volume of 0.60 ± 0.07 m SLE (including peripheral glaciers). While the Radic and Hock (2010) assessment is presently the most widely used for values for glacier volume and area, their assessment still depends on upscaling of the present global inventory which is only ca. 48% complete. [PLACEHOLDER FOR SECOND ORDER DRAFT: the new inventory may be in place by early 2012]

The absence of marine-terminating glaciers from most conventional mass-balance measurement programs resulted in underestimates of total glacier losses. This deficiency was partially corrected by Cogley (2009a), who obtained totals ca. 40% greater than the values without geodetic observations for the period 2001-2004. Dyurgerov (2010) accounted for overestimates of total loss rate by correcting for declining glacier area during loss (as well as making other corrections); the revised rate of sea level rise from glaciers for the period 1961–2003 increased by 14% (0.58 mm yr^{-1} SLE in the 2010 analysis from 0.51 mm yr^{-1} SLE in the 2005 analysis), but for the period 2000–2004, the revised rate declined 16% (0.88 mm yr^{-1} SLE in the 2010 analysis from 1.05 mm yr^{-1} SLE in the 2005 analysis).

Compilation and upscaling of observations indicate that it is very likely that the long-term (since ca. mid-19th century; see Leclerqc et al. (2011) net decline of global glacier volume has continued in recent decades. The overall rate of decline is likely to be accelerating, but the trends inferred from observations are highly variable, and on pentadal intervals, most commonly used for averaging glacier mass balance data, the trend is not consistent. Using an improved glacier inventory, Cogley (2009a) assessed recent loss rates from glaciers, including those glaciers on the periphery of the Greenland and Antarctic ice sheets, at 0.92 ± 0.05 mm yr^{-1} SLE for 2005–2009, and 0.94 ± 0.04 mm yr^{-1} SLE for 1993 – 2009. The largest loss rates came from Arctic Canada and Alaska, but the missing peripheral glaciers surrounding the ice sheets were estimated to be significant contributors as well, adding an additional ca. 25% to the total loss rate. For comparison, AR4 reported loss rates of 0.50 ± 0.18 mm yr^{-1} SLE for 1961–2004, and 0.77 ± 0.22 mm yr^{-1} SLE for 1991–2004, with the largest sea level contributions from Arctic Canada, Alaska, and High Mountain Asia. Significant uncertainties remain in the estimates of glacier loss rates, arising from 1) an improved but still incomplete glacier inventory, especially for the peripheral glaciers surrounding the ice sheets; 2) spatially sparse and temporally patchy observations; 3) exclusion in some observational methods of calving losses.

13.4.3 Greenland and Antarctica Ice-Sheet Contributions

Knowledge of the contribution of the Greenland and Antarctic ice sheets to sea level changes comes primarily from satellite and airborne surveys. Three main techniques are employed (Chapter 4): the mass budget method, repeat altimetry, and temporal variation in the Earth's gravity field. The strengths and weaknesses of these methods are discussed in Section 4.4.1. The Greenland ice sheet's mass budget comprises its surface mass budget (the sum of ablation which is primarily ice and snow melt and subsequent runoff, and accumulation primarily snowfall) and outflow (the release of ice bergs). Antarctica's mass budget comprises accumulation and outflow in the form of calving and ice flow into floating (and therefore sea level neutral) ice shelves.

Observations indicate that Greenland is very likely to be experiencing a net loss of mass, and this loss is likely to have increased over the last two decades. Drawn from the assessment made in Chapter 4 (Section 4.4.2.2), Greenland's contribution was 0.34 ± 0.06 mm yr^{-1} between 1993 and 2009, and 0.61 ± 0.18 mm yr^{-1} between 2005 and 2009. Antarctica is also likely to be in a state of net mass loss and its contribution to sea level is also likely to be increasing through time (Section 4.4.2.3). The associated rate of sea level rise was an average of 0.24 ± 0.09 mm yr^{-1} between 1993 and 2009, and 0.40 ± 0.19 mm yr^{-1} over the period 2005 to 2009. The contribution of both ice sheets is 0.58 ± 0.15 mm yr^{-1} over 1993–2009 and 1.01 ± 0.37 mm yr^{-1}

over 2005-2009. For context, the AR4's assessment was 0.21 ± 0.07 mm yr^{-1} for Greenland and 0.21 ± 0.35 mm yr^{-1} for Antarctica, over the period 1993 to 2003.

13.4.4 Land-Water Storage Contributions

Changes in land-water storage in response to climate change and variability and direct human-induced effects have the potential to contribute to sea level change. Apart from ice sheets and glaciers, fresh water on land is stored in rivers, lakes, human-made reservoirs, wetlands and inundated areas, the root zone (upper few meters of the soil), aquifers (ground water reservoirs), and snow pack at high latitudes and altitudes.

Estimates of climate related land-water storage changes over the past two decades rely on global hydrological models because corresponding observations are inadequate. Using atmospheric reanalyses as external forcing, model-based studies (Milly et al., 2003; Ngo-Duc et al., 2005) found no long-term climatic trend in total water storage. While snow is the dominant contribution to seasonal GMSL variations (Milly et al., 2003), its long-term contribution to sea level is negligible, a result recently confirmed from a 20-year long satellite-based observational record of snow mass (Biancamaria et al., 2011).On the other hand, models report large interannual, decadal, and multidecadal fluctuations in land-water storage, equivalent to several millimetres of sea level (Ngo-Duc et al., 2005). Recent studies showed that interannual variability in observed GMSL is correlated with ENSO indices (Nerem et al., 2010) and is inversely related to ENSO-driven changes of land-water storage, especially in the tropics (Llovel et al., 2011); specifically, sea level tends to be higher during El Niño events because ocean precipitation increases (especially in the North Pacific) and land precipitation decreases. The reverse happens during La Niña events as seen very clearly during the 2010–2011 La Nina Event (Figure 13.3).

Direct human interventions on land-water storage induce sea level change (Gornitz, 2001; Huntington, 2008; Lettenmaier and Milly, 2009; Sahagian, 2000). The largest contributions come from groundwater withdrawal (for agriculture, industrial, and domestic use) and reservoir filling behind dams, but urbanization, wetland drainage, land-use and land-cover changes, and deforestation also play a role. Over the past half-century, tens of thousands of dams have been constructed to create artificial reservoirs, offsetting some of the sea level rise that would otherwise have occurred. Several attempts have been made to estimate the corresponding total volume of water stored in artificial reservoirs (Chao, 1995; Gornitz, 2001; Vorosmarty, 2002). Chao et al. (2008) reconstructed the history of water impoundment in the nearly 30,000 reservoirs built during the 20th century and estimated the average contribution to sea level by dams and artificial reservoirs at~ –0.55 mm yr^{-1} SLE during the last half-century with a stabilization in recent years, suggesting that without dam building, past sea level rise would have been larger. Lettenmaier and Milly (2009) suggested a slightly smaller contribution since ~1940–1950, of ~ –0.35 mm yr^{-1} SLE, and stabilization since year 2000. However, other human-induced factors may at least partly cancel this effect, the main candidate being groundwater depletion (i.e., the excess of water withdrawal over recharge). Estimates of this factor show considerable uncertainty. For example, Wada et al. (2010) estimated this effect at 0.8 ± 0.1 mm yr^{-1} SLE since 1960 while Milly et al. (2010) proposed a lower value of 0.2–0.3 mm yr^{-1} SLE for recent years. Using Konikow's (2011) estimate for ground waters (of 0.12 mm yr^{-1} SLE for 1900–2008), Church et al. (2011b) estimated a net effect of dams and ground water mining on the order of –0.1 ± 0.2 mm yr^{-1} SLE over 1970–2008. Because of increased water demand in highly populated arid regions, future increases in groundwater mining may lead to sea level rise, especially as the effect of dams has already declined and is projected to decline in future decades (Lettenmaier and Milly, 2009).

Additional information on global land-water storage is provided by satellite gravity measurements from the GRACE satellite mission. GRACE measures temporal changes of the vertically integrated water column (surface waters, soil moisture, groundwater) and thus cannot separate the contribution of individual reservoirs nor distinguish between climate and anthropogenic effects. The GRACE-based total water volume trend in the world's largest river basins since 2002 is small and not significantly different from zero in equivalent sea level (Llovel et al., 2010b; Ramillien et al., 2008). However, the GRACE results suffer from low spatial resolution and contamination by GIA (Lettenmaier and Milly, 2009). For example, in some river basins adjacent to mountain ranges (e.g., Indus, Ganges, Brahmaputra), GRACE cannot clearly separate land hydrology from glacier mass changes (Matsuo and Heki, 2010), whereas at high latitudes, estimates of GRACE-based water storage change are strongly affected by GIA uncertainty.

In summary, model-based and GRACE-based estimates of total land-water storage indicate that climate-related trends are small and do not contribute more than ~ 0.1–0.2 mm yr^{-1} to observed sea level rise. This is unlike human-induced changes, which is several times larger in amplitude over the second half of the 20th century. The two main contributions (ground water pumping and water impoundment behind dams), however, more or less cancel each other. At interannual time scales, climate-related changes in land-water storage produce several mm of SLE and are mostly related to ENSO events.

13.4.5 Ocean Mass Observations from GRACE (2002–2010)

Since 2002, GRACE has directly measured changes in ocean mass (Cazenave et al., 2009; Chambers, 2006; Chambers et al., 2004; Chambers et al., 2010; Leuliette; Miller 2009; Llovel et al., 2010a). These measurements represent the sum of total land-ice plus land-water components, and thus provide an independent assessment of the latter contributions. Because of the poor spatial resolution of the GRACE observations, however, measures must be taken to prevent land signals from leaking into the ocean estimates. Depending on which GRACE processing center's gravity solutions are used and on the post-processing applied to the data, errors on estimated ocean mass change can reach 0.5 mm yr^{-1} (Quinn; Ponte 2010). GRACE is also sensitive to mass redistribution associated with GIA and requires an associated correction that ranges from ~1.2 mm yr^{-1} to ~1.7 mm yr^{-1} depending on the GIA model used (Chambers et al., 2010; Paulson et al., 2007; Peltier, 2009; Tamisiea, 2011), adding uncertainty to GRACE-based ocean mass estimates.

GRACE estimates of the increase in global average ocean mass since 2002 range from 1–1.5 mm yr^{-1} SLE (Leuliette and Willis, 2011), which is somewhat less than estimates of the mass change made from other sources. Possible explanations for these differences include a portion of the meltwater from glaciers that is being stored on the continents rather than running into the oceans, GIA correction uncertainty, and residual errors in the GRACE estimates.

The simultaneous availability of altimeter, GRACE, and Argo measurements provides a means of testing these relatively new observation systems. In terms of global averages, the sum of global ocean mass from GRACE and global thermosteric sea level change from Argo should almost equal the total sea level change observed by satellite altimetry, although there is still a missing contribution from the deep ocean below 2000 m. A number of studies have compared these data sets over 2003–2008/2009 and found good agreement on seasonal timescales, but less agreement on interannual timescales (Leuliette; Miller 2009; Llovel et al., 2010a; Willis et al., 2008). A longer data time series from these observing systems is needed to provide useful constraints on closure of the sea level budget.

In summary, ocean mass has been increasing at a rate of 1.1 ± 0.6 mm yr^{-1} SLE over 2005–2010 (Leuliette and Willis, 2011), which agrees within the error bars with independent estimates computed from observations of total sea level (altimetry) and thermosteric sea level (Argo), but is significantly lower than independent estimates of the glacier, Greenland, and Antarctic contributions (Table 13.1). The reason for this disagreement is still undetermined, but could result from an underestimate of the measurements errors, or a physical cause such as a portion of the glacier melt being stored on the continents instead of running into the oceans.

13.4.6 Summary of Observed Budget

The observed budget of GMSL changes is divided into the period since 1971 (when significantly more ocean data became available and systematic glacier reconstructions began), since 1993 (the satellite altimeter era), and since 2005 (the ARGO era). The numbers provided in Table 13.1 are based on direct estimates for the contributions (input from Chapters 3 and 4 for thermal expansion and land ice, and from Church et al. (2011b) for land-water storage). Over all time periods considered, the sea level budget (direct observations of total sea level compared to the sum of the component contributions) is closed within uncertainties.

Table 13.1: Global mean sea level budget (mm yr^{-1}) over different time intervals from observations (updated values available in SOD) and from model-based contributions. Uncertainties are 5–95%. The AOGCM historical integrations end in 2005; projections for RCP 4.5 are used for 2006–2010. The thermosteric, glacier and ice-sheet SMB

contributions are computed from the CMIP5 results following the methods of Appendix 13.A. The ice-sheet dynamics contributions are estimated as described in the text.

Source	1901–1990	1971–2010	1993–2010	2005–2010
Observed contributions				
Thermosteric		0.70 ± 0.13	1.0 ± 0.3	0.75 ± 0.15
Glaciers	0.50 ± 0.43	0.72 ± 0.06	0.94 ± 0.07	0.92 ±0.08
Greenland		0.14 ± 0.04[a]	0.34 ± 0.10	0.61 ± 0.30
Antarctica		0.10 ± 0.06[a]	0.24 ± 0.15	0.40 ± 0.31
Land water storage		–0.1 ± 0.2	–0.1 ± 0.2	–0.15 ± 0.1
Total		1.6 ± 0.3	2.4 ± 0.4	2.5 ± 0.5
Modelled contributions				
Thermosteric	0.30 ± 0.24	0.80 ± 0.28	1.32 ± 0.47	1.14 ± 0.78
Glaciers	0.53 ± 0.30	0.89 ± 0.42	1.13 ± 0.52	1.26 ± 0.50
Greenland SMB	0.05 ± 0.06	0.09 ± 0.10	0.12 ± 0.13	0.14 ± 0.14
Antarctic SMB	–0.08 ± 0.16	–0.19 ± 0.21	–0.26 ± 0.25	–0.29 ± 0.26
Greenland dynamics		0.07 ± 0.02	0.17 ± 0.05	0.31 ± 0.15
Antarctic dynamics		0.10 ± 0.06	0.24 ± 0.15	0.40 ± 0.31
Total[b]		1.7 ± 0.6	2.6 ± 0.8	2.8 ± 1.0
Modelled Greenland SMB for observed climate[c]		0.06 ± 0.08	0.20 ± 0.17	0.39 ± 0.28
Observed total	~1.7 ± 0.3	1.7 ± 0.18	±0.5	2.8 ± 0.5

Notes:
(a) Estimated as the weighted sum of the mean for 1993–2010 and zero for 1971–1992, assuming the ice-sheets to have been in mass balance for the earlier years.
(b) Including observed land water storage.
(c) Difference from the mean SMB of 1961–1990 in the models of Table 13.3. This difference equals the sea level contribution from Greenland SMB changes if the ice sheet is assumed to have been near zero mass balance during 1961–1990 (Hanna et al., 2005). This row is shown for comparison and is not included in the total.

13.4.7 Modeled Global Budget

The closure of the observational budget for recent periods within uncertainties (Section 13.4.6) represents a significant advance since the AR4 in physical understanding of the causes of past GMSL change, and provides a basis for critical evaluation of models of these contributions (introduced in Section 13.2) in order to assess their reliability for making projections (Sections 13.5 and 13.6.1.1).

GMSL rise due to thermal expansion is approximately proportional to the increase in ocean heat content (Körper et al., submitted; Russell et al., 2000), and both of these can be calculated from AOGCM simulations (Section 13.5.1). Experiments have been carried out with CMIP3 and CMIP5 AOGCMs forced with historical time-dependent anthropogenic change in atmospheric composition since the late 19th century, in most cases also including natural forcing due to volcanic aerosol and to variations in solar irradiance. These experiments provide the basis for the statistical detection of climate change and its attribution to forcing agents (Chapter 10). Domingues et al. (2008) compared GMSL due to thermal expansion of the upper 700 m of the ocean in observations with CMIP3 historical experiments. For 1961–1999, the simulations with both anthropogenic and natural forcing had substantially smaller increasing trends than those without the natural forcing, because the natural volcanic forcing tends to cool the climate system and reduce ocean heat uptake (Levitus et al., 2001). On average, the models including natural forcing agreed better with the variability in the observations and their trends were about 10% less than the observed trends, but closer to the observations than the models without natural forcing.

Historical GMSL rise due to thermal expansion simulated by CMIP5 models is shown in Table 13.1 and Figure 13.4a. The rate of thermal expansion increases during the 20th century because the ocean takes up heat more rapidly as the climate warms. The model-mean rate for 1971–2010 is close to observations. For 1993–2010 the model-mean rate exceeds that observed, probably because ocean warming in the AOGCMs during the first decade of the 21st century is at least as large as in the late 1990s, whereas in observations there has been a decreased rate of ocean warming, possibly due in part to increased negative aerosol radiative forcing (Church et al., 2011b) not included in the model simulations. Following the major volcanic

eruptions in 1963, 1982 and 1991, the rate of expansion is substantially larger than the 20th century average, as the ocean rebounds from the impact of the volcanic forcing (Church et al., 2005; Gregory et al., 2006).

Gregory (2010) suggested that AOGCMs in general may underestimate ocean heat uptake in historical simulations, because the models are usually spun up without volcanic forcing, whose imposition during the 20th century therefore represents a net negative forcing relative to the control climate, whereas in reality volcanic eruptions should give zero long-term forcing, because they are a normal part of the system. The hypothesis is that the apparent long persistence of the oceanic cooling following the 1883 eruption of Krakatau in the CMIP3 historical simulations (Delworth et al., 2005; Gleckler et al., 2006a; Gleckler et al., 2006b; Gregory et al., 2006) is an artifact of experimental design. Comparison of CMIP3 historical experiments with and without volcanic forcing indicates that this effect could lead to an underestimate of 0.1–0.2 mm yr^{-1} of thermosteric GMSL rise on average during the 20th century. This effect is not included in the results in Table 13.1 and Figure 13.4a and the projections for the 21st century.

[INSERT FIGURE 13.4 HERE]

Figure 13.4: Modeled and observed global-mean sea level contributions and total sea level from the 1960s to the present. All curves have an arbitrary offset and are set to zero in 1971, shortly after a significant increase in the number of ocean observations. The coloured curves are for various model simulations of (a) thermal expansion, (b) glacier melting, (c) Greenland and Antarctic surface mass balance, observed changes in terrestrial storage and the dynamic response of the ice sheets, (d) total sea level and (e) the model and observed trends in sea level. In each panel the observational time series is shown in black (dashed, and solid for the altimeter record). The total model uncertainty range is in light grey.

Process-based model parameters used in projecting global glacier mass changes (Section 13.5.2) are mainly derived from or calibrated against some measure of observed recent past glacier mass balance (Bahr et al., 2009; Marzeion et al., 2011; Meier et al., 2007; Radic and Hock, 2011; Raper and Braithwaite, 2005). Hence they cannot be independently evaluated against observations. The only exception for global glacier projections is the model of Zuo and Oerlemans (1997), used for projections by Gregory and Oerlemans (1998) van de Wal and Wild (2001) and Slangen et al. (2011); it employs glacier mass-balance sensitivities obtained from idealised perturbation studies of models for individual glaciers and applied to glaciers worldwide according to climatological conditions. The AR4 obtained a global glacier mass balance sensitivity to global-mean temperature change of 0.61 ± 0.12 mm yr^{-1} K^{-1} (standard error) from this model. This is probably an underestimate of the true value, partly because newer inventories have a larger global glacier area (Leclercq et al., 2011). Regression of the area-weighted global glacier mass balance time series for 1950–2010 (Cogley 2009a), subsequently extended, see Chapter 4) against HadCRUT3 global mean surface air temperature (Brohan et al., 2006) yields a greater sensitivity of 1.07 ± 0.26 mm yr^{-1} K^{-1} (standard error) and indicates that glaciers would be in steady state in a climate whose global SAT was 0.28 K cooler than the mean of 1865–1894 (cf. Section 10.6.3.1 of Meehl et al., 2007). Employing this sensitivity with global-mean temperature change from CMIP5 historical simulations gives glacier contributions to GMSL shown in Table 13.1 and Figure 13.4b. This method of simulation of global glacier mass balance is a semi-empirical model analogous to that of Rahmstorf (2007) (Section 13.6.1.2). Since the GCMs reproduce the observed temperatures, the glacier model, by construction reproduces the glacier observations for recent decades (Table 13.1, Figure 13.4b). Observed glacier mass loss began in the 19th century, before substantial anthropogenic influence on climate.

Projections of future changes in the SMB of the Antarctic and Greenland ice sheets are made using regional climate models and statistical downscaling models (Section 13.5.3). Table 13.2 compares results from simulations of recent past decades using various models of these kinds and from global reanalysis products for Antarctica.

The average and standard deviation of model-based accumulation (precipitation minus sublimation) estimates from the Greenland models in Table 13.2 is 589 ± 77 Gt yr^{-1}, which agrees with published observation-based accumulation maps, e.g., 513 ± 41 Gt yr^{-1} by Bales et al. (2009) and 591 ± 83 Gt yr^{-1} by Burgess et al. (2010). Drifting snow erosion is small over the Greenland ice sheet. For SMB (accumulation minus ablation), the models of Table 13.2 give 333 ± 96 Gt yr^{-1} for 1961–1990. All the models indicate that Greenland ice sheet SMB started decreasing in the early 1990s, on average by 3% per year. This results in a significant and increasing contribution to the rate of GMSL rise (Table 13.1, Figure 13.4c). The largest trends are found in models with coupled snow and atmosphere simulations (RACMO2 and MAR). As there

is no significant trend in accumulation in any of these models, this trend is caused almost entirely by increased melt and subsequent runoff (Figure 13.5). This tendency is related to pronounced regional warming, which might be partly associated with anomalous NAO variability in recent years, not necessarily attributable to anthropogenic climate change (Chapter 10). AOGCM historical simulations do not reproduce this effect, since they are not constrained to simulate actual decadal variability once they have been initialized (Chapter 11). Consequently the AOGCM-based method used for projection of Greenland SMB (Section 13.5.3.1 and Appendix 13.A) does not show as strong a tendency towards increasing contribution to GMSL (Table 13.1).

[INSERT FIGURE 13.5 HERE]

Figure 13.5: Annual-mean surface mass balance (accumulation minus ablation) for the Greenland Ice Sheet, simulated by regional climate models for the period 1960–2010.

Accumulation (precipitation minus sublimation) approximates SMB in Antarctica, since surface ablation is negligible in the present climate. There are model uncertainties in Antarctic accumulation because drifting snow processes, which remove an estimated 7% of the accumulated snow (Lenaerts et al., submitted), and snow hydrology are not accounted for by global models, and the ice sheet's steep coastal slopes are not well captured by coarse model grids. There are also uncertainties in observation-based estimates of Antarctic SMB, which rely on sparse accumulations measurements with very little coverage in high-accumulation areas. Observation-based SMB estimates of the Antarctic ice-sheet (e.g., 1768 ± 49 Gt yr^{-1} in Arthern et al., 2006) are generally lower than model-based SMB estimates (1923 ± 184 Gt yr^{-1} for the average of models in Table 13.2).

For the Antarctic ice-sheet, interannual variability in accumulation is dominated by changes in precipitation. However, global reanalysis data have been shown to contain spurious trends in the southern hemisphere, related to changes in the observing system, e.g., the introduction of new satellite observations (Bromwich et al., 2011; Bromwich et al., 2007). This problem also potentially affects RCMs that are forced at the boundaries of their limited-area domain by global reanalyses. In the models of which the temporal variability is deemed most reliable, no significant trend is present in accumulation over recent decades. This agrees with observation-based studies (Anschütz et al., 2009; Monaghan et al., 2006) and implies that Antarctic SMB change has not contributed significantly to changes in the rate of GMSL rise. However, AOGCM simulations show a tendency to increased accumulation in the recent past. Consequently the AOGCM-based method used for projection of Antarctic SMB (Appendix 13.A) indicates a small negative contribution to GMSL in recent decades (Table 13.2), which has not been observed (Chapter 4). If this means that AOGCMs are incorrect in projecting an increase in Antarctic temperature and precipitation (Section 13.5.3.2), it implies an underestimate in projections of GMSL rise (Section 13.6.1.3).

When calibrated appropriately, dynamical ice-sheet models (Section 13.2.3) can reproduce the rapid changes in ice-sheet outflow observed in recent decades (e.g., Graversen et al. (2011) for Greenland; Gladstone et al. (submitted), for Pine Island Glacier in Antarctica). However, the magnitude of the dynamic change is not well-constrained from observations. Comparison of the observed Greenland contribution to GMSL in 1993–2010 and 2005–2010 with the Greenland SMB contribution of the observed climate for the same periods (Table 13.1) suggests that the remainder, which is attributed to recent dynamical change, is about ~40% of the total. Rignot et al. (2011) evaluate trends in SMB and outflow since 1992, when the ice sheets are assumed to be near balance; their results indicate dynamics accounts for ~60% of the total. These results are both consistent with the AR4 assumption that dynamical change caused about half of the observed imbalance for Greenland. For Antarctica, if there is no significant SMB trend, the entire observed imbalance must be caused entirely by dynamical change, as assumed by the AR4.

The sum of the process-based model contributions and the estimates for ice-sheet dynamical change and anthropogenic change in terrestrial water storage (Section 13.4.4) is consistent with the observed rate of GMSL rise for 1971–2010 and 1993–2010. This satisfactory explanation of GMSL rise in terms of the models and methods used to project the contributions is a further scientific advance relative to the AR4. If the AOGCMs reproduced recent regional climate changes, as discussed above, the ice-sheet SMB contributions would be more positive resulting in better agreement. The trends in sea level are also shown in Figure 13.4e. The models all show a gradual increase in rate during the period, with a pronounced increase in

the trend following the eruption of Mt Pinatubo in 1991; both of these characteristics are also observed in the GMSL record estimated from tide gauges.

Table 13.2: Surface mass balance and rates of change for the ice sheets calculated from ice sheet surface mass balance models. The sea level equivalent is shown for the model averages. Negative SMB means positive sea level rise and vice-versa. Uncertainties are one standard deviation.

Reference and model[a]	SMB[b] Gt yr^{-1}	SMB trend 1991–2010 Gt yr^{-2}	SMB anomaly[c] 1971–2010 Gt yr^{-1}	SMB anomaly[c] 1993–2010 Gt yr^{-1}	SMB anomaly[c] 2005–2010 Gt yr^{-1}
Greenland	**1961–1990**				
RACMO2, Ettema et al. (2009), 11 km RCM	410 ± 110	–12.7 ± 3.5	–25 ± 118	–82 ± 110	–170 ± 86
MAR, Fettweis et al. (2011), 25 km RCM	423 ± 112	–16.9 ± 3.4	–42 ± 138	–130 ± 120	–231 ± 79
PMM5, Box et al. (2009), 25 km RCM	357 ± 65	–8.9 ± 3.1	–1 ± 70	–38 ± 80	–82 ± 76
ECMWFd, Hanna et al. (submitted), 5 km PDD	279 ± 99	–7.3 ± 3.7	–8 ± 102	–43 ± 97	–86 ± 68
SnowModel, Mernild and Liston (submitted), 5 km EBM	194 ± 77	–9.4 ± 2.6	–32 ± 90	–68 ± 88	–129 ± 85
Average	333 ± 96	–11.0 ± 3.8	–22 ± 17	–72 ± 37	–140 ± 62
Antarctica	**1979–2010**				
RACMO2, Lenaerts et al. (submitted) 27 km RCM	2060 ± 116				
JRA25, 125 km RA	2042 ± 128				
ERAi, 80 km RA	1610 ± 98				
MERRA, 55 km RA	1918 ± 134				
CFSR, 38 km RA	1985 ± 111				
Average	1923 ± 184				

Notes:
(a) The approximate spatial resolution is stated and the model type denoted by PDD = positive degree day, EBM = energy balance model, RCM = regional climate model, RA = global reanalysis model. The reanalyses are due to Bromwich et al. (2011).
(b) Different ranges of years are used for Greenland and Antarctica, as shown.
(c) Difference from the mean SMB of 1961–1990.

[START BOX 13.1 HERE]

Box 13.1: The Global Energy Budget

A fundamental aspect of the Earth's climate system is the global energy balance, which is dependent on many phenomena of the system. At the top of the atmosphere (TOA), the boundary of the climate system, the balance involves shortwave radiation received from the sun, shortwave radiation reflected and long-wave radiation emitted by the Earth (Chapter 1). There are also significant transfers of energy between components (atmosphere, Chapter 2; ocean, Chapter 3; cryosphere, Chapter 4) of the climate system (Trenberth et al., 2009) and from one location to another (particularly from the equatorial region towards the poles) by the atmosphere and the ocean. The ocean has stored over 90% of the increase in energy in the climate system over recent decades (Box 3.1), resulting in ocean thermal expansion and hence sea level rise (Chapter 9, Section 13.4). Thus the energy and sea level budgets are linked and must be consistent (Church et al., 2011b).

For understanding climate change, a critical question is how the Earth's energy budget is changing over years to decades and longer. Tracking this energy flow is a critical element in understanding climate variability and change (Trenberth 2009, 2010; Trenberth and Fasullo, 2010). Here we focus on the Earth's global energy budget since 1970, the period when near global observational data coverage is available. The rate of storage of energy in the Earth system must be equal to the net downward radiative flux at the TOA. In analysing climate change, we regard this flux as being the difference between radiative forcing, due to

changes imposed on the system, and the radiative response by the system, due to the climate change that results from the forcing.

The radiative forcing of the climate system (Chapter 8) has increased since 1970 as a result of a increase in solar irradiance (the cumulative energy input from solar forcing 1970–2010 is only about 40 x 10^{21} J), increases in well-mixed (long-lived) greenhouse gas concentrations (giving almost 1400 x 10^{21} J) and contributions from changes in short-lived greenhouse gases (tropospheric and stratospheric ozone and stratospheric water vapour; giving over 200 x 10^{21} J; Box 13.1, Figure 1a). The total cumulative energy input from these components from 1970 to 2010 amounts to about 1600 x 10^{21} J, and the energy flux is increasing with time. Volcanic eruptions inject aerosols into the stratosphere, reflecting some of the incoming solar radiation, and thus give a negative radiative forcing, which persists for a couple of years, and partly offsets the increased forcing from greenhouse gases. Since 1970, two major eruptions (El Chichón in Mexico in 1982 and Mt Pinatubo in the Philippines in 1991) and other smaller eruptions have offset almost 250 × 10^{21} J of the increased energy flow. Changes in the surface albedo from land use change have led to a greater reflection of short-wave radiation back to space, totalling about 100 x 10^{21} J. Tropospheric aerosols have a greater influence; they predominantly reflect sunlight and enhance brightness of clouds which reflects more sunlight, reinforcing their negative radiative forcing. However, black carbon, including that on snow and ice, are a positive radiative forcing. The estimates of the total aerosol forcing reported in Chapter 7 offset almost 800 × 10^{21} J of the greenhouse gas forcing, leaving an energy gain of about 520 × 10^{21} J over this period (Box 13.1, Figure 1a).

[INSERT BOX 13.1, FIGURE 1 HERE]

Box 13.1, Figure 1: The Earth's energy budget from 1970 through 2010. **(a)** The cumulative energy into the Earth system from changes in solar forcing, well-mixed and short-lived greenhouse gases, changes in surface albedo, volcanic forcing and tropospheric aerosol forcing are shown by the coloured lines and these are added to give the total energy changes (dashed black line). **(b)** The cumulative energy from (a), with an expanded scale, is balanced by the warming of the Earth system (energy absorbed in the melting of ice and warming the atmosphere, the land and the ocean) and an increase in outgoing radiation inferred from temperature change of a warming Earth. These terms are represented by the time-varying thicknesses of the coloured regions. The residuals in the cumulative energy (red lines) for a climate feedback parameter λ of 1.25 ± 0.5 W m^{-2} K^{-1} (equivalent to an equilibrium climate sensitivity of 3°C with a range from 2.1°C (λ of 1.75 W m^{-2} K^{-1}) to 4.9°C (λ of 0.75 W m^{-2} K^{-1}), are indicated by the solid and dashed red lines. The uncertainties quoted are one standard deviation.

As the climate system warms, energy is lost to space through increased outgoing radiation. This radiative response by the system is predominantly due to increased thermal grey-body radiation as a function of temperature, but is modified by climate feedbacks, such as changes in water vapour, surface albedo and cloud, which affect both outgoing long-wave and reflected shortwave radiation. The TOA fluxes have been measured by the Earth Radiation Budget Experiment (ERBE) satellites from 1985 to 1999 (Wong et al., 2006) and the Cloud and the Earth's Radiant Energy System (CERES) satellites from March 2000 to the present (Loeb et al., 2009). The TOA radiative flux measurements are highly precise, allowing identification of changes in the Earth's net energy budget from year to year within the ERBE and CERES missions (Kato 2009; Stackhouse 2010), but the calibration of the instruments is not sufficiently accurate to allow determination of the absolute TOA energy flux or to provide continuity across missions (Loeb et al., 2009). (Murphy et al., 2009) used the variability in the ERBE and CERES TOA radiation data (Chapter 2) to infer the additional net outgoing radiation $\lambda \Delta T$ from the warming Earth. Combining this with globally averaged surface temperature data, they obtain the climate feedback parameter λ, which is related to the equilibrium climate sensitivity (see Box 12.1). For a mid range value of λ of 1.25 ± 0.5 W m^{-2} K^{-1} (equivalent to an equilibrium climate sensitivity of 3°C, with a range from 2.1°C (λ of 1.75 W m^{-2} K^{-1}) to 4.9°C (λ of 0.75 W m^{-2} K^{-1})), the estimated additional net outgoing radiation results in a loss of energy of about 400 × 10^{21} J (Box 13.1, Figure 1b). The uncertainties quoted are one standard deviation.

The ocean's large capacity to store heat means that temperatures increase slowly. If the radiative forcing were fixed, the climate system would eventually warm sufficiently that the radiative response would balance the radiative forcing, and there would be zero net heat flux into the system. However, the forcing is increasing, and so the climate system is not in radiative equilibrium (Hansen et al., 2005), and has stored about 225 x 10^{21} J since 1970 [Box 3.1]. This storage provides strong evidence of a changing climate. The majority of this additional heat is in the upper 750 m of the ocean but there is also warming in the deep and abyssal ocean. The associated thermal expansion of the ocean has contributed about 40% of the observed sea

level rise since 1970 (Section 13.4.2.2.6; (Church et al., 2011b). The ocean is continuing to warm and will continue to do so for centuries even if greenhouse gas emissions cease (Solomon et al., 2009). A small amount of additional heat has been used to warm the continents, warm and melt glacial and sea ice, and warm the atmosphere (See Box 3.1 and Box 13.1, Figure 1b).

The residual in the energy budget in 2010 (Box 13.1, Figure 1b, red line) is less than 85×10^{21} J (about 16% of the total positive energy flux of 520×10^{21} J) for the central value of climate sensitivity of 3°C. A positive residual means that the cumulative forcing is apparently greater than the heat lost and stored by the system. For a λ of 1.75 W m^{-2} K^{-1} (climate sensitivity of 2.1°C) the residual would be more negative whereas for a λ of 0.75 W m^{-2} K^{-1} (climate sensitivity of 4.9°C), the residual would be positive. The residual increases in magnitude to almost -150×10^{21} J in the mid 1990s. For the central value of λ, the negative tendency of the residual up to the mid 1990s in Figure 1b (red solid line) and the subsequent positive tendency are equivalent to global energy fluxes of about –0.4 W m^{-2} and 0.3 W m^{-2} respectively. A possible explanation could be that the aerosol forcing is overestimated through the 1980s and early 1990s but is underestimated for the last 15 years. Church et al. (2011b) suggest such a change could relate to the almost doubling of fossil fuel use in developing nations (Le Quere et al., 2009) and the associated increase in sulphur emission in south and east Asia from 2000 (Lu 2010; Streets et al., 2009). Hofmann et al. (2009) and Vernier et al. (2011) observe that aerosols are increasingly carried into the upper troposphere/lower stratosphere by deep convection. Nevertheless, with any of these choices, the residual is smaller than the uncertainties and confirms our understanding of climate change and provides evidence that no major forcings of climate are omitted in current climate assessments (Footnote 13.1).

In addition to these forced variations in Earth's energy budget, there is also internal variability on decadal time scales. Observations and models indicate that a decade of steady or even decreasing surface temperature can occur in a warming world (Easterling; Wehner 2009). GCM simulation indicate these periods are associated with a transfer of heat from the upper to the deeper ocean, of order 0.1 W m^{-2} (Katsman; van Oldenborgh 2011; Meehl et al., 2011), with a near steady (Meehl et al., 2011) or an increased radiation to space (Katsman; van Oldenborgh 2011), again of order 0.1 W m^{-2}. While these natural fluctuations represent a large amount of heat, they are significantly smaller than the forced variations in the Earth's energy budget.

These independent estimates of radiative forcing, observed heat storage and surface warming combine to give an energy budget for the Earth that is very likely closed, and is consistent with our best estimate of climate sensitivity. Changes in the Earth's energy storage are thus a powerful observation for the detection and attribution of climate change (Gleckler et al., submitted; Huber; Knutti submitted) as well as a constraint on climate sensitivity (see Chapter 9, Box 12.1) and future warming.

[INSERT FOOTNOTE 13.1 HERE]

Footnote 13.1: The geothermal heat flux is small (less than 2×10^{21} J; (Pollack et al., 1993) and changes little over the time period considered. Although increasing rapidly, the energy released by the burning of fossil fuels is also small, less than 1×10^{21} J (US Energy Information Administration, http://www.eia.gov/pub/international/iealf/Table1.xls).

[END BOX 13.1 HERE]

13.5 Projected Contributions to GMSL

13.5.1 Ocean Heat Uptake and Thermosteric Sea Level Rise

Over 90% of the net energy increase of the climate system on multiannual timescales is stored in the ocean (Box 3.1). In projections of the early decades of the 21st century, the upper ocean dominates the heat uptake, and heat content rises roughly linearly with global mean surface air temperature (SAT) (Körper et al., submitted; Pardaens et al., 2011c). On multidecadal timescales under scenarios of steadily increasing radiative forcing, the global mean rate of ocean heat uptake is approximately proportional to the global mean SAT change from equilibrium (Gregory, 2000; Gregory and Forster, 2008; Rahmstorf, 2007a), with the constant of proportionality (in W m^{-2} K^{-1}) being the ocean heat uptake efficiency κ. Thus the rate of thermosteric sea level rise is projected to increase during the 21st century, and it will increase more rapidly under scenarios of greater warming (Meehl et al., 2007). The rate of thermal expansion can be scaled with

reasonable accuracy to radiative forcing or SAT change in order to make an estimate for one scenario based on model results for another scenario at a particular time in the future, provided that the scenarios have a sufficiently similar time profile (Gregory and Forster, 2008; Katsman et al., 2008; Meehl et al., 2007).

Because the ocean integrates the surface heat flux, annual time series of thermosteric sea level rise show less interannual variability than time series of global SAT, and thermal expansion projections following different scenarios do not significantly diverge for several decades. Scenarios assuming strong mitigation of greenhouse gas emissions begin to show a reduced rate of thermal expansion beyond about 2040, and the amount by 2100 is about one-third less than in a typical non-mitigation scenario (Körper et al., submitted; Pardaens et al., 2011c; Washington et al., 2009).

The ocean heat uptake efficiency quantifies the effect of ocean heat uptake on moderating time-dependent climate change (Raper et al., 2002). In the model average of CMIP3 AOGCMs, κ is about half the magnitude of the climate feedback parameter α. Accordingly, the transient climate response ($=F_{2\times}/(\alpha+\kappa)$, (where $F_{2\times}$ is the radiative forcing due to doubling CO_2) for the model average is about two-thirds of the equilibrium climate sensitivity ($=F_{2\times}/\alpha$) (Dufresne; Bony 2008; Gregory; Forster 2008). For a given forcing scenario, a larger proportion of the uncertainty in projected ocean heat uptake comes from the uncertainty in the climate feedback parameter than from the uncertainty in the ocean heat uptake efficiency (Knutti and Tomassini, 2008; Raper et al., 2002).

In the ocean interior, heat is transported by large-scale motion, eddies and turbulent mixing, the last of which is parametrised as thermal diffusion. Observed thermal expansion in the upper 700 m is well matched by an upwelling-diffusion model with observationally determined parameters by Marčelja (2010) with differences from Domingues et al. (2008) being typically less than 4 mm; using AR4 global SAT projections, this model gives thermal expansion projections in the lower half of the AR4 SRES ranges. Observed ocean heat uptake has been used in conjunction with observed global SAT change to constrain the ocean thermal diffusivity and hence projections of thermal expansion in EMICs (Knutti; Tomassini 2008; Sokolov et al., 2010). For scenario A1B, Sokolov et al. (2010) obtained a range of thermal expansion projections which was lower than the AR4 range when using the observational dataset of Levitus et al. (2005) as a constraint, and greater than AR4 when using Domingues et al. (2008). From these studies with simpler models, it appears that observations of heat uptake could have the potential to constrain significantly the representation of relevant ocean heat transport processes in AOGCMs.

Ocean heat uptake and thermal expansion take place not only while atmospheric GHG concentrations are rising, but continue for many centuries after stabilization of radiative forcing, at a rate which declines only slowly (Figure 13.5) (Meehl et al., 2005; Meehl et al., 2007; Solomon et al., 2009). This is because the timescale for warming the deep ocean is much longer than for the shallow ocean (Gregory, 2000; Held et al., 2010). While the approximation that the rate of thermosteric sea level rise increases with the temperature elevation above preindustrial is valid for initial periods of increasing temperature, the rate is reduced when temperature stabilization begins (Schewe et al., 2011). The rate and the stabilization timescale for thermal expansion depend on the GHG stabilization level. For the highest scenarios RCP8.5 thermosteric sea level rise can reach up to 2m in the year 2500. Nonlinear changes in ocean circulation, particularly due to a reduction in deep water formation, can also have a large effect on global ocean heat uptake (Fluckiger et al., 2006; Levermann et al., 2005; Vellinga; Wood 2008). Since the thermal expansivity of sea water is greater at higher temperature and higher pressure, the amount of thermal expansion for a given heat uptake depends on the distribution of warming in the ocean (Körper et al., submitted; Russell et al., 2000).

[INSERT FIGURE 13.6 HERE]

Figure 13.6: [PLACEHOLDER FOR SECOND ORDER DRAFT: CMIP5 results for the period beyond 2100 will be added.] Observed [tbc] and modelled thermosteric sea level rise for 1950 to 2100 [tbc] [Approximately scaled results for ocean heat content on right hand axis. Upper 700 m or full depth or both and for all RCPs to be decided.]

13.5.2 Glaciers

The 21st-century sea level contribution from glaciers presented in the AR4 assessment (Meehl et al., 2007) ranged from 0.06 to 0.15 m SLE across the range of scenarios, while four subsequently published estimates include 0.08 to 0.37 m SLE (Meier et al., 2007), 0.17 to 0.55 m SLE (Pfeffer et al., 2008), 0.15 to 0.39 m

SLE (Bahr et al., 2009), and 0.09 to 0.16 m SLE (Radic; Hock 2010). Each of the post-AR4 projections involves different limiting assumptions, and each employs significantly different approaches. All are influenced by the improving but still incomplete global glacier inventory, the practical difficulties of modelling large numbers (>200,000) of glaciers (see Section 13.4.2), accounting for the dynamic response of an unknown fraction of marine-terminating glaciers, and accurately accounting for land hydrology interception of runoff from non-marine inland glaciers. The variety of approaches used in the projections referenced above was motivated partly by the difficulties imposed by these obstacles.

The absence of a complete global inventory of glaciers may be one of the greatest sources of uncertainty both for present-day mass balance evaluation (Chapter 4, Section 4.3.2), and for projections, since the inventory is required for initial conditions in numerical models, for future placement of glaciers in latitude, longitude, and altitude during model evolution (where they sample future climatically-determined mass balance environments), and for categorization of glaciers by size class in scaling computations. The global inventory is evolving rapidly, as are power-law scaling estimates of the aggregate volume of glaciers based on measured areas (see Chapter 4). Since the AR4 projections, Cogley (2009b) and Radic and Hock (2010) extended the global inventory to ca. 48% of estimated global glacier covered area, and produced new estimates of global glacier area and volume (Table 13.3), including improved estimates of areas and volumes of glaciers surrounding the Greenland and Antarctic ice sheets. This volume of 0.6 ± 0.7 m compares to the smaller estimates used in the AR4 of 0.15, 0.24 and 0.37 m SLE, not including the glaciers around the ice sheets. Further improvements of the inventory are anticipated in early 2012.

Meier et al. (2007), Pfeffer et al. (2008), and Bahr et al. (2009) made analyses that attempted to circumvent missing data and modelling capabilities to constrain projections of future sea level rise. Meier et al. (2007) compiled present-day observed loss rates for glaciers, most of which were available only to 2005, and extrapolated individual records forward one year to create a common start date of 2006 for a combined extrapolation of observations from the Greenland and Antarctic ice sheets. The observations were then extrapolated forward to 2100 under two scenarios: fixed future rates (GT yr^{-1}) and fixed future trends (GT yr^{-2}). The two projections led to total sea level contributions of 0.10 ± 0.02 m SLE for fixed future rate and 0.24 ± 0.13 m SLE for fixed future trend. By simply extrapolating observed rates forward, all the problems associated with the incomplete glacier inventory, treatment of mass balance, adjustment of glacier size and area, etc. are eliminated, but realistic dynamic response and the control of future behaviour through GCM input to a mass balance model is sacrificed. The fixed future trend projection depends critically on the time period of observations for which the initial rate and trend is defined, and both projections depend on the assumption that the processes that controlled the rates during the observation period continue to do so during the period of extrapolation (essentially an assumption of statistical stationarity). Whether this is true for glaciers or ice sheets on century time scales is unknown, but several studies indicate that time scales for dynamics of individual glacier systems is highly variable, ranging from decades to centuries (Calkin et al., 2001; Joughin et al., 2008).

Pfeffer et al. (2008) made a series of calculations designed initially to establish limits on maximum sea level rise from all land-ice sources, with the primary focus on testing hypothesized extreme sea level projections from the ice sheets. Like Meier et al. (2007), the Pfeffer et al. model did not depend on detailed knowledge of the distribution of glaciers, mass balance models, or future climate. Rather, global average surface mass balance and calving discharge rates required to meet certain sea level targets were calculated, and the plausibility of the demands required to meet those assumptions was examined. For global glaciers, a low-range, but not minimum, sea level contribution of 0.17 m SLE by 2100 was calculated by scaling the increase in surface mass balance to the increase in calving loss according to the ratio defined for the Greenland ice sheet following a doubling of Greenland outlet glacier speed (the scaling was taken from Greenland since data on marine-terminating glaciers are lacking); another low-range estimate of 0.24 m SLE by 2100 was calculated using the Meier et al., constant-rate extrapolation for comparison. A maximum sea level contribution from glaciers was estimated, again by scaling the surface mass balance-to-calving ratio from Greenland, where outlet glacier speeds were increased to the highest rates deemed reasonable; the maximum sea level contribution for glaciers was 0.55 m SLE. However, the calving contribution of the 0.55 m estimate, 0.47 m SLE, may be greater than the total glacier ice accessible through marine-terminating outlets, so this may be an overestimate. Without a global accounting of the fraction of glacier area drained through marine-terminating outlets, this question is difficult to resolve definitively. Because of the extremely approximate nature of the calculations, uncertainties in the Pfeffer et al. projections were not assigned.

Bahr et al. (2009) used volume-area scaling to calculate the global mass loss required to restore glacier accumulation area ratios (AAR) to an equilibrium value $AAR_0 = 0.57$ from their 1997–2006 global average value of 0.44, assuming either that future AARs do not move any further out of equilibrium than at present (i.e., no further decline in AAR) or that AARs continue to move away from equilibrium (i.e., continue to decline) at the present-day rate. Their result ranges from 0.18 ± 0.03 (assuming no further decline in AARs) to 0.37 ± 0.02 m SLE (assuming AARs continue to decline for the next 40 years at rates observed for the past 40 years). These projections refer to an eventual steady state and are not specific projections for 2100; no time scale for re-equilibration to $AAR_0 = 0.57$ is given. Bahr et al.'s method depends on the assumption that such an intrinsic equilibrium value, or AAR_0, exists, although no theoretical underpinning for the relationship has been discovered. However, long-term observations of AARs are strikingly consistent. For 86 glaciers compiled by Dyurgerov (2010), $AAR_0 = 0.57 \pm 0.01$; for approximately 30,000 Eurasian and European glaciers compiled by Bahr (1997), $AAR_0 = 0.58 \pm 0.11$. If the value $AAR_0 \sim 0.57$ holds for equilibrium conditions in general, then the Bahr et al. calculation is a robust lower bound on sea level rise. Also, Bahr et al.'s projection neglected the potential role of marine-terminating dynamics, and is thus a lower bound for this reason as well.

Of the four projections published since 2007, Radic and Hock (2011) is the closest in method to the projections detailed in AR4 and the study that draws most directly on GCM-derived climate forcing (although only a single SRES scenario, A1B, was used). Like a number of other previous model projections, Radic and Hock simulated future mass balance using GCM output to obtain future temperature and precipitation, and a mass-balance model to calculate accumulation and ablation from climate variables determined at future times and positions on the Earth's surface. While early models were unable to account for details such as the effect of declining glacier area (e.g., Gregory and Oerlemans, 1998), later analyses (e.g., van de Wal and Wild, 2001) used power-law scaling (Bahr et al., 1997) to do so. Raper and Braithwaite (2006) introduced methods to allow the hypsometry (area-elevation distribution) of modelled glaciers to adapt to changes in elevation as well as total area, thus permitting, for example, the retreat of glaciers to higher, stable altitudes in warming conditions. Radic and Hock's (2011) analysis was distinctive from these previous models in several regards. Rather than apply a tuned mass balance model directly to aggregate glacier areas *en masse*, Radic and Hock (2011) calculated mass balance parameters as functions of position and elevation and applied the model to a calibration suite of 36 glaciers, from which mass balance sensitivity parameters were calculated and applied individually to each of 122,867 glaciers and ice caps in the WGI-XF inventory (Cogley, 2009a). The result was then upscaled to the remaining uninventoried global glaciers, approximately 266 x 10^3 km^2 in aggregate area, which includes the peripheral glaciers surrounding the ice sheets (totalling 77,386 ± 29,866 km^2, or ca. 32% of the global total (Radic and Hock, 2010)). These latter glaciers had been left out of the calculations of Raper and Braithwaite (2006). For the A1B scenario, Radic and Hock's calculation projects a sea level contribution from glaciers of 0.124 ± 0.037 m by 2100. The AR4 projections did not include a contribution from peripheral glaciers surrounding the ice sheets, but simply added 20% to the calculated projections from other glaciers on the basis of the estimated contemporary fractional peripheral glacier contribution to give a total of 0.07 to 0.17 m in 2095. Radic and Hock approximated glacier area-elevation distributions and their adjustment over time following the principals detailed in Raper and Braithwaite (2006). The implications of the handling of the time response of glaciers and evolution of area and hypsometry have not been fully explored. Another significant limitation of the Radic and Hock analysis (as well as with its predecessors) is its exclusion of the effects of dynamics associated with marine-terminating glaciers. Since all changes in models of this type are driven by climate parameters translated into surface mass balance variables, the role of calving instability and rapid discharge of ice into the ocean cannot enter into any of these projections.

The sea level rise projections made after AR4 are summarized in Table 13.3 below. The values given for the glacier contribution, in sea level equivalent by 2100, range from 0.035 to 0.37 m. Since the seven studies listed employed very different methodologies, the meaning of an average and standard deviation is unclear and is not calculated. Several points regarding the comparison of these recent projections to each other and to those presented at the time of the AR4 should be emphasized. Peripheral glaciers surrounding the Greenland and Antarctic ice sheets can be modelled more realistically following the publication of Radic and Hock's (2010) re-evaluation of global glacier volume and area distributions, so the total volume of global glaciers is effectively larger than at the time of AR4, and improvements over the factor of 1.2 used in AR4 to account for the peripheral glaciers may be expected. Of the seven newer studies, Radic and Hock (2011),

Slangen et al. (2011), Marzeion et al. (2011) and Bahr et al. (2009) used inventory data and excluded consideration of calving losses, while Meier et al. (2007) and Pfeffer et al. (2008) integrated aggregate rates, including calving. Meier et al. (2007) and Pfeffer et al. (2008) are essentially rate-extrapolation methods, although the strategy behind the extrapolation is very different in the two studies. To the extent that calving is a part of the observations that initiate the extrapolations, Meier et al. (2007) and Pfeffer et al. (2008) considered dynamics, and Pfeffer et al. (2008) considered calving explicitly, albeit very simply, by making separate calculations for dynamic losses and surface mass balance losses. Pfeffer et al. (2008) made and additional projection ("High 1") of 0.55 m, not tabulated here, which is most likely an overestimate. It was designed specifically to exclude unrealistically high estimates at a high level of confidence, and is a robust tool for excluding larger unrealistic values, but not for excluding smaller unrealistic values, and as such is not in itself a good projection estimate.

Of the six newer studies, Radic and Hock (2011), Slangen et al. (2011), and AR5 Method (described in Section 13.6.1.1) are most similar to the models used for projections in AR4. All three methods take advantage of a significantly improved glacier inventory (Cogley, 2009a) and Radic and Hock (2011) used a new method for applying a calibrated mass balance model to each glacier in the WGI-XF inventory individually. Nevertheless, some important uncertainties remain. The use of a triangular area-elevation distribution imposes restrictions on the Accumulation Area Ratio (AAR) that may artificially influence a glacier's mass balance; power-law scaling is implemented in a way that requires that the value of a poorly constrained multiplier relating area to volume be defined. Compromises like these are commonplace in numerical models, but have potentially substantial effects on model outcomes. A systematic investigation of the effect of such method details in all projection models could provide an informative view of overall model uncertainty.

Bahr et al. (2009) computed the committed glacier contribution to sea level rise at the current temperature level to be 0.184 ± 0.033 m. Under a continuous global temperature increase, the contribution becomes more uncertain mainly due to the incomplete inventory and approximations in hypsometric adjustment as well as the uncertainty in climate forcing. At some point in the future, the declining size of the glacier reservoir will start to influence the loss rate, although what this effect will be and how long it will take to manifest itself is not clear. If the collective response time of glaciers is fast compared to the time scale of their disappearance, then the area distribution will adjust with the shrinking volume, and loss rates may decline as the area exposed to surface mass balance declines. Alternatively, if the collective response time is slow compared to the time scale of their disappearance, then the area distribution will not have time to adjust, and the glaciers will largely thin in place with little effect on area. In that case there is less likely to be any area-reduction effect on loss rates. A GCM-forced mass balance model (Marzeion et al., 2011) was computed beyond the 21st century and results in sea level contributions of up to 0.4 m for high-emission scenarios and 0.29 m for low-emission scenarios. An upper limit of the glacier contribution is the total amount of ice currently stored in glaciers which amounts to 0.60 ± 0.07 m SLE (including peripheral glaciers) (Radic and Hock, 2010).

[INSERT FIGURE 13.7 HERE]

Figure 13.7: Projected sea level rise from glaciers according to model calculations from seven recent analyses, with AR4 glacier projections for comparison. Mean projections only are shown in each case. Calving losses are considered in the Pfeffer (2008) and Meier (2007) projections, but excluded in the Radic and Hock (2011), Bahr et al. (2009), Slangen et al. (2011), Marzeion et al. (2011), and AR5 method projections. Radic and Hock, Slangen, and AR5 projections are GCM-driven models using the SRES A1B scenario; the Marzeion projection uses the CMIP RCP4.5. PGIC in Marzeion curves refers to peripheral glaciers and ice caps surrounding the Greenland and Antarctic Ice Sheets. Curves for Radic and Hock and for Marzeion are a mean of ten different GCM model inputs.

Other uncertainties exist which are harder to evaluate. These include the potential for near-term rapid dynamic response from marine-terminating glaciers. Rapid dynamic response from glaciers does not have the potential long-term effect that ice sheet dynamics has because glaciers do not have significant marine-grounded ice volumes, but the potential for significant short-term contributions is large. Between 1996 and 2007, Columbia Glacier, on Alaska's south coast, lost mass at an average rate of 7.65 GT yr^{-1}, or 0.0211 mm yr^{-1} SLE, approximately 0.7% of the rate of global sea level rise during this period (Rasmussen et al., 2011). Columbia Glacier, with a total volume of approximately 150 km^3, cannot contribute to sea level at such a rate for very long, but marine-terminating glaciers of this size can be significant factors on decadal scales.

Another source of uncertainty, largely unexamined at this time, is land hydrology interception of glacier runoff. Glacier mass loss rates are generally assumed to be sea level gains, with no delay or interception by surface or aquifer storage. Glacier complexes located near coasts but not exclusively discharging directly into the ocean (e.g., Patagonia, Alaska's Chugach and St. Elias Ranges) can probably be assumed to unaffected by land hydrology interception, or if runoff is intercepted, the storage capacity of narrow coastal zones will be limited and the long-term effect on interception will probably be negligible. For interior regions like High Mountain Asia, however, interception by land hydrology may be significant but is presently poorly understood and very difficult to constrain by observations. Studies of groundwater changes in regions downstream of the Himalayas generally show overall depletion, not storage (Rodell et al., 2009), but the fate of glacier runoff from High Mountain Asia remains an important but unsolved problem.

Table 13.3: Glacier Projections

Reference	Projected SLR at 2100 (m)	Notes
Radic and Hock (2011)	0.09–0.16	A1B scenario Average of 10 GCMs Calving excluded
Meier et al. (2007)		
Fixed rate	0.08–0.12	Extrapolation Calving included
Fixed trend	0.11–0.37	
Pfeffer et al. (2008)		
Low projection 1	0.17	Limit seeking analysis Calving included
Low projection 2	0.24	
Bahr et al. (2009)		
Present AAR	0.12	Exponential approach to long-term steady-state Calving excluded
Continued AAR decline	0.24	
Slangen et al. (2011)	0.16	A1B scenario Calving excluded
Marzeion et al. (2011)		
Excluding glaciers peripheral to ice sheets	0.035–0.063	A1B Scenario Average of 10 GCMs Calving excluded
Excluding glaciers peripheral to ice sheets	0.046–0.082	
AR5 Method		
Low	0.12	A1B scenario
Medium	0.15	
High	0.18	
Full Range of projections	**0.035–0.37**	

13.5.3 Ice-Sheet Surface Mass Balance Change

Uncertainty in projections of the contribution from Greenland and Antarctic surface mass balance (SMB) to sea level change arises from uncertainties in the magnitude of global climate change, the relation of the ice-sheet regional climate change to global climate change, and the response of the SMB to regional climate change. The effect on SMB from changing topography is small during the 21st century. For instance, in an experiment with CO_2 initially increasing at 1% per year and then stabilising after 140 years at $4 \times CO_2$, Vizcaíno et al. (2010) found that SMB changes were not discernibly affected by the changing geometry of the ice sheets until about year 150 in Antarctic and about year 250 in Greenland, consistent with earlier results (Huybrechts and De Wolde, 1999). Models show an increasingly negative SMB for Greenland under global warming (Huybrechts et al., 2011b; Vizcaino et al., 2010) during the 21st century and beyond. By contrast, Antarctic SMB is projected to be positive under global warming during the 21st century, since low surface temperatures inhibit large-scale surface melt while precipitation increases with warming air temperatures and associated moisture content (Uotila et al., 2007). Beyond 2100, coupled climate models of

intermediate complexity project a positive SMB for low-emission scenarios and a negative SMB for high-emission scenarios (Section 13.6.2), due to the competition of surface melt and enhanced snow fall. [PLACEHOLDER SECOND ORDER DRAFT: ice2sea experiments to be included.]

13.5.3.1 Greenland

Like the AR4, all recent studies have indicated a positive sea level contribution from Greenland SMB because the increase in ablation (mostly runoff) outweighs that in accumulation (mostly snowfall). Several recent studies can be readily compared with one another and the AR4 because they are all based on CMIP3 AOGCM results with scenario SRES A1B (see Table 13.4). Most of these studies carried out time-dependent simulations, thus removing the need to scale the results, as was necessary with the time-slice simulations available at the time of the AR4.

Yoshimori and Abe-Ouchi (in press) used CMIP3 AOGCM results with a temperature-index method at high resolution. They found that the inter-model spread in global surface air temperature change accounts for about 60% of the spread in the change of projected Greenland ablation. Two important contributions to the remaining spread are the surface air temperature in the model control climate, which affects the magnitude of warming because surface air temperature over ice cannot rise far above the freezing point, and the weakening of the AMOC, which affects the magnitude of warming over Greenland. As in the AR4, the projected sea level contributions by 2100 for scenario A2 were similar to those for scenario A1B.

Using CMIP3 AOGCM climate change simulations, Fettweis et al. (2008) applied a regression relationship, derived from RCM simulations of the recent past between annual anomalies in climate and in Greenland SMB simulated with an EBM, to obtain projections; these have a similar mean and narrower range than the AR4 projections. Their regression method depends on the assumption that a relationship derived from past variability will also hold for future forced climate change. Franco et al, (2011) found similar results when using the same method and a subset of CMIP3 models assessed to have the most realistic simulation of present-day Greenland climate. With this method, Fettweis et al. (2011) projected sea level rise during the 21st century of about 0.07 and 0.14 m for RCP 4.5 and 8.5, respectively, using results from the CanESM2 model.

Several studies indicate that the uncertainty in the SMB modelling is comparable to the uncertainty from global climate change projections. Comparing results from time-slice integrations at a range of resolutions with the ECHAM5 global atmosphere model, Bengtsson et al. (submitted) found that precipitation and ablation are both larger when simulated at lower horizontal resolution. They suggest that these effects are consequences of topography being generally lower when represented at lower horizontal resolution. This allows precipitation to spread further inland because it reduces topographic barriers, and enhances ablation because there is more area at lower, warmer, altitudes. Graversen et al. (2011) found that climate change modelling alone gave a range similar to the AR4 for the Greenland SMB contribution to sea level under SRES A1B, but they obtained a wider range of results when also allowing for uncertainties associated with the PDD method and ice-sheet dynamics (see Section 13.5.4). Greve et al. (2011) applied the same CMIP3 ensemble-mean AOGCM climate from SRES A1B experiments to two thermomechanical ice-sheet models (SICOPOLIS and IcIES). Because AOGCM climate deviates from observed, imposing it at 2004 produces a sudden large change in SMB, which is markedly different for the two ice-sheet models, owing to different choices of PDD factors, and this results in different changes in ice-sheet mass during the 21st century.

Using AOGCM results with CO_2 initially increasing at 1% per year and then stabilising after 140 years at 4 × CO_2, Bougamont et al. (2007) found that a PDD method gave larger ablation and smaller refreezing than an EBM, resulting in almost twice as large an increase in Greenland runoff. A comparison of three different regional climate models forced by the same AOGCM results for SRES A1B (Rae et al., submitted) showed that the simulated SMB was particularly sensitive to the snow-albedo parameterisations of melting and on the allowance for refreezing of runoff. Using an EBM in a regional climate model with boundary conditions from an AOGCM, Mernild et al. (2010) projected a larger Greenland SMB sea level contribution for SRES A1B than the corresponding PDD-based AR4 projection, possibly because refreezing was smaller than estimated by the AR4 method. These three studies all point to the particular importance of refreezing in making projections of Greenland SMB change.

Table 13.4: Contribution to sea level rise from change in the surface mass balance of the Greenland ice sheet during the 21st century under scenario SRES A1B. Where given, ranges are 5–95% estimated from the published results and indicate the uncertainty due to the climate change modelling, except where noted otherwise.

Reference	Model[a]	Contribution to Global Mean Sea Level Rise			
		starting from	up to	amount (m)[b]	rate (mm yr^{-1})[b]
AR4 (Meehl et al., 2007)	20 km PDD	1990	2090–2099	0.01–0.08	0.3–1.9
Bengtsson et al. (submitted)[c]	60 km (T213) EBM	1959–1989	2069-2099	—	1.4
Fettweis et al. (2008)	TI from 25 km EBM	1970–1999	2090–2099	0.03–0.05	0.3–1.0
Graversen et al. (2011)	10 km PDD	2000	2100	0.02–0.08 0.00–0.17[d]	0.0–2.1[d]
Greve et al. (2011)[e]	10 km PDD	2004–2013	2090-2099	—	–0.5, 0.3
Mernild et al. (2010)	25 km EBM	1990–1999	2070–2080	0.12	1.9
Rae et al. (submitted)[f]	25 km EBM	1980–1999	2090-2099	0.01, 0.04, 0.06	0.3,1.2,1.5
Yoshimori and Abe-Ouchi (in press)	1–2 km TI	1980–1999	2100	0.02–0.13	0.2–2.0

Notes:
(a) The spatial resolution is stated and the SMB method denoted by TI = temperature index, PDD = positive degree day, EBM = energy balance model.
(b) The amount of sea level rise is the time-integral of the SMB contribution from the period or date labelled "starting from" to the one labelled "up to". The rate of sea level rise applies to the latter period or date alone.
(c) This experiment used time-slices, with boundary conditions from an AOGCM, rather than a simulation of the complete century, so results are not available for the amount. The rate shown is the difference in SMB contribution between the "starting from" and "up to" periods.
(d) Range including uncertainty in SMB modelling, ice-sheet dynamical modelling and choice of emission scenario (B1, A1B or A2) as well as uncertainty in climate modelling.
(e) Results are given for two ice-sheet models (SICOPOLIS and IcIES) using the same AOGCM climate boundary conditions. The rate given is the increase between the "starting from" period and the "up to" period.
(f) Results are given for three RCMs driven with boundary conditions from the same AOGCM.

Beyond 2100, coupled climate ice-sheet models project an increasingly negative surface mass balance (SMB) for the Greenland ice sheet for all warming scenarios (Driesschaert et al., 2007; Mikolajewicz et al., 2007a, 2007b; Ridley et al., 2005; Swingedouw et al., 2008; Vizcaino et al., 2010; Vizcaino et al., 2008; Winguth et al., 2005). A nonlinear increase in ice loss from Greenland with increasing regional radiative forcing is found across different scenarios (Driesschaert et al., 2007). The nonlinearity arises from the increase in both the length of the ablation season and the daily amount of melting.

Surface mass balance on Greenland is controlled by regional climate which is influenced by interactions with sea-ice distribution and atmospheric and oceanic circulation. On multi-centennial time scales, Swingedouw et al. (2008) found enhanced ice loss from Greenland in a coupled simulation in which ice topography and melt water flux influence the ocean and atmospheric circulation as well as sea ice distribution. They also found that interactive changes of the Antarctic ice sheet results in reduced ice loss from Antarctica. Vizcaino et al. (2010) found the opposite effect, mainly due to the effect of topographic changes on the surface temperature, but less pronounced in amplitude.

Due to reduced regional temperature on Greenland, Mikolajewicz et al. (2007a) and Vizcaino et al. (2008) found strongly reduced ice loss from Greenland in scenarios with a cessation of the Atlantic thermohaline circulation (THC). Apart from these situations, the SMB becomes increasingly negative with increasing global mean temperature. Some models find a threshold temperature increase beyond which the Greenland Ice Sheet reduces to less than 30% of its present volume as detailed in Section 13.5.3.2.

13.5.3.2 Possible Irreversibility of Greenland Ice Loss and Associated Temperature Threshold

Model results suggest that, like other climatic subsystems (see Section 12.6.4.4), the Greenland Ice Sheet exhibits a strongly nonlinear and potentially irreversible response to external forcing. There is a critical threshold in surface warming when the total surface mass balance over Greenland becomes negative. If warming less than this threshold of sustainability is maintained for several millennia, the ice sheet will lose mass but will reach a steady state in which most of Greenland is still covered with ice (Driesschaert et al., 2007; Greve, 2000; Ridley et al., 2010a). If a greater warming is maintained indefinitely, the majority of the Greenland Ice Sheet will be lost via changes in SMB over many centuries or millennia. This nonlinear behaviour is caused by a combination of the surface-elevation feedback (because lower elevations experience more melt) and the surface-albedo feedback (because darker surfaces such as debris-covered ice experience more melt), both of which tend to speed deglaciation. Gregory and Huybrechts (2006) estimated the threshold global mean temperature to be between 3.1 ± 0.8°C above pre-industrial by application of the sufficient condition of negative surface mass balance.

The loss of the ice sheet is not inevitable because it has a long timescale. If the CO_2 concentration declines before the ice sheet is eliminated, the ice sheet might regrow. In the light of future GHG emissions, the time scale of ice loss is competing with the time scale of temperature decline after a reduction of GHG emissions (Allen et al., 2009; Solomon et al., 2009; Zickfeld et al., 2009). The outcome therefore depends on both the CO_2 concentration and on how long it is sustained. Charbit et al. (2008) found that loss of the ice sheet is inevitable for cumulative emissions about 3000 GtC, but a partial loss followed by regrowth occurs for cumulative emissions less than 2500 GtC. (Ridley et al., 2010b) identified three steady states of the ice sheet. If the CO_2 concentration is returned to pre-industrial when more than 20–40% of the ice sheet has been lost, it will regrow only to 80% of its original volume due to a local climate feedback in one region; if 50% or more, it regrows to 20–40% of the original.

13.5.3.3 Antarctica

Projections of Antarctic SMB changes over the 21st century as assessed by the AR4 under SRES scenarios indicated a negative contribution to sea level because precipitation increase outweighed any ablation increases over the ice-sheet marginal areas and the Antarctic Peninsula. Post-AR4 assessments of CMIP-3 climate change experiments confirm the consistency of the projected Antarctic precipitation increase (Bracegirdle et al., 2008b; Uotila et al., 2007). Several studies (Bengtsson et al., 2011; Krinner et al., 2007; Uotila et al., 2007) have shown that this precipitation increase is directly linked to atmospheric warming via the increased moisture holding capacity of warm air. Atmospheric circulation changes only modulate this continental signal on regional scales, particularly near the ice-sheet margins, and are an order of magnitude smaller on the continental scale than the thermodynamic changes (Uotila et al., 2007). The simulated SMB is, however, strongly influenced by sea ice (Swingedouw et al., 2008) and ocean surface conditions particularly near the ice-sheet margins. This strong dependence suggests that the use of anomaly methods in regional climate and SMB projections with global or regional atmospheric models can give more accurate results (Krinner et al., 2007). Genthon et al. (2009) reported a tendency for higher resolution models to simulate a stronger future precipitation increase because of better representation of coastal precipitation processes, although Bengtsson et al. (2011) found that this can be compensated for by an opposite sensitivity of the simulated ablation changes to model resolution.

While coupled climate-ice-sheet models do not show any significant contribution from Antarctic SMB to GMSL during the 21st century, the Antarctic SMB becomes negative contributing positively to sea level rise in simulations of high-emission scenarios beyond the 21st century (Huybrechts et al., 2011b; Vizcaino et al., 2010) (Section 13.6.2).

[INSERT FIGURE 13.8 HERE]

Figure 13.8: [PLACEHOLDER FOR SECOND ORDER DRAFT: Observed and projected surface mass balance and dynamical contributions from 1950 to 2100.]

[PLACEHOLDER FOR SECOND ORDER DRAFT: Further results from ice2sea RCM EBM simulations of Greenland and Antarctic SMB change to be included. This will help clarify whether EBM and PDD methods are systematically different for Greenland, or if this is confounded by other factors such as how to calculate anomalies or interpolate. Several sets of relationships from these various studies between global climate

change (measured by global temperature change) and ice sheet SMB change to be compared to assess the model uncertainty in projections, and applied in combination to RCP global temperature projections.]

[PLACEHOLDER FOR SECOND ORDER DRAFT: Add assessment of ability of coarse resolution models to reproduce and project precipitation on Antarctica here: regional climate models, e.g., RACMO, via GCMs to EMICs. The model evaluation chapter will provide an assessment of the ability of these models to reproduce and project future precipitation on Antarctica.]

13.5.4 Ice-Sheet Dynamical Changes

Projections of the contribution to sea level rise from dynamical change are still in their infancy. The AR4 was unable to quantify the SLR that may be caused by these effects. Since the publication of the AR4, a great deal of effort has been invested in understanding these effects as well as developing a new generation of ice-sheet models that are capable of simulating them. We are therefore now in a position to make meaningful projections of SLR due to ice-sheet dynamics over the next century, although much uncertainty still exists in our basic understanding of the effects and our ability to model them.

The effects themselves are mostly associated with the flux of ice (outflow) leaving an ice sheet where it impinges on the ocean. In the case of Greenland, this is primarily by the calving of ice bergs into fjords. In Antarctica, it is associated with the flow of ice across the grounding line which separates ice resting on bedrock (at least some of which is not currently displacing ocean water) and floating ice shelves (which already displace their weight in ocean water and therefore have an insignificant influence on SLR). A second mechanism affecting Greenland is the enhanced lubrication of the ice-sheet bed by increased amounts of surface melt water. The link between this mechanism and SLR is less obvious because in itself accelerated flow simply redistributes mass within the ice sheet; this mass must still be lost (by enhanced surface melt or calving) for there to be a SLR contribution. For any of these processes to be simulated accurately, two criteria must be met: the local climate forcing (be it atmospheric or oceanic) must be correctly modelled; and the basic mechanisms themselves must be simulated satisfactorily (which in itself offers strong challenges in terms of the process included in a model and its numerical implementation).

Changes in the coastal seas surrounding Greenland and Antarctica are now recognised as being very important in ultimately triggering dynamic changes. The most likely links are between water temperature at depth and ice berg calving (in Greenland) and submarine melt experienced by ice shelves (Antarctica). Observational evidence supported by modelling suggests that many of the observed changes in ice dynamics may have been triggered by episodic extensions of relatively warm water into close proximity with the ice sheets (Holland et al., 2008a; Jacobs et al., 2011; Thoma et al., 2008). Confidence in the ability of AOGCMs to adequately represent these regional phenomena is low. Yin et al. (2011) assessed output from 19 AOGCMs under scenario A1B to determine how subsurface temperatures are projected to evolve around the ice sheets. They showed decadal-mean warming of 1.7–2.0°C around Greenland and 0.5–0.6°C around Antarctica between 1951–2000 and 2091–2100. With few exceptions, this type of forcing has yet to be included in simulations of future ice-sheet dynamics.

In this subsection, we assess the literature available on which to make projections of SLR over the next century and assess the likelihood of the current mass loss from the Antarctic ice sheet leading to its irreversible decline. Several papers discussed below do not disaggregate dynamical effects from SMB and give only total contributed SLR, nonetheless we have attempted to extract some meaningful numbers from these papers. Given the considerable uncertainties associated with these processes, the figures given in this section are for total sea level rise over the 21st century and no attempt is made to disaggregate this information to finer temporal resolutions. In addition, the literature does not yet support assessment based on multiple emission scenarios.

13.5.4.1 Greenland

Simulations of the effect of future dynamical change on the Greenland Ice Sheet need to address the effects of iceberg calving and flow lubrication by surface melt water. The simulation of calving is hampered by inadequate understanding of the links between climate change and ice berg production (in particular the role

of fjord water temperature) and poor knowledge of the subglacial bedrock topography underlying many outlet glaciers and believed to be crucial in determining the extent of calving-based retreat.

Widespread dynamic thinning of the Greenland Ice Sheet occurred south of 66°N between 1996 and 2000, and extended to 70°N by 2005, with a doubling of mass loss (0.27 ± 0.09 mm yr^{-1} to 0.67 ± 0.12 mm yr^{-1} equivalent SLR) due to this thinning over the period (Rignot; Kanagaratnam 2006). GRACE and GPS measurements further identified increased mass loss that expanded from southeastern Greenland up much of western Greenland between 2005 and 2010 (Khan et al., 2010; Luthcke et al., 2006; Wouters et al., 2008). The spatial pattern of thinning is linked predominantly to marine-terminating outlet glaciers, suggesting that accelerated flow triggered calving based retreat (Pritchard et al., 2009; Sole et al., 2008).

The dynamics of Helheim Glacier, East Greenland over the last decade is simulated using a flow line model with calving based on a relatively simple flotation criterion (Nick et al., 2009). The modeled 7-km retreat of the calving front from one bathymetric ridge to another reproduces observed patterns of thinning and velocity change (including subsequent slow down). Over a 50-year period, this retreat contributes an average ~0.001 mm yr^{-1} additional outflow (~2% of the steady-state outflow), while a more extreme scenario in which retreat continues for an additional 5.5 km contributes an average addition of 0.003 mm yr^{-1}. Further retreat is limited by the decreasing water depths of the fjord.

Observations (Bartholomew et al., 2010; Das et al., 2008; Joughin et al., 2008; Sundal et al., 2011) suggest that basal lubrication by surface melt water does occur and increases peak summer flow by two to three times the winter background, but a simple positive relation between increased melt and enhanced ice flow now seems unlikely, and the two may even be negatively correlated. Although there has been considerable progress in our ability to model the interactions of surface meltwater with the bed (Schoof, 2010), only preliminary attempts have so far been made to incorporate this into predictive ice-sheet models. The presence of large quantities of melt water within the ice sheet may trigger other effects that influence ice dynamics related to the release of latent heat (Phillips et al., 2010).

Price et al. (2011) assessed the long-term response of the ice sheet by employing a three-dimensional model that includes longitudinal stresses and is tuned to represent present-day ice-flow patterns. The model is forced to reproduce the observed recent thinning of the ice sheet's three main outlet glaciers and is then allowed to evolve to a new equilibrium, which requires ~100 years. The long-term response to present-day thinning amounts to over 75% of the total sea level Greenland contribution. The future SLR to be expected as a consequence of the recent observed outlet glacier retreat is 1.0 ± 0.4 mm from the three modeled glaciers by 2100, and 6 ± 2 mm when scaled to include all outlet glaciers. Further prediction requires an assessment of how regularly future calving based retreat will occur. Total dynamic SLR varies between 10 and 45 mm over the next century when the repeat interval between successive retreats is varied between 50 and 10 years.

Vizcaino et al. (2010) and Huybrechts et al. (2011b) conducted simulations using coupled climate and ice-sheet models for experiments with two and four times preindustrial concentrations of atmospheric carbon dioxide. Although both ice-sheet models include crude representations of calving, they omit several dynamical effects thought to be important on decadal to centennial time scales, such as basal lubrication by surface melt water and the longitudinal transmission of stresses. Their projected rates of SLR are therefore dominated by changing SMB with an ill-constrained calving component. Huybrechts et al. (2011b) made the important point that calving decreases from a maximum at the start of the experiment to zero when the ice sheet has retreated from direct contact with the ocean. In their work, this typically takes 500 years and happens after the associated SLR is 0.8 m.

Greve et al. (2011) reported results from the SICOPOLIS and IcIES ice-sheet models for projected response to climate change for the next 500 years. Both models are of traditional design and do not include several dynamical effects thought to be important on decadal to century time scales, in particular they do not admit longitudinal stress transmission. Forcing comes from an ensemble average of 18 AR4 models for the A1B scenario (climate after the first century is held fixed) and a day-degree SMB scheme is employed. The models generated SLR of 0.30 m (SICOPOLIS) and 0.05 m (IcIES) in the next century and SLR of 0.79 m and 0.25 m over 500 years, respectively. These experiments were repeated with a doubling of the basal sliding coefficient, which attempts to assess the effect of enhanced basal lubrication as larger amounts of

surface melt water penetrate to the ice-sheet bed. Doubling sliding equates to a fourfold increase in flow over the (typically) four-month melt season, which is very high but not totally unreasonable in comparison with observations (e.g., Bartholomew et al., 2010). These experiments show an increase in associated SLR of 0.22 m (SICOPOLIS) and 0.12 m (IcIES), which represents an estimate of the dynamic component).

Graversen et al. (2011) assessed the effect of dynamical change on the ice sheet using a model that does not include longitudinal stresses by increasing the simulated flow of outlet glaciers by ~20% per decade for different periods of time varying from 1990–2008 only to the entire 21st century. This adds a maximum of 25 mm to the SLR expected in this century.

Ren et al. (2011) employed an ice-flow model based on the Navier-Stokes equations to simulate the response of Greenland under the A1B scenario using output from MIROC3.2(hires) and CCSM3. The AOGCM output is used to drive an energy-balance model of SMB. A range of models is employed to simulate basal sliding, which is empirically linked to the production of surface melt water. The authors note a 10% increase in ice velocity over the next 500 years, which they attribute to the lower viscosity of warming ice. This explanation appears unlikely and no supporting evidence is given. It is not clear what affect this increased velocity has on the ice sheet's mass budget and no figures are given that allow the dynamic and SMB effects to be separated. Associated SLR reaches a maximum of 66 mm by 2100.

Pfeffer et al. (2008) developed low and high scenarios for potential SLR contribution from Greenland dynamics. The former assumes a first-decade doubling of outlet glacier velocity throughout the ice sheet, which contributes 93 mm SLR in the 21st century. The latter scenario assumes an order of magnitude increase on the same time scale which contributes 0.47 m.

Katsman et al. (2011) estimated the contribution of calving to SLR using a similar methodology. They assumed a doubling of discharge to 2050 (followed by a rapid slowdown to original values) for marine terminating outlet glaciers in the east and south. In the north and for Jakobshavn Isbrae, they assumed a quadrupling by 2100. Their final estimate is 100 mm SLR.

We divide our assessment of dynamics into calving and basal lubrication. For the former, the studies by Price et al. (2011), Katsman et al. (2011), and Pfeffer et al. (2008) (low scenario) suggest a SLR contribution of 0.05–0.1 m, which can be taken as an upper bound of the likely range. The high scenario of Pfeffer et al. (2008) provides a plausibility limit of 0.47 m. For basal lubrication, the literature is still very poorly developed and the figure of 0.22 m from Greve et al. (2011) is taken as a plausibility limit given uncertainty in the applied forcing. A plausibility limit for SLR is therefore 0.69 m (derived by simple addition). A lower bound is given by the SLR to which the ice sheet is already committed by its response to past changes in calving, which is given by Price et al. (2011) as 6 ± 2 mm.

Table 13.5: Published estimates of the contribution of changing ice dynamics to global-mean sea level rise. Types of estimate are indicates as * for process model and + for physically-based constraint.

Ice Mass	Source	Total Contribution to 21st Century Global-Mean Sea Level Rise (m)	
		Likely upper bound	*'Plausibility' Scenario*
Pine Island/Thwaites	Pfeffer et al. (2008)+	0.11	0.39
Pine Island	Joughin et al. (2010)*	0.02–0.03	
	Gladstone et al. (2011)*	0.04–0.07	
Antarctica	Pfeffer et al. (2008)+	0.12	0.55
	Pollard and de Conto (2009)*		0.33
	Katsman et al. (2011)+	0.17 to 0.15 ("modest")	0.41 ("severe")
Antarctic Peninsula	Pfeffer et al. (2008)+	0.01	0.06
Greenland	Pfeffer et al. (2008)+	0.09	0.47
	Katsman et al. (2011)+	0.10	
	Price et al. (2011)*	0.01–0.05	
	Graversen et al. (2011)*	0.03	

Greve et al. (2011)*	0.12–0.22

13.5.4.2 Antarctica

Two main mechanisms have been identified that may affect the dynamics controlling mass loss from the Antarctic ice sheet in the next century. Both are related to the floating ice shelves that fringe much of the ice sheet. The first relates to increasing submarine melt experienced by these shelves leading to their thinning and acceleration. The second relates to the increased potential for melt ponds to form on the upper surface of ice shelves, which may destabilize them.

A recent example of the fracture-based collapse of an ice shelf caused by surface melt water is the Larsen B ice shelf; similar collapses have also occurred along the length of Antarctic Peninsula (Pritchard; Vaughan 2007). Morris and Vaughan (2003) identified a threshold mean annual air temperature of –5°C for the collapse of these ice shelves. There is potential for the larger ice shelves of the main Antarctic ice sheet to experience similar collapses if air temperatures should warm sufficiently. This may then be associated with the acceleration of grounded ice outflow (as was the case for Larsen B: De Angelis and Skvarca, 2003; Rignot et al., 2004; Scambos, 2004) with associated SLR.

Bracegirdle et al. (2008a) analysed the output of 19 AOGCMs for the A1B and 20C3M scenarios. They find a significant mean annual warming of <2.5°C between 2004–2023 and 2080–2099. Mean annual air temperatures are thought to be between –14°C and –25°C on the major ice shelves of Antarctica (Comiso, 2000) so that warming in the next century will likely not be sufficient to initiate collapse using the Morris and Vaughan (2003) threshold. Fykes et al. (2010), however, do find high surface melt over these ice shelves by 2500 using an intermediate complexity model with an emissions scenario based on A2.

Mass loss from dynamical change in Antarctica is now focussed on Pine Island, Thwaites and Smith glaciers draining the West Antarctic ice sheet, and Cook and Totten glaciers draining the East Antarctic ice sheet (Pritchard et al., 2009; Rignot et al., 2008; Shepherd and Wingham, 2007). These ice streams are grounded on bedrock well below sea level, which has raised concerns about the unstable landward migration of their grounding lines and associated mass loss (see Box 13.2). The grounding line of Pine Island Glacier (PIG) appears to have retreated from a bedrock ridge ~30 km from the current grounding line into water that is roughly twice as deep (Jenkins et al., 2010). Numerical modelling of ocean circulation forced by atmospheric reanalyses for 1980–2005 suggests that upwelling of relatively warm Circumpolar Deep Water on to the continental shelf occurred between the late 1980 and early 1990s, thus possibly inducing the contemporaneous onset of acceleration and thinning of Pine Island Glacier (Thoma et al., 2008).

Joughin et al., (2010) used a model of PIG with a migrating grounding line and constrained by observations of the contemporary velocity field to simulate the effects of a prescribed increase in oceanic melt and a forced loss of basal traction within ~25 km of the grounding line. Simulated rates of thinning agreed with observations for the period 2003–2008. The model is potentially capable of simulating unstable grounding line retreat, but retreat is actually limited to ~25 km and a new equilibrium position was found within 100 years. The sea level contribution predicted by the most extreme of these experiments is 27 mm over the next century with more likely melt scenarios generating <18 mm. These figures can be compared with an extrapolation based on contemporary thinning rates (Wingham et al., 2009) that yields 30 mm SLR over 130–140 years.

Gladstone et al. (submitted) employed a flowline model which incorporates longitudinal and transverse stresses to simulate PIG from 1900 to 2200. The ice-flow model is coupled to a box model of circulation under an ice shelf so that the melt rates that the shelf experiences do not have to be prescribed. This box model is forced by ocean temperatures simulated by the BRIOS ocean model forcing using HadCM3 output for scenario A1B. The ocean model predicts a ~ 2°C rise in subsurface water temperature between 1990 and 2100, which is towards the high end of the Yin et al.'s (2011) analysis for West Antarctica using global AOGCMs with coarser resolution than BRIOS. A 5000-member ensemble is used to explore parameter uncertainty and individual experiments are approved or rejected on the basis of agreement with observations. Within the accepted experiments, two states exist: one where retreat is stabilized 50–90 km behind the present grounding line and another that is characterized be complete collapse from 2150 onwards. The

partially deglaciated state is similar to (although somewhat more pronounced than) the simulation of Joughin et al. (2010). The majority of ice within the main PIG ice stream is grounded well below sea level and is already displacing ocean water; its loss therefore has a reduced impact on sea level. SLR associated with the collapsed state is 14 mm by 2100 and 3.1 cm by 2200, which is likely to be an underestimate of true SLR because volume loss from areas adjacent to the ice stream flow line is not the incorporated. An estimate of this latter effect increases SLR by 2100 to 42–70 mm based on an area 100–200 km wide on either side of the ice stream thinning partially.

Pfeffer et al., (2008) estimated potential SLR over the 21st century on the basis of a doubling of velocity in the next decade for Pine Island and Thwaites Glaciers in West Antarctica, with the velocity of the two East Antarctic systems remaining at present-day values. This low scenario contributes 124 mm with a further 12 mm attributed to the glaciers of the Antarctic Peninsula. A high scenario is developed in which Pine Island and Thwaites Glaciers accelerate in the first decade to the highest known outlet glacier velocity and the East Antarctic glaciers' velocity increases by an order of magnitude on the same timescale. This scenario is deemed high but still plausible in terms of the ice flow it demands, and contributes SLR of 552 mm with an additional 59 mm from the Antarctic Peninsula.

Katsman et al. (2011) used a similar methodology to develop modest and severe scenarios. The former is based on the continuation of recent trends of increasing ice velocities in West Antarctica, the Antarctic Peninsula and the marine-based sectors of East Antarctic ice sheet. This scenario would see 70 to 150 mm SLR contribution from Antarctica. The severe scenario attempts to capture the consequences of the collapse of the West Antarctic Ice Sheet through grounding-line retreat. In this scenario, ice loss from East and West Antarctica increases to eight times the values required to balance surface accumulation (based on observations of glacier acceleration generated by the collapse of the Larsen B ice shelf, Scambos et al., (2004)). This scenario has a SLR contribution of 0.41 m.

Little et al. (submitted) developed a statistical framework for projecting the SLR generated by Antarctic ice dynamics. They employ scenarios in which outflow from the major drainage basins of the ice sheet is assumed to grow linearly or quadratically. Outflow from Pine Island and Thwaites Glaciers is extrapolated from observed trends. Other catchments are simulated using a statistical sampling of the rate of increase of outflow and how tightly correlated this rate is between individual drainage basins. Using the quadratic growth curve, Pine Island and Thwaites Glaciers are 99% certain to yield less than ~0.16 m SLR by 2100. If the growth curve is tuned using the modelling results of Joughin et al. (2010), this value falls to 82 mm. For the whole of Antarctica over the next century, SLR in excess of 0.4 m is found to require local rates of increased outflow that are far greater than historical trends or continental wide increases in outflow for which there is no evidence.

The geometry of a collapsed West Antarctic Ice Sheet can be modelled using the assumption that grounding lines only stabilise in areas where bedrock topography rises in the inland direction (Bamber et al., 2009). Once the location of a stable grounding line has been established, an ice flow model can estimate the associated ice thickness configuration. The volume of lost ice is estimated at 3.3 ± 0.2 m SLE (including an estimate of adjoining ice drawn down from East Antarctica and the effect the lithosphere's elastic response) compared to 4.8 m for loss of all ice in West Antarctica and the Peninsula (Bamber et al., 2009). Additional contributions are possible from East Antarctica, which also has large, potentially unstable areas currently resting below sea level (Ferraccioli et al., 2009).

A model with a coarse (10- to 40-km) numerical grid that included a parameterization of grounding line migration (Schoof, 2007a) was used to simulate the evolution of the West Antarctic ice sheet over the past five million years (Pollard and DeConto, 2009). The simulations, which were driven by fluctuations in the melt rate experienced by ice shelves, show the sporadic collapse of the ice sheet during this period. Collapse from maximum glacial configurations occurs in response to smoothly varying forcing and produces configurations ranging from similar to the present day to remnant ice cover over bedrock archipelagos. Collapses occur on timescales of one to a few thousand years when melt rates are increased by a factor of 20 for ice shelves in topographically-sheltered locations and doubled for exposed shelves, suggesting a stability threshold of approximately 5°C for intermediate-depth ocean warming (Pollard and DeConto, 2009). Assuming a minimum time for collapse of 1,000 years and the Bamber et al., (2009) revised sea level figure, this equates to SLR of 0.3 m century^{-1}.

The studies by Gladstone et al. (submitted) (with enhancement discussed above but for Pine Island only), Katsman et al. (2011), Little et al. (submitted) and Pfeffer et al. (2008) (low scenario) suggest a SLR contribution of 0.07–0.15 m, which can be taken as an upper bound of the likely range. The high scenarios of Katsman et al. (2011)and Pfeffer et al. (2008) provide a plausibility limit of 0.4 to 0.55 m, which is suggested by Little et al. (submitted) to be exceptionally unlikely. An estimate based on deglaciation of the West Antarctic ice sheet in 1,000 years yields 0.33 m. The plausibility limit is therefore 0.33–0.55 m. A lower bound of 18–27 mm is provided by Joughin et al. (2010) in which SLR is limited to the partial deglaciation of PIG.

Beyond the 21st century, feedbacks between atmosphere, ocean and ice sheet require the application of coupled climate-ice-sheet models (Swingedouw et al., 2008; Vizcaino et al., 2010). Currently available continental scale ice-sheet models which are coupled to global climate models cannot resolve the oceanic processes beneath the ice shelf which determines basal ice-shelf melting processes. Currently applied parameterizations assume changes in basal melting to be determined by the ocean temperature offshore of the ice shelf. Furthermore, the dynamics in the transition zone between ice sheet and ice shelf which determine the ice flow across the grounding line relevant for Antarctica's sea level contribution is parameterized in all continental ice-sheet models of Antarctica. Finally, information on the dynamic properties of the bedrock which determines the friction between ice and ground is missing. Consequently, confidence in the models' ability to adequately represent 21st century changes in solid ice discharge under global warming is low.

On the other hand, already coarse resolution climate-ice-sheet models reveal the importance of interaction between ocean, ice and atmosphere. For example, Swingedouw et al., (2008) found strongly reduced ice loss from Antarctica in a coupled model. In their simulations, freshwater discharge from Antarctica produces a strong halocline and thereby inhibits sea-ice melting under warming which leads to a reduction in regional warming around Antarctica of up to 10°C. In contrast, Hattermann and Levermann (2010) found that freshwater release from basal melting may enhance the gyre circulation along the Antarctic coast and thereby enhance heat transport towards the ice shelves and melting. As a consequence, a realistic range of sea level contribution from Antarctica on centennial time scales might be much larger than currently revealed by models.

Currently available coupled climate-ice-sheet models show no net-ice loss from Antarctica during the 21st century independent of the scenario (Huybrechts et al., 2011a; Vizcaino et al., 2010). That means that in these models the ice loss compensates the additional snow fall due to enhanced atmospheric water content. Beyond the year 2100, ice loss exceeds the enhanced precipitation in scenarios above 560 ppm CO_2-equ., while the ice sheet gains mass for lower scenarios (Section 13.6.2).

13.5.4.3 Possible Irreversibility of Ice Loss from West Antarctica

As detailed in Box 13.2 and section 12.6.4.4, large areas of the West Antarctic Ice Sheet might be subject to potential self-accelerated ice loss via the marine ice sheet instability (Schoof, 2007a; Weertman, 1961). On West Antarctica, ice of about 3.7 m SLE is grounded below current sea level with downward sloping bedrock and thereby potentially subject to instability (Bamber et al., 2009). Paleo records suggest that such abrupt ice discharge occurred several times during warm periods of the last 5 million years (Naish et al., 2009). Currently available models are able to capture such self-accelerated discharge. (Bamber et al., 2009) reproduced the paleo-records with a forced ice-sheet model at 25 km resolution and parameterized ice flow across the grounding line.

Temperatures at which past discharge occurred are reported to be 1–2°C above present-day temperature. These simulations showed a sea level rise of about 7 m during time spans of 1000–7000 years with approximately equal contributions from West and East Antarctica.

In East Antarctica, enough ice is grounded below sea level to cause about 13 m SLE rise and is thus potentially subject to the marine ice-sheet instability. However, no available model results or paleo records have indicated the possibility of self-accelerated ice discharge from these regions.

13.5.4.4 Summary Assessment

In summary, it is very likely that dynamic change within the Greenland and Antarctic ice sheet will lead to SLR during the next century. A lower bound of the likely range is 22 mm, while a likely upper bound is 0.25 m (both derived by simple addition). A limit based on plausibility is 1.24 m for SLR from ice sheet dynamics. It is important to stress that, with very few exceptions, many of the effects thought to be important will not have responded fully by 2100 so that SLR after this date is very likely to continue, most likely at an accelerating rate.

[START BOX 13.2 HERE]

Box 13.2: History of the Marine Ice-Sheet Instability Hypothesis

Marine ice sheets rest on bedrock that is submerged below sea level (often by 2–3 km). They are fringed by floating ice shelves which are fed by flow from the grounded ice across a grounding line (GL). This GL is free to migrate both seawards and landwards as a consequence of the local balance between the weight of ice and displaced ocean water, and it is this feature that gives rise to the marine ice-sheet instability (MISI).

The most researched marine ice sheet is the West Antarctic Ice Sheet (WAIS) where approximately 75% (or 1.55×10^6 km^2) of the ice sheet's area currently rests on bedrock below sea level. The East Antarctic ice sheet (EAIS), however, also has appreciable areas grounded below sea level (~35% or 3.39×10^6 km^2) in particular around the Totten and Cook Glaciers.

The MISI has a long history based on theoretical discussions which were started by Weertman (1974) and Mercer (1978), and have seen many refinements over the subsequent years. The advent of satellite-based observation has given fresh impetus to this debate; in particular, work on the GL retreat and thinning of Pine Island (PIG), Thwaites (TG) and Smith Glaciers (all WAIS) has highlighted the importance in understanding the MISI to projections of the ice sheet's future contribution to sea level rise.

Two main triggers to the MISI have been identified, both of which have relevance to contemporary polar climate change. The first is the presence of warmer ocean water under ice shelves, which may lead to enhanced submarine melt (Jenkins et al., 2010). The second is the presence of melt water ponds on the surface of the ice shelf, which tend to increase crevassing and led to the collapse of the Larsen B ice shelf (LBIS) over the course of two months (Rott et al., 1996).

The first essential ingredient of the MISI is the observation that the flux of ice leaving an ice sheet across the GL (outflow) is likely to increase as ice thickness at the GL increases. This relationship is likely to be nonlinear so that any change in thickness will have an exaggerated effect on outflow. The second ingredient is that the bedrock on which the ice sheet rests slopes down towards the centre of the ice sheet, which is indeed the case for much of the WAIS. If an external trigger causes ice to thin, then flotation dictates that the GL must retreat. This new GL position will be associated with deeper bedrock and thicker ice so that outflow increases. This increased outflow leads to further thinning and continued, unstable retreat. The retreat can be stopped if the GL encounters a bedrock rise (so that both thickness and outflow decrease) or other factors not in the simple MISI model intervene, such as reduced submarine melt, sea level fall adjacent to the grounding line from isostatic and gravitational effects of mass loss (Gomez et al., 2010c; Gomez et al., submitted) or enhanced lateral drag slowing flow (Joughin et al., 2010).

Early studies of this phenomenon were based on models that only considered effects at the GL itself and not in the context of the wider ice sheet-shelf system. Further, they were not based on a formal derivation from the basic laws of mechanics thought to control ice-sheet flow. It was therefore unclear whether the instability that these early works demonstrated was a robust prediction or was due to the particular assumptions made in the model's derivation. Questions were raised about an ice sheet's ability to adjust its flow close to the GL so that ice-shelf changes are not felt by the rest of the ice mass (Hindmarsh, 1993). Recently, however, a more complete analysis from first principles has been developed (Schoof, 2007a). This suggest that the all-important relation between thickness and flow at the GL exists and has a power ~5 (i.e., that a 10% increase in thickness leads to a 61% increase in flux).

The collapse of the LBIS provided a natural experiment that demonstrated the linkage between an ice shelf and the flow of grounded ice draining into it. The collapse was associated with a two-to-eightfold speed up of the glaciers draining into the collapsed sector of the ice shelf, while the flow of glaciers draining into a surviving sector was unaltered (Rignot et al., 2004; Scambos, 2004). This suggests that the shelf-sheet link exists and has important implications for the future evolution of the far more significant PIG and THW systems of the WAIS.

The recent strides made in placing MISI on a sound analytical footing are, however, limited to the analysis of steady states. Numerical modelling is required to make the predictions of GL retreat rates that are required in SLR projections. There are major challenges in designing models whose results do not depend in a qualitative way on the details of their numerical design. Problems arise at the GL because, in addition to flotation, the stress regime within the ice mass (and hence the way that it flows) changes abruptly as a consequence of the loss of basal traction as the ice loses contact with the underlying bedrock (Pattyn et al., 2006). This is the topic of active research, and a combination of more complete modelling of the GL stress regime (Morlighem et al., 2010) and the use of very high-resolution models (Durand, 2009) is showing promise.

[END BOX 13.2 HERE]

13.5.5 Anthropogenic Effects on Terrestrial Water Storage

Human activities change terrestrial water storage and hence sea level. These activities vary with socioeconomic development, and may also be sensitive to climate change. Their future global contributions have been little studied in the published peer-reviewed scientific literature.

For extraction of groundwater in excess of natural recharge, we consider two possibilities. The first assumes that this contribution to sea level rise continues throughout the 21st century at the rate of 0.35 ± 0.07 mm yr^{-1} assessed for 1993–2008 by Church et al. (2011b) and Konikow (2011), amounting to 22–44 mm (from 1986–2005 to 2081–2100 i.e., 95 years). The second follows Rahmstorf et al. (2011) in assuming that the groundwater extraction estimates of Wada et al. (2010) can be scaled up in the future with global population, in which case it amounts to about 100 mm by the end of the century.

For impoundment of water in reservoirs, we assume either that it continues throughout the 21st century at the rate of -0.30 ± 0.15 mm yr^{-1} SLE estimated for 1993–2008 by Church et al. (2011b) on the basis of Chao et al. (2008), giving a negative SLE change of 5–52 mm over 95 years, or that it is zero after 2010 i.e., little further net impoundment (cf. Lettenmaier and Milly, 2009). Regarding the latter, we note that a zero contribution still requires further construction of reservoirs, as sedimentation reduces the existing storage volume. These scenarios indicate a range of 0–50 mm of global-mean sea level fall.

This assessment leads to a range of –30 to +100 mm for the net contribution from anthropogenic change in terrestrial water storage over the 21st century. This range includes the range of 0–40 mm assumed by Katsman et al. (2008). Because of the limited information on which this assessment is based, we have low confidence in the range, and we cannot give ranges for individual RCP scenarios.

13.6 Projections of Global Mean Sea Level Rise

13.6.1 Projections for the 21st Century

13.6.1.1 Process-Based Projections

Process-based projections for GMSL rise during the 21st century based on results from nine CMIP5 AOGCMs under the RCP scenarios are shown in Figure 13.9 and Table 13.6 for the mean of 2081–2100 relative to the mean of 1986–2005 (a period of 95 years). They are the sum of contributions for which existing models and projections are compared and evaluated in Sections 13.4.7 and 13.5. Thermal expansion is available from CMIP5. Land ice SMB changes are calculated from CMIP5 global mean surface air

temperature projections using parameterisations that are derived from observations and more detailed simulations. Possible ice-sheet dynamical changes are assessed from the published literature, which does not yet provide a sufficient basis for making projections related to particular emissions scenarios. Projections of changes in land-water storage due to human intervention are also treated as independent of emissions scenario. The methods used to make the projections are described in greater detail in Appendix 13.A. The ranges given are 5–95% confidence intervals characterising the systematic uncertainty in modelling the contributions. We assess the likelihood of and our confidence in these projections in Section 13.6.1.3.

Time series of GMSL and its rate of rise are shown in Figure 13.10. The central projections for GMSL in all scenarios lie within a range of 0.05 m until the middle of the century, because the divergence of the climate projections has a delayed effect owing to the time-integrating characteristic of sea level. By the end of the century (2081 to 2100 compared to 1985 to 2005), they have a spread of about 0.2 m, with RCP2.6 giving least (0.27–0.50 m) and RCP8.5 most (0.41–0.71 m). RCP4.5 and RCP6.0 are very similar at the end of the century (both 0.32–0.56 m), but RCP4.5 has a greater rate of rise earlier in the century, RCP6.0 later. In all scenarios, the rate of rise initially increases, beginning from its recent value of ~3 mm yr^{-1}. The rate of rise becomes roughly constant (central projection of ~4.5 mm yr^{-1}) in RCP2.6 before the middle of the century, and in RCP4.5 and RCP6.0 by the end of the century, but acceleration continues throughout the century in RCP8.5 (central projection reaching ~10 mm yr^{-1}). Even in RCP2.6, the rate of rise does not decrease significantly. In all scenarios, the average rate of GMSL rise during the 21st century is very likely to exceed the average rate during 1971–2010.

In all scenarios, thermal expansion is the largest contribution, accounting for 30-50% of the total in the central projections. Glaciers are next largest. By 2100, about a third of the present glacier volume is projected to be eliminated under RCP8.5, and about a quarter under RCP2.6. Contributions from changes in SMB and dynamics of the Greenland ice-sheet are both positive and of similar size; for the Antarctic ice-sheet they are both larger in magnitude, but SMB change gives a negative contribution (see discussion in Sections 13.4.7 and 13.6.1.3).

For scenario SRES A1B, the projection is 0.37–0.65 m. In the AR4, projections were given for 2090–2099 relative to 1990 (a period of 105 years). For 2090–2099, we obtain 0.40–0.70 m relative to 1996, to which about 0.02 m should be added for GMSL rise 1990–1995 in order to compare with the AR4 projections for the same scenario, which was 0.21–0.48 m. The largest increase relative to the AR4 is from land ice dynamics, for which the central projection is 0.13 m in this scenario. This term was largely omitted in the AR4 because a basis in published literature was not available at that time to make projections.

[INSERT FIGURE 13.9 HERE]

Figure 13.9: Projections with ranges and median values for global mean sea level rise and its contributions in 2081–2100 relative to 1986–2005 for the four RCP scenarios and scenario SRES A1B used in the AR4. The contributions from ice-sheet dynamical change and anthropogenic land water storage are independent of scenario, and are treated as having uniform probability distributions. The projections for global-mean sea level rise are regarded as likely ranges with medium confidence. See discussion in Sections 13.6.1.1 and 13.6.1.3 and Annex 13.A for methods.

[INSERT FIGURE 13.10 HERE]

Figure 13.10: Projections of (a) GMSL rise relative to 1986–2005 and (b) the rate of GMSL rise as a function of time for the four RCP scenarios and scenario SRES A1B. The solid lines show the median and the dashed lines the likely range for each scenario.

Table 13.6: Projections with likely ranges (5–95% uncertainties) and median values for global-mean sea level rise and its contributions in metres in 2081–2100 relative to 1986–2005 for the four RCP scenarios, and rates of GMSL rise in mm yr^{-1} in 2081–2100.

	RCP26			RCP45			RCP60			RCP85		
	5%	50%	95%	5%	50%	95%	5%	50%	95%	5%	50%	95%
Thermal expansion	0.09	0.14	0.18	0.12	0.17	0.22	0.13	0.18	0.23	0.19	0.25	0.32
Glaciers	0.09	0.12	0.15	0.10	0.14	0.17	0.10	0.13	0.16	0.12	0.16	0.19
Greenland ice-sheet SMB	0.01	0.02	0.05	0.01	0.03	0.07	0.01	0.03	0.07	0.02	0.05	0.13
Antarctic ice-sheet SMB	–0.08	–0.04	–0.02	–0.09	–0.05	–0.02	–0.09	–0.05	–0.02	–0.12	–0.06	–0.03

Greenland ice-sheet dyn	0.00	0.05	0.09									
Antarctic ice-sheet dyn	0.01	0.07	0.13			These terms are scenario-independent						
Land water storage	–0.03	0.03	0.08									
Sea level rise	0.27	0.38	0.49	0.31	0.43	0.56	0.32	0.44	0.56	0.41	0.55	0.70
Rate of sea level rise	3.0	4.9	6.9	4.0	6.1	8.3	4.9	7.2	9.6	6.6	9.8	13.8
Sea level rise at 2100	0.30	0.43	0.56	0.35	0.49	0.64	0.37	0.51	0.65	0.47	0.64	0.84

13.6.1.2 Semi-Empirical Projections

The semi-empirical approach regards changes in sea level as an integrated response of the entire climate system, reflecting changes in the dynamics and thermodynamics of the atmosphere, ocean and cryosphere; it explicitly does not attribute sea level rise to its individual physical components. Semi-empirical models use simple physically motivated relationships, with parameters determined from observational time series, to predict GMSL from either global mean surface air temperature (Grinsted et al., 2010; Horton et al., 2008; Rahmstorf, 2007a; Rahmstorf et al., 2011; Vermeer and Rahmstorf, 2009) or radiative forcing (Jevrejeva et al., 2009; 2010; 2011). The paleo record provides strong evidence for a relationship between GMSL and these predictors on glacial/interglacial timescales (Section 13.3.1). Semi-empirical models have adopted various analytical formulations for describing and projecting GMSL changes as a function of the same predictors and applied them to multidecadal timescales.

The development of semi-empirical models was motivated by two problems. First, process-based ice-sheet dynamical models were not available to simulate recent accelerations in ice flow and make projections with confidence (Sections 13.2 and 13.5.4). Second, in previous assessments, known observed and simulated contributions to GMSL from thermal expansion, glaciers and ice sheets did not completely account for observed sea level rise during the 20th century (Church et al., 2001; Gregory et al., 2006). For example, the AR4 assessed the mean observational rate for 1961–2003 as 1.8 ± 0.5 mm yr^{-1}, and the sum of terms as 1.1 ± 0.5 mm yr^{-1} (Bindoff et al., 2007; Hegerl et al., 2007). With the central estimates, only about 60% of observed sea level rise was thus explained, and the potential implication was that projections using process-based models which reproduce only those known contributions would underestimate future sea level rise (Grinsted et al., 2010; Jevrejeva et al., 2009; Rahmstorf 2007a). Recent improvements in observational data sets for ocean warming and land ice mean that observed contributions to sea level rise since about 1970 can now account for GMSL (Section 13.4) (Church et al., 2011b; Domingues et al., 2008; Moore et al., 2011), although process-based models are not yet available for all contributions (Section 13.4.7). While semi-empirical models do not solve the two problems that motivated their development, they provide an alternative approach for projecting GMSL, as well as for exploring the sensitivity of sea level to various forcing factors.

Semi-empirical models are designed to reproduce the observed sea level record over their period of calibration, which provides them with model parameters needed to make projections (Grinsted et al., 2010; Jevrejeva et al., 2009; Rahmstorf, 2007a; Vermeer and Rahmstorf, 2009). A test of the predictive skill of the models requires simulating a part of the observed record which has not been used for calibration. To do this, Rahmstorf (2007b) calibrated against observed GMSL rise for 1880–1940 and projected 1940–2000, obtaining results within 0.02 m of observed, while Grinsted et al. (2010), using Brohan et al. (2006) or Moberg et al. (2005) temperature for calibration, projected a rate of rise for 1993 to 2006 of 2.0–4.9 mm yr^{-1} or 3.1–4.9 mm yr^{-1} respectively (5–95% ranges), compared to the altimeter estimate of 3.3 ± 0.4 mm yr^{-1}.

Three kinds of issues relating to calibration of semi-empirical models have been discussed in the literature. First, the GMSL estimates used for training the models are based on limited observations and are thus uncertain. There has been debate about whether the projections of Rahmstorf (2007a) may be sensitive to their statistical treatment of the temporal variability in the instrumental record of sea level change (Holgate et al., 2007; Rahmstorf, 2007b; Schmith et al., 2007). Rahmstorf et al. (2011) reported that GMSL projections for the RCP 4.5 scenario for 2100 varied by ±0.04 m for values within a range of 0–25 years for the embedding dimension used for temporal smoothing during the calibration.

Second, there may be sensitivity to the choice of datasets used for calibration. Rahmstorf et al. (2011) obtained central projections under RCP 4.5 for 2100 within a range of about ±0.10 m based on calibration with the GMSL datasets of Church and White (2006), Jevrejeva et al. (2008) and Kemp et al. (2011), but their projections calibrated with the dataset of Church and White (2011) were about 0.3 m lower (Table 13.7), even though the two Church and White (2011) GMSL datasets differ at all times by less than one standard deviation (on average by less than 50% of one standard deviation). While Rahmstorf et al. (2011) argued that the Church and White (2011) data imply model parameters that are inconsistent with reconstructed paleo-temperatures, the result also raises the possibility that there may be a substantial but as yet uninvestigated sensitivity of the Vermeer and Rahmstorf (2009) model to statistically insignificant features of the calibration dataset. Grinsted et al. (2010) and Jevrejeva et al. (2010; 2011; 2011) addressed this issue by using an inverse Monte-Carlo technique to determining their model parameters, effectively sampling a larger observational space determined by the uncertainty covariance matrix of their GMSL estimate. A question remains, however, as to whether Grinsted et al. (2010) fully sampled the observational space, as represented for example by the Church and White (2006, 2011) and Wenzel and Schroeter (2010) GMSL estimates. Grinsted et al. (2010) also investigated the sensitivity to the temperature dataset used as predictor, and Jevrejeva et al. (2010) the sensitivity to radiative forcing as predictor (Table 13.7). In the latter case, three datasets gave median projections under RCP 4.5 for 2100 within a range of about ±0.20 m.

Third, Vermeer and Rahmstorf (2009) demonstrated that contributions to GMSL rise which are not caused by contemporaneous climate change or radiative forcing should be subtracted from the observational sea level record before calibrating a semi-empirical model, because otherwise they may be implicitly scaled up or down with future climate change, particularly if they correlate with the semi-empirical predictors of sea level change. Such contributions include groundwater depletion and storage of water by dams. Rahmstorf et al. (2011) found that their projections were about 0.25 m smaller if they did not exclude reservoir storage. Making these exclusions, however, adds uncertainty to semi-empirical model projections because the terms to be excluded, and their time-dependence, are themselves uncertain.

Because of the above issues and structural differences between the models, projections from the semi-empirical models for the 21st century have a wide range (the spread of their central values for the A1B scenario is more than 50% of the average; Table 13.7).

Making projections with a semi-empirical model assumes that sea level in the future will respond as it has in the past to radiative forcing or climate change. This may not hold if potentially non-linear physical processes do not scale in the future in ways which can be calibrated from the past (Rahmstorf et al., 2011; Vermeer and Rahmstorf, 2009; von Storch et al., 2008). These considerations imply unquantified systematic uncertainty in semi-empirical models, which could lead to overestimated or underestimated projections. Four such effects have been discussed in the literature.

First, AOGCMs indicate that the ocean heat uptake efficiency tends to decline as warming continues and heat penetrates more deeply (Gregory and Forster, 2008). A linear scaling of the rate of global ocean heat uptake with global SAT determined from the past will thus overestimate future time-integrated heat content change and the consequent thermosteric sea level rise on a century timescale. Rahmstorf (2007a) found that the linear scaling overestimated by 0.12 m (about 30%) the thermal expansion simulated by a climate model with a 3D ocean from 1990 to 2100 under scenario SRES A1FI. A more accurate simulation can be achieved by taking into account the vertical profile of warming, at least by distinguishing the upper (mixed layer) and lower (thermocline) layers (Held et al., 2010; Vermeer and Rahmstorf, 2009). The Vermeer and Rahmstorf (2009) model gives improved agreement.

Second, the appropriate choice for the formulation of the semi-empirical model may depend on the nature of the climate forcing, and could therefore differ between past and future. Von Storch et al. (2008) analysed output from a simulation of the past millennium with the ECHO-G model in order to calibrate a relationship, of the form used by Rahmstorf (2007a), between global mean SAT and the contribution of thermal expansion to the rate of sea level rise. They found that the relationship varies with time, implying that its projections would not be reliable. In response, Vermeer and Rahmstorf (2009) argued that the sea level variations of the last millennium arise predominantly from episodic volcanic forcing and cannot be adequately simulated by the semi-empirical model of Rahmstorf (2007a) because it was intended to simulate the response to sustained forcing on multidecadal timescales.

Third, the sensitivity of glaciers to warming will tend to decrease as the ablating area and the remaining volume decrease (Section 13.5.2). On the other hand, glaciers at high latitudes which currently have negligible surface melting will begin to ablate as the climate becomes warmer, giving an increase in sensitivity (Rahmstorf et al., 2011) (Section 13.5.2). Estimating the balance of these two effects will require detailed modelling of glacier SMB.

Fourth, future rapid dynamical changes in ice-sheet dynamics could substantially increase sea level rise (Section 13.5.4). In order for large ice-sheet dynamical changes to be predictable from the instrumental record, such changes must have contributed substantially to sea level rise during the period of calibration. However, it is likely that they have contributed only a small part of the observed sea level rise during recent decades (about 20% since 1993 and likely less for earlier decades; Chapter 4). This phenomenon is therefore not likely to be the reason why semi-empirical projections are larger than process-based projections.

Table 13.7: Global-mean sea level rise (m) from the year indicated to 2100 projected by semi-empirical models and compared with the IPCC AR4 projection.

	From	5%	50%	95%
Scenario SRES A1B				
IPCC AR4[c]	1990	0.22	0.37	0.50
IPCC AR4[c,d]	1990	0.22	0.43	0.65
Rahmstorf (2007a)[a]	1990	-	0.85	-
Horton et al. (2008)[b]	2000	0.62	0.74	0.88
Vermeer and Rahmstorf (2009)	1990	0.98	1.24	1.56
Grinsted et al. (2010) with Brohan et al. (2006) temperature for calibration	1990	0.32	0.83	1.34
Grinsted et al. (2010) with Moberg et al. (2005) temperature for calibration	1990	0.91	1.12	1.32
Jevrejeva et al. (2010) with Goosse et al. (2005) forcing for calibration	1990	0.60	0.75	1.15
Jevrejeva et al. (2010) with Crowley et al. (2003) forcing for calibration	1990	0.63	0.86	1.06
Jevrejeva et al. (2010) with Tett et al. (2007) forcing for calibration	1990	0.87	1.15	1.40
Scenario RCP 4.5				
Rahmstorf et al. (2011) with Church and White (2006) for calibration	2000	0.84	1.01	1.28
Rahmstorf et al. (2011) with Jevrejeva et al. (2008) for calibration	2000	0.91	1.15	1.49
Rahmstorf et al. (2011) with Church and White (2011) for calibration	2000	0.62	0.73	0.91
Rahmstorf et al. (2011) with proxy data for calibration	2000	0.69	0.95	1.32
Jevrejeva et al. (2011)[e]	1990	0.52	0.74	1.10

Notes:
(a) Uncertainty range not given.
(b) The mean value and the range across the 11 GCMs are shown.
(c) Extrapolated to 2100 using the projected rates of sea level rise for 2000–2099 in Table 10.7 of Meehl et al., (2007).
(d) Including scaled-up ice-sheet discharge given in Table 10.7 of Meehl et al. (2007) as an illustration of the possible magnitude of this effect.
(e) Results given are the average of three different semi-empirical models.

13.6.1.3 Likely Ranges and Bounds

The AR4 (Meehl et al., 2007) presented model-based projections of GMSL rise during the 21st century, but did not provide a best estimate, principally because the scientific understanding of the time was not sufficient to allow an assessment of the effects of rapid changes in ice-sheet dynamics, and these effects were consequently not included in the ranges given by the AR4. For the SRES A1B scenario, the AR4 range was 0.21–0.48 m, and for the highest-emissions scenario A1FI it was 0.26–0.59 m. If the acceleration of ice-sheet outflow, observed in the last two decades, increased linearly with global mean surface air temperature, the AR4 maximum projections would be raised by 0.1–0.2 m. The AR4 was unable to exclude larger values or to assess their likelihood.

Since the publication of the AR4, motivated by policy needs, upper bounds of between 0.9 and 2.4 m for GMSL rise by 2100 have been obtained by three other approaches (Nicholls et al., 2011), namely semi-empirical models (Section 13.6.1.2), analogues from past climates (Section 13.3.1), and physical constraints on ice-sheet dynamics (Section 13.5.4). The broad range of values reflects the different methodologies, which consider different constraining factors and sources of evidence. Whereas a best estimate and a likely range are well-defined in their purpose, in that they aim to equal and to encompass the true value, an upper bound is not uniquely defined, because it depends on the subjective choice of constraints that are to be tested to the limit.

The confidence that can be placed in projections by the various kinds of method must be considered. Confidence arises from the nature, quantity, quality and consistency of the evidence. For process-based projections, which use the results from models of individual contributions (Section 13.6.1.1), confidence comes most importantly from our understanding of the modelled physical processes, the consistency of the models with wider physical understanding of those processes as elements of the climate system, the agreement of modelled and observed contributions, and the agreement of observed and modelled GMSL (Section 13.4.7; Chapters 9 and 10, Box 13.1 on budgets).

Semi-empirical models (Section 13.6.1.2) make projections by calibrating a physically motivated relationship between GMSL and some other parameter of the climate system in the past and applying it to the future, without quantifying the contributory physical processes. If we had no physical understanding of the causes of sea level rise, the semi-empirical approach to projections would be the only possible one, but extrapolation beyond the range of calibration implies uncertainty that is difficult to quantify. As a result, there is no consensus about the reliability of semi-empirical model projections.

Although the semi-empirical model projections in Table 13.7 cover a wide range, they all project significantly higher GMSL rise than process-based models. It is important to establish whether the semi-empirical projections are physically plausible. Since ocean thermal expansion and glacier contributions are comparatively well understood and simulated, the only suggested explanation in terms of processes is that semi-empirical models may allow for rapid ice-sheet dynamical change in response to future climate change (Grinsted et al., 2010; Little et al., submitted). Our assessment is that this is unlikely to be the reason for the difference, because the ice sheets did not contribute a substantial proportion of GMSL rise during most of the period of the data used for calibration (Sections 13.4.6 and 13.4.7), and hence any relationship of rapid ice-sheet dynamical change to global climate change cannot be determined from the data. Moreover, our current understanding of the causes of recent dynamical change in Greenland and Antarctica is that they have been triggered by local changes in ocean temperature (Holland et al., 2008a; Jacobs et al., 2011; Thoma et al., 2008). A link to global surface temperature or radiative forcing is not likely to be strong on the century timescale. Hence we consider that rapid ice-sheet dynamical changes could not be reliably extrapolated from the observed data on which semi-empirical models are calibrated.

A third approach to obtaining an upper bound examines rates of sea level change in the paleo-record. Rapid GMSL rise has occurred during glacial terminations, continuing even after sea level and climate have reached interglacial states, at rates of up to about 1 m century^{-1} averaged over centuries (Section 13.3.1.2). However, these rates are dominated by large ice-sheets that no longer exist, and a better analogue for the future comes from past interglaciations. There is reliable evidence of GMSL rise at 0.10–0.25 m century^{-1} averaged over centuries during the LIG, partly due to the effect of insolation on ice-sheet SMB as well as a warmer climate (Section 13.3.1.1.2).

The fourth approach is to obtain an upper bound from physical constraints. By considering kinematic limits on outflow from the ice sheets, Pfeffer et al. (2008) argued that scenarios of GMSL rise exceeding 2 m by 2100 are physically untenable, such as the scenario of Hansen et al. (2007) giving 5 m. Pfeffer et al. (2008) constructed a "high" scenario of 2 m of sea level rise by 2100, and Katsman et al. (2011) of 1.1 m. Although Pffefer et al. (2008) and Katsman et al. (2011) consider their scenarios to be physically possible, they are unable to quantify their likelihood, because these scenarios are based on assumptions, rather than being related to observations of the response of the Greenland and Antarctic ice-sheets to climate change or variability on century timescales. Their scenarios involve contributions of ~0.5 m from Antarctica. This is much greater than any process-based projections of dynamical ice-sheet change (Section 13.5.4), and would require a discharge growth rate similar to that observed in recent decades for the Pine Island Glacier to be sustained in all drainage basins of the entire ice sheet for the whole century (Little et al., submitted).

Projections of GMSL rise during the 21st century (and in following centuries, see Section 13.6.2) must be accompanied by an indication of confidence in order for them to be practically useful. There is a relationship between the level of confidence and the width of the range delimited. Extremely high bounds to GMSL rise in the 21st century can easily be set with confidence, but being physically unachievable makes them of little value. We attempt to define a narrower range that may be more useful but which is by necessity accompanied by lower confidence. In our assessment, GMSL rise during the 21st century for each RCP scenario is likely to lie within the range given by the process-based projections (Section 13.6.1.1). Although they are constructed using 5–95% confidence intervals for individual processes, we are not able to assert that GMSL rise is very likely to lie within these ranges because we have only medium confidence in our assessment. Under the RCP 4.5 scenario, for example, GMSL is likely to rise by 0.35–0.64 m by 2100 relative to 1986–2005, with a median estimate of 0.49 m. Under RCP 8.5, the scenario with the highest radiative forcing, the likely range reaches 0.84 m, similar to the lower estimate of Pfeffer et al. (2008). Larger values cannot be excluded, but the current state of scientific understanding is insufficient for evaluating their probability. On the other hand, we have high confidence that the time-mean rate of GMSL rise during the 21st century is very likely to exceed the rate observed during 1971–2010.

The agreement of process-based models with observations and physical understanding is a cause for confidence and an advance since the AR4, but other factors restrict our confidence. First, observations do not show an increase in Antarctic precipitation, which is projected by models; if this term were smaller than indicated by models or entirely absent in the future, our projections would be raised by up to 0.07 m (assuming uncorrelated errors). Second, understanding of rapid changes in ice-sheet dynamics is still very limited. Third, there is no published literature that quantifies observational constraints or the effect of carbon-cycle uncertainties on GMSL rise, such as there is for surface air temperature. For this reason we have lower confidence in our projections than can be placed in projections of global-mean suface air temperature change (Chapter 12). [PLACEHOLDER FOR SECOND ORDER DRAFT: Explain and if possible reconcile the treatments of Chapter 12 and Chapter 13]. Fourth, we do not know why semi-empirical models give higher projections, which might point to some presently unidentified or underestimated contribution. Progress on all of these is needed in order to attain high confidence in GMSL projections.

13.6.2 Projections Beyond the 21st Century

The Representative Concentration Pathways (RCPs), as applied in Sections 13.5 and 13.6.1, are defined up to the year 2100. The Extended Concentration Pathways (ECPs) have been introduced for the period between 2100 and 2300 (Meinshausen et al., 2011). These time periods are not sufficient to capture the full impact of sea level rise, since oceanic warming as well as continental ice responds to changes in external forcing on centennial to millennial time scales. While this section will focus on a time horizon up to the year 2500, it should be noted that sea level is very likely to continue to rise beyond 2500 unless global mean temperatures decline (e.g., Gillett et al., 2011; Huybrechts et al., 2011a; Solomon et al., 2009).

A number of model simulations of ice sheets and oceanic warming apply scenarios different from the ECPs. Consequently, sea level projections beyond the year 2100 have been grouped here into scenarios in which atmospheric GHG concentration does not exceed 560 ppm CO_2-equivalent and into those that exceed 560 ppm. A synthesis of the different sea level contributions is provided in Table 13.8 and Figure 13.11 for the end of each century until the year 2500. Thermal expansion contributions were obtained from coarse-

resolution coupled climate models (Gillett et al., 2011; Schewe et al., 2011; Solomon et al., 2009; Vizcaino et al., 2008). Contributions from the Greenland and Antarctic ice sheets were obtained with climate models of comparable complexity coupled to continental ice-sheet models (Huybrechts et al., 2011a; Vizcaino et al., 2010). Glacier projections were obtained by application of the method by Marzeion et al. (2011) to the CMIP-5 model output for scenarios and models that were integrated up to the year 2300.

The uncertainty range of the total sea level change has been computed assuming independence between different contributions; i.e., displayed uncertainties are for the total sea level change range from the sum of all the minimum contributions to the sum of all maximum contributions compared to Section 13.6.1 where the uncertainties are added in quadrature. This approach is adopted because of the limited number of simulations available. The underlying assumption of independence might not always be justified which would change the uncertainty range. It is chosen here for two main reasons: (1) a number of projections result from simulations of only one component relevant for sea level (2) in cases where fully coupled models where applied confidence is low that the interdependence of uncertainties is modelled realistically. For example, the ice loss from Greenland and Antarctica are determined by the regional temperature and precipitation field. Confidence in whether the interdependence of these remote regions is well captured in the coarse-resolution models that are applied is low.

[INSERT FIGURE 13.11 HERE]

Figure 13.11: Sea level projections beyond the year 2100 are grouped into scenarios which exceed 560 ppm CO_2-equivalent (upper panel) and those who do not (lower panel). Coloured bars comprise the entire range of available model simulations. Horizontal lines provide the specific model simulations. Total sea level represents the sum of the different components assuming independence of the different contributions. Grey shaded bars exhibit the likely range for the 21st century projection from Figure 13.9 with the median as the horizontal line. [PLACEHOLDER FOR SECOND ORDER DRAFT: More simulations will be added including from the model intercomparison projects SeaRise and Ice2Sea.]

[PLACEHOLDER FOR SECOND ORDER DRAFT: Add figure with sea level pattern according to ice sheet contributions in 2500.]

In summary, projections show positive contributions to sea level from thermal expansion, glaciers and the Greenland ice sheet. Due to enhanced precipitation under warming, Antarctica has a negative contribution to sea level in scenarios limited by 560 ppm CO_2-equivalent. For scenarios above 560 ppm CO_2-equivalent, Antarctic SMB is contributing positively to GMSL. As discussed in Section 13.5.4.2, confidence in the models capability to project sea level contributions from dynamic ice-sheet changes in Greenland and Antarctica is low, due to inadequate representation of ice shelves, ice-ocean interaction and the dynamics within fast flowing ice streams. In Greenland, dynamic mass loss is limited by topographically defined outlets regions. Solid-ice discharge induced from interaction with the ocean is furthermore self-limiting because retreat of the ice sheet results in increasingly less contact with the ocean and less mass loss by iceberg calving (Graversen et al., 2011; Pfeffer et al., 2008; Price et al., 2011). By contrast, the bedrock topography of Antarctica is such that a retreating ice sheet will remain in contact with the ocean. Due to topography that is declining landward, especially in West Antarctica, this may lead to enhanced rates of mass loss as the ice retreats. While the model used by Huybrechts et al. (2011a) is in principle capable of capturing this marine ice sheet instability (see Box 13.2), confidence in the models ability to capture the associated time scale is low. The model used by Vizcaino et al., (2010) does not represent the ice shelf dynamics and is thereby lacking a fundamental process that can trigger the instability. As stated by the authors, low confidence needs to be attributed to the model's ability to project future solid ice discharge from Antarctica. It is thus likely that the contributions from Antarctica as depicted in Figure 13.11 underestimate the real future contribution.

The total sea level change in 2500 in scenarios up to 560 ppm CO_2-equivalent ranges from 0.03 to 1.22 m and for scenarios above 560 ppm CO_2-equivalent from 1.72 to 5.59 m. The semi-empirical method applied by Jevrejeva (2011) yields similar values of 0.13-1.74 m below 560 ppm CO_2-equivalent and 1.03–5.79 m above 560 ppm CO_2-equivalent. For increasing GMT, sea level is very likely to continue to rise beyond the year 2500 as shown by available model simulations of thermal expansion and ice sheets that were computed beyond 2500 (Driesschaert et al., 2007; Gillett et al., 2011; Goelzer et al., 2011; Huybrechts et al., 2011b; Mikolajewicz et al., 2007c; Rahmstorf and Ganopolski, 1999; Ridley et al., 2005; Schewe et al., 2011;

Solomon et al., 2009; Swingedouw et al., 2008; Vizcaino et al., 2010; Vizcaino et al., 2008; Winguth et al., 2005) and by the semi-empirical approach.

Table 13.8: Uncertainty range of sea level contribution and total sea level change for low and high scenarios as obtained from model simulations.

Contribution	Scenario	2200	2300	2400	2500
Thermal expansion	low	0.23–0.27	0.26–0.32	0.24–0.38	0.22–0.41
Glaciers	low	0.07–0.23	0.09–0.26	0.11[(a)]	0.12[(a)]
Greenland ice sheet	low	0.05–0.17	0.08–0.33	0.11–0.52	0.14–0.75
Antarctic ice sheet	low	–0.17 – –0.02	–0.25– –0.04	–0.36 – –0.05	–0.45 – –0.06
Total	low	0.17–0.44	0.17–0.86	0.10–0.95	0.03–1.22
Thermal expansion	high	0.36–1.07	0.52–1.49	0.62–1.76	0.71–1.97
Glaciers	high	0.09–0.32	0.13–0.40	0.15[(a)]	0.17[(a)]
Greenland ice sheet	high	0.13–0.50	0.31–1.19	0.51–1.94	0.73–2.57
Antarctic ice sheet	high	–0.04–0.01	0.02–0.19	0.06–0.51	0.11–0.88
Total	high	0.55–1.90	0.98–3.27	1.34–4.36	1.72–5.59

Notes:
(a) The value is based on one simulation only.

13.7 Regional Sea Level Change

Regional sea level change results from the combination of a global sea level change and from regional controls, which may or may not be related to this global averaged rise. Regional differences from the global average may be substantial and have complex spatial patterns determined by ocean dynamical processes, movements of the sea floor and changes in gravity due to water mass redistribution (e.g., land ice, groundwater) in the climate system. Ocean processes include a dynamical redistribution of water masses and a change of water-mass properties caused by winds, air-sea heat and freshwater fluxes, and ocean currents, and they are usually associated with natural climate modes. Since the characteristic time scales of these processes are different, their relative contribution to regional sea level variability or change will depend fundamentally on the time scale considered.

13.7.1 Interpretation of Past Regional Sea Level Change

As discussed in Chapter 3, precise observations of regional sea level exist only since the start of satellite altimetry in 1993. Over the period 1993–2010, the rate of sea level change estimated from altimetry varied regionally between –4 mm yr^{-1} and +15 mm yr^{-1} (Figure 1, FAQ 13.1), with the largest rates of 10–15 mm yr^{-1} in the western Pacific being up to about four times the global mean value of 3.2 mm yr^{-1}. Higher-than-global averaged rates were also observed in the North Atlantic around Greenland and in the Southern Ocean. Rates lower than the global mean were observed in the northeastern Pacific and in the eastern Pacific along the western coasts of North and South America. However, tide gauge data indicate that those trends can vary substantially from decade to decade and most likely the patterns shown in the figure do not represent long-term trends in regional sea level, but rather natural climate variability.

Estimates of sea level changes over periods longer than the altimeter era depend fundamentally on tide-gauge observations, which at a few locations exist for several decades or longer (Woodworth et al., 2011b). Because long tide-gauge time series have a sparse spatial distribution, techniques are required that combine these longer time series with the comprehensive spatial coverage of the satellite altimeter data to reconstruct past regional sea level variability. Church et al. (2004) and a number of subsequent studies (Church and White, 2006, 2011; Hamlington et al., 2011; Llovel et al., 2010a; Meyssignac et al., 2011a; Ray and Douglas, submitted; Wenzel and Schroter, 2010) applied one such technique whereby they used an

expansion of the altimetry data (or sea level data from ocean reanalyses) in terms of Empirical Orthogonal Functions (EOFs) backward in time to describe the spatial variability of sea level before the satellite era.

Although uncertainties remain in sea level reconstructions, spatial trend patterns over the past 50 years are very likely significantly different from those observed over the recent altimetry era, and have a magnitude that is 3–4 times lower because they are less dominated by the decadal variability, a result also found in ocean reanalyses over similar time spans (Carton et al., 2005; Kohl and Stammer, 2008). However, altimetry-era like patterns can be observed at several selected periods in the past, which suggests that ongoing regional sea level changes are largely associated with low-frequency internal modes of the ocean (Meyssignac et al., 2011b; White et al., 2005b). This low-frequency (multi-decadal) variability may significantly amplify in some areas the global mean sea level rise while in other areas may reduce it. For example, Becker et al. (2011) argued that because of the ENSO-related low-frequency variability, total sea level rise since 1950 at the Tuvalu islands is 3 times larger than the global mean.

Most of the regional sea level changes observed or reconstructed during recent decades appear to be steric in nature (Ishii and Kimoto, 2009; Levitus et al., 2005; Levitus et al., 2009; Lombard et al., 2005a; Lombard et al., 2005b). Moreover, thermosteric changes observed in the upper ocean over the altimetry era appear primarily responsible for the observed regional trend patterns, although in some regions (e.g., Atlantic Ocean) halosteric effects are also important and can reduce or enhance thermosteric changes. Ocean models and reanalyses-based results (Carton et al., 2005; Stammer et al., 2011; Wunsch and Heimbach, 2007) as well as ocean circulation models without data assimilation (Lombard et al., 2009) confirm these results.

Observations and reanalysis (Stammer et al., 2011) over the last half of the 20th century both agree in showing that steric spatial patterns are not stationary but are part of decadal sea level variability and fluctuate both in space and time as part of climate modes of the coupled ocean-atmosphere system, such as the El Niño-Southern Oscillation (ENSO), the North Atlantic Oscillation (NAO) and the Pacific Decadal Oscillation (PDO) (Di Lorenzo et al., 2010; Levitus et al., 2005; Lombard et al., 2005a; Lozier et al., 2010). These changes appear to be primarily caused by changing wind fields and associated changes in the ocean circulation (Kohl and Stammer, 2008), and are to a large extent associated with climate modes of variability internal to the coupled climate system and associated changes in the oceans flow field. For example, the large rates of sea level rise in the western tropical Pacific and the fall in the eastern Pacific over the period 1993-2010 correspond to an increase in the strength of the trade winds in the central and eastern tropical Pacific (Merrifield, 2011; Timmermann et al., 2010) over the same period. The long-term sea level trend from 1958 to 2001 in the tropical Pacific can also be explained as the ocean's dynamical response to variations in the wind forcing (Qiu and Chen, 2006; Timmermann et al., 2010). Han et al. (2010) suggested that regional changes of sea level in the Indian Ocean that have emerged since the 1960s are driven by changing surface wind associated with a combined enhancement of Hadley and Walker cells. Similar magnitude variations in the wind forcing and associated regional sea level are very likely to occur over coming decades.

13.7.2 GCM Projections/Predictions, Climate Modes and Forced Response

Existing climate models simulate only the dynamical component of sea level plus a global sea level change due to the uptake of heat or the addition of fresh water from terrestrial sources. Resulting regional sea level change projections over the 21st century can be expected to result partly from changing wind forcing (with associated redistribution of ocean properties) and partly from changes in the ocean heat and freshwater content and the associated dynamical adjustment. Both will be superimposed on the trend of global mean sea level rise.

Observations of regional sea level changes over the recent decade indicate that it is likely that local sea level changes for the next few decades will be dominated by interannual to decadal sea level variability caused by internal (dynamical) variability of the climate system, with good correspondence between regional sea level variability and changes in upper-ocean heat and salt content. To a large extent, this variability will result from a redistribution of ocean properties by natural climate modes in the coupled system, with wind remaining the primary driver of changes in the ocean circulation. However, climate modes and internal variability may change in the future relative to present conditions (Yin et al., 2010) which will complicate sea level projections on these time scales.

The CMP5 model ensemble simulates strong interannual variability in the tropical Pacific and Indian Oceans (>10 cm, RMS) associated with ENSO and dynamics of the equatorial current system (Figure 13.12a). Similar variability amplitudes are also apparent in the North Atlantic Current and over the southern ocean. In projections for the 21st century, the interannual variability of dynamic sea level weakens significantly in the South Pacific and parts of the Indian Ocean. (Figure 13.12b). In contrast, decadal variability is likely to increase in amplitude over the North Pacific, the tropical Pacific and the eastern subtropical Atlantic.

[INSERT FIGURE 13.12 HERE]

Figure 13.12: (a) RMS Interannual dynamic sea level variability (mm) in a CMIP5 multimodel ensemble (7 models total), built from the historically-forced experiments during the period 1951–2005; (b) Changes in the ensemble average inter-annual dynamic sea level variability (std. dev.; in mm) in 2081–2100 relative to 1986–2005. The projection data (2081-2100) is from the RCP4.5 experiment.

The contribution of long-term trends in sea level due to increased global heat uptake or changes in the freshwater content is likely to prevail over variability toward the end of the 21st century (to be quantified in SOD). In particular, the contribution of global ocean heat storage to regional steric sea level anomalies is very likely to gain importance with time as the climate-warming signal increasingly penetrates into the deep ocean (Pardaens et al., 2011b). This will make the uptake of heat a strong contributor to the predicted steric sea level rise on a centennial time scale. As an example, for the last three decades of the 21st century, the AR4 climate model ensemble mean shows significant heat storage in the tropical Atlantic and in a band in the Southern Ocean around 45°S (Yin et al., 2010). About half of this heat is stored in the ocean below 700 m depth. In the SRES A1B scenarios over the course of the 21st century, the ensemble mean shows significant ocean heat storage in almost the entire world ocean. Exceptions are some subpolar regions in the Atlantic and the Southern Ocean, and parts of the Arctic. The pattern resembles the ensemble mean thermosteric sea level rise. Similar to the 20th century simulations, the high-latitude deep ocean plays an important role for ocean heat up-take (see also Landerer et al., 2007).

Recent analyses have detected changes in the ocean salinity structure (Durack and Wijffels, 2010) that may be important for future regional steric sea level changes. Halosteric effects can be important, and in some regions can dominate, especially in regions of high-latitude water mass formation where we also expect long-term heat and freshwater uptake to take place (e.g., in the subpolar North Atlantic, the Arctic, the Southern Ocean) (Pardaens et al., 2011a; Yin et al., 2010). It is likely that in the future thermosteric changes will dominate the steric variations in the Southern Ocean, halosteric changes will dominate in the Arctic and strong compensation between thermosteric and halosteric change will characterise the Atlantic (Pardaens et al., 2011a). Because of anticipated increased atmospheric moisture transport from low to high latitudes (Pardaens et al., 2003), future halosteric anomalies are likely to be negative in the North Atlantic basin and partly compensate the thermosteric sea level increase there. However, they are positive in the Arctic Ocean and dominate regional sea level anomalies (Yin et al., 2010).

[PLACEHOLDER FOR SECOND ORDER DRAFT: add CMIP5 results and discuss the differences between models.]

Projections of steric sea level changes toward the end of the 21st century, displayed in Figure 13.13 as an ensemble mean over 7 CMIP5 models, reveal a clear regional pattern in steric sea level change, in which the Southern Ocean shows a net decline, while the remaining global ocean displays complex ridge-and-trough structures in a generally rising sea level. For example, in the North Atlantic, sea level rises strongest along the North Atlantic Current, but less so further to the south. A similar dipole pattern was induced in CMIP3 results by a weakening of the AMOC which leads to a local steric sea level rise east of North America, which drives more waters toward the shelf, directly impacting northeastern North America (Landerer et al., 2007; Levermann et al., 2005; Yin et al., 2010). Suzuki et al. (2005) compared changes in mean dynamic sea level in 2080–2100 relative to 1980–2000 as obtained form a low and a high-resolution ocean component of a coupled model. The authors conclude that changes are comparable, but that the high-resolution model presents enhanced details due to ocean eddy dynamics.

The spread of the ensemble is shown in the lower panel of the figure and indicates that all regions showing an enhanced sea level toward the end of the 21st century coincide with those showing the largest uncertainty.

[INSERT FIGURE 13.13 HERE]

Figure 13.13: (a) CMIP5 ensemble mean projection of the steric sea level in 2081–2100 relative to 1986–2005 computed from 7 models (in mm), using the RCP4.5 experiment. The figure includes the globally averaged steric sea level increase. (b) RMS spread (deviation) of the ensemble mean (mm).

Over time scales longer than a few days, the ocean adjusts nearly isostatically to regional changes in atmospheric pressure relative to its instantaneous mean over the ocean (i.e., inverted barometer effect). Sea level pressure is projected to increase over the subtropics and mid-latitudes (depressing sea level) and decrease over high latitudes (raising sea level), especially over the Arctic (order several millibars by the end of the 21st century) associated with a poleward expansion of the Hadley Circulation and a poleward shift of the storm tracks of several degrees latitude, with a consequent increase in cyclonic circulation patterns over the high-latitude Arctic and Antarctic regions (Held and Soden, 2006). The Arctic might therefore become a region where the atmospheric inverse barometer effect will contribute positively to the halosteric sea level rise (Yin et al., 2010). Stammer and Hüttemann (2008) showed that coupled climate models that do not include the effect of changes in atmospheric moisture content on sea level pressure will underestimate future regional loading effects by up to 2 cm.

13.7.2.1 Summary Assessment

There is high confidence that regional sea level changes over the next few decades will be dominated by interannual to decadal sea level variability caused by internal (dynamical) variability of the climate system. It is likely (medium to high confidence) that the contribution of long-term trends in sea level due to increased global heat uptake or changes in the freshwater content will progressively dominate regional pattern of sea level change toward the end of the 21st century, at least for the upper end of the projections. Nevertheless there is a consensus that the redistribution of heat and salt in the ocean as a response to changing winds will always be a significant factor to regional sea level changes which to first order will not project on global mean sea level.

13.7.3 Response to Freshwater Forcing

13.7.3.1 Dynamic Ocean Response to Freshwater Forcing

Enhanced freshwater fluxes derived from an increase in ice-sheet melt water at high latitudes results in a regional pattern of sea level rise. This addition of freshwater to the ocean is communicated around the ocean basins within days, resulting in an increase in global mean sea level (Gower, 2010; Lorbacher et al., submitted). However, an increase in freshwater from Greenland melting results in an additional basin-wide steric response of the North Atlantic on timescales of a few years, communicated via boundary waves, equatorial Kelvin waves, and westward propagating baroclinic Rossby waves (Stammer, 2008). An associated complete baroclinic adjustment of the global ocean might take as long as 500 years.

The adjustment of the ocean to high-latitude meltwater input also involves atmospheric and oceanic teleconnections. Stammer et al. (2011) suggested a rapid communication of sea level changes due to Greenland melt water pulses to other basins via an atmospheric bridge, triggering an ENSO-like response in the Pacific within just a few months. The atmospheric bridge from the tropical North Atlantic into the Arctic is particularly important and sensitive to the mean atmospheric state, which is poorly simulated in many coupled GCMs. On longer-than-decadal time scales, the freshwater input to the North Atlantic raises sea level in the Arctic Ocean and reverses the Bering Strait throughflow, transporting colder, fresher water from the Arctic Ocean into the North Pacific (Hu et al., 2010) and causing a large part of the North Pacific cooling (Okumura et al., 2009).

Meltwater forcing in the subpolar North Atlantic also causes changes of the AMOC, which in turn causes dynamic changes of sea level in the North Atlantic, particularly in its northwestern region. The combination of this dynamic sea level rise and the global mean sea level exposes northeastern North America to some of the fastest and largest sea level rise during this century (Yin et al., 2009). Lorbacher et al. (2010) showed that the diagnosed patterns of sea-surface height (SSH) anomalies associated with changes in the AMOC in the North Atlantic depend on the time scales of interest. Model hindcast simulations for 1958–2004 showed that

the pattern is primarily related to the wind-driven variability of the AMOC and gyre circulation on interannual time scales and is not useful as a "fingerprint" of longer term changes in the AMOC due to Greenland melting because the ability to detect such a trend is low along the Gulf Stream. More favourable signal-to-noise ratios are found in the subpolar gyre and the eastern North Atlantic, where a significant imprint in SSH is apparent after about 20 years.

13.7.3.2 Earth and Gravitational Response to Contemporary Surface Water Mass Redistribution

Ice-sheet melting and corresponding water mass redistribution between the cryosphere, the land and the oceans causes solid Earth and rotational responses to the varying loads and distinctive regional changes in the gravity field and sea level ("fingerprints") (Gomez et al., 2010b; Mitrovica et al., 2009; Mitrovica et al., 2001; Riva et al., 2010b) (see FAQ 13.1). Most existing studies have presented results that do not define a specific rate of polar ice-sheet mass loss (Mitrovica et al., 2001) or are based on end-member scenarios of ice retreat, such as from the West Antarctic ice sheet (Bamber et al., 2009; Gomez et al., 2010b; Mitrovica et al., 2009) and marine-based parts of the East Antarctic ice sheet (Gomez et al., 2010b). All of these studies demonstrate that the sea level response to these events includes a large departure from the mean value, whereby regions experiencing mass loss are subject to relative sea level fall up to several times the global average rise from these mass contributions, whereas in the far field the sea level rise is larger (up to about 30%) than the global average rise from these mass contributions (Gomez et al., 2010a; Mitrovica et al., 2009; Mitrovica et al., 2001) (Gomez et al., 2010a). A difference in the maximum predicted rise (relative to the global mean) between groups has been shown to be due to the accuracy with which water expulsion from the deglaciated marine basins is calculated (Gomez et al., 2010b; Mitrovica et al., 2011). Note that these changes are in addition to the ongoing response to past changes (e.g., glacial isostatic adjustment in response to the most recent deglaciation).

Currently, the ice-sheet fingerprints have not yet been detected in the observations and thus are likely small to date compared to steric effects. However, with further ice-sheet melting, it is likely that they will begin to dominate the regional patterns of sea level change (Kopp et al., 2010). These fingerprints will dominate most quickly nearest the melting ice sheets where the precise pattern of the sea level response is sensitive to the detailed melt geometry

Water mass redistributions associated with land hydrology changes may also produce spatially variable 'fingerprints" in sea level (Fiedler and Conrad, 2010). In particular regional changes in the terrestrial storage of water (in addition to loss of ice) can lead to a sea level response on interannual and longer time scales, specifically near large river basins (Riva et al., 2010a).

13.7.3.3 Summary Assessment

It is likely (high confidence) that in 21st century regional sea level changes, there will be a significant contribution arising from melting polar ice masses in the form of a dynamical steric response of the ocean and in the form of a solid Earth and rotational responses to varying loads of polar ice masses and distinctive regional changes in the gravity field. While the former contribution can project on global mean sea level increase, there is high confidence that it will be most prominent on regional and basin scales. Both contributions to first order would be volume conserving such that a resulting sea level decline around shrinking polar ice masses will lead to an increase in sea level over the rest of the ocean.

13.7.4 Net Regional SSH Changes on Decadal to Centennial Time Scales

The net regional SSH changes over the next decades are likely to be dominated by dynamical changes (mass redistribution and steric components) superimposed on a global sea level rise. Accordingly, natural variability of sea level will continue to lead to periods of lower and higher regional sea levels. However, during the 21st century, the mean rise will progressively dominate over the natural variability in mean sea level, at least for the upper end of the projections.

Net regional sea level projections for the 21st century are a composite of (1) the impacts of steric and dynamic changes as projected by AOGCMs, (2) mass changes of the ocean from glaciers and ice sheets, including the regional patterns from both contemporary and past changes in land ice, (3) changes in the

atmospheric loading, and (4) vertical land motion. Katsman et al. (2011) and Slangen et al. (2011); see also Church et al. (2011b) estimated net regional sea level projections based on AR4 climate model projections. To do so, they adopted the 21st century land-ice changes estimated by Meehl et al. (2007), with the exception of using more recent information on glaciers (Radic and Hock, 2010). Hu et al. (2011) suggested that steric and dynamical sea- level changes can potentially increase the sea level increase near the northeastern coast of North America and in the western Pacific.

[PLACEHOLDER FOR SECOND ORDER DRAFT: add CMIP5 results and discuss the differences between models.]

Slangen et al. (2011) and Church et al. (2011a) have combined these fingerprints and GIA with the AR4 projections to provide regional patterns of sea level change in the 21st century. These results suggest that for the 21st century, past, present and future loss of land ice is likely to remain an important contributor to spatial structures in sea level change.

Figure 13.14 shows regional sea level projections based on CMIP5 climate model projections. These results show the fingerprint of a sea level fall in proximity to ablating ice masses, leading to rates of maximum rise at low to mid latitudes due to this ice melt and GIA processes. The contribution from ongoing viscous deformation from past changes in land ice is generally small relative to that due to contemporary ice changes and steric processes, except in regions that experienced large ice loss during the most recent deglaciation (e.g., Canada and northwest Eurasia), where this signal was shown to be of equal amplitude. The dynamic ocean contribution in response to the influx of freshwater associated with land-ice loss (Section 13.7.2.1.2) was not considered in their analysis. Land vertical motion can also contribute significantly to projected sea level changes; in some regions land uplift might be significant, leading to a decrease of relative sea level.

[INSERT FIGURE 13.14 HERE]

Figure 13.14: [PLACEHOLDER FOR SECOND ORDER DRAFT: CMPI5 results.] Ensemble mean RSL contribution (m) of ice sheets (upper left), glaciers (upper right), steric changes (lower left) and GIA (lower right) for scenario A1B between 1980–1999 and 2090–2099. White shading in upper left panel indicates the mass loss regions on AIS and GIS (from Slangen et al., 2011).

The ensemble mean sea level anomaly pattern (Figure 13.15) reveals that many regions are likely to experience regional sea level changes that differ substantially from the global mean, with a maximum that is greater than twice the global mean as well as regions where a substantial fall in sea level is expected. The ensemble spread appears to be dominated by the spread in the steric contribution, which remains poorly understood. Spatial variations are apparent which in many places can lead to reduction of net sea level relative to a global mean, for example by more than 1 m close to polar ice sheets. For individual locations, the one sigma uncertainty in the ensemble is approximately 20 cm.

[INSERT FIGURE 13.15 HERE]

Figure 13.15: [PLACEHOLDER FOR SECOND ORDER DRAFT: CMPI5 results.] Ensemble mean sea level anomaly (m) with respect to global mean RSL change (0.47 m) for scenario A1B between 1980–1999 and 2090–2099 (from Slangen et al., 2011). Global mean = 0.47 m; range = –3.65 to +1.01 m.

[PLACEHOLDER FOR SECOND ORDER DRAFT: To be expanded/updated when CMIP projections are available – will show global results and some key locations around the globe.]

The combination of the natural variability and the projected sea level rise from the AR4 has been considered for a number of islands in the westerns Pacific Ocean (Australian Bureau of Meteorology and CSIRO, 2011). For example, in Palau (8°N, 135°E) in the western equatorial Pacific (Figure 13.16), the available historical record indicates monthly variability in mean sea level has been about 36 cm (5–95% range, after removal of the seasonal signal; dashed lines in Figure 13.16). It is likely that a similar range will continue through the 21st century. By 2090, the average projected sea level for the A1B scenario of 38 cm (with a 5 to 95% range of 18 to 59 cm) is greater than any observations of monthly mean sea level in the instrumental record. Of course, monthly variability and extreme sea levels from winds and waves associated with weather phenomena (Section 13.8) need to be considered in addition to these projections of mean sea level.

[INSERT FIGURE 13.16 HERE]

Figure 13.16: [PLACEHOLDER FOR SECOND ORDER DRAFT: CMPI5 results. To be expanded/updated f when CMIP projections are available – will show results for some key locations around the globe.] Observed and projected relative sea level change near Palau. The observed *in situ* relative sea level records (since the late 1970s) are indicated in blue, with the satellite record (since 1993) in green. The gridded sea level at Cook Islands (since 1950, from Church and White, 2011) is shown in red. The projections for the A1B scenario (5–95% uncertainty range) are shown by the shaded region from 1990–2100. The range of projections for the A1B, A2 and B1 scenarios by 2100 are also shown by the bars on the right. The dashed lines are an estimate of interannual variability in sea level (5–95% range about the long-term trends) and indicate that individual monthly averages of sea level can be above or below longer term averages.

13.7.4.1 Summary Assessment

It is very likely (high confidence) that in the 21st century, net sea level change will have a strong regional pattern which will lead to significant deviations in local and regional sea level change from a global mean. There is a consensus that future regional sea level change will result from a combination of dynamical ocean changes, mass changes of the ocean from glaciers and ice sheets, including the regional patterns from both contemporary and past changes in land ice, changes in the atmospheric loading, and vertical land motions, with relative contributions from each varying significantly across the oceans. It is likely (high confidence) that over large parts of the ocean regional sea level rise will be positive, but that amplitudes can vary by a factor of 2-3 relative to the global sea level crease.

13.7.5 Uncertainties and Sensitivity to Ocean/Climate Model Formulations and Parameterizations

Sea level is a property of the ocean connected to nearly all dynamical and thermodynamical processes over the full ocean column, from the surface fluxes to the ocean bottom. Improvements in the skill of a sea level projection require a reduction in the limitations of ocean models, such as through the use of (1) better parameterizations of unresolved physical processes, (2) improved numerical algorithms for such processes as tracer advection, (3) refined grid resolution to better represent such features as boundary currents and mesoscale eddies, and (4) the elimination of obsolete assumptions that have a direct impact on sea level (e.g., rigid lid and virtual tracer fluxes). Among the many limiting approximations made in ocean models, the Boussinesq approximation has been found to only marginally impact regional patterns (i.e., deviations from global mean) when directly compared to non-Boussinesq simulations (Losch et al., 2004), thus lending greater confidence in Boussinesq models for addressing questions of regional sea level change. Furthermore, for global sea level, the now standard a posteriori adjustment of Greatbatch (1994) accurately incorporates the missing global steric effect.

Coarse-resolution ocean-climate simulations require a parameterization of mesoscale and smaller eddies, but the parameterizations as well as the details of their numerical implementations can greatly impact the simulation. The Southern Ocean is an example, whereby projections for the 21st century suggest a drop in sea level associated with an increase in ACC transport largely arising from changes in winds (Yin et al., 2010; Pardaens et al., 2011b). As shown by Farneti et al. (2010), however, the coarse climate models may be over-estimating the ACC response to wind changes. Better implementations of eddy parameterizations reduce such biases (Farneti and Gent, 2011; Gent and Danabasoglu, 2011), and they form the basis for some, but not all, of the CMIP5 simulations. Moreover, Vinogradov and Ponte (2011) suggested that as one considers regional sea level variability and its relevant dynamics and forcing, mesoscale ocean features become important factors on a sub-decadal time scale.

Even with a perfect ocean model, skill in sea level projections depends on skill of the coupled climate model in which errors impacting sea level may originate from non-ocean components. Furthermore, initialization is fundamental to the prediction problem, particularly for simulation of low-frequency climate variability modes (Meehl et al., 2010). Projections of land-ice melting and the resultant sea level rise patterns also have large uncertainties, with additional uncertainties arising from GIA models such as the mantle viscosity structure. Each of the many uncertainties and errors results in considerable spread in the projected patterns of sea level changes in the CMIP3 models used as part of AR4, which is similar to the spread seen in the TAR models (Pardaens et al., 2011b; Slangen et al., 2011).

13.8 21st Century Projections of Sea Level Extremes and Waves

Climate change is likely to affect extreme sea levels and ocean waves in two principal ways. First, extra-tropical and tropical storms are the key drivers of extreme wave and water-level events, so that changes in intensity, frequency, duration, and path of these storms will have impacts on wave and water-level extremes. Second, sea level rise adds to the heights of sea level extremes, regardless of how the storm-related component evolves. Sea level rise also may increase the threat of coastal inundation due to wave runup. Here we assess projections for extreme water levels and waves based on estimates of future storminess and sea level rise.

13.8.1 Changes in Sea Level Extremes

As discussed in the AR4 (Bindoff et al., 2007) and confirmed by more recent studies (Menéndez and Woodworth, 2010), statistical analyses of tide-gauge observations have shown an increase in observed sea level extremes worldwide that are caused primarily by an increase in MSL (Chapter 3). Because tide-gauge stations are commonly situated in protected sites, they do not monitor the effects of changes in wave heights on sea level extremes over time. There has been some indication that the amplitude and phase of tidal heights have exhibited long-term change (Müller et al., 2011), but their impacts on extreme levels are not well understood.

Dominant modes of climate variability also have a measureable influence on extreme sea levels in many regions, particularly the El Niño–Southern Oscillation (ENSO) and the North Atlantic Oscillation (NAO) (reviewed by (Lowe et al., 2010; Walsh et al., 2011). These impacts are due to water-level anomalies associated with the climate mode, as well as mode-related changes in storminess.

13.8.2 Projections of Extreme Sea Levels

13.8.2.1 Recent Projection Assessments

The AR4 assessed projections of storm surges for a few regions (Europe, Australia, the Bay of Bengal) based on a limited number of dynamical modeling studies (Christensen et al., 2007). Their results generally indicated higher magnitude surges in future scenarios; however, confidence in these projections was low because of the wide spread in AOGCM and RCM projections. Lowe et al. (2010) completed a comprehensive review of changes in observed extremes and their driving forces and future projections, and concluded that the increases in the observed sea level extremes in the 20th century occurring primarily through an increase in MSL apply to the projections for the 21st century as well.

Studies since the AR4 have also considered extreme sea levels in other regions, including the relative contributions of sea level rise and storminess on projected extremes. As summarized by the SREX assessment (Seneviratne et al., 2012), most projections for the end of the 21st century find it likely that extremes will continue to track MSL, while some studies find that changes in storminess will cause additional changes in extreme surges in the 21st century. The SREX assessment (Seneviratne et al., 2012) reported also that it is likely that global tropical cyclone frequency will decrease or remain roughly constant, but medium confidence is assigned to the projection that the frequency of the most intense storms will increase in some ocean basins. Uncertainties in projections of the frequency and track of cyclones make it difficult to project how these changes will impact particular regions. Similarly, while the SREX and the current assessment (Chapter 14) find that it is likely that there has been a poleward shift in the main northern and southern extra-tropical cyclone tracks during the last 50 years, and that regional changes may be substantial, there is only low confidence in region-specific projections.

13.8.2.2 Projections Based on Dynamical Models

Projected changes in storminess have been assessed by directly applying climate-model forcing to a storm-surge model. Using three regionally downscaled GCMs for A2, B2 and A1B scenarios, Debernard and Roed (2008) found statistically significant changes between 1961–1990 and 2071–2100 of an 8–10% increase in the 99th percentile surge heights, mainly during the winter season along the coastlines of the eastern North Sea and the northwestern British Isles, and decreases south of Iceland. Using a downscaled GCM under an A1B scenario, Wang et al. (2008) projected a significant increase in wintertime storm surges around most of Ireland between 1961–1990 and 2031–2060. Sterl et al. (2009) concatenated the output from a 17-member

ensemble of A1B simulations from a GCM over the model periods 1950–2000 and 2050–2100 into a single longer time series to estimate 10,000-year return values of surge heights (relative to mean sea level) along the Dutch coastline. No statistically significant change in this value was projected for the 21st century because projected wind-speed changes were not associated with the maximum surge-generating northerlies. These studies demonstrate that the results are sensitive to the particular choice of GCM or RCM, therefore indicating uncertainties associated with the projections. Unnikrishnan et al. (2011) used RCM simulations to force a storm-surge model for the Bay of Bengal and found that the combined effect of sea level rise and RCM projections for the A2 scenario (2071–2100) gave an increase in 100-year return levels of total sea level, (including tides), varying between 0.40 and 0.67 m (about 5–20%) along the northern part of the east coast of India compared to those in the base line (1961–1990) scenario.

Several regional projections of storm surges attempted to assess the relative contribution of the two main causative factors, sea level rise and changes in projected atmospheric fields, on the changes in future sea level extremes. Studies by McInnes et al. (2009) for southeastern Australia, Brown et al. (2010) for the eastern Irish Sea, and Woth et al. (2006) for the North Sea showed that sea level rise has a greater potential than meteorological changes to increase extreme sea levels by the end of the 21st century in these locations. Using six hypothetical hurricanes that produce approximate 100-year return levels, Smith et al. (2010) found that on the southeastern Louisiana coast in the regions of large surges, the effect of mean sea level rise on simulated surges was linear. However, in the regions of moderate surges (2–3 m), particularly in wetland-fronted areas, the increase in surges was very large (by 1–3 m).

They showed that sea level rise alters the speed of propagation of surges and their amplification varied in different regions of the coast. Harper et al. (2009) constructed populations of synthetic cyclones representing current climate in tropical Australia to force storm-surge models, and perturbed them to represent projected future climates. They found a relatively small impact of a 10% increase in tropical cyclone intensity for the 1-in-100 year total sea level (including tides), compared with the projected sea level rise off the tropical east coast of Australia.

13.8.2.3 Projections Based on Statistical Methods

There have been some statistical methods used to project extreme sea level, mostly at local scales. Cayan et al. (2008) constructed hourly time series of sea level for the 21st century for three tide gauge stations in California by adding (i) the predicted tides, (ii) sea level rise projections, (iii) sea level fluctuations and (iv) a contribution due to the ENSO mode. Sea level fluctuations were derived by first developing a regression relation between the 20th century observed sea level fluctuations and fluctuations in sea level pressure and wind stress and then applying this to the 21st century CM2.1 projection of sea level pressure and wind stress. The contribution due to the ENSO mode was estimated through a regression relation derived for the 20th century between NINO 3.4 SSTs and smoothed observed sea level at tide gauge stations in California. Analysis of the resulting hourly time series for the 21st century showed that towards the low-end SRES scenario of sea level rise, extremes changed similar to those of MSL, while towards the high-end scenario of sea level rise, the frequency and magnitude of extremes increased considerably relative to those experienced in the 20th century. In the Gulf of Mexico, Mousavi et al. (2011) developed a simple relationship between hurricane-induced storm surges, sea level rise and hurricane intensification through increased SSTs for three modeled major historical cyclones, and found that the dynamic interaction of surge and sea level rise lowered or amplified the surge at different points within a shallow coastal bay.

13.8.2.4 Sea Level Allowance for Extreme Events

Based on the assumption that projected increase in extreme sea levels is largely due to an increase in MSL, Hunter (2010) described a method of combining observations of present sea level extremes with the projections of sea level rise to obtain a "sea level allowance." This allowance is calculated so that the expected frequency of flooding events is preserved. It is based on the projected rise in mean sea level and its uncertainty, and on the variability of tides and storm surges (which are parameterised by the scale parameter of their Gumbel distribution). The method was applied to 198 tide gauge stations over the globe, yielding estimates of the scale parameter (a measure of the variability of high sea levels), which varied between 0.05 and 0.20 m for 90% of the stations considered (Hunter, in press) (Figure 13.17). Figure 13.17 shows that early in the 21st century, when the uncertainty is small, the allowance is approximately the projected central

value of the sea level rise. However, later in the century, when the uncertainty in the projections is larger, the sea level allowance tends towards the upper limits of the projected rise.

13.8.2.5 Summary Assessment

To conclude, there is medium-to-high confidence that 21st century projected increases in extreme sea levels will occur, primarily through an increase in MSL. There is low confidence in the projected regional variations of the sea level rise (Section 13.7), and also in the (likely small) changes in the contribution to extreme sea levels by storm surges caused by atmospheric forcing alone. If the expected frequency of flooding of coastal infrastructure is not to increase, the allowance for sea level rise needs to be greater than the central sea level rise projections.

[INSERT FIGURE 13.17 HERE]

Figure 13.17: Sea level allowance based on scale parameters of 0.05 and 0.20 m (covering 90% of the global range) for the A1FI projections. For each scale parameter, there are two curves (for 0.20 m the two curves are not distinguishable): the upper one is based on fitting a normal uncertainty distribution to the 5 to 95-percentile limits, while the lower one is based on a raised-cosine distribution. Also shown are the mean and the 5 to 95-percentile range of projections based on the A1FI emission scenario and a combination of the results of the TAR and AR4.

13.8.3 Projections of Ocean Waves

Wave-field variability is dictated by changes in the major wind systems, especially in the main tropical and extra-tropical storm tracks. Prevailing wind and storm characteristics are known to vary with natural modes of climate variability (see Chapter 14), and a number of studies have related changes in wave climatologies with climate modes, notably ENSO (Adams et al., 2008; Allan and Komar, 2006; Menéndez et al., 2008), the NAO (Izaguirre et al., 2010; Woolf et al., 2002), and SAM (Hemer et al., 2010a; Izaguirre et al., 2011). The primary challenges for wave projection efforts are to determine what anthropogenic-driven changes in winds are likely to occur, to separate these effects from natural variability, and to translate these changes into wave-field climatologies on a global and regional scale.

13.8.3.1 Storm Projections and Ocean Waves

The AR4 assessment, the SREX assessment (Seneviratne et al., 2012) and the current assessment (Chapter 3) have reviewed evidence for positive, as well as negative, wave-height trends based on in-situ observations. Trends and variability in wave heights since the early 1990s have been described using satellite altimeter data (Hemer et al., 2010a; Izaguirre et al., 2011; Young et al., 2011). Based on in-situ and altimeter observations, it is likely that wave heights have increased in the North Pacific over the past century, in the North Atlantic since the 1950s, and the Southern Ocean over the last two decades (Chapter 3). Nevertheless, the observational record is sparse in space and time, which limits attempts to separate anthropogenic from natural controls on wave-height changes. Wang et al. (2009) concluded that the effects of anthropogenic forcing are detectable during winter months at high latitudes, particularly in the northeastern North Atlantic. However, their simulations, based on geostrophic wind energy, underestimate observed wave-height changes during 1955-2004, which increases the uncertainty about this finding.

For long-term wind projections, the SREX (Seneviratne et al., 2012) and current (Chapter 14) assessments report a likely poleward shift in mid-latitude winter storm tracks, with less certainty regarding future changes in tropical cyclones. In the Southern Hemisphere, this shift is likely associated with a trend toward a positive SAM phase, with an increase in wind speeds. In general, there is low confidence in basin-specific projections of tropical cyclones. As noted in Chapter 14, projections for ENSO remain uncertain, and model projections show that the NAO tends toward a more positive phase, but the amplitude change is slight.

13.8.3.2 Wave Projections Based on Climate Models

Although uncertainties remain regarding future storm patterns, there has been recent progress in translating climate model outputs into wave projections. The AR4 reported projected increases in global SWHs in a future warmer climate from a single statistical projection of Wang and Swail (2006). The projected conditions were consistent with increased wind speeds associated with mid-latitude storms, but considered

only a limited five-member ensemble for a single future emission scenario (SRES A2), leading to high, or unquantified, uncertainty. Wave parameters other than SWH were not considered in the assessment.

Since the AR4, several methods of deriving wave-climate projections have been pursued, largely involving dynamical (Andrade et al., 2007; Debernard et al., 2002; Debernard; RØEd 2008; Grabemann and Weisse, 2008; Hemer, submitted; Hemer et al., submitted-b; Leake et al., 2007; Lionello et al., 2008; Mori et al., 2010) and statistical methods (Caires et al., 2006; Wang and Swail, 2006; Wang et al., 2010). In the dynamical approach, climate model (global or regionally downscaled) derived surface fields force a spectral wave model that generates the wave prediction. Bias-adjustments can be applied to the climate model surface forcing (Hemer, submitted; Hemer et al., submitted-b; Wang et al., 2010). The statistical approach uses current climate reanalyses to establish a statistical relationship between atmospheric conditions (e.g., MSLP, 10-m winds) and SWH. The statistical relationship established is then applied to climate model projections to derive SWH projections, under the assumption that the statistics are stationary. These relationships can be derived from global or regional scale studies.

These multiple approaches introduce a further level of uncertainty within wave-climate projections in addition to scenario-specific inter- and intra-climate model uncertainties common to other climatological parameters. Wave projection studies to date have been carried out largely in isolation without adequate quantification of the uncertainty inherent in the different approaches (Hemer et al., 2010b). A collaborative intercomparison program is now underway with the aim of assessing the robustness of available wind-wave climate projections, as well as isolating dominant sources of uncertainty (Coordinated Ocean Wave Climate Projections (COWCLIP); (Hemer et al., submitted-c).

Few global wave-climate projections exist. Global dynamical projections under an SRES A1B future emission scenario (Mori et al., 2010) are qualitatively consistent with the statistical projections of Wang and Swail (2006) discussed in the AR4 (under an SRES A2 scenario), and quantitative comparisons are underway as part of the COWCLIP program. The region with the largest projected change is the high southern latitudes, where mean SWH at the end of the 21st century is approximately 0.3–0.4 m higher than the present-day mean. Mori et al. (2010) projected extreme SWH in the equatorial Pacific (50-year SWH) to increase by 60% over present-day values, mostly due to projected changes in tropical cyclone intensity and frequency.

A number of dynamical wave-projection studies have been carried out with a regional focus. For the Mediterranean Sea, Lionello et al. (2010; 2008) projected a widespread shift of the wave-height distribution to lower values by the mid-21st century under an SRES A1B scenario, implying a decrease in mean and extreme wave heights. Several studies have developed wave-climate projections in the North Sea using statistical and dynamical approaches. Despite several of these being derived from the same GCM and emission scenarios (SRES B2 and A2), projected changes in wave height over the 21st century span a broad range from a 21 cm (4%) decrease in extreme heights (Leake et al., 2009) to an insignificant change in SWH (Caires et al., 2008; Debernard; RØEd 2008) to a 35 cm (5–8%) increase in extreme wave heights with greater (less) contribution of westerly directed waves in the eastern (western) North Sea (Grabemann and Weisse, 2008). The range of uncertainty observed in projected conditions results from different regional dynamical downscaling models and different approaches to developing wave projections.

Dynamical wave-climate projection studies have also been carried out for open coasts of the North Atlantic. Under the A2, B2 and A2B scenarios, Leake et al. (2009) projected larger waves at the end of the 21st century south of the UK, but smaller waves to the north. Along the Portuguese coast, Andrade et al. (2007) found while there was no projected change in SWH under the SRES A2 scenario, there was a projected rotation in wave direction so that waves had a greater northerly orientation at the end of the 21st century.

Using a dynamical approach to determine projected change in wave conditions on the Australian east coast, Hemer (submitted) and Hemer et al. (submitted-a) reported a small projected decrease in mean SWH (<5cm) and a southerly rotation of wave direction under SRES A2 and B1 scenarios, consistent with a projected southward shift of the sub-tropical ridge in the forcing fields.

[INSERT FIGURE 13.18 HERE]

Figure 13.18: [PLACEHOLDER FOR SECOND ORDER DRAFT: COWCLIP results - will present overview of wave projections based on studies to date, with indication of robustness between studies.]

13.8.3.3 Projections of Coastal Waves and Inundation

Coastal inundation is strongly impacted by wave runup, which is a combination of increased coastal water levels associated with breaking waves (wave setup) and variable water levels associated with shoaling waves and lower frequency infragravity waves. When storm-driven waves and surges coincide with the occurrence of high tides, coastal flooding becomes increasingly large. Wave runup scales with offshore SWH (Stockdon et al., 2006) hence climate-related projections of offshore SWH generally apply to coastal runup (Ruggiero, 2008). The uncertainties inherent in specifying future storminess also limit confidence in projections of runup, as they do for SWH.

In addition, sea level rise is a robust component of future climate change, and the impact of sea level rise on runup warrants consideration. Along sandy beaches and exposed shorelines, runup does not scale with water level (Stockdon et al., 2006), hence sea level rise is an independent additive term in runup projections, as in the case of extreme storm surge heights. The impact of sea level rise on coastal morphology is a separate issue that is reviewed in the SREX report (Seneviratne et al., 2012). Along coastlines protected by shallow fringing reefs, such as tropical islands and atolls, components of wave runup do scale with water level (Péquignet et al., 2011). Along these shorelines, sea level rise likely will have a two-fold impact on inundation as water level and runup energy increase. The effect will be mitigated to the extent that the depth of fringing reef platforms can keep pace with sea level rise under the impacts of climate change (Hoegh-Guldberg et al., 2007).

13.8.3.4 Summary Assessment

Sea and swell waves reflect changes in surface winds and storm patterns, hence it is likely that climate change will have a significant impact on SWHs and other wave properties. Dynamical and statistical techniques for wave projections are improving, and ensemble assessments of wave-model projections are beginning to quantify uncertainties. Nevertheless, wave projections ultimately are only as good as the wind fields used to generate them, and significant uncertainties are involved in the specification of future winds, particularly storm winds. Accordingly, wave projections are presented with low confidence, with medium confidence assigned to wave-field changes associated with the poleward migration of winter storm tracks at mid-latitudes, which in the Southern Ocean is associated with a trend toward a more positive SAM state and more energetic waves.

13.9 Synthesis and Key Uncertainties

It is virtually certain that global averaged sea level has been rising through the 20th century and into the early 21st, that there has been an increase in the rate of rise since preindustrial times, that we know the major contributions to this rise, and that sea level will continue to rise during the 21st century and beyond. Figure 13.19 provides a schematic representation of the major changes affecting past and future sea level change.

The evidence for historical sea level rise comes from coastal and island sea level measurements around the world, with the longest tide-gauge records dating back to the 18th century. Since the early 1990s, satellite altimeters have allowed the first global perspective on sea level variability and rise and have revealed its complex temporal and spatial structure as well as the ongoing global average rise. Geological data support the long tide-gauge records that there has been an increase in the rate of rise from the order of a few tenths of a mm yr^{-1} over the last two millennia to a value approaching 2 mm yr^{-1} for the 20th century. The altimeter data and the *in situ* data indicate an increase to over 3 mm yr^{-1} since 1993. Our understanding using both observations and models has improved such that we now have a quantitative explanation for the observed rise over recent decades. However, details of the variability of sea level change over recent millennia, when the acceleration to modern values occurred, how large any 20th century acceleration was and the regional distribution of 20th century sea level rise remain uncertain.

The major contributions to sea level rise over the last 40 years have come from ocean thermal expansion, particularly of the upper layers of the ocean, and the melting of glaciers. There have also been smaller

contributions from melting of the Greenland Ice Sheet and most recently an increase in ice discharge from both the Greenland and Antarctic ice sheets. While the first three of these are directly related to warming atmospheric temperatures, the increased ice discharge is thought to be related to ocean temperature changes through regional changes in ocean circulation. The relationship of these circulation changes to climate change remains unclear. There has also been a contribution from changes in terrestrial water storage unrelated to climate change. The models are now reproducing the observed faster rate of rise since 1993. However, our understanding is far from perfect with inadequate knowledge about the longer-term ocean contribution, particularly in the southern hemisphere and the deep ocean, inadequate inventories and rates of change of glaciers, and inadequate understanding and models of the ice sheets. Solving these uncertainties, particularly those related to the ice sheets, is central to improved projections.

The oceans, glaciers and the ice sheets all have long time scales. As a result, they will all continue to contribute to sea level change and it is virtually certain that global averaged sea level will continue to rise during the 21st century and very likely for centuries after 2100. Major contributions will come from ocean thermal expansion and glacier melting, increased melting on Greenland, with these positive contributions partly offset by increased accumulation on Antarctica. The amount of increased ice discharge from the ice sheets is uncertain but on the multi-century time scales this is likely to be the dominant cause of sea level change.

There remains uncertainty about the rate of rise during the 21st century with semi-empirical models projecting a larger rate of rise than process-based models. The improved explanation of historical sea level rise from process-based models gives greater confidence to their projections which lie in the range 0.27 to 0.50 m for RCP2.6, 0.32to 0.56 m for RCP4.5 and RCP6.0, 0.41 to 0.71 m for RCP8.5 (2081 to 2100 compared to 1986 to 2005). The paleo evidence also indicates upper limits for the rates of rise during relevant but incomplete analogues of about 1 m century^{-1}. The largest uncertainty in projecting 21st century (and beyond) sea level rise relates to the inadequately understood behaviour of the ice sheets.

The distribution of sea level change is likely to be non-uniform. Wind patterns directly impact the regional distribution of sea level on interannual and decadal time scales and this variability will be the dominant signal over the next few decades. However, as the mean rise progresses, changes in winds, ocean circulation (and ocean temperatures and salinities), the distribution of water around the globe and hence the Earth's gravitational field and vertical land motion will all impact the regional distribution of sea level rise. At the current time we have little understanding of the reasons for the differences between the regional projections from climate models. However, while the pattern of change remains uncertain, it is very likely that over the majority of the ocean regional sea level rise will be positive.

Higher sea levels have already affected the frequency that extreme sea level thresholds are exceeded. For many locations, this is very likely to continue with rising sea levels, whether or not there is a change in storm frequency or intensity.

The rate of rise is relatively independent of greenhouse gas emission trajectories for the next several decades and there is a long-term commitment to future rise even with substantial reductions in greenhouse gas emissions. However, by 2100 and particularly on the longer time scales, different emission scenarios have an increasingly large impact on sea level rise, and higher emission scenarios may commit the world to metres of sea level rise, particularly if warming thresholds are crossed leading to potentially irreversible sea level rise on millennial time scales. Knowledge of these thresholds and rates of change are inadequate. However, the available paleo evidence indicates that during the last interglaciation, when temperatures were at values we could reach during the 21st century, sea levels were metres higher than present-day values; older paleo evidence indicates even higher sea levels are possible. This requires meter-scale contributions from the ice sheets as ocean thermal expansion and glacier melting would be insufficient to explain the observations.

[INSERT FIGURE 13.19 HERE]

Figure 13.19: Schematic diagram of the major changes that influenced sea level during the 20th century and will potentially to drive sea level change during the 21st century and beyond.

[START FAQ 13.1 HERE]

FAQ 13.1: Why does Local Sea Level Change Differ from the Global Average?

Local sea level change departs from the global average value because the processes that cause sea levels to change (some climate related and others not) do not result in only a globally uniform signal. For example, ocean warming and land-ice melting will contribute not only to global mean sea level rise in the future, but both of these processes will also result in spatially variable patterns of sea level change. On the other hand, some processes such as changes in the wind forcing will only influence regional sea levels.

Observations of sea-surface height (SSH) change from satellite altimetry since 1993 illustrate that sea level does not rise uniformly. FAQ 13.1, Figure 1a shows average rates of SSH change (in mm yr^{-1}) for the period 1993 to 2010 determined from satellite altimetry. Using these observations, the global average rate of change is 3.2 ± 0.5 mm yr^{-1}, or a total rise in global mean SSH of 5.4 ± 0.85 cm over the 17-year period. FAQ 13.1, Figure 1a shows that, in many areas, average rates of local SSH change deviated significantly from the global mean rate during this period. For example, the western Pacific Ocean experienced rates of rise about three times greater than the global mean value. In contrast, the eastern Pacific Ocean is characterised by rates that are lower than the global mean value, with much of the west coast of the Americas experiencing a SSH fall during this period.

Due to the relatively short time period spanned by the satellite observations, it is important to note that the spatial pattern shown in FAQ 13.1, Figure 1a is strongly influenced by processes operating on interannual to decadal timescales (such as El Nino and the Pacific Decadal Oscillation). SSH trends evaluated over a longer time period (40 years and longer) would look substantially different since the influence of these relatively short-term processes on longer term trends is relatively small. Measurements from a small selection of tide gauges illustrate this point (also shown in FAQ 13.1, Figure 1a). Note that these data measure vertical motion of the sea surface relative to the sea floor, and so the signal due to land motion has been estimated and removed so that the tide gauge and satellite data sets can be compared. At the locations where tide gauge data are shown in FAQ 13.1, Figure 1a, the average rate of change determined is, in general, substantially different from the altimeter rate. Note that the tide gauge data clearly show the high-amplitude shorter term (decadal and less) changes that are evident in the spatial pattern of the altimeter measurements (FAQ 13.1, Figure 1a; e.g., El Nino and Pacific Decadal Oscillation).

Much of the spatial variability captured by the satellite measurements was due to changes in ocean temperature and salinity (steric sea level). Changes in local ocean temperature and salinity are intimately linked to atmosphere-ocean interactions over decadal timescales, particularly changes in wind forcing and associated changes in the ocean flow field. Input of glacial meltwater has also influenced the density structure of the oceans, probably leading to some of the spatial variability shown in FAQ 13.1, Figure 1a. Glacial meltwater influences the temperature, salinity and density structure of the ocean where it is input and also at distance from the source as the salinity and temperature anomalies propagate outwards, thus affecting SSH changes over relatively large areas through changes in ocean density (steric change) and the associated changes in ocean circulation.

In addition to the processes that cause changes in SSH and thus contribute to the observations shown in FAQ 13.1, Figure 1a, changes in sea level can also be affected by vertical motion of the ocean floor. Indeed, it is the relative vertical motion between the ocean surface and ocean floor that governs the relative change in sea level at a given coastal location; it is this quantity, known as relative sea level, that is used to assess the risk of flooding over a given time period. While rapid vertical ocean-floor displacements are possible (e.g., through the occurrence of earthquakes), on time scales of decades to millennia, steady ductile deformation of rock deep within the Earth is one of the primary natural process through which vertical land motion influences relative sea level change. There is considerable spatial variability in this secular component of vertical land motion across the globe and so, in order to capture the full spatial variability in relative sea level change, the ocean floor component should be added to the SSH component.

On regional to global scales, vertical land motion is dominated by two processes: deformation due to the transfer of mass on the Earth's surface (isostasy) and deformation due to plate tectonics. The latter can be significant in specific areas, particularly those near convergent plate margins (e.g., Japan, Chile). In most areas at present, the ongoing isostatic adjustment associated with the large transfer of water mass from ice

sheets to oceans during the recent glacial-interglacial transition (approximately 20,000 years to 6,000 years before present) is the dominant contributor to vertical land motion. A model estimate of the contribution of this process to contemporary vertical land motion is shown in FAQ 13.1, Figure 1b. Locations where large ice sheets once existed (e.g., northern North America; Fennoscandinavia) are characterised by regions of sea-floor uplift (sea level fall) exceeding values of 10 mm yr^{-1}. In these areas, the sea-floor component of sea level change dominates that due to SSH change. Peripheral to these regions are well-defined areas of sea-floor subsidence with rates up to several mm yr^{-1} which contribute to an enhanced relative sea level rise (e.g., east and west coasts of North America; southern shore of the North Sea). These regions of isostatically driven sea-floor uplift and subsidence result from the melting of large ice sheets during the most recent glacial-interglacial transition (i.e., ice unloading). There are also more subtle signals embedded in FAQ 13.1, Figure 1b associated with the addition of melt water to the ocean basins and the consequent loading of the ocean floor and changes in Earth rotation associated with the isostatic deformation. For example, the enhanced sea-floor uplift adjacent to southern South America is due to both of these effects.

A large amount of land ice currently exists on the Earth in the form of glaciers and ice sheets (Greenland and Antarctica). Melting of these reservoirs results in vertical motion of both SSH and the ocean floor. An example of model output due to contemporary (as opposed to past) melting of the Greenland and Antarctic ice sheets is shown in FAQ 13.1, Figure 1c. The model prediction shows that sea levels fall within a region peripheral to the melt sources and rise by an amount greater than the global mean value in low-to-mid latitude areas distant from the melting ice sheets. This is due to the influence of the ice sheet changes on the Earth's gravity field as mass is transferred from land (in the form of ice) to the oceans. The mass transfer also results in deformation of the solid (rocky) Earth and changes in Earth rotation which contribute to the total signal shown in FAQ 13.1, Figure 1c. Contemporary melting of land ice (the large ice sheets in this case) is another example of a process that leads to a distinct spatial pattern in sea level change.

In summary, a variety of processes lead to height changes of the ocean surface and ocean floor that have distinct spatial signatures. The combination of these processes leads to a pattern of total sea level change that is complex and varies through time as the relative contribution of each process changes. While the global average change is a useful integrated value that is sensitive to the contribution of climatic processes (land-ice melting and ocean warming) and represents a good first order estimate of relative sea level change at many coastal locations, it is evident from the above discussion that departures from the global average can be large and should also be considered when projecting regional to local changes in sea level. Projections at these scales are necessary to accurately evaluate the risk of flooding at specific localities.

[INSERT FAQ 13.1, FIGURE 1. HERE]

FAQ 13.1, Figure 1. (a) Sea-surface height (SSH) trends (in mm yr^{-1}) from October 1992 to December 2010 from satellite altimetry. Also shown are time series from selected tide gauge stations (red lines) for the period 1950 to 2010. Note that the tide gauge data have been corrected for vertical land motion due to glacial isostatic adjustment. For comparison, an estimate of global mean sea level change (and associated uncertainty) is also shown (black line) with each tide gauge time series. (b) A map of present-day vertical sea-floor motion associated with the on-going deformation of the solid Earth due to the large reduction in land-ice volume that occurred between about 20,000 and 6,000 years before present. Note that, this deformation influences the gravity field and thus also contributes to relative sea level through changes in SSH. (c) Model output showing relative sea level change due to melting of the Greenland ice sheet and the West Antarctic ice sheet at rates of 0.5 mm yr^{-1} each (giving a global mean value of 1 mm yr^{-1}). In this case, the spatial pattern reflects vertical changes in both SSH and the sea floor in response to the contemporary re-distribution of mass between the ice sheets and the oceans.

[END FAQ 13.1 HERE]

[START FAQ 13.2 HERE]

FAQ 13.2: Will the Greenland and Antarctic Ice Sheets Contribute to Sea Level Change?

The Greenland, West and East Antarctic ice sheets (GIS, WAIS and EAIS, respectively) are the largest reservoirs of freshwater on the planet, and have contributed to sea level change over geological and recent times. They gain mass through accumulation (snowfall) and lose it by surface ablation (mostly ice melt where air temperatures are warm enough) and outflow at their marine boundary either by flow to a floating

ice shelf or ice berg calving. Likely increases in accumulation will cause global mean sea level to fall, while likely increases in surface ablation and increases in outflow, about which we have less confidence, will cause it to rise. Fluctuations in these mass fluxes depend on a range of processes both internal to the ice sheet and externally linked to changes in the atmosphere and oceans; however, we are confident that sources of mass loss will exceed sources of mass gain so that a continuing positive contribution to global sea level can be expected over the next century.

Over many millennia, the slow horizontal flow of an ice sheet carries mass from areas of net accumulation (generally in the high-elevation interior) to net loss (generally at the low-elevation periphery and the coastal perimeter). At present, Greenland loses roughly half of its accumulated ice by surface ablation and half by calving; whereas Antarctica loses virtually all its accumulation by outflow to ice shelves, where it is lost by calving and the submarine melt. Ice shelves displace ocean water and their loss therefore has a negligible effect on sea level.

In EAIS, some studies using satellite radar altimetry suggest that snowfall has increased, while recent atmospheric modelling and satellite gravimetric observations find no significant increase. This apparent disagreement may be because long-term trends are masked by the strong inter-annual variability of snowfall. Projections of 21st century Antarctic snowfall suggest significant increases are likely, deriving primarily from the increased ability of the warmer polar atmosphere to hold moisture with regional changes in atmospheric circulation playing a secondary role.

Air temperatures around Antarctica are very likely to remain too cold for substantial surface ablation. Satellite-based and field observations suggest that a small number of localised coastal regions are currently experiencing enhanced outflow, manifested as ice-surface lowering. These areas (primarily Pine Island and Thwaites Glaciers of WAIS, Totten and Cook Glaciers of EAIS) all lie within km-deep bedrock troughs and occupy positions towards the edge of Antarctica's continental shelf. The increase in outflow is likely to have been triggered by regional ocean warming.

Although the area of Antarctica affected by enhanced outflow is many times smaller than that experiencing increased snow accumulation, mass loss by this means is likely to currently exceed mass gain. Projecting outflow during the 21st century is a research challenge requiring improvements in our ability to simulate changes in the grounding line that separates floating ice from that resting on bedrock, and interactions between ice shelves and the ocean affecting submarine melting. The theory of 'marine ice sheet instability' relies on the idea that the outflow from an ice sheet resting on bedrock below sea level grows as ice thickness at the grounding line increases; on bedrock that slopes downward towards the ice-sheet centre this then leads a vicious circle of increased outflow, retreat into thicker ice and further increases in outflow. This process could then potentially result in the rapid loss of sectors of the ice sheet as grounding lines retreat along troughs and basins that deepen towards the ice sheet's interior. Such an unstable collapse could be independent of climate forcing, and could occur on timescales of centuries (for individual troughs) to millennia (for WAIS and sectors of EAIS). Much research effort is currently focused on understanding how important this theoretical concept is for WAIS and EAIS.

In the more northerly Antarctic Peninsula, there is a well-documented record of ice-shelf collapse that is very likely related to increased surface melting caused by atmospheric warming over recent decades. The collapse and associated thinning of glaciers draining into these ice shelves has had a positive but minor effect on sea level, as will any further such events in the Peninsula. Current projections of 21st century climate suggest that this process is unlikely to affect the stability of the large ice shelves of the WAIS and EAIS.

Estimates of the contribution of the Antarctic ice sheets to sea level over the last few decades vary widely. There are indications that enhanced outflow (primarily in WAIS) is beginning to outweigh increases in snow accumulation (primarily in EAIS) implying a tendency towards sea level rise. In the future, the effects of marine instability may become important but current evidence is insufficient to unambiguously identify the precursor of such an unstable retreat.

In Greenland, a range of observations suggests that accumulation rates have increased slightly over the interior of the ice sheet, most likely related to a warmer atmosphere. Despite the large area affected, however, this mass gain is more than compensated by increases in mass loss through increased surface

ablation and outflow. Mass loss due to surface ablation is very likely to have doubled since the early 1990s and this trend will very likely continue over the next century as more of the ice sheet experiences surface ablation for longer fractions of the year. Indeed, projections for the 21st century suggest that increasing mass loss will very likely dominate over weakly increasing accumulation. The refreezing of melt water within the snow pack high up on the ice sheet offers an important (though perhaps temporary) dampening effect on the relation between atmospheric warming and mass loss.

Ice berg calving from many of Greenland's major outlet glaciers is very likely to have increased significantly over the last decade, and constitutes an appreciable additional mass loss. This appears to be related to the intrusion of warm water into the coastal seas around Greenland but it is not clear whether this phenomenon is related to inter-decadal variability (such as the North Atlantic Oscillation) or a longer-term trend, and there are recent indications that many outlet glaciers are now slowing. Although this makes projections of its effect on 21st century outflow difficult, it does highlight the sensitivity of outflow to ocean warming. The impacts of increased amounts of surface melt water on basal lubrication and the ability of ice to deform more easily may lead to greater rates of flow but the link to increased outflow is presently unclear.

The Greenland ice sheet has contributed to a rise in global mean sea level over the last few decades and this trend will very likely increase over the next century. In contrast to Antarctica, no large-scale instabilities are known that could generate an abrupt increase in the rate of sea level rise but it is likely that a threshold exists so that continued shrinkage may become irreversible even assuming a return to pre-industrial climate on centennial time scales. While mass loss through the calving of ice bergs may increase in future decades, this process will eventually end as the ice margin retreats onto bedrock above sea level where the bulk of the ice sheet resides.

[INSERT FAQ 13.2, FIGURE 1 HERE]

FAQ 13.2, Figure 1: Current and future (circa 2100) ice-sheet processes associated with sea level rise. (upper left) Greenland Ice Sheet during the last decade showing areas experiencing thinning more than 0.2 m yr^{-1} (red), thickening more than 0.2 m yr^{-1} (dark blue). Contemporary equilibrium line altitude (ELA) is shown as a dashed line. (lower left) Schematic illustration of Greenland projections for 2090–2099 showing ELA and area greater than 200 m below sea level, suggesting that future interaction with the oceans will be limited. (upper right) Antarctic ice sheets during the last decade indicating areas experiencing thinning and thickening (same colour scale). (lower right) Schematic illustration of Antarctic projections for 2090–2099 showing coincidence of areas currently experiencing thinning and areas grounded below sea level that are connected to the ocean.

[END FAQ 13.2 HERE]

References

Ablain, M., A. Cazenave, G. Valladeau, and S. Guinehut, 2009: A new assessment of the error budget of global mean sea level rate estimated by satellite altimetry over 1993–2008. *Ocean Sci.*, **5,** 193-201.

Adams, P. N., D. L. Inman, and N. E. Graham, 2008: Southern California Deep-Water Wave Climate: Characterization and Application to Coastal Processes. *Journal of Coastal Research***,** 1022-1035.

Allan, J. C., and P. D. Komar, 2006: Climate Controls on US West Coast Erosion Processes. *Journal of Coastal Research***,** 511-529.

Allen, M., D. Frame, C. Huntingford, C. Jones, J. Lowe, M. Meinshausen, and N. Meinshausen, 2009: Warming caused by cumulative carbon emissions towards the trillionth tonne. *Nature*, **458,** 1163-1166.

Amundson, J. M., M. Fahnestock, M. Truffer, J. Brown, M. P. M. P. Luthi, and R. J. Motyka, 2010: Ice melange dynamics and implications for terminus stability, Jakobshavn Isbræ, Greenland. *JOURNAL OF GEOPHYSICAL RESEARCH*, **115,** F01005.

Andrade, C., H. O. Pires, R. Taborda, and M. C. Freitas, 2007: Projecting future changes in wave climate and coastal response in Portugal by the end of the 21st century. *Journal of Coastal Research*, **Special Issue 50,** 263-257.

Andrade, C., Pires, H.O., Taborda, R., Freitas, M.C., 2007: Projecting future changes in wave climate and coastal response in Portugal by the end of the 21st century. *Journal of Coastal Research*, **Special Issue 50,** 263-257.

Anschütz, H., and Coauthors, 2009: Revisiting sites of the South Pole Queen Maud Land Traverses in East Antarctica: Accumulation data from shallow firn cores. *Journal of Geophysical Research-Atmospheres*, **114**.

Arthern, R., D. Winebrenner, and D. Vaughan, 2006: Antarctic snow accumulation mapped using polarization of 4.3-cm wavelength microwave emission. *Journal of Geophysical Research-Atmospheres*, **111,** -.

Bahr, D. B., and M. Dyurgerov, 1999: Characteristic mass-balance scaling with valley glacier size. *Journal of Glaciology*, **45,** 17-21.

Bahr, D. B., M. Dyurgerov, and M. F. Meier, 2009: Sea level rise from glaciers and ice caps: A lower bound. *Geophysical Research Letters*, **36,** 4.

Bales, R., and Coauthors, 2009: Annual accumulation for Greenland updated using ice core data developed during 2000-2006 and analysis of daily coastal meteorological data. *Journal of Geophysical Research-Atmospheres*, **114,** -.

Bamber, J. L., R. E. M. Riva, B. L. A. Vermeersen, and A. M. LeBrocq, 2009: Reassessment of the Potential Sea level Rise from a Collapse of the West Antarctic Ice Sheet. *Science*, **324,** 901-903.

Bartholomew, I., P. Nienow, D. Mair, A. Hubbard, M. A. King, and A. Sole, 2010: Seasonal evolution of subglacial drainage and acceleration in a Greenland outlet glacier. *Nature Geoscience*, **3,** 408-411.

Becker, M., B. Meyssignac, W. Llovel, A. Cazenave, and T. Delcroix, 2011: Sea level variations at Tropical Pacific Islands since 1950. *Global and Planetary Change*.

Beckley, B. D., and Coauthors, 2010: Assessment of the Jason-2 Extension to the TOPEX/Poseidon, Jason-1 Sea-Surface Height Time Series for Global Mean Sea Level Monitoring. *Marine Geodesy*, **33,** 447-471.

Bedford, D., 1996: A new digitized glacier inventory for the Former Soviet Union and China., C. Haggerty, Ed.

Bengtsson, L., S. Koumoutsaris, and K. Hodges, 2011: Large-scale surface mass balance of land ices from a comprehensive atmosphere model. *Surveys in Geophysics*, **32,** 459-474.

——, submitted: Large-scale surface mass balance of land ices from a comprehensive atmosphere model. *Surveys in Geophysics*.

Benn, D. I., C. R. Warren, and R. H. Mottram, 2007: Calving processes and the dynamics of calving glaciers. *Earth-Science Reviews*, **82,** 143-179.

Biancamaria, S., A. Cazenave, N. Mognard, W. Llovel, and F. Frappart, 2011: Satellite-based high latitude snow volume trend, variability and contribution to sea level over 1989/2006. *Glob. Planetary Change*, **75,** 99-107.

Bindoff, N. L., and Coauthors, 2007: Observations: Oceanic climate change and sea level. *Climate change 2007: the physical science basis*, S. Solomon, and D. Qin, Eds., Cambridge Univ. Press, 385-432.

Blum, M. D., and H. H. Roberts, 2009: Drowning of the Mississippi Delta due to insufficient sediment supply and global sea level rise. *Nature Geoscience*, **2,** 488-491.

Bougamont, M., and Coauthors, 2007: The impact of model physics on estimating the surface mass balance of the Greenland Ice Sheet. *Geophys. Res. Lett.*, **34,** L17501.

Box, J., L. Yang, D. Bromwich, and L. Bai, 2009: Greenland Ice Sheet Surface Air Temperature Variability: 1840-2007. *Journal of Climate*, **22,** 4029-4049.

Bracegirdle, T. J., W. M. Connolley, and J. Turner, 2008a: Antarctic climate change over the twenty first century. *Journal of Geophysical Research-Atmospheres*, **113,** 13.

——, 2008b: Antarctic climate change over the twenty first century. *Journal of Geophysical Research-Atmospheres*, **113**.

Broerse, D., L. Vermeersen, R. Riva, and W. van der Wal, 2011: Ocean contribution to co-seismic crustal deformation and geoid anomalies: Application to the 2004 December 26 Sumatra-Andaman earthquake. *Earth and Planetary Science Letters*, **305,** 341-349.

Brohan, P., J. J. Kennedy, I. Harris, S. F. B. Tett, and P. D. Jones, 2006: Uncertainty estimates in regional and global observed temperature changes: A new data set from 1850. *Journal of Geophysical Research-Atmospheres*, **111**.

Bromwich, D., J. Nicolas, and A. Monaghan, 2011: An Assessment of Precipitation Changes over Antarctica and the Southern Ocean since 1989 in Contemporary Global Reanalyses. *Journal of Climate*, **24,** 4189-4209.

Bromwich, D., R. Fogt, K. Hodges, and J. Walsh, 2007: A tropospheric assessment of the ERA-40, NCEP, and JRA-25 global reanalyses in the polar regions. *Journal of Geophysical Research-Atmospheres*, **112,** -.

Brown, J., A. Souza, and J. Wolf, 2010: Surge modelling in the eastern Irish Sea: present and future storm impact. *Ocean Dynamics*, **60,** 227-236.

Burgess, E., R. Forster, J. Box, E. Mosley-Thompson, D. Bromwich, R. Bales, and L. Smith, 2010: A spatially calibrated model of annual accumulation rate on the Greenland Ice Sheet (1958-2007). *Journal of Geophysical Research-Earth Surface*, **115,** -.

Caires, S., V. R. Swail, and X. L. Wang, 2006: Projection and Analysis of Extreme Wave Climate. *Journal of Climate*, **19,** 5581-5581-5589,5591-5593,5596-5597,5599,5601-5605.

Caires, S., J. Groeneweg, and A. Sterl, 2008: Past and future changes in North Sea extreme waves. *ICCE 2008*, Hamburg.

Calkin, P. E., G. C. Wiles, and D. J. Barclay, 2001: Holocene coastal glaciation of Alaska. *Quaternary Science Reviews*, **20,** 449-461.

Carton, J. A., B. S. Giese, and S. A. Grodsky, 2005: Sea level rise and the warming of the oceans in the Simple Ocean Data Assimilation (SODA) ocean reanalysis. *J. Geophys. Res.*, **110**.

Cayan, D., P. Bromirski, K. Hayhoe, M. Tyree, M. Dettinger, and R. Flick, 2008: Climate change projections of sea level extremes along the California coast. *Climatic Change*, **87,** 57-73.

Cazenave, A., and W. Llovel, 2010: Contemporary Sea Level Rise. *Annual Review of Marine Science*, **2,** 145-173.

Cazenave, A., and Coauthors, 2009: Sea level budget over 2003-2008: A reevaluation from GRACE space gravimetry, satellite altimetry and Argo. *Global and Planetary Change*, **65,** 83-88.

Chambers, D. P., 2006: Evaluation of new GRACE time-variable gravity data over the ocean. *Geophys. Res. Lett.*, **33**.

Chambers, D. P., J. Wahr, and R. S. Nerem, 2004: Preliminary observations of global ocean mass variations with GRACE. *Geophys. Res. Lett.*, **31,** doi:10.1029/2004GL020461.

Chambers, D. P., J. M. Wahr, M. Tamisiea, and R. S. Nerem, 2010: Ocean Mass from GRACE and Glacial Isostatic Adjustment. *J. Geophys. Res.*, **115**.

Chao, B. F., 1995: Anthropogenic impact on global geodynamics due to reservoir water impoundment. *Geophys. Res. Lett.*, **22,** 3529-3532.

Chao, B. F., Y. H. Wu, and Y. S. Li, 2008: Impact of artificial reservoir water impoundment on global sea level. *Science*, **320,** 212-214.

Charbit, S., D. Paillard, and G. Ramstein, 2008: Amount of CO(2) emissions irreversibly leading to the total melting of Greenland. *Geophysical Research Letters*, **35,** 5.

Christensen, J. H., and Coauthors, 2007: Regional climate projections. *Climate Change, 2007: The Physical Science Basis.*, Cambridge University Press.

Church, J., N. White, and J. Arblaster, 2005: Significant decadal-scale impact of volcanic eruptions on sea level and ocean heat content. *Nature*, **438,** 74-77.

Church, J., J. Gregory, N. White, S. Platten, and J. Mitrovica, 2011a: Understanding and Projecting Sea Level Change. *Oceanography*, **24,** 130-143.

Church, J. A., and N. J. White, 2006: A 20th century acceleration in global sea level rise. *Geophysical Research Letters*, **33**.

——, 2011: Sea level Rise from the Late 19th to the Early 21st Century. *Surveys in Geophysics*, **32,** 585-602.

Church, J. A., P. L. Woodworth, T. Aarup, and W. S. Wilson, Eds., 2010: *Understanding sea level rise and variability*. Wiley-Blackwell, 428 pp.

Church, J. A., N. J. White, R. Coleman, K. Lambeck, and J. X. Mitrovica, 2004: Estimates of the regional distribution of sea level rise over the 1950-2000 period. *Journal of Climate*, **17,** 2609-2625.

Church, J. A., and Coauthors, 2001: Changes in sea level. *Climate change 2001: The scientific basis. Contribution of Working Group I to the Third Assessment Report of the Intergovernmental Panel on Climate Change*, Cambridge University Press, 639-693.

Church, J. A., and Coauthors, 2011b: Revisiting the Earth's sea level and energy budgets from 1961 to 2008. *Geophysical Research Letters*, **38**.

Clarke, P., D. Lavallee, G. Blewitt, T. van Dam, and J. Wahr, 2005: Effect of gravitational consistency and mass conservation on seasonal surface mass loading models. *Geophysical Research Letters*, **32,** L08306.

Cogley, J. G., 2009a: Geodetic and direct mass-balance measurements: comparison and joint analysis. *Annals of Glaciology*, **50,** 96-100.

——, 2009b: A more complete version of the World Glacier Inventory. *Annals of Glaciology*, **50,** 32-38.

Colville, E., A. Carlson, B. Beard, R. Hatfield, J. Stoner, A. Reyes, and D. Ullman, 2011: Sr-Nd-Pb Isotope Evidence for Ice-Sheet Presence on Southern Greenland During the Last Interglacial. *Science*, **333,** 620-623.

Comiso, J. C., 2000: Variability and trends in Antarctic surface temperatures from in situ and satellite infrared measurements. *Journal of Climate*, **13,** 1674-1696.

Crowley, T. J., S. K. Baum, K.-Y. Kim, G. C. Hegerl, and W. T. Hyde, 2003: Modeling ocean heat content changes during the last millennium. *Geophys. Res. Lett.*, **30**.

Das, S. B., I. Joughin, M. D. Behn, I. M. Howat, M. A. King, D. Lizarralde, and M. P. Bhatia, 2008: Fracture propagation to the base of the Greenland Ice Sheet during supraglacial lake drainage. *Science*, **320,** 778-781.
De Angelis, H., and P. Skvarca, 2003: Glacier surge after ice shelf collapse. *Science*, **299,** 1560-1562.
de Berg, W. J. V., M. R. van den Broeke, C. H. Reijmer, and E. van Meijgaard, 2006: Reassessment of the Antarctic surface mass balance using calibrated output of a regional atmospheric climate model. *Journal of Geophysical Research-Atmospheres*, **111,** 15.
Debernard, J., Ø. Sætra, and L. P. Røed, 2002: Future wind, wave and storm surge climate in the northern North Atlantic. *Climate Research*, **23,** 39-49.
Debernard, J. B., and L. P. RØEd, 2008: Future wind, wave and storm surge climate in the Northern Seas: a revisit. *Tellus A*, **60,** 427-438.
Delworth, T. L., V. Ramaswamy, and G. L. Stenchikov, 2005: The impact of aerosols on simulated ocean temperature and heat content in the 20th century. *Geophysical Research Letters*, **32**.
Di Lorenzo, E., and Coauthors, 2010: Central Pacific El Nino and decadal climate change in the North Pacific Ocean. *Nature Geoscience*, **3,** 762-765.
Domingues, C. M., J. A. Church, N. J. White, P. J. Gleckler, S. E. Wijffels, P. l. M. Barker, and J. R. Dunn, 2008: Improved estimates of upper-ocean warming and multi-decadal sea level rise. *Nature*, **453,** 1090.
Douglas, B. C., 2001: Sea level change in the era of the recording tide gauge. *Sea level rise, History and consequences*, B. C. Douglas, M. S. Kearney, and S. P. Leatherman, Eds., Academic Press, 37-64.
Driesschaert, E., and Coauthors, 2007: Modeling the influence of Greenland ice sheet melting on the Atlantic meridional overturning circulation during the next millennia. *Geophysical Research Letters***,** ARTN L10707, DOI 10.1029/2007GL029516.
Dufresne, J.-L., and S. Bony, 2008: An assessment of the primary sources of spread of global warming estimates from coupled atmosphere-ocean models. *J. Climate*, **21,** 5135-5144.
Durack, P. J., and S. E. Wijffels, 2010: Fifty-Year Trends in Global Ocean Salinities and Their Relationship to Broad-Scale Warming. *Journal of Climate*, **23,** 4342-4362.
Durand, G., O. Gagliardini, T. Zwinger, E. Le Meur, and R. C. A. Hindmarsh, 2009: Full Stokes modeling of marine ice sheets: influence of the grid size. *Annals of Glaciology*, **50,** 109-114.
Dutton, A., and K. Lambeck, submitted: Ice volume and sea level during the last interglacial. *Science*.
Dyurgerov, M., M. Meier, and University of Colorado Boulder. Institute of Arctic and Alpine Research., 2005: *Glaciers and the changing earth system : a 2004 snapshot.* Institute of Arctic and Alpine Research, University of Colorado, 117 p. pp.
Dyurgerov, M. B., 2010: Reanalysis of Glacier Changes: From the IGY to the IPY, 1960-20080130-3686, 116 pp pp.
Easterling, D. R., and M. F. Wehner, 2009: Is the climate warming or cooling? *Geophys. Res. Lett.*, **36,** L08706.
Ericson, J., C. Vorosmarty, S. Dingman, L. Ward, and M. Meybeck, 2006: Effective sea level rise and deltas: Causes of change and human dimension implications. *Global and Planetary Change*, **50,** 63-82.
Ettema, J., M. van den Broeke, E. van Meijgaard, W. van de Berg, J. Bamber, J. Box, and R. Bales, 2009: Higher surface mass balance of the Greenland ice sheet revealed by high-resolution climate modeling. *Geophysical Research Letters*, **36,** -.
Farneti, R., and P. R. Gent, 2011: The effects of the eddy-induced advection coefficient in a coarse-resolution coupled climate model. *Ocean Modelling*, **39,** 135-145.
Farneti, R., T. L. Delworth, A. J. Rosati, S. M. Griffies, and F. Zeng, 2010: The Role of Mesoscale Eddies in the Rectification of the Southern Ocean Response to Climate Change. *Journal of Physical Oceanography*, **40,** 1539-1557.
Farrell, W. E., and J. A. Clark, 1976: On postglacial sea level. *Geophysical Journal of the Royal Astronomical Society*, **46,** 647-667.
Ferraccioli, F., E. Armadillo, T. Jordan, E. Bozzo, and H. Corr, 2009: Aeromagnetic exploration over the East Antarctic Ice Sheet: A new view of the Wilkes Subglacial Basin. *Tectonophysics*, **478,** 62-77.
Fettweis, X., E. Hanna, H. Gallee, P. Huybrechts, and M. Erpicum, 2008: Estimation of the Greenland ice sheet surface mass balance for the 20th and 21st centuries. *Cryosphere*, **2,** 117-129.
Fettweis, X., A. Belleflame, M. Erpicum, B. Franco, and S. Nicolay, 2011: Estimation of the sea level rise by 2100 resulting from changes in the surface mass balance of the Greenland ice sheet. *Climate Change - Geophysical Foundations and Ecological Effects*, J. Blanco, and H. Kheradmand, Eds., Intech, 503-520.
Fiedler, J. W., and C. P. Conrad, 2010: Spatial variability of sea level rise due to water impoundment behind dams. *Geophysical Research Letters*, **37,** -.
Fluckiger, J., R. Knutti, and J. White, 2006: Oceanic processes as potential trigger and amplifying mechanisms for Heinrich events. *Paleoceanography*, **21,** -.
Franco, B., X. Fettweis, M. Erpicum, and S. Nicolay, 2011: Present and future climates of the Greenland ice sheet according to the IPCC AR4 models. *Climate Dynamics*.
Fyke, J. G., L. Carter, A. Mackintosh, A. J. Weaver, and K. J. Meissner, 2010: Surface Melting over Ice Shelves and Ice Sheets as Assessed from Modeled Surface Air Temperatures. *Journal of Climate*, **23,** 1929-1936.
Gehrels, W. R., B. Hayward, R. M. Newnham, and K. E. Southall, 2008: A 20th century acceleration of sea level rise in New Zealand. *Geophysical Research Letters*, **35**.

Gehrels, W. R., and Coauthors, 2006: Rapid sea level rise in the North Atlantic Ocean since the first half of the nineteenth century. *Holocene*, **16,** 949-965.
Gent, P. R., and G. Danabasoglu, 2011: Response to Increasing Southern Hemisphere Winds in CCSM4. *Journal of Climate*, **24,** 4992-4998.
Genthon, C., G. Krinner, and H. Castebrunet, 2009: Antarctic precipitation and climate-change predictions: horizontal resolution and margin vs plateau issues. *Annals of Glaciology***,** 55-60.
Gillett, N., V. Arora, K. Zickfeld, S. Marshall, and A. Merryfield, 2011: Ongoing climate change following a complete cessation of carbon dioxide emissions. *Nature Geoscience***,** 83-87.
Gladstone, R. M., A. J. Payne, and S. L. Cornford, 2010a: Parameterising the grounding line in flow-line ice sheet models. *Cryosphere*, **4,** 605-619.
Gladstone, R. M., V. Lee, A. Vieli, and A. J. Payne, 2010b: Grounding line migration in an adaptive mesh ice sheet model. *Journal of Geophysical Research-Earth Surface*, **115**.
Gladstone, R. M., and Coauthors, 2011: Pine Island Glacier calibrated prediction with a flowline model.
Gladstone, R. M., and Coauthors, submitted: Pine Island Glacier calibrated prediction with a flowline model.
Gleckler, P., T. Wigley, B. Santer, J. Gregory, K. AchutaRao, and K. Taylor, 2006a: Krakatoa's signature persists in the ocean. *Nature*, **439,** 675-675.
Gleckler, P., K. AchutaRao, J. Gregory, B. Santer, K. Taylor, and T. Wigley, 2006b: Krakatoa lives: The effect of volcanic eruptions on ocean heat content and thermal expansion. *Geophysical Research Letters*, **33,** -.
Gleckler, P. J., and Coauthors, submitted: Robust evidence of human-induced global ocean warming on multi-decadal time scales. *Nature Climate Change*.
Goelzer, H., P. Huybrechts, M. Loutre, H. Goosse, T. Fichefet, and A. Mouchet, 2011: Impact of Greenland and Antarctic ice sheet interactions on climate sensitivity. *Climate Dynamics*, **37,** 1005-1018.
Goldberg, D., D. M. Holland, and C. Schoof, 2009: Grounding line movement and ice shelf buttressing in marine ice sheets. *Journal of Geophysical Research-Earth Surface*, **114**.
Gomez, N., J. X. Mitrovica, M. E. Tamisiea, and P. U. Clark, 2010a: A new projection of sea level change in response to collapse of marine sectors of the Antarctic Ice Sheet. *Geophysical Journal International*, **180,** 623-634.
Gomez, N., J. Mitrovica, M. Tamisiea, and P. Clark, 2010b: A new projection of sea level change in response to collapse of marine sectors of the Antarctic Ice Sheet. *Geophysical Journal International*, **180,** 623-634.
Gomez, N., J. X. Mitrovica, P. Huybers, and P. U. Clark, 2010c: Sea level as a stabilizing factor for marine-ice-sheet grounding lines. *Nature Geoscience***,** 850-853.
Gomez, N., D. Pollard, J. X. Mitrovica, P. Huybers, and P. U. Clark, submitted: Evolution of a coupled marine ice sheet - sea level model. *Journal of Geophysical Research*.
Good, P., J. M. Gregory, and J. A. Lowe, 2011: A step-response simple climate model to reconstruct and interpret AOGCM projections. *Geophysical Research Letters*, **38**.
Goosse, H., H. Renssen, A. Timmermann, and R. S. Bradley, 2005: Internal and forced climate variability during the last millennium: a model-data comparison using ensemble simulations. *Quaternary Science Reviews*, **24,** 1345-1360.
Gornitz, V., 2001: Impoundment, groundwater mining, and other hydrologic transformations: Impacts on global sea level rise. *Sea Level Rise, History and Consequences*, B. C. Douglas, M. S. Kearney, and S. P. Leatherman, Eds., Academic Press, 97-119.
Gouretski, V., and K. Koltermann, 2007: How much is the ocean really warming? *Geophysical Research Letters*, **34,** -.
Gower, J. F. R., 2010: Comment on "Response of the global ocean to Greenland and Antarctic ice melting" by D. Stammer. *Journal of Geophysical Research-Oceans*, **115**.
Grabemann, I., and R. Weisse, 2008: Climate change impact on extreme wave conditions in the North Sea: an ensemble study. *Ocean Dynamics*, **58,** 199-212.
Graversen, R. G., S. Drijfhout, W. Hazeleger, R. van de Wal, R. Bintanja, and M. Helsen, 2011: Greenland's contribution to global sea level rise by the end of the 21st century. *Climate Dynamics*, **37,** 1427-1442.
Greatbatch, R. J., 1994: A NOTE ON THE REPRESENTATION OF STERIC SEA LEVEL IN MODELS THAT CONSERVE VOLUME RATHER THAN MASS. *Journal of Geophysical Research-Oceans*, **99,** 12767-12771.
Gregory, J., 2000: Vertical heat transports in the ocean and their effect an time-dependent climate change. *Climate Dynamics***,** 501-515.
——, 2010: Long-term effect of volcanic forcing on ocean heat content. *Geophysical Research Letters*, **37,** -.
Gregory, J., and J. Oerlemans, 1998: Simulated future sea level rise due to glacier melt based on regionally and seasonally resolved temperature changes. *Nature*, **391,** 474-476.
Gregory, J. M., and P. Huybrechts, 2006: Ice-sheet contributions to future sea level change. *Philosophical Transactions of the Royal Society a-Mathematical Physical and Engineering Sciences*, **364,** 1709-1731.
Gregory, J. M., and P. M. Forster, 2008: Transient climate response estimated from radiative forcing and observed temperature change. *J. Geophys. Res.*, **113,** D23105.
Gregory, J. M., J. A. Lowe, and S. F. B. Tett, 2006: Simulated global-mean sea level changes over the last half-millennium. *J. Climate*, **19,** 4576-4591.
Greve, R., 2000: On the response of the Greenland ice sheet to greenhouse climate change. *Climatic Change***,** 289-303.
Greve, R., F. Saito, and A. Abe-Ouchi, 2011: Initial results of the SeaRISE numerical experiments with the models SICOPOLIS and IcIES for the Greenland ice sheet. *Annals of Glaciology*, **52,** 23-30.

Grinsted, A., J. Moore, and S. Jevrejeva, 2010: Reconstructing sea level from paleo and projected temperatures 200 to 2100 ad. *Climate Dynamics*, **,** 461-472.
Hamlington, B. D., R. R. Leben, R. S. Nerem, and K.-Y. Kim, 2011: Reconstructing sea level using cyclostationary empirical orthogonal functions. *J. Climate*, **in press**.
Han, W. Q., and Coauthors, 2010: Patterns of Indian Ocean sea level change in a warming climate. *Nature Geoscience*, **3,** 546-550.
Hanna, E., P. Huybrechts, I. Janssens, J. Cappelen, K. Steffen, and A. Stephens, 2005: Runoff and mass balance of the Greenland ice sheet: 1958-2003. *Journal of Geophysical Research-Atmospheres*, **110,** -.
Hanna, E., and Coauthors, submitted: Greenland Ice Sheet surface mass balance 1870 to 2100 based on Twentieth century reanalysis, and links with global climate forcing. *Journal of Geophysical Research*.
Hansen, J., M. Sato, P. Kharecha, G. Russell, D. Lea, and M. Siddall, 2007: Climate change and trace gases. *Philosophical Transactions of the Royal Society a-Mathematical Physical and Engineering Sciences*, 1925-1954.
Hansen, J., and Coauthors, 2005: Earth's Energy Imbalance: Confirmation and Implications. *Science*, **308,** 1431-1435.
Harper, B., T. Hardy, L. Mason, and R. Fryar, 2009: Developments in storm tide modelling and risk assessment in the Australian region. *Natural Hazards*, **51,** 225-238.
Hattermann, T., and A. Levermann, 2010: Response of Southern Ocean circulation to global warming may enhance basal ice shelf melting around Antarctica. *Climate Dynamics*, 741-756.
Hearty, P. J., J. T. Hollin, A. C. Neumann, M. J. O'Leary, and M. McCulloch, 2007: Global sea level fluctuations during the Last Interglaciation (MIS 5e). *Quaternary Science Reviews*, **26,** 2090-2112.
Hegerl, G. C., and Coauthors, 2007: Understanding and attributing climate change. *Climate Change 2007: The Physical Science Basis. Contribution of Working Group I to the Fourth Assessment Report of the Intergovernmental Panel on Climate Change*, Cambridge University Press.
Held, I., M. Winton, K. Takahashi, T. Delworth, F. Zeng, and G. Vallis, 2010: Probing the Fast and Slow Components of Global Warming by Returning Abruptly to Preindustrial Forcing. *Journal of Climate*, 2418-2427.
Held, I. M., and B. J. Soden, 2006: Robust responses of the hydrological cycle to global warming. *Journal of Climate*, **19,** 5686-5699.
Hemer, M. A., submitted: Climate and variability bias adjustment of climate model-derived winds for a southeast Australian dynamical wave model. *Ocean Dynamics*.
Hemer, M. A., J. A. Church, and J. R. Hunter, 2010a: Variability and trends in the directional wave climate of the Southern Hemisphere. *International Journal of Climatology*, **30,** 475-491.
Hemer, M. A., K. McInnes, and R. Ranasinghe, submitted-a: Exploring uncertainty in regional East Australian wave climate projections. *International Journal of Climatology*.
Hemer, M. A., K. L. McInnes, and R. Ranasinghe, submitted-b: Exploring uncertainty in regional East Australian wave climate projections. *International Journal of Climatology*.
Hemer, M. A., X. L. Wang, J. A. Church, and V. R. Swail, 2010b: COORDINATING GLOBAL OCEAN WAVE CLIMATE PROJECTIONS. *Bulletin of the American Meteorological Society*, **91,** 451-451-454.
Hemer, M. A., X. L. Wang, R. Weisse, V. R. Swail, and C. Team, submitted-c: Community advancing wind-waves climate science: the COWCLIP project. *Bulletin of the American Meteorological Society*.
Hindmarsh, R. C. A., 1993: Qualitative dynamics of marine ice sheet. *Ice in the climate system*, W. R. Peltier, Ed., Springer-Verlag, 67-99.
Hoegh-Guldberg, O., and Coauthors, 2007: Coral reefs under rapid climate change and ocean acidification. *Science*, **318,** 1737-1742.
Hofmann, D., J. Barnes, M. O'Neill, M. Trudeau, and R. Neely, 2009: Increase in background stratospheric aerosol observed with lidar at Mauna Loa Observatory and Boulder, Colorado. *Geophys. Res. Lett.*, **36,** L15808.
Holgate, S., S. Jevrejeva, P. Woodworth, and S. Brewer, 2007: Comment on "A semi-empirical approach to projecting future sea level rise". *Science*, **317,** 2.
Holgate, S. J., 2007: On the decadal rates of sea level change during the twentieth century. *Geophysical Research Letters*, **34**.
Holgate, S. J., and P. L. Woodworth, 2004: Evidence for enhanced coastal sea level rise during the 1990s. *Geophysical Research Letters*, **31,** -.
Holland, D. M., R. H. Thomas, B. De Young, M. H. Ribergaard, and B. Lyberth, 2008a: Acceleration of Jakobshavn Isbrae triggered by warm subsurface ocean waters. *Nature Geoscience*, **1,** 659-664.
Holland, P. R., A. Jenkins, and D. M. Holland, 2008b: The response of ice shelf basal melting to variations in ocean temperature. *Journal of Climate*, **21,** 2558-2572.
Horton, R., C. Herweijer, C. Rosenzweig, J. P. Liu, V. Gornitz, and A. C. Ruane, 2008: Sea level rise projections for current generation CGCMs based on the semi-empirical method. *Geophysical Research Letters*, **35,** 5.
Hu, A., G. A. Meehl, W. Han, and J. Yin, 2011: Effect of the potential melting of the Greenland Ice Sheet on the Meridional Overturning Circulation and global climate in the future. *Deep-Sea Research Part Ii-Topical Studies in Oceanography*, **58,** 1914-1926.
Hu, A. X., and Coauthors, 2010: Influence of Bering Strait flow and North Atlantic circulation on glacial sea level changes. *Nature Geoscience*, **3,** 118-121.
Huber, M., and R. Knutti, submitted: Anthropogenic and antural warming inferred from changes in Earth's energy balance. *Nature Geoscience*.

Hunter, J., 2010: Estimating sea level extremes under conditions of uncertain sea level rise. *Climatic Change*, **99,** 331-350.
Hunter, J., in press: A simple technique for estimating an allowance for uncertain sea level rise. *Climatic Change*.
Huntington, T. G., 2008: Can we dismiss the effect of changes in land-based water storage on sea level rise? *Hydrological Processes*, **22,** 717-723.
Huybrechts, P., and J. De Wolde, 1999: The dynamic response of the Greenland and Antarctic ice sheets to multiple-century climatic warming. *J. Climate*, **12,** 2169-2188.
Huybrechts, P., H. Goelzer, I. Janssens, E. Driesschaert, T. Fichefet, H. Goosse, and M. Loutre, 2011a: Response of the Greenland and Antarctic Ice Sheets to Multi-Millennial Greenhouse Warming in the Earth System Model of Intermediate Complexity LOVECLIM. *Surveys in Geophysics*, **32,** 397-416.
Huybrechts, P., H. Goelzer, I. Janssens, E. Driesschaert, T. Fichefet, H. Goosse, and M. F. Loutre, 2011b: Response of the Greenland and Antarctic Ice Sheets to Multi-Millennial Greenhouse Warming in the Earth System Model of Intermediate Complexity LOVECLIM. *Surveys in Geophysics*, **32,** 397-416.
Ishii, M., and M. Kimoto, 2009: Reevaluation of historical ocean heat content variations with time-varying XBT and MBT depth bias corrections. *Journal of Oceanography*, **65,** 287-299.
Izaguirre, C., F. J. Méndez, M. Menéndez, and I. J. Losada, 2011: Global extreme wave height variability based on satellite data. *Geophysical Research Letters*, **38,** L10607.
Izaguirre, C., F. J. Mendez, M. Menendez, A. Luceño, and I. J. Losada, 2010: Extreme wave climate variability in southern Europe using satellite data. *J. Geophys. Res.*, **115,** C04009.
Jacobs, S. S., A. Jenkins, C. F. Giulivi, and P. Dutrieux, 2011: Stronger ocean circulation and increased melting under Pine Island Glacier ice shelf. *Nature Geoscience*, **4,** 519-523.
Jenkins, A., P. Dutrieux, S. S. Jacobs, S. D. McPhail, J. R. Perrett, A. T. Webb, and D. White, 2010: Observations beneath Pine Island Glacier in West Antarctica and implications for its retreat. *Nature Geoscience*, **3,** 468-472.
Jevrejeva, S., A. Grinsted, and J. Moore, 2009: Anthropogenic forcing dominates sea level rise since 1850. *Geophysical Research Letters*, **36,** L20706.
Jevrejeva, S., J. Moore, and A. Grinsted, 2010: How will sea level respond to changes in natural and anthropogenic forcings by 2100? *Geophysical Research Letters*, **37,** L07703.
Jevrejeva, S., J. C. Moore, and A. Grinsted, 2011: Sea level projections to AD 2500 with a new generation of climate change scenarios. *Global and Planetary Change*, **80-81,** 14-20.
Jevrejeva, S., A. Grinsted, J. C. Moore, and S. Holgate, 2006: Nonlinear trends and multiyear cycles in sea level records. *Journal of Geophysical Research-Oceans*, **111,** -.
Jevrejeva, S., J. C. Moore, A. Grinsted, and P. L. Woodworth, 2008: Recent global sea level acceleration started over 200 years ago? *Geophys. Res. Lett.*, **35**.
Johnson, G., and N. Gruber, 2007: Decadal water mass variations along 20 degrees W in the Northeastern Atlantic Ocean. *Progress in Oceanography*, **73,** 277-295.
Johnson, G., S. Mecking, B. Sloyan, and S. Wijffels, 2007: Recent bottom water warming in the Pacific Ocean. *Journal of Climate*, **20,** 5365-5375.
Joughin, I., B. E. Smith, and D. M. Holland, 2010: Sensitivity of 21st century sea level to ocean-induced thinning of Pine Island Glacier, Antarctica. *Geophysical Research Letters*, **37,** 5.
Joughin, I., S. B. Das, M. A. King, B. E. Smith, I. M. Howat, and T. Moon, 2008: Seasonal speedup along the western flank of the Greenland Ice Sheet. *Science*, **320,** 781-783.
Jouzel, J., and Coauthors, 2007: Orbital and millennial Antarctic climate variability over the past 800,000 years. *Science*, **317,** 793-796.
Kaser, G., J. G. Cogley, M. B. Dyurgerov, M. F. Meier, and A. Ohmura, 2006: Mass balance of glaciers and ice caps: Consensus estimates for 1961-2004. *Geophysical Research Letters*, **33,** -.
Kato, S., 2009: Interannual Variability of the Global Radiation Budget. *Journal of Climate*, **22,** 4893-4907.
Katsman, C., W. Hazeleger, S. Drijfhout, G. Oldenborgh, and G. Burgers, 2008: Climate scenarios of sea level rise for the northeast Atlantic Ocean: a study including the effects of ocean dynamics and gravity changes induced by ice melt. *Climatic Change*, **91,** 351-374.
Katsman, C. A., and G. J. van Oldenborgh, 2011: Tracing the upper ocean's “missing heat&#8221. *Geophys. Res. Lett.*, **38,** L14610.
Katsman, C. A., and Coauthors, 2011: Exploring high-end scenarios for local sea level rise to develop flood protection strategies for a low-lying delta - the Netherlands as an example. *Climate Dynamics*.
Kemp, A., B. Horton, J. Donnelly, M. Mann, M. Vermeer, and S. Rahmstorf, 2011: Climate related sea level variations over the past two millennia. *Proceedings of the National Academy of Sciences of the United States of America*, **108,** 11017-11022.
Khan, S. A., J. Wahr, M. Bevis, I. Velicogna, and E. Kendrick, 2010: Spread of ice mass loss into northwest Greenland observed by GRACE and GPS. *Geophysical Research Letters*, **37**.
Knutti, R., and L. Tomassini, 2008: Constraints on the transient climate response from observed global temperature and ocean heat uptake. *Geophys. Res. Lett.*, **35,** L09701.
Kohl, A., and D. Stammer, 2008: Decadal sea level changes in the 50-year GECCO ocean synthesis. *Journal of Climate*, **21,** 1876-1890.

Konikow, L. F., 2011: Contribution of global groundwater depletion since 1900 to sea level rise. *Geophysical Research Letters*, **38**.
Kopp, R., J. Mitrovica, S. Griffies, J. Yin, C. Hay, and R. Stouffer, 2010: The impact of Greenland melt on local sea levels: a partially coupled analysis of dynamic and static equilibrium effects in idealized water-hosing experiments A letter. *Climatic Change***,** 619-625.
Kopp, R. E., F. J. Simons, J. X. Mitrovica, A. C. Maloof, and M. Oppenheimer, 2009: Probabilistic assessment of sea level during the last interglacial stage. *Nature*, **462,** 863-U851.
Körper, J., and Coauthors, submitted: The effect of aggressive mitigation on sea level rise and sea ice changes. *Climate Dynamics*.
Kouketsu, S., and Coauthors, 2011: Deep ocean heat content changes estimated from observation and reanalysis product and their influence on sea level change. *Journal of Geophysical Research-Oceans*, **116,** -.
Krinner, G., O. Magand, I. Simmonds, C. Genthon, and J. L. Dufresne, 2007: Simulated Antarctic precipitation and surface mass balance at the end of the twentieth and twenty-first centuries. *Climate Dynamics*, **28,** 215-230.
Lambeck, K., 1988: *Geophysical Geodesy*. Oxford Science Publications, 1-710 pp.
Lambeck, K., and S. M. Nakiboglu, 1984: Recent global changes in sea level. *Geophysical Research Letters*, **11,** 959-961.
Lambeck, K., C. Smither, and M. Ekman, 1998: Tests of glacial rebound models for Fennoscandinavia based on instrumented sea- and lake-level records. *Geophysical Journal International*, **135,** 375-387.
Lambeck, K., M. Anzidei, F. Antonioli, A. Benini, and A. Esposito, 2004: Sea level in Roman time in the Central Mediterranean and implications for recent change. *Earth and Planetary Science Letters***,** 563-575.
Lambeck, K., C. D. Woodroffe, F. Antonioli, M. Anzidei, R. M. Gehrels, J. Laborel, and A. J. Wright, 2010: Paleoenvironmental records, geophysical modelling, and reconstruction of sea level trends and variability on centennial and longer timescales. *Understanding Sea level Rise and Variability*, J. A. Church, P. L. Woodworth, T. Aarup, and W. S. Wilson, Eds., Wiley-Blackwell, 61-121.
Landerer, F. W., J. H. Jungclaus, and J. Marotzke, 2007: Regional dynamic and steric sea level change in response to the IPCC-A1B scenario. *Journal of Physical Oceanography*, **37,** 296-312.
Le Quere, C., M. R. Raupach, J. G. Canadell, G. Marland, and et al., 2009: Trends in the sources and sinks of carbon dioxide. *Nature Geosci*, **2,** 831-836.
Leake, J., J. Wolf, J. Lowe, J. Hall, and R. Nicholls, 2009: Response of marine climate to future climate change: application to coastal regions. *International Conference on Coastal Engineering, 5*, World Scientific Publishing, Singapore.
Leake, J., and Coauthors, 2007: Predicted wave climate for the UK: towards and integrated model of coastal impacts of climate change. *The 10th conference on Estuarine and Coastal Modelling*, Newport, Rhode Island, American Society of Civil Engineers, 393-406.
Leclercq, P. W., J. Oerlemans, and J. G. Cogley, 2011: Estimating the Glacier Contribution to Sea level Rise for the Period 1800-2005. *Surveys in Geophysics*, **32,** 519-535.
Lemke, P., and Coauthors, 2007: Observations: Changes in Snow, Ice and Frozen Ground. *Climate Change 2007: The Physical Science Basis. Contribution of Working Group I to the Fourth Assessment Report of the Intergovernmental Panel on Climate Change*, Cambridge University Press.
Lenaerts, J. T. M., M. R. van den Broeke, W. J. van de Berg, E. van Meijgaard, and P. K. Munneke, submitted: A new high-resolution surface mass balance map of Antarctica (1989-2009) based on regional atmospheric climate modeling. *Geophysical Research Letters*.
Lettenmaier, D. P., and P. C. D. Milly, 2009: Land waters and sea level. *Nature Geoscience*, **2,** 452-454.
Leuliette, E. W., and L. Miller, 2009: Closing the sea level rise budget with altimetry, Argo, and GRACE. *Geophysical Research Letters*, **36,** -.
Leuliette, E. W., and R. Scharroo, 2010: Integrating Jason-2 into a Multiple-Altimeter Climate Data Record. *Marine Geodesy*, **33,** 504-517.
Leuliette, E. W., and J. K. Willis, 2011: Balancing the Sea Level Budget. *Oceanography*, **24,** 122-129.
Levermann, A., A. Griesel, M. Hofmann, M. Montoya, and S. Rahmstorf, 2005: Dynamic sea level changes following changes in the thermohaline circulation. *Climate Dynamics***,** 347-354.
Levitus, S., J. Antonov, and T. Boyer, 2005: Warming of the world ocean, 1955-2003. *Geophys. Res. Lett.*, **32,** L02604.
Levitus, S., J. Antonov, J. Wang, T. Delworth, K. Dixon, and A. Broccoli, 2001: Anthropogenic warming of Earth's climate system. *Science*, **292,** 267-270.
Levitus, S., J. I. Antonov, T. P. Boyer, R. A. Locarnini, H. E. Garcia, and A. V. Mishonov, 2009: Global ocean heat content 1955-2008 in light of recently revealed instrumentation problems. *Geophysical Research Letters*, **36,** -.
Lionello, P., M. B. Galati, and E. Elvini, 2010: Extreme storm surge and wind wave climate scenario simulations at the Venetian littoral. *Physics and Chemistry of the Earth, Parts A/B/C*.
Lionello, P., S. Cogo, M. B. Galati, and A. Sanna, 2008: The Mediterranean surface wave climate inferred from future scenario simulations. *Global and Planetary Change*, **63,** 152-162.
Lisiecki, L., and M. Raymo, 2005: A Pliocene-Pleistocene stack of 57 globally distributed benthic delta O-18 records. *Paleoceanography***,** ARTN PA1003, DOI 10.1029/2004PA001071.
Little, C. M., M. Oppenheimer, and N. M. Urban, submitted: Assessing ice sheet driven sea level rise using a probabilistic, bottom-up approach *Nature Climate Change*.

Llovel, W., S. Guinehut, and A. Cazenave, 2010a: Regional and interannual variability in sea level over 2002-2009 based on satellite altimetry, Argo float data and GRACE ocean mass. *Ocean Dynamics*, **60,** 1193-1204.
Llovel, W., M. Becker, A. Cazenave, J. F. Cretaux, and G. Ramillien, 2010b: Global land water storage change from GRACE over 2002-2009; Inference on sea level. *Comptes Rendus Geoscience*, **342,** 179-188.
Llovel, W., and Coauthors, 2011: Terrestrial waters and sea level variations on interannual time scale. *Global and Planetary Change*, **75,** 76-82.
Loeb, N., and Coauthors, 2009: Toward Optimal Closure of the Earth's Top-of-Atmosphere Radiation Budget. *Journal of Climate***,** 748-766.
Lombard, A., G. Garric, and T. Penduff, 2009: Regional patterns of observed sea level change: insights from a 1/4A degrees global ocean/sea-ice hindcast. *Ocean Dynamics*, **59,** 433-449.
Lombard, A., A. Cazenave, P. Y. Le Traon, and M. Ishii, 2005a: Contribution of thermal expansion to present-day sea level change revisited. *Global and Planetary Change*, **47,** 1-16.
Lombard, A., A. Cazenave, K. DoMinh, C. Cabanes, and R. S. Nerem, 2005b: Thermosteric sea level rise for the past 50 years; comparison with tide gauges and inference on water mass contribution. *Global and Planetary Change*, **48,** 303-312.
Lorbacher, K., J. Dengg, C. W. Boning, and A. Biastoch, 2010: Regional Patterns of Sea Level Change Related to Interannual Variability and Multidecadal Trends in the Atlantic Meridional Overturning Circulation. *Journal of Climate*, **23,** 4243-4254.
Lorbacher, K., S. J. Marsland, J. A. Church, S. M. Griffies, and D. Stammer, submitted: Rapid barotrophic sea level rise from ice-sheet melting scenarios. *Journal of Geophysical Research*.
Losch, M., A. Adcroft, and J. M. Campin, 2004: How sensitive are coarse general circulation models to fundamental approximations in the equations of motion? *Journal of Physical Oceanography*, **34,** 306-319.
Lowe, J. A., and Coauthors, 2010: *Past and Future Changes in Extreme Sea Levels and Waves.* Wiley-Blackwell, 326-375 pp.
Lozier, M. S., V. Roussenov, M. S. C. Reed, and R. G. Williams, 2010: Opposing decadal changes for the North Atlantic meridional overturning circulation. *Nature Geoscience*, **3,** 728-734.
Lu, Z., Streets, D. G., Zhang, Q., Wang, S., Carmichael, G. R., Cheng, Y. F., Wei, C., Chin, M., Diehl, T., and Tan, Q., 2010: Sulfur dioxide emissions in China and sulfur trends in East Asia since 2000. *Atmos. Chem. Phys.*, **10,** 6311-6331, doi:6310.5194/acp-6310-6311-2010.
Luthcke, S. B., and Coauthors, 2006: Recent Greenland ice mass loss by drainage system from satellite gravity observations. *Science*, **314,** 1286-1289.
Lyman, J. M., and Coauthors, 2010: Robust warming of the global upper ocean. *Nature*, **465,** 334-337.
Marcelja, S., 2010: The timescale and extent of thermal expansion of the global ocean due to climate change. *Ocean Science*, **6,** 179-184.
Marzeion, B., M. Hofer, A. H. Jarosch, G. Kaser, and T. Mölg, 2011: A minimal model for reconstructing interannual mass balance variability of glaciers in the European Alps. *The Cryosphere Discuss.*, **5,** 2799-2839.
Maslin, M., and Coauthors, 2000: Palaeoreconstruction of the Amazon River freshwater and sediment discharge using sediments recovered at Site 942 on the Amazon Fan. *Journal of Quaternary Science***,** 419-434.
Matsuo, K., and K. Heki, 2010: Time-variable ice loss in Asian high mountains from satellite gravimetry. *Earth and Planetary Science Letters*, **290,** 30-36.
McInnes, K., I. Macadam, G. Hubbert, and J. O'Grady, 2009: A modelling approach for estimating the frequency of sea level extremes and the impact of climate change in southeast Australia. *Natural Hazards*, **51,** 115-137.
McKay, N., J. Overpeck, and B. Otto-Bliesner, 2011: The role of ocean thermal expansion in Last Interglacial sea level rise. *Geophysical Research Letters*, **38,** -.
Meehl, G. A., A. X. Hu, and C. Tebaldi, 2010: Decadal Prediction in the Pacific Region. *Journal of Climate*, **23,** 2959-2973.
Meehl, G. A., J. M. Arblaster, J. T. Fasullo, A. Hu, and K. E. Trenberth, 2011: Model-based evidence of deep-ocean heat uptake during surface-temperature hiatus periods. *Nature Clim. Change*, **1,** 360-364.
Meehl, G. A., and Coauthors, 2005: How much more global warming and sea level rise? *Science*, **307,** 1769-1772.
Meehl, G. A., and Coauthors, 2007: Global climate projections. *Climate Change 2007: The Physical Science Basis. Contribution of Working Group I to the Fourth Assessment Report of the Intergovernmental Panel on Climate Change*, Cambridge University Press.
Meier, M. F., and Coauthors, 2007: Glaciers dominate Eustatic sea level rise in the 21st century. *Science*, **317,** 1064-1067.
Meinshausen, M., and Coauthors, 2011: The RCP Greenhouse Gas Concentrations and their Extension from 1765 to 2300. *Climatic Change*, **submitted**.
Menéndez, M., and P. L. Woodworth, 2010: Changes in extreme high water levels based on a quasi-global tide-gauge data set. *J. Geophys. Res.*, **115,** C10011.
Menéndez, M., F. J. Méndez, I. J. Losada, and N. E. Graham, 2008: Variability of extreme wave heights in the northeast Pacific Ocean based on buoy measurements. *Geophysical Research Letters*, **35,** L22607.
Mercer, J. H., 1978: WEST ANTARCTIC ICE SHEET AND CO2 GREENHOUSE EFFECT - THREAT OF DISASTER. *Nature*, **271,** 321-325.

Mernild, S. H., and G. E. Liston, submitted: Greenland freshwater runoff. Part II: Distribution and trends, 1960-2010. *Journal of Climate*.
Mernild, S. H., G. E. Liston, C. A. Hiemstra, and J. H. Christensen, 2010: Greenland Ice Sheet Surface Mass-Balance Modeling in a 131-Yr Perspective, 1950-2080. *Journal of Hydrometeorology*, **11,** 3-25.
Merrifield, M. A., S. T. Merrifield, and G. T. Mitchum, 2009: An Anomalous Recent Acceleration of Global Sea Level Rise. *J. Climate*, **22,** 5772–5781.
Merrifield, M. A., and M.E. Maltrud, 2011: Regional sea level trends due to a Pacific trade wind intensification. *Geophys. Res. Letter*, **38,** L21605.
Meyssignac, B., W. Llovel, M. Becker, and A. Cazenave, 2011a: An assessment of two-dimensional past sea level reconstructions over 1950-2009 based on tide gauge data and different input sea level grids. *Surveys in Geophysics*, **in review**.
Meyssignac, B., W. Llovel, A. Cazenave, D. Salas, and Y. Melia, 2011b: Spatial trend patterns in observed sea level: Internal variability or anthropogenic signature? *Climate Dynamics*, **in review**.
Mikolajewicz, U., M. Vizcaino, J. Jungclaus, and G. Schurgers, 2007a: Effect of ice sheet interactions in anthropogenic climate change simulations. *Geophysical Research Letters*, **34,** L18706.
——, 2007b: Effect of ice sheet interactions in anthropogenic climate change simulations. *Geophysical Research Letters***, 34,** L18706.
Mikolajewicz, U., M. Groger, E. Maier-Reimer, G. Schurgers, M. Vizcaino, and A. Winguth, 2007c: Long-term effects of anthropogenic CO2 emissions simulated with a complex earth system model. *Climate Dynamics***,** 599-631.
Miller, K. G., and Coauthors, submitted: The high tide of the warm Pliocene: Implications of global sea level for Antarctic deglaciation. *Geology*.
Miller, L., and B. C. Douglas, 2007: Gyre-scale atmospheric pressure variations and their relation to 19th and 20th century sea level rise. *Geophysical Research Letters*, **34,** L16602.
Milly, P. C. D., A. Cazenave, and M. C. Gennero, 2003: Contribution of climate-driven change in continental water storage to recent sea level rise. *Proceedings of the National Academy of Sciences of the United States of America*, **100,** 13158-13161.
Milly, P. C. D., and Coauthors, 2010: Terrestrial water-storage contributions to sea level rise and variability. *Understanding Sea level Rise and Variability*, J. A. Church, P. L. Woodworth, T. Aarup, and W. S. Wilson, Eds., Blackwell Publishing Ltd.
Milne, G., and J. Mitrovica, 2008: Searching for eustasy in deglacial sea level histories. *Quaternary Science Reviews***,** 2292-2302.
Milne, G., W. Gehrels, C. Hughes, and M. Tamisiea, 2009: Identifying the causes of sea level change. *Nature Geoscience*, **2,** 471-478.
Milne, G. A., and J. X. Mitrovica, 1998: Postglacial sea level change on a rotating Earth. *Geophysical Journal International*, **133,** 1-19.
Mitchum, G. T., R. S. Nerem, M. A. Merrifield, and W. R. Gehrels, 2010: Modern sea level change estimates. *Understanding sea level rise and variability*, J. A. Church, P. L. Woodworth, T. Aarup, and W. S. Wilson, Eds., Wiley-Blackwell.
Mitrovica, J. X., N. Gomez, and P. U. Clark, 2009: The Sea level Fingerprint of West Antarctic Collapse. *Science*, **323,** 753-753.
Mitrovica, J. X., M. E. Tamisiea, J. L. Davis, and G. A. Milne, 2001: Recent mass balance of polar ice sheets inferred from patterns of global sea level change. *Nature*, **409,** 1026-1029.
Mitrovica, J. X., N. Gomez, E. Morrow, C. Hay, K. Latychev, and M. E. Tamisiea, 2011: On the robustness of predictions of sea level fingerprints. *Geophysical Journal International***,** in press.
Moberg, A., D. M. Sonechkin, K. Holmgren, N. M. Datsenko, and W. Karlen, 2005: Highly variable Northern Hemisphere temperatures reconstructed from low- and high-resolution proxy data. *Nature*, **433,** 613-617.
Monaghan, A. J., and Coauthors, 2006: Insignificant change in Antarctic snowfall since the International Geophysical Year. *Science*, **313,** 827-831.
Moore, J. C., S. Jevrejeva, and A. Grinsted, 2011: The historical global sea level budget. *Annals of Glaciology*.
Mori, N., T. Yasuda, H. Mase, T. Tom, and Y. Oku, 2010: Projection of Extreme Wave Climate Change under Global Warming. *Hydrological Research Letters*, **4,** 15-19.
Morlighem, M., E. Rignot, H. Seroussi, E. Larour, H. Ben Dhia, and D. Aubry, 2010: Spatial patterns of basal drag inferred using control methods from a full-Stokes and simpler models for Pine Island Glacier, West Antarctica. *Geophysical Research Letters*, **37**.
Morris, E. M., and D. G. Vaughan, 2003: Spatial and temporal variation of surface temperature on the Antarctic Peninsula and the limit of viability of ice shelves. *Antarctic Peninsula Climate Variability: Historical and Paleoenvironmental Perspectives*, **79,** 61-68.
Moucha, R., A. Forte, J. Mitrovica, D. Rowley, S. Quere, N. Simmons, and S. Grand, 2008: Dynamic topography and long-term sea level variations: There is no such thing as a stable continental platform. *Earth and Planetary Science Letters*, **271,** 101-108.
Mousavi, M., J. Irish, A. Frey, F. Olivera, and B. Edge, 2011: Global warming and hurricanes: the potential impact of hurricane intensification and sea level rise on coastal flooding. *Climatic Change*, **104,** 575-597.

Müller, M., B. K. Arbic, and J. X. Mitrovica, 2011: Secular trends in ocean tides: Observations and model results. *J. Geophys. Res.*, **116,** C05013.
Muhs, D., K. Simmons, and B. Steinke, 2002: Timing and warmth of the Last Interglacial period: new U-series evidence from Hawaii and Bermuda and a new fossil compilation for North America. *Quaternary Science Reviews*, **21,** 1355-1383.
Muhs, D. R., K. R. Simmons, R. R. Schumann, and R. B. Halley, 2011: Sea level history of the past two interglacial periods: new evidence from U-series dating of reef corals from south Florida. *Quaternary Science Reviews*, **30,** 570-590.
Murphy, D. M., S. Solomon, R. W. Portmann, K. H. Rosenlof, P. M. Forster, and T. Wong, 2009: An observationally based energy balance for the Earth since 1950. *J. Geophys. Res.*, **114,** D17107.
Naish, T., G. Wilson, G. Dunbar, and P. Barrett, 2008: Constraining the amplitude of Late Oligocene bathymetric changes in western Ross Sea during orbitally-induced oscillations in the East Antarctic Ice Sheet: (2) Implications for global sea level changes. *Palaeogeography Palaeoclimatology Palaeoecology***,** 66-76.
Naish, T., and Coauthors, 2009: Obliquity-paced Pliocene West Antarctic ice sheet oscillations. *Nature*, **458,** 322-U384.
Nerem, R. S., D. P. Chambers, C. Choe, and G. T. Mitchum, 2010: Estimating Mean Sea Level Change from the TOPEX and Jason Altimeter Missions. *Marine Geodesy*, **33,** 435-446.
Ngo-Duc, T., K. Laval, J. Polcher, A. Lombard, and A. Cazenave, 2005: Effects of land water storage on global mean sea level over the past half century. *Geophysical Research Letters*, **32,** -.
Nicholls, R. J., and Coauthors, 2011: Sea level rise and its possible impacts given a 'beyond 4 degrees C world' in the twenty-first century. *Philosophical Transactions of the Royal Society a-Mathematical Physical and Engineering Sciences*, **369,** 161-181.
Nick, F. M., A. Vieli, I. M. Howat, and I. Joughin, 2009: Large-scale changes in Greenland outlet glacier dynamics triggered at the terminus. *Nature Geoscience*, **2,** 110-114.
Nick, F. M., C. J. van der Veen, A. Vieli, and D. I. Benn, 2010: A physically based calving model applied to marine outlet glaciers and implications for the glacier dynamics. *Journal of Glaciology*, **56,** 781-794.
Okumora, Y. M., C. Deser, and A. Hu, 2009: North Pacific climate response to freshwater focring in the subarctic North Atlantic: oceanic and atmospheric pathways. *Journal of Climate*, **22,** 1424-1445.
Okumura, Y. M., C. Deser, A. Hu, A. Timmermann, and S. P. Xie, 2009: North Pacific Climate Response to Freshwater Forcing in the Subarctic North Atlantic: Oceanic and Atmospheric Pathways. *Journal of Climate*, **22,** 1424-1445.
Overpeck, J. T., B. L. Otto-Bliesner, G. H. Miller, D. R. Muhs, R. B. Alley, and J. T. Kiehl, 2006: Paleoclimatic evidence for future ice-sheet instability and rapid sea level rise. *Science*, **311,** 1747-1750.
Pardaens, A., J. M. Gregory, and J. Lowe, 2011a: A model study of factors influencing projected changes in regional sea level over the twenty-first century. *Climate Dynamics*, **in press**.
——, 2011b: A model study of factors influencing projected changes in regional sea level over the twenty-first century. *Climate Dynamics*, **36,** 2015-2033.
Pardaens, A. K., H. T. Banks, J. M. Gregory, and P. R. Rowntree, 2003: Freshwater transports in HadCM3. *Climate Dynamics*, **21,** 177-195.
Pardaens, A. K., J. A. Lowe, S. Brown, R. J. Nicholls, and D. de Gusmao, 2011c: Sea level rise and impacts projections under a future scenario with large greenhouse gas emission reductions. *Geophysical Research Letters*, **38**.
Pattyn, F., A. Huyghe, S. De Brabander, and B. De Smedt, 2006: Role of transition zones in marine ice sheet dynamics. *Journal of Geophysical Research-Earth Surface*, **111,** 10.
Paulson, A., S. J. Zhong, and J. Wahr, 2007: Inference of mantle viscosity from GRACE and relative sea level data. *Geophysical Journal International*, **171,** 497-508.
Peltier, W. R., 2001: Global glacial isostatic adjustment and modern instrumental records of relative sea level history. *Sea level rise: History and consequences*, B. C. Douglas, M. S. Kearney, and S. P. Leatherman, Eds., Academic Press, 65-95.
Peltier, W. R., 2004: Global glacial isostasy and the surface of the ice-age Earth. *Annual Reviews of Earth and Planetary Science*, **32,** 111-149.
Peltier, W. R., 2009: Closure of the budget of global sea level rise over the GRACE era: the importance and magnitudes of the required corrections for global glacial isostatic adjustment. *Quaternary Science Reviews*, **28,** 1658-1674.
Péquignet, A. C., J. Becker, M. Merrifield, and S. Boc, 2011: The dissipation of wind wave energy across a fringing reef at Ipan, Guam. *Coral Reefs*, **30,** 71-82.
Pfeffer, W. T., 2007: A simple mechanism for irreversible tidewater glacier retreat. *Journal of Geophysical Research-Earth Surface*, **112**.
Pfeffer, W. T., J. T. Harper, and S. O'Neel, 2008: Kinematic constraints on glacier contributions to 21st-century sea level rise. *Science*, **321,** 1340-1343.
Phillips, T., H. Rajaram, and K. Steffen, 2010: Cryo-hydrologic warming: A potential mechanism for rapid thermal response of ice sheets. *Geophysical Research Letters*, **37**.
Pollack, H. N., S. J. Hurter, and J. R. Johnson, 1993: Heat flow from the Earth's interior: Analysis of the global data set. *Rev. Geophys.*, **31,** 267-280.
Pollard, D., and R. DeConto, 2009: Modelling West Antarctic ice sheet growth and collapse through the past five million years. *Nature***,** 329-U389.

Price, S. F., A. J. Payne, I. M. Howat, and B. E. Smith, 2011: Committed sea level rise for the next century from Greenland ice sheet dynamics during the past decade. *Proceedings of the National Academy of Sciences of the United States of America*, **108,** 8978-8983.
Pritchard, H. D., and D. G. Vaughan, 2007: Widespread acceleration of tidewater glaciers on the Antarctic Peninsula. *Journal of Geophysical Research-Earth Surface*, **112**.
Pritchard, H. D., R. J. Arthern, D. G. Vaughan, and L. A. Edwards, 2009: Extensive dynamic thinning on the margins of the Greenland and Antarctic ice sheets. *Nature*, **461,** 971-975.
Purkey, S. G., and G. C. Johnson, 2010: Warming of Global Abyssal and Deep Southern Ocean Waters between the 1990s and 2000s: Contributions to Global Heat and Sea Level Rise Budgets. *Journal of Climate*, **23,** 6336-6351.
Qiu, B., and S. M. Chen, 2006: Decadal variability in the large-scale sea surface height field of the South Pacific Ocean: Observations and causes. *Journal of Physical Oceanography*, **36,** 1751-1762.
Quinn, K. J., and R. M. Ponte, 2010: Uncertainty in ocean mass trends from GRACE. *Geophysical Journal International*, **181,** 762-768.
Radic, V., and R. Hock, 2010: Regional and global volumes of glaciers derived from statistical upscaling of glacier inventory data. *Journal of Geophysical Research-Earth Surface*, **115,** -.
——, 2011: Regionally differentiated contribution of mountain glaciers and ice caps to future sea level rise. *Nature Geoscience*, **4,** 91-94.
Rae, J., and Coauthors, submitted: Twenty-first century climate change in Greenland: A comparative analysis of three Regional Climate Models, 1-43 pp.
Rahmstorf, S., 2007a: A semi-empirical approach to projecting future sea level rise. *Science*, **315,** 368-370.
——, 2007b: Response to comments on "A semi-empirical approach to projecting future sea level rise". *Science*, **317**.
Rahmstorf, S., and A. Ganopolski, 1999: Long-term global warming scenarios computed with an efficient coupled climate model. *Climatic Change*, **43,** 353-367.
Rahmstorf, S., M. Perrette, and M. Vermeer, 2011: Testing the robustness of semi-empirical sea level projections. *Climate Dynamics*.
Ramillien, G., J. S. Famiglietti, and J. Wahr, 2008: Detection of Continental Hydrology and Glaciology Signals from GRACE: A Review. *Surveys in Geophysics*, **29,** 361-374.
Raper, S. C. B., and R. J. Braithwaite, 2005: The potential for sea level rise: New estimates from glacier and ice cap area and volume distributions. *Geophysical Research Letters*, **32**.
——, 2006: Low sea level rise projections from mountain glaciers and icecaps under global warming. *Nature*, **439,** 311-313.
Raper, S. C. B., J. M. Gregory, and R. J. Stouffer, 2002: The role of climate sensitivity and ocean heat uptake on AOGCM transient temperature response. *J. Climate*, **15,** 124-130.
Rasmussen, L. A., H. Conway, R. M. Krimmel, and R. Hock, 2011: Surface mass balance, thinning and iceberg production, Columbia Glacier, Alaska, 1948-2007. *Journal of Glaciology*, **57,** 431-440.
Ray, R. D., and B. C. Douglas, submitted: Experiments in reconstructing twentieth-century sea levels. *Progress in Oceanography*.
Raymo, M., J. Mitrovica, M. O'Leary, R. DeConto, and P. Hearty, 2011: Departures from eustasy in Pliocene sea level records. *Nature Geoscience*, **4,** 328-332.
Ren, D. D., R. Fu, L. M. Leslie, J. L. Chen, C. R. Wilson, and D. J. Karoly, 2011: The Greenland Ice Sheet Response to Transient Climate Change. *Journal of Climate*, **24,** 3469-3483.
Ridley, J., J. Gregory, P. Huybrechts, and J. Lowe, 2010a: Thresholds for irreversible decline of the Greenland ice sheet. *Climate Dynamics***,** 1065-1073.
Ridley, J., J. M. Gregory, P. Huybrechts, and J. Lowe, 2010b: Thresholds for irreversible decline of the Greenland ice sheet. *Climate Dynamics*, **35,** 1065-1073.
Ridley, J. K., P. Huybrechts, J. M. Gregory, and J. A. Lowe, 2005: Elimination of the Greenland ice sheet in a high CO2 climate. *Journal of Climate*, **18,** 3409-3427.
Rignot, E., and P. Kanagaratnam, 2006: Changes in the velocity structure of the Greenland ice sheet. *Science*, **311,** 986-990.
Rignot, E., I. Velicogna, M. R. van den Broeke, A. Monaghan, and J. Lenaerts, 2011: Acceleration of the contribution of the Greenland and Antarctic ice sheets to sea level rise. *GEOPHYSICAL RESEARCH LETTERS*, **38**.
Rignot, E., G. Casassa, P. Gogineni, W. Krabill, A. Rivera, and R. Thomas, 2004: Accelerated ice discharge from the Antarctic Peninsula following the collapse of Larsen B ice shelf. *Geophysical Research Letters*, **31**.
Rignot, E., J. L. Bamber, M. R. Van Den Broeke, C. Davis, Y. H. Li, W. J. Van De Berg, and E. Van Meijgaard, 2008: Recent Antarctic ice mass loss from radar interferometry and regional climate modelling. *Nature Geoscience*, **1,** 106-110.
Riva, R. E. M., J. L. Bamber, D. A. Lavallee, and B. Wouters, 2010a: Sea level fingerprint of continental water and ice mass change from GRACE. *Geophysical Research Letters*, **37,** L19605.
——, 2010b: Sea level fingerprint of continental water and ice mass change from GRACE. *Geophysical Research Letters*, **37,** -.
Robinson, A., R. Calov, and A. Ganopolski, 2011: Greenland ice sheet model parameters constrained using simulations of the Eemian Interglacial. *Climate of the Past*, **7,** 381-396.

Rodell, M., I. Velicogna, and J. S. Famiglietti, 2009: Satellite-based estimates of groundwater depletion in India. *Nature*, **460,** 999-U980.
Roemmich, D., and Coauthors, 2010: Global Ocean Warming and Sea Level Rise. *Understanding sea level rise and variability*, J. Church, P. L. Woodworth, T. Aarup, and S. Wilson, Eds., Blackwell Publishing.
Rohling, E. J., K. Grant, C. Hemleben, M. Siddall, B. A. A. Hoogakker, M. Bolshaw, and M. Kucera, 2008: High rates of sea level rise during the last interglacial period. *Nature Geoscience*, **1,** 38-42.
Rott, H., P. Skvarca, and T. Nagler, 1996: Rapid collapse of northern Larsen Ice Shelf, Antarctica. *Science*, **271,** 788-792.
Ruggiero, P., 2008: Impacts of climate change on coastal erosion and flood probability in the US Pacific. *Solutions to Coastal Disasters 2008*, 158-169.
Russell, G. L., V. Gornitz, and J. R. Miller, 2000: Regional sea level changes projected by the NASA/GISS atmosphere-ocean model. *Clim. Dyn.*, **16,** 789-797.
S., R., 2007: A semi-empirical approach to projecting future sea level rise. 368-370.
Sahagian, D., 2000: Global physical effects of anthropogenic hydrological alterations: sea level and water redistribution. *Global and Planetary Change*, **25,** 39-48.
Scambos, T. A., J. A. Bohlander, C. A. Shuman, and P. Skvarca, 2004: Glacier acceleration and thinning after ice shelf collapse in the Larsen B embayment, Antarctica. *Geophysical Research Letters*, **31**.
Schewe, J., A. Levermann, and M. Meinshausen, 2011: Climate change under a scenario near 1.5 °C of global warming: monsoon intensification, ocean warming and steric sea level rise. *Earth Syst. Dynam.*, **2,** 25-35.
Schmith, T., S. Johansen, and P. Thejll, 2007: Comment on "A semi-empirical approach to projecting future sea level rise". *Science*, **317**.
Schoof, C., 2007a: Ice sheet grounding line dynamics: Steady states, stability, and hysteresis. *Journal of Geophysical Research-Earth Surface*, **112**.
——, 2007b: Marine ice-sheet dynamics. Part 1. The case of rapid sliding. *Journal of Fluid Mechanics*, **573,** 27-55.
——, 2010: Ice-sheet acceleration driven by melt supply variability. *Nature*, **468,** 803-806.
Seneviratne, S., et al., 2012: *Changes in Climate Extremes and their impacts on the natural Physical Environment. Special Report on Managing the Risks of Extreme Events and Disasters to Advance Climate Change Adaptation (SREX).* IPCC. (in press).
Shepherd, A., and D. Wingham, 2007: Recent sea level contributions of the Antarctic and Greenland ice sheets. *Science*, **315,** 1529-1532.
Slangen, A. B. A., C. A. Katsman, R. S. W. van de Wal, L. L. A. Vermeersen, and R. E. M. Riva, 2011: Towards regional projections of twenty-first century sea level change based on IPCC SRES scenarios. *Climate Dynamics*.
Smith, J. M., M. A. Cialone, T. V. Wamsley, and T. O. McAlpin, 2010: Potential impact of sea level rise on coastal surges in southeast Louisiana. *Ocean Engineering*, **37,** 37-47.
Sokolov, A. P., C. E. Forest, and P. H. Stone, 2010: Sensitivity of climate change projections to uncertainties in the estimates of observed changes in deep-ocean heat content. *Climate Dynamics*, **34,** 735-745.
Sole, A., T. Payne, J. Bamber, P. Nienow, and W. Krabill, 2008: Testing hypotheses of the cause of peripheral thinning of the Greenland Ice Sheet: is land-terminating ice thinning at anomalously high rates? *Cryosphere*, **2,** 205-218.
Solomon, S., G.-K. Plattner, R. Knutti, and P. Friedlingstein, 2009: Irresversible climate change due to carbon dioxide emissions. *Proceedings of the National Academy of Science*, **106,** 1704-1709.
Solomon, S., and Coauthors, Eds., 2007: *Climate Change 2007: The Physical Science Basis*. Cambridge University Press, 940 pp.
Stackhouse, P. W., Jr., T. Wong, N. G. Loeb, D. P. Kratz, A. C. Wilber, D. R. Doelling, and L. C. Nguyen, 2010: Earth Radiation Budget at top-of-atmosphere [in "State of the Climate in 2009"]. *Bull. Amer. Meteor. Soc.*, **91,** S41.
Stammer, D., 2008: Response of the global ocean to Greenland and Antarctic ice melting. C06022.
Stammer, D., and S. Huttemann, 2008: Response of regional sea level to atmospheric pressure loading in a climate change scenario. *Journal of Climate*, **21,** 2093-2101.
Stammer, D., N. Agarwal, P. Herrmann, A. Kohl, and C. R. Mechoso, 2011: Response of a Coupled Ocean-Atmosphere Model to Greenland Ice Melting. *Surveys in Geophysics*, **32,** 621-642.
Sterl, A., H. van den Brink, H. de Vries, R. Haarsma, and E. van Meijgaard, 2009: An ensemble study of extreme North Sea storm surges in a changing climate. *Ocean Science Discussions*, **6,** 1031-1059.
Stockdon, H. F., R. A. Holman, P. A. Howd, and A. H. Sallenger Jr, 2006: Empirical parameterization of setup, swash, and runup. *Coastal Engineering*, **53,** 573-588.
Stone, J., G. Balco, D. Sugden, M. Caffee, L. Sass, S. Cowdery, and C. Siddoway, 2003: Holocene deglaciation of Marie Byrd Land, West Antarctica. *Science*, **299,** 99-102.
Streets, D. G., and Coauthors, 2009: Anthropogenic and natural contributions to regional trends in aerosol optical depth, 1980–2006. *J. Geophys. Res.*, **114,** D00D18.
Sundal, A. V., A. Shepherd, P. Nienow, E. Hanna, S. Palmer, and P. Huybrechts, 2011: Melt-induced speed-up of Greenland ice sheet offset by efficient subglacial drainage. *Nature*, **469,** 522-U583.
Suzuki, T., and Coauthors, 2005: Projection of future sea level and its variability in a high-resolution climate model: Ocean processes and Greenland and Antarctic ice-melt contributions. *Geophysical Research Letters*, **32**.

Swingedouw, D., T. Fichefet, P. Huybrechts, H. Goosse, E. Driesschaert, and M. Loutre, 2008: Antarctic ice-sheet melting provides negative feedbacks on future climate warming. *Geophysical Research Letters*, ARTN L17705, DOI 10.1029/2008GL034410.

Syvitski, J., and Coauthors, 2009: Sinking deltas due to human activities. *Nature Geoscience*, **2,** 681-686.

Tamisiea, M. E., 2011: Ongoing glacial isostatic contributions to observations of sea level change. *Geophysical Journal International*, **186,** 1036-1044.

Tamisiea, M. E., E. M. Hill, R. M. Ponte, J. L. Davis, I. Velicogna, and N. T. Vinogradova, 2010: Impact of self-attraction and loading on the annual cycle in sea level. *Journal of Geophysical Research*, **115,** C07004.

Tett, S. F. B., and Coauthors, 2007: The impact of natural and anthropogenic forcings on climate and hydrology since 1550. *Climate Dynamics*, **28,** 3-34.

Thoma, M., A. Jenkins, D. Holland, and S. Jacobs, 2008: Modelling Circumpolar Deep Water intrusions on the Amundsen Sea continental shelf, Antarctica. *Geophysical Research Letters*, **35**.

Thompson, W., and S. Goldstein, 2005: Open-system coral ages reveal persistent suborbital sea level cycles. *Science*, 401-404.

Timmermann, A., S. McGregor, and F. F. Jin, 2010: Wind Effects on Past and Future Regional Sea Level Trends in the Southern Indo-Pacific. *Journal of Climate*, **23,** 4429-4437.

Trenberth, K. E., 2009: An imperative for climate change planning: tracking Earth's global energy. *Current Opinion in Environmental Sustainability*, **1,** 19-27.

——, 2010: Global change: The ocean is warming, isn't it? *Nature*, **465,** 304-304.

Trenberth, K. E., and J. T. Fasullo, 2010: Tracking Earth's Energy. *Science*, **328,** 316-317.

Trenberth, K. E., J. T. Fasullo, and J. Kiehl, 2009: Earth's Global Energy Budget. *Bulletin of the American Meteorological Society*, **90,** 311-323.

Unnikrishnan, A. S., M. R. R. Kumar, and B. Sindhu, 2011: Tropical cyclones in the Bay of Bengal and extreme sea level projections along the east coast of India in a future climate scenario. *Current Science (India)*, **101,** 79-83.

Uotila, P., A. H. Lynch, J. J. Cassano, and R. I. Cullather, 2007: Changes in Antarctic net precipitation in the 21st century based on Intergovernmental Panel on Climate Change (IPCC) model scenarios. *Journal of Geophysical Research-Atmospheres*, **112**.

van de Berg, W., M. van den Broeke, J. Ettema, E. van Meijgaard, and F. Kaspar, 2011: Significant contribution of insolation to Eemian melting of the Greenland ice sheet. *Nature Geoscience*, **4,** 679-683.

Van de Wal, R. S. W., and M. Wild, 2001: Modelling the response of glaciers to climate change by applying volume-area scaling in combination with a high resolution GCM. *Climate Dynamics*, **18,** 359-366.

Vaughan, D. G., and J. R. Spouge, 2002: Risk estimation of collapse of the West Antarctic Ice Sheet. *Climatic Change*, **52,** 65-91.

Vellinga, M., and R. Wood, 2008: Impacts of thermohaline circulation shutdown in the twenty-first century. *Climatic Change*, **91,** 43-63.

Vermeer, M., and S. Rahmstorf, 2009: Global sea level linked to global temperature. *Proceedings of the National Academy of Science*, **106,** 21527-21532.

Vernier, J. P., L. W. Thomason, and J. Kar, 2011: CALIPSO detection of an Asian tropopause aerosol layer. *Geophys. Res. Lett.*, **38,** L07804.

Vinogradov, S. V., and R. M. Ponte, 2011: Low-frequency variability in coastal sea level from tide gauges and altimetry. *Journal of Geophysical Research-Oceans*, **116**.

Vizcaino, M., U. Mikolajewicz, J. Jungclaus, and G. Schurgers, 2010: Climate modification by future ice sheet changes and consequences for ice sheet mass balance. *Climate Dynamics*, **34,** 301-324.

Vizcaino, M., U. Mikolajewicz, M. Groger, E. Maier-Reimer, G. Schurgers, and A. Winguth, 2008: Long-term ice sheet-climate interactions under anthropogenic greenhouse forcing simulated with a complex Earth System Model. *Climate Dynamics*, 665-690.

von Schuckmann, K., and P. Y. Le Traon, submitted: How well can we derive Global Ocean Indicators from Argo data? *Ocean Science*.

von Storch, H., E. Zorita, and J. F. Gonzalez-Rouco, 2008: Relationship between global mean sea level and global mean temperature in a climate simulation of the past millennium. *Ocean Dynamics*, **58,** 227-236.

Vorosmarty, C. J., 2002: Global water assessment and potential contributions from Earth Systems Science. *Aquatic Sciences*, **64,** 328-351.

Wada, Y., L. P. H. van Beek, C. M. van Kempen, J. W. T. M. Reckman, S. Vasak, and M. F. P. Bierkens, 2010: Global depletion of groundwater resources. *Geophysical Research Letters*, **37,** -.

Walsh, K. J. E., K. McInnes, and J. L. McBride, 2011: Climate change impacts on tropical cyclones and extreme sea levels in the South Pacific – a regional assessment. *Global and Planetary Change*.

Wang, S., R. McGrath, J. Hanafin, P. Lynch, T. Semmler, and P. Nolan, 2008: The impact of climate change on storm surges over Irish waters. *Ocean Modelling*, **25,** 83-94.

Wang, X., and V. Swail, 2006: Climate change signal and uncertainty in projections of ocean wave heights. *Climate Dynamics*, **26,** 109-126.

Wang, X., V. Swail, F. Zwiers, X. Zhang, and Y. Feng, 2009: Detection of external influence on trends of atmospheric storminess and northern oceans wave heights. *Climate Dynamics*, **32,** 189-203.

Wang, X. L., V. R. Swail, and A. Cox, 2010: Dynamical versus statistical downscaling methods for ocean wave heights. *International Journal of Climatology*, **30,** 317-332.
Warrick, R. A., and J. Oerlemans, 1990: Sea level rise. *Climate Change, The IPCC Scientific Assessment*, J. T. Houghton, G. J. Jenkins, and J. J. Ephraums, Eds., Cambridge University Press, 260-281.
Warrick, R. A., C. Le Provost, M. F. Meier, J. Oerlemans, and P. L. Woodworth, 1996: Changes in sea level. *Climate Change 1995, The Science of Climate Change*, J. T. Houghton, L. G. Meira Filho, B. A. Callander, N. Harris, A. Klattenberg, and K. Maskell, Eds., Cambridge University Press, 359-405.
Washington, W. M., and Coauthors, 2009: How much climate change can be avoided by mitigation? *Geophys. Res. Lett.*, **36**.
Watts, A. B., 2001: *Isostasy and Flexure of the Lithosphere.* Cambridge University Press, 458 pp.
Weertman, J., 1961: STABILITY OF ICE-AGE ICE SHEETS. *Journal of Geophysical Research*, **66,** 3783-&.
——, 1974: Stability of the junction of an ice sheet and ice shelf. *Journal of Glaciology*, **13,** 3-13.
Wenzel, M., and J. Schroter, 2010: Reconstruction of regional mean sea level anomalies from tide gauges using neural networks. *Journal of Geophysical Research-Oceans*, **115**.
White, N., J. Church, and J. Gregory, 2005a: Coastal and global averaged sea level rise for 1950 to 2000. *Geophysical Research Letters*, **32,** -.
White, N. J., J. A. Church, and J. M. Gregory, 2005b: Coastal and global averaged sea level rise for 1950 to 2000. *Geophysical Research Letters*, **32,** -.
Wijffels, S., and Coauthors, 2008: Changing Expendable Bathythermograph Fall Rates and Their Impact on Estimates of Thermosteric Sea Level Rise. *Journal of Climate*, **21,** 5657-5672.
Willis, J. K., D. P. Chambers, and R. S. Nerem, 2008: Assessing the globally averaged sea level budget on seasonal to interannual timescales. *Journal of Geophysical Research-Oceans*, **113,** -.
Wingham, D. J., D. W. Wallis, and A. Shepherd, 2009: Spatial and temporal evolution of Pine Island Glacier thinning, 1995-2006. *Geophysical Research Letters*, **36**.
Winguth, A., U. Mikolajewicz, M. Groger, E. Maier-Reimer, G. Schurgers, and M. Vizcaino, 2005: Centennial-scale interactions between the carbon cycle and anthropogenic climate change using a dynamic Earth system model. *Geophysical Research Letters***,** ARTN L23714, DOI 10.1029/2005GL023681.
Wong, T., B. Wielicki, R. Lee, G. Smith, K. Bush, and J. Willis, 2006: Reexamination of the observed decadal variability of the earth radiation budget using altitude-corrected ERBE/ERBS nonscanner WFOV data. *Journal of Climate***,** 4028-4040.
Woodworth, P. L., M. Menendez, and W. R. Gehrels, 2011a: Evidence for Century-Timescale Acceleration in Mean Sea Levels and for Recent Changes in Extreme Sea Levels. *Surveys in Geophysics*, **32,** 603-618.
Woodworth, P. L., W. R. Gehrels, and R. S. Nerem, 2011b: Nineteenth and Twentieth Century Changes in Sea Level. *Oceanography*, **24,** 80-93.
Woodworth, P. L., N. J. White, S. Jevrejeva, S. J. Holgate, J. A. Church, and W. R. Gehrels, 2009: Evidence for the accelerations of sea level on multi-decade and century timescales. *International Journal of Climatology***,** 777-789.
Woolf, D. K., P. G. Challenor, and P. D. Cotton, 2002: Variability and predictability of the North Atlantic wave climate. *J. Geophys. Res.*, **107,** 3145.
Woppelmann, G., and Coauthors, 2009: Rates of sea level change over the past century in a geocentric reference frame. *Geophysical Research Letters*, **36,** -.
Woth, K., R. Weisse, and H. von Storch, 2006: Climate change and North Sea storm surge extremes: an ensemble study of storm surge extremes expected in a changed climate projected by four different regional climate models. *Ocean Dynamics*, **56,** 3-15.
Wouters, B., D. Chambers, and E. J. O. Schrama, 2008: GRACE observes small-scale mass loss in Greenland. *Geophysical Research Letters*, **35,** 5.
Wunsch, C., and D. Stammer, 1997: Atmospheric loading and the oceanic "inverted barometer" effect. *Reviews of Geophysics*, **35,** 79-107.
Wunsch, C., and P. Heimbach, 2007: Practical global oceanic state estimation. *Physica D-Nonlinear Phenomena*, **230,** 197-208.
Yin, J. J., M. E. Schlesinger, and R. J. Stouffer, 2009: Model projections of rapid sea level rise on the northeast coast of the United States. *Nature Geoscience*, **2,** 262-266.
Yin, J. J., S. M. Griffies, and R. J. Stouffer, 2010: Spatial Variability of Sea Level Rise in Twenty-First Century Projections. *Journal of Climate*, **23,** 4585-4607.
Yin, J. J., J. T. Overpeck, S. M. Griffies, A. X. Hu, J. L. Russell, and R. J. Stouffer, 2011: Different magnitudes of projected subsurface ocean warming around Greenland and Antarctica. *Nature Geoscience*, **4,** 524-528.
Yoshimori, M., and A. Abe-Ouchi, in press: Sources of spread in multi-model projections of the Greenland ice-sheet surface mass balance. *Journal of Climate*.
Young, I. R., S. Zieger, and A. V. Babanin, 2011: Global Trends in Wind Speed and Wave Height. *Science*, **332,** 451-455.
Zemp, M., M. Hoelzle, and W. Haeberli, 2009: Six decades of glacier mass-balance observations: a review of the worldwide monitoring network. *Annals of Glaciology*, **50,** 101-111.

Zickfeld, K., M. Eby, H. Matthews, and A. Weaver, 2009: Setting cumulative emissions targets to reduce the risk of dangerous climate change. *Proceedings of the National Academy of Sciences of the United States of America*, **106,** 16129-16134.

Zuo, Z., and J. Oerlemans, 1997: Contribution of glacier melt to sea level rise since AD 1865: a regionally differentiated calculation. *Climate Dynamics*, **13,** 835-845.

Appendix 13.A: Methods of Sea Level Projections for the 21st Century

Annual timeseries for change in global-mean surface air temperature and GMSL rise due to thermal expansion in the historical period and during the 21st century under RCP scenarios (Section 13.5.1) were obtained from CMIP5 AOGCMs. Where CMIP5 results were not available for a particular AOGCM and scenario, they were estimated by the method of Good et al. (2011) using the response of that AOGCM to an instantaneous quadrupling of CO_2 concentration. The same method was used to estimate the CMIP5 projections for scenario SRES A1B. Uncertainties were derived from the CMIP5 ensemble by treating the model spread as a normal distribution. As in the AR4, the temperature and expansion timeseries were chosen from their distributions in a perfectly correlated way, but all other uncertainties were assumed independent and combined by Monte Carlo. For input to the land ice projections (Section 13.6.1.1), the projections for global surface air temperature change $T(t)$ were expressed as anomalies relative to the time-mean of 1865–1894 and adjusted to have the same time-mean anomaly for 1986–2005 with respect to 1865–1894 as in observations (Brohan et al., 2006). For simulation of past land-ice changes (Section 13.4.7), the historical simulations of $T(t)$ were similarly expressed as anomalies with respect to 1865–1894, but not adjusted.

The rate of global glacier mass loss $r_g = -\mathrm{d}M_g/\mathrm{d}t$, where M_g is global glacier mass and t is time, was parametrised according to $r_g = s\,(T - T_0)\,(M_g/M_0)^{1.65}$, where s is the global glacier mass balance sensitivity to T, obtained by linear regression of observations of r_g against T (Section 13.4.7), giving $s = 1.07 \pm 0.26$ mm $\mathrm{yr}^{-1}\,\mathrm{K}^{-1}$ (standard error). The final factor in r_g represents the reduction in sensitivity as glacier area is lost, where $M_0 = 0.6$ m SLE (Radić and Hock, 2010) is the value of M_g at the start of the projections in 1986. This form for r_g and the exponent were derived by Meehl et al. (2007) in the AR4 (Section 10.A.2). We used this method because it is a convenient parametrisation in terms of T that gives results close to those of the more detailed model of Radić and Hock (2011) (Section 13.5.2). To make projections, we chose s randomly from a normal distribution representing its uncertainty, and $T_0 = 0.32 - 0.65/s$, which gives $T_0 = -0.28$ K for the central value of s. T_0 is the value of T for a climate in which glaciers were in steady state i.e., $r_g = 0$.

Changes in ice-sheet SMB were computed from T using quadratic fits to the results of Gregory and Huybrechts (2006), as in the AR4 (Section 10.A.4). The fits were treated as equally probable. We used this method because it is a convenient parametrisation in terms of T that gives results close to those of several other models described in Section 13.5.3. However, the more recent models for Greenland on average give results which are larger by 20% than the AR4 method, and they indicate that an uncertainty of 30% arises from different treatments of Greenland SMB. Therefore to represent the ranges of these models, we multiply the results of the Greenland quadratic fits by 1.2 and add an additional normally distributed random uncertainty of 30%.

The contributions from ice-sheet dynamics at the start of the projections were taken to be half of the observed rate of loss for 2005–2010 from Greenland and all of that for Antarctica (Section 13.4.7). The contributions reach 0.004–0.100 m at 2100 from Greenland and 0.018–0.150 m from Antarctica; these are the likely ranges from our assessment of existing studies (Section 13.5.4). For each ice-sheet, a quadratic function of time was fitted which begins at the minimal initial rate and reaches the minimum final amount, and another for the maxima. Time series for the dynamic contribution lying between these extremes were constructed as combinations of the extreme time series using a random and uniform linear weight. The same method was followed for the anthropogenic terrestrial water storage contribution (initial rates from Section 13.4.6 and final amounts from Section 13.5.5).

Appendix 13.B: Components and Total Projected Sea Level Change

[PLACEHOLDER FOR SECOND ORDER DRAFT: Table 13.B.1]

Chapter 13: Sea-Level Change

Coordinating Lead Authors: John A. Church (Australia), Peter U. Clark (USA)

Lead Authors: Anny Cazenave (France), Jonathan Gregory (UK), Svetlana Jevrejeva (UK), Anders Levermann (Germany), Mark Merrifield (USA), Glenn Milne (Canada), R. Steven Nerem (USA), Patrick Nunn (Australia), Antony Payne (UK), W. Tad Pfeffer (USA), Detlef Stammer (Germany), Alakkat Unnikrishnan (India)

Contributing Authors: David Bahr (USA), Jason E. Box (USA), David H. Bromwich (USA), Mark Carson (Germany), William Collins (UK), Xavier Fettweis (Belgium), Piers Forster (UK), Alex Gardner, Peter Good (UK), Rune Grand Graversen (Sweden), Ralf Greve (Japan), Stephen Griffies (USA), Edward Hanna (UK), Mark Hemer (Australia), Regine Hock (USA), Simon J. Holgate (UK), John Hunter (Australia), Philippe Huybrechts (Belgium), Gregory Johnson (USA), Georg Kaser (Austria), Caroline Katzman (Netherlands), Gerhard Krinner (France), Jan Lanaerts (Netherlands), Ben Marzeion (Austria), Kathleen L. McInnes (Australia), Sebastian Mernild (USA), Ruth Mottram (Denmark), Gunnar Myhre (Norway), J.P. Nicholas (USA), Valentina Radic (Canada), Jamie Rae (UK), Jan H. van Angelen (Netherlands), Willem J. van de Berg (Netherlands), Michiel van den Broeke (Netherlands), Masakazu Yoshimori (Japan)

Review Editors: Jean Jouzel (France), Roderik van de Wal (Netherlands), Philip L. Woodworth (UK), Cunde Xiao (China)

Date of Draft: 16 December 2011

Notes: TSU Compiled Version

Figures

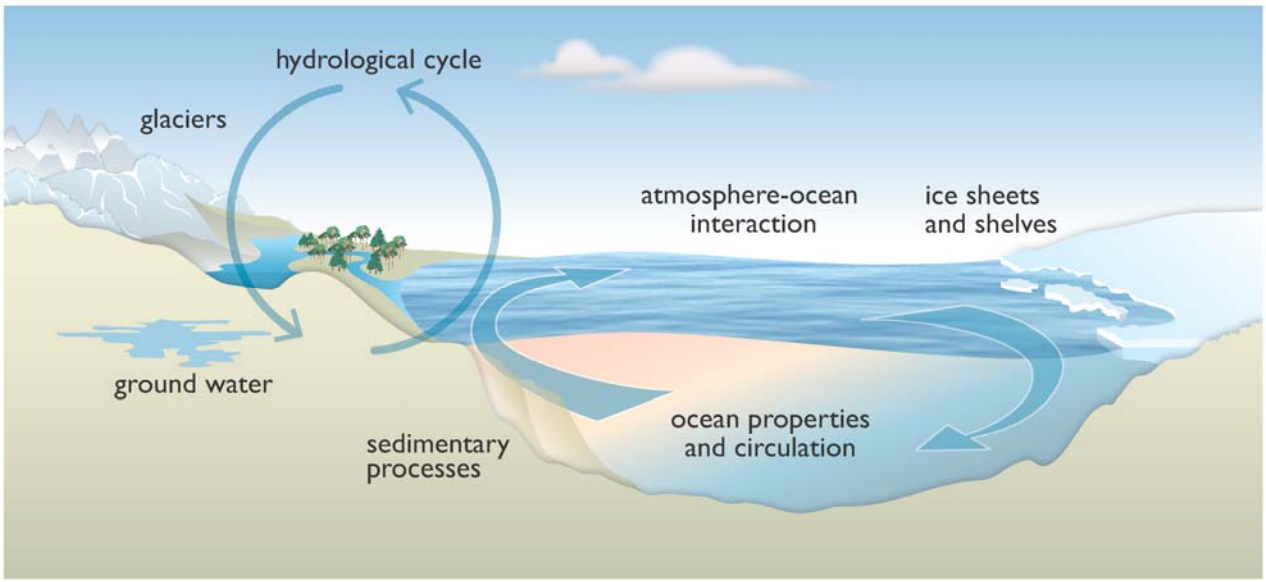

Figure 13.1: Schematic diagram illustrating climate sensitive processes that can influence sea level. Changes in any one of the components or processes shown will result in a sea level change. The term 'ocean properties' refers to ocean temperature, salinity and density, which influence and are dependent on ocean circulation. The term “sedimentary processes” includes erosion, deposition and compaction of sediment.

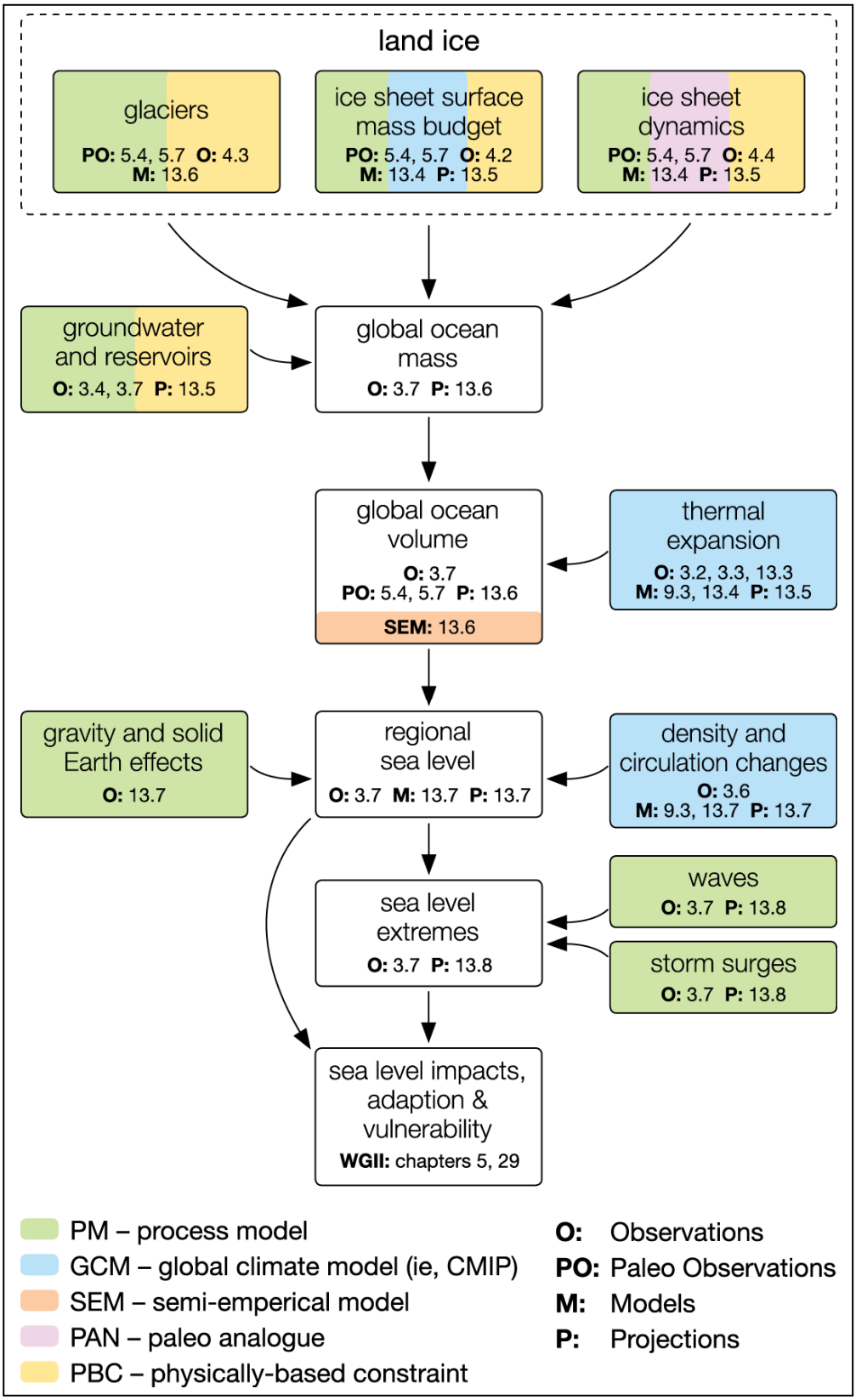

Figure 13.2: Schematic representation of key processes that contribute to sea level change and are considered in this report. Colouring of individual boxes indicates the types of models and approaches used in projecting the contribution of each process to future sea level change. The diagram also serves as an index to the sections in this report that are relevant to the assessment of sea level projections via numbers given at the bottom of each box.

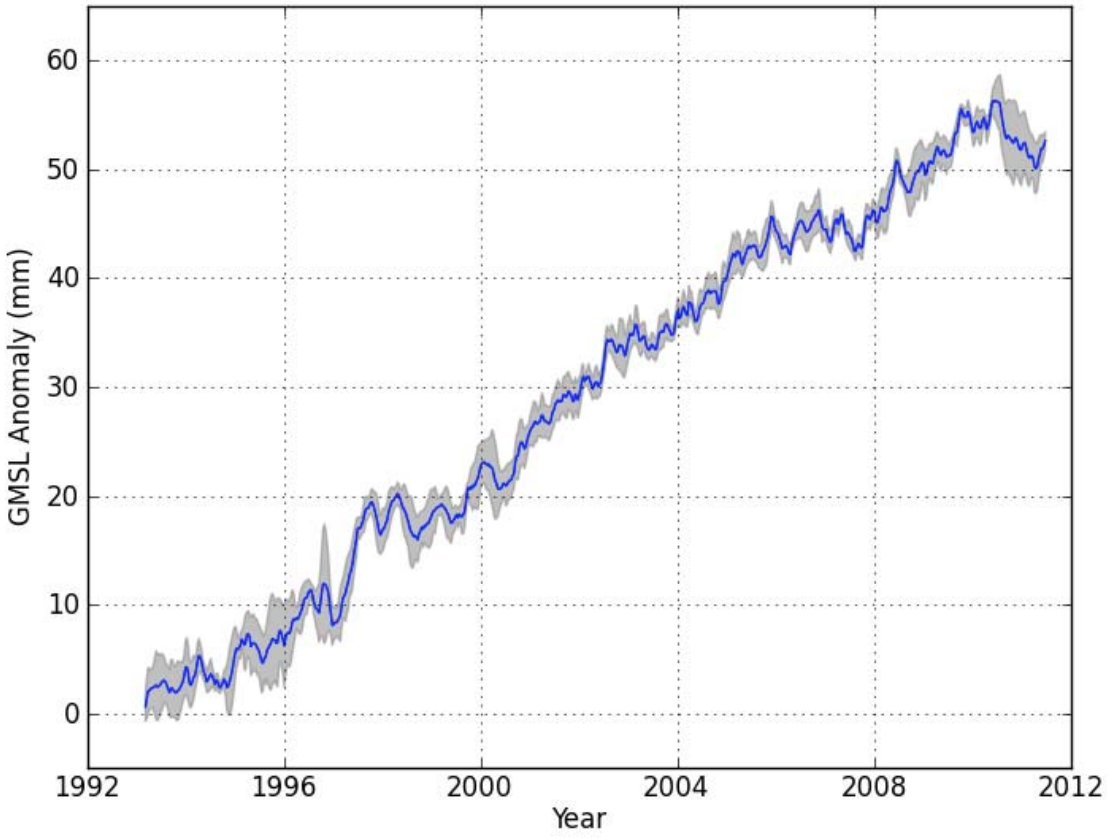

Figure 13.3: Global mean sea level variations over 1993-2011 computed from an ensemble mean of five different analyses of altimeter data from the TOPEX/Poseidon, Jason-1, and Jason-2 satellite missions (Ablain et al., 2009; Beckley et al., 2010; Church and White, 2011; Leuliette and Scharroo, 2010; Nerem et al., 2010). Annual and semi-annual variations have been removed and 60-day smoothing has been applied. The secular trend is 3.2 mm yr^{-1} after correcting for GIA (0.3 mm yr^{-1}). The gray shading represents 95% certainties based on the standard deviation of the different analyses.

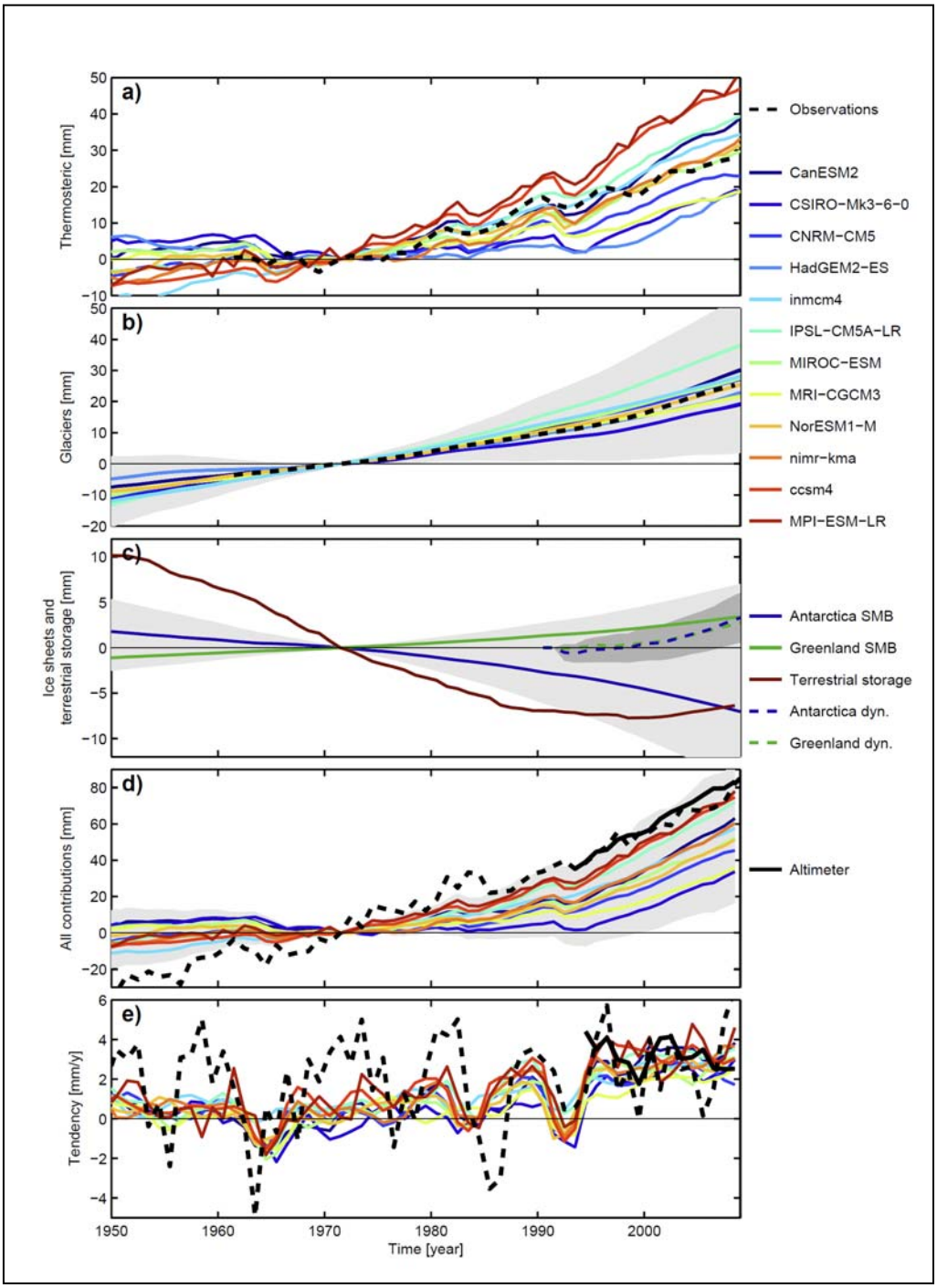

Figure 13.4: Modeled and observed global-mean sea level contributions and total sea level from the 1960s to the present. All curves have an arbitrary offset and are set to zero in 1971, shortly after a significant increase in the number of ocean observations. The coloured curves are for various model simulations of (a) thermal expansion, (b) glacier melting, (c) Greenland and Antarctic surface mass balance, observed changes in terrestrial storage and the dynamic response of the ice sheets, (d) total sea level and (e) the model and observed trends in sea level. In each panel the observational time series is shown in black (dashed, and solid for the altimeter record). The total model uncertainty range is in light grey.

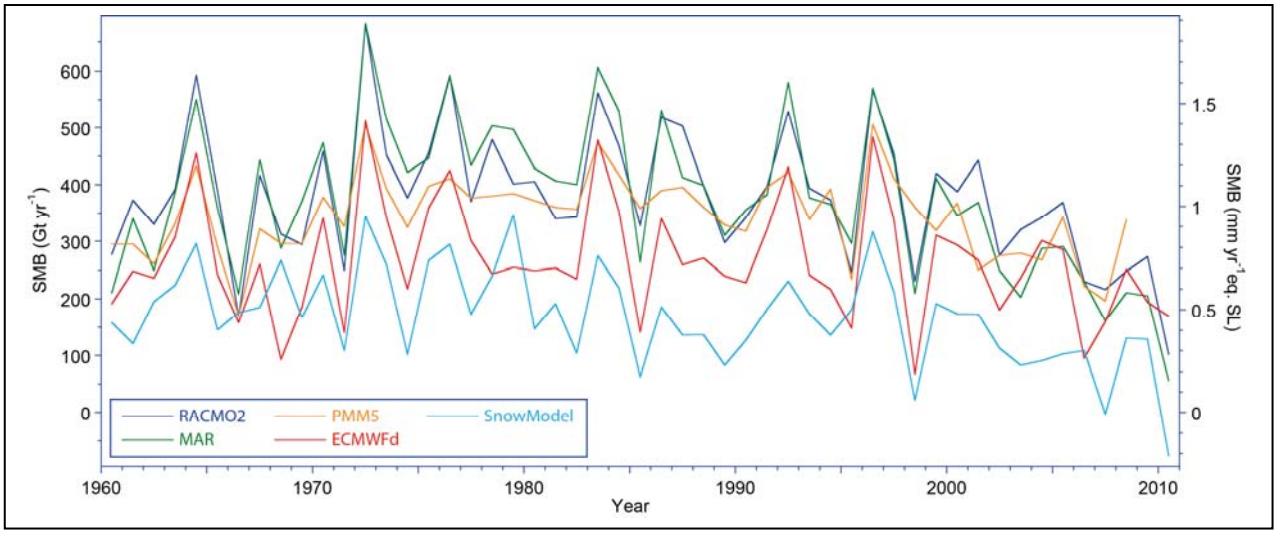

Figure 13.5: Annual-mean surface mass balance (accumulation minus ablation) for the Greenland Ice Sheet, simulated by regional climate models for the period 1960–2010.

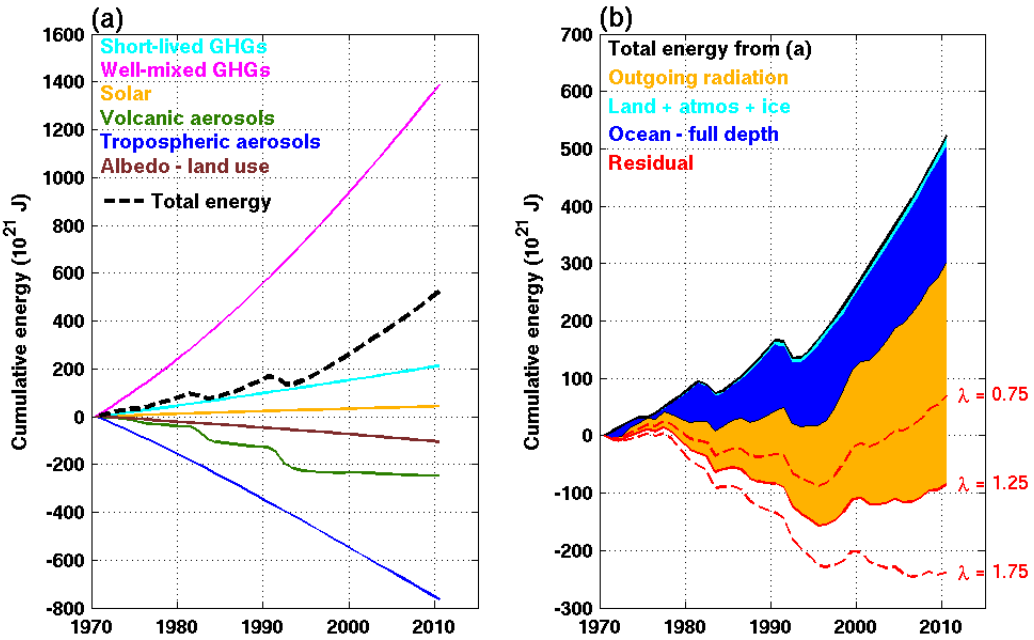

Box 13.1, Figure 1: The Earth's energy budget from 1970 through 2010. **(a)** The cumulative energy into the Earth system from changes in solar forcing, well-mixed and short-lived greenhouse gases, changes in surface albedo, volcanic forcing and tropospheric aerosol forcing are shown by the coloured lines and these are added to give the total energy changes (dashed black line). **(b)** The cumulative energy from (a), with an expanded scale, is balanced by the warming of the Earth system (energy absorbed in the melting of ice and warming the atmosphere, the land and the ocean) and an increase in outgoing radiation inferred from temperature change of a warming Earth. These terms are represented by the time-varying thicknesses of the coloured regions. The residuals in the cumulative energy (red lines) for a climate feedback parameter λ of 1.25 ± 0.5 W m^{-2} K^{-1} (equivalent to an equilibrium climate sensitivity of 3°C with a range from 2.1°C (λ of 1.75 W m^{-2} K^{-1}) to 4.9°C (λ of 0.75 W m^{-2} K^{-1}), are indicated by the solid and dashed red lines. The uncertainties quoted are one standard deviation.

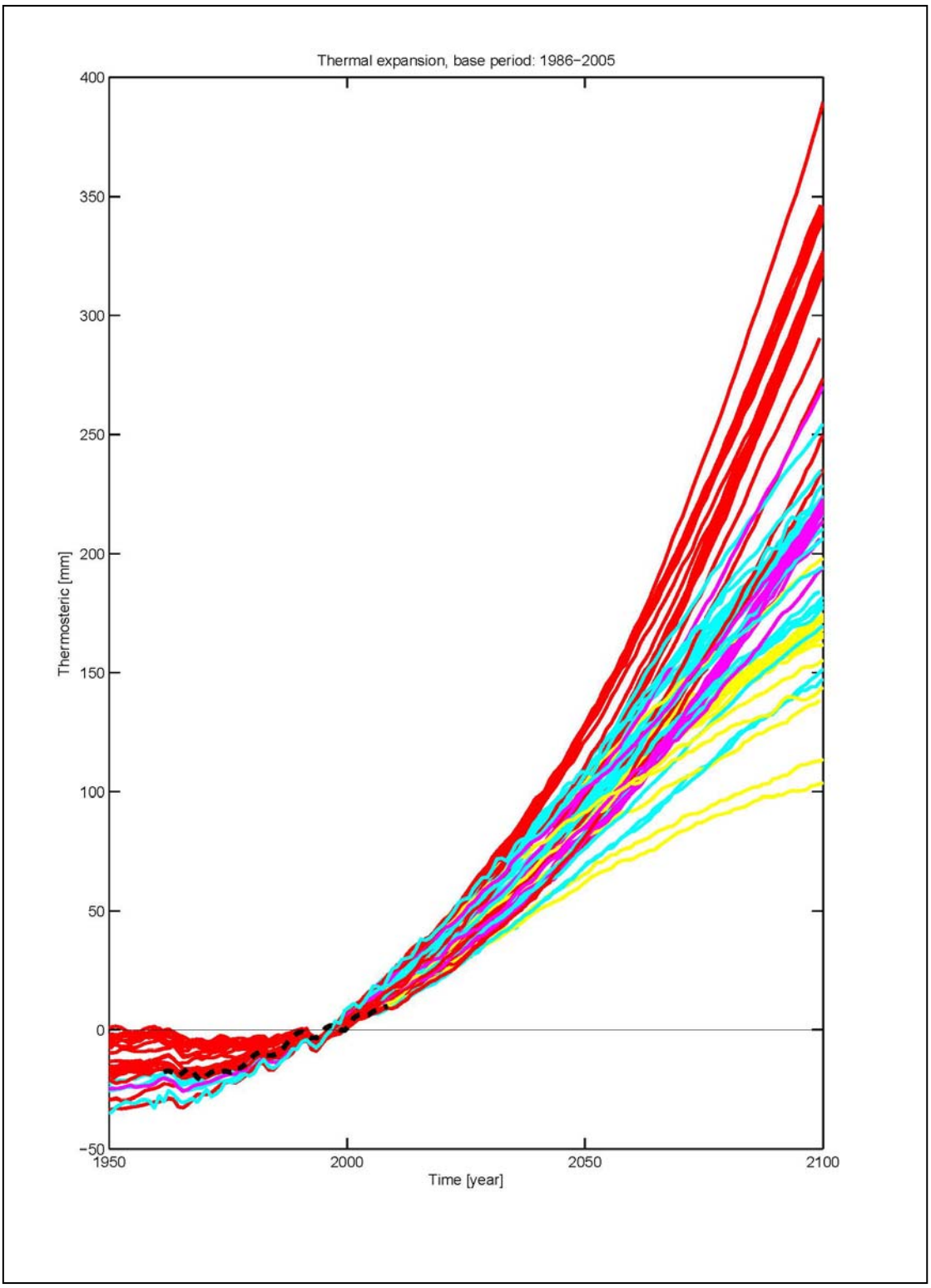

Figure 13.6: [PLACEHOLDER FOR SECOND ORDER DRAFT: CMIP5 results for the period beyond 2100 will be added.] Observed [tbc] and modelled thermosteric sea level rise for 1950 to 2100 [tbc] [Approximately scaled results for ocean heat content on right hand axis. Upper 700 m or full depth or both and for all RCPs to be decided.]

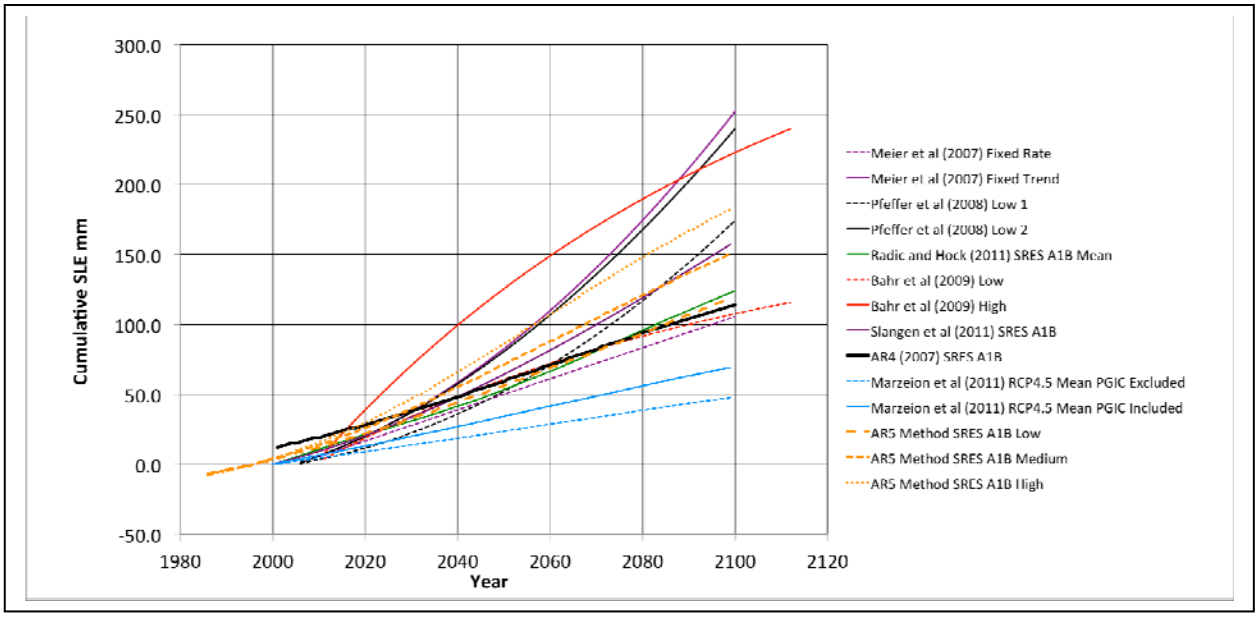

Figure 13.7: Projected sea level rise from glaciers according to model calculations from seven recent analyses, with AR4 glacier projections for comparison. Mean projections only are shown in each case. Calving losses are considered in the Pfeffer (2008) and Meier (2007) projections, but excluded in the Radic and Hock (2011), Bahr et al. (2009), Slangen et al. (2011), Marzeion et al. (2011), and AR5 method projections. Radic and Hock, Slangen, and AR5 projections are GCM-driven models using the SRES A1B scenario; the Marzeion projection uses the CMIP RCP4.5. PGIC in Marzeion curves refers to peripheral glaciers and ice caps surrounding the Greenland and Antarctic Ice Sheets. Curves for Radic and Hock and for Marzeion are a mean of ten different GCM model inputs.

Figure 13.8: [PLACEHOLDER FOR SECOND ORDER DRAFT: Observed and projected surface mass balance and dynamical contributions from 1950 to 2100.]

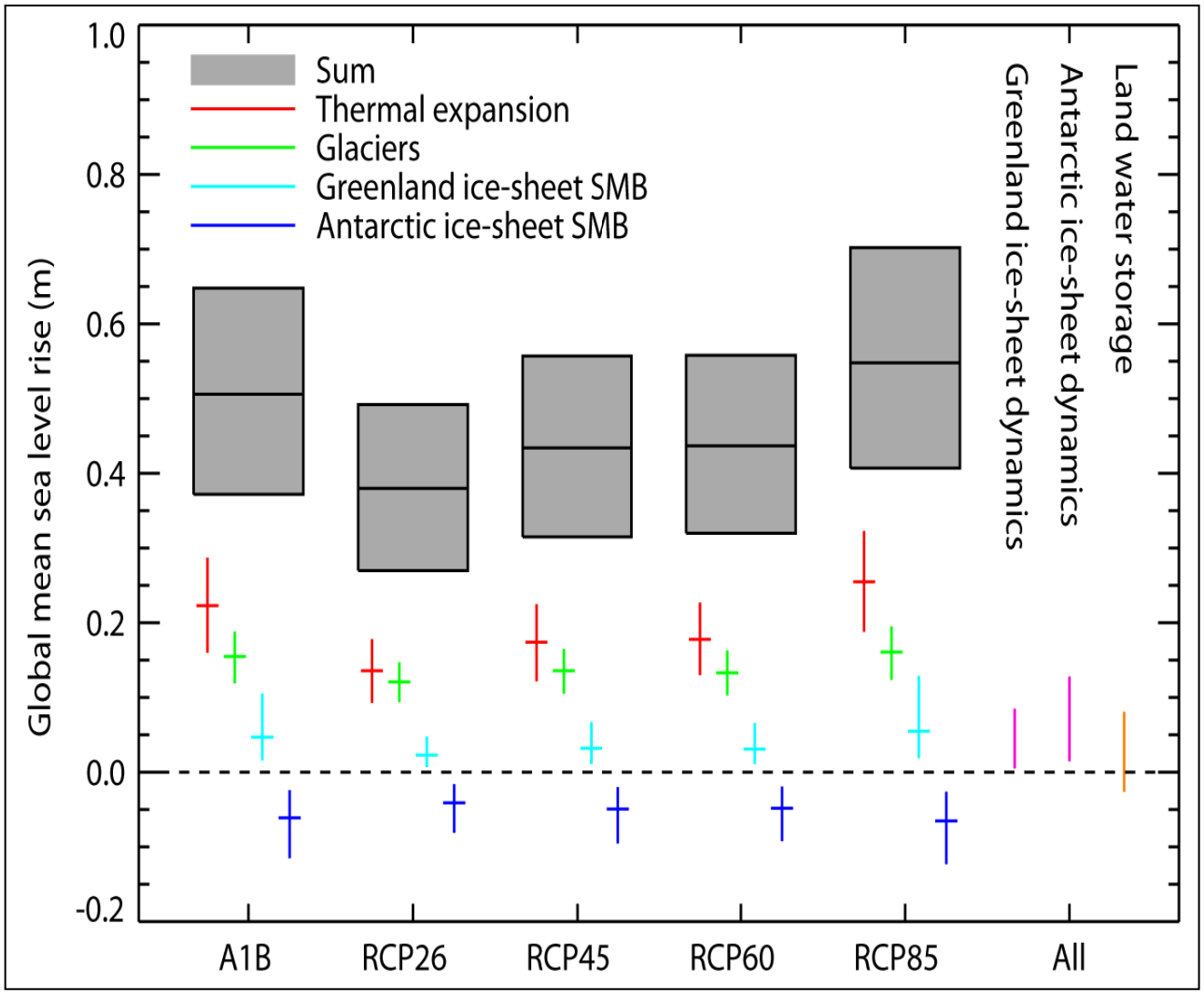

Figure 13.9: Projections with ranges and median values for global mean sea level rise and its contributions in 2081–2100 relative to 1986–2005 for the four RCP scenarios and scenario SRES A1B used in the AR4. The contributions from ice-sheet dynamical change and anthropogenic land water storage are independent of scenario, and are treated as having uniform probability distributions. The projections for global-mean sea level rise are regarded as likely ranges with medium confidence. See discussion in Sections 13.6.1.1 and 13.6.1.3 and Annex 13.A for methods.

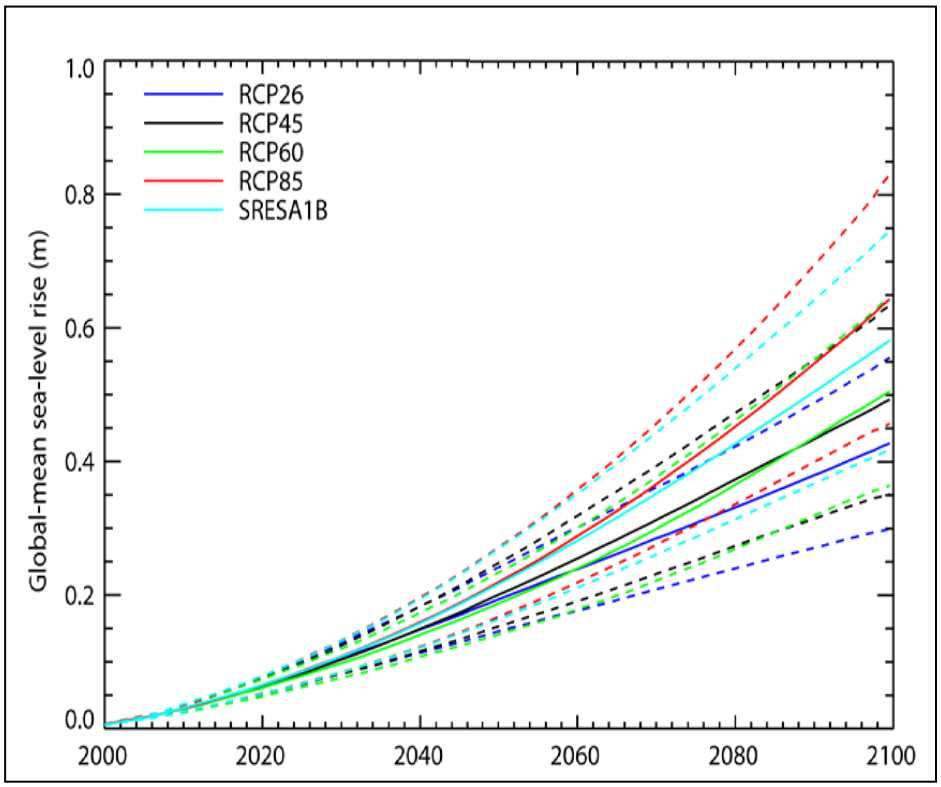

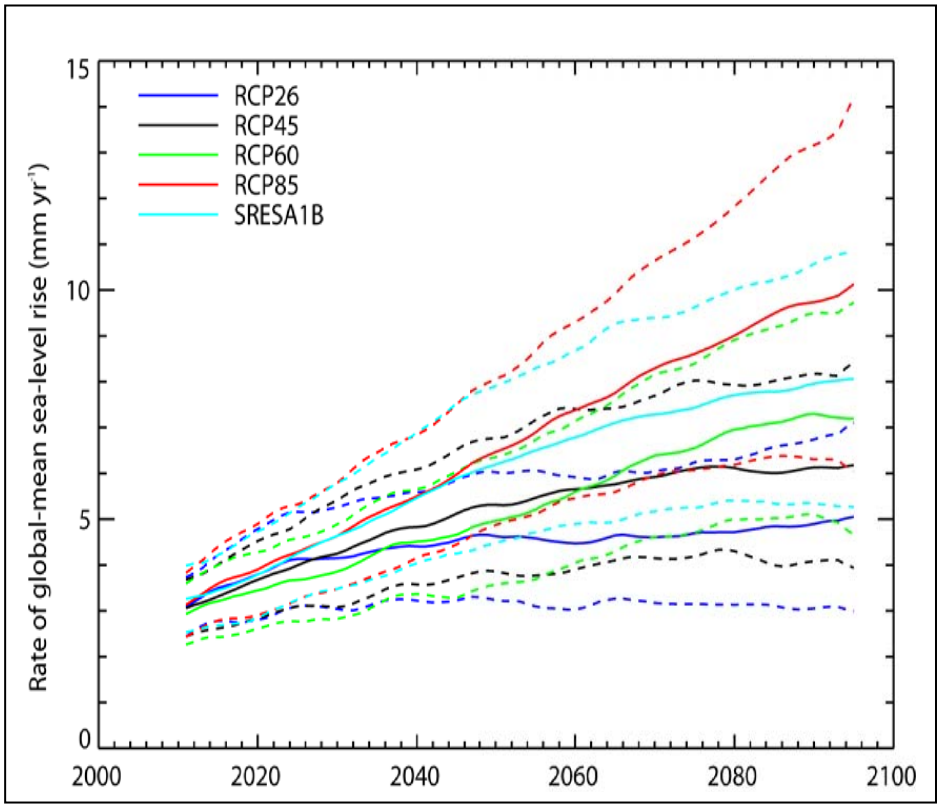

Figure 13.10: Projections of (a) GMSL rise relative to 1986–2005 and (b) the rate of GMSL rise as a function of time for the four RCP scenarios and scenario SRES A1B. The solid lines show the median and the dashed lines the likely range for each scenario.

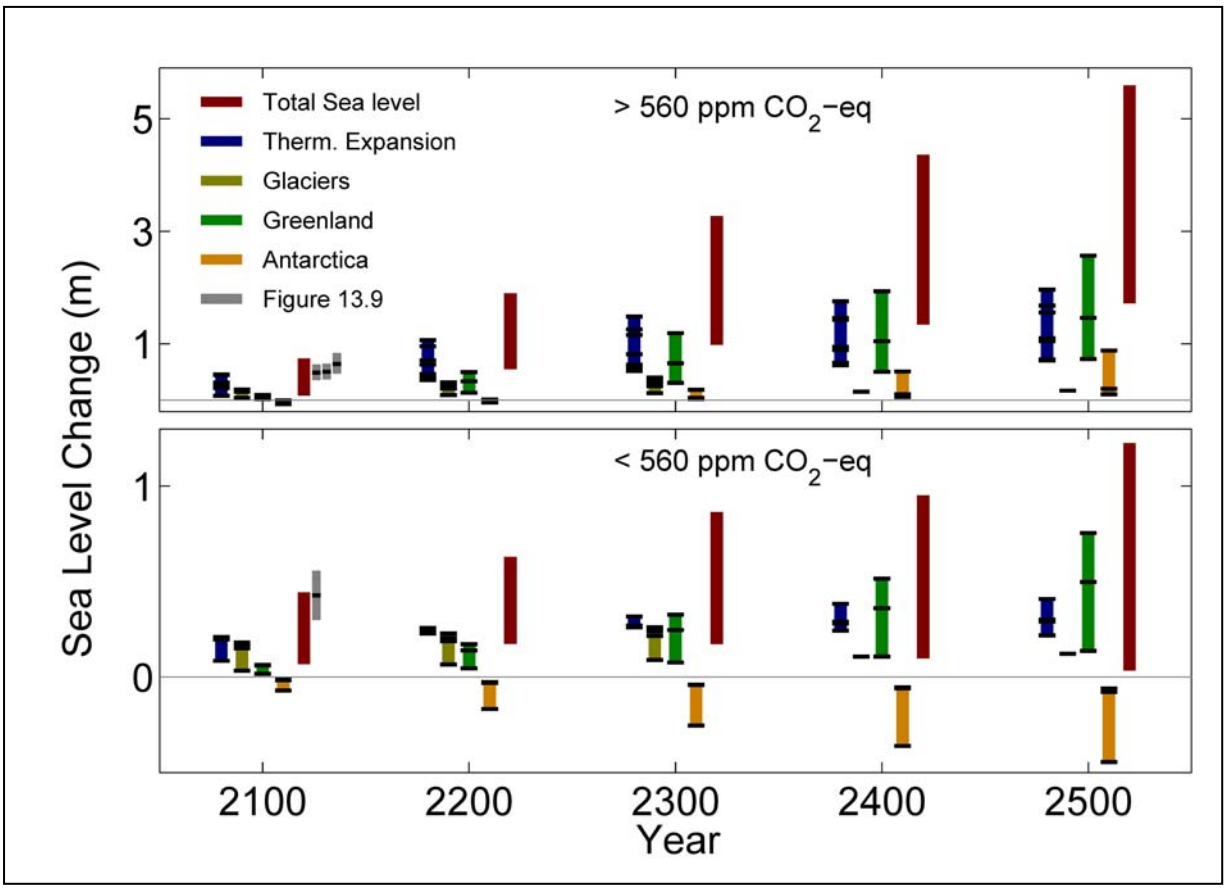

Figure 13.11: Sea level projections beyond the year 2100 are grouped into scenarios which exceed 560 ppm CO_2-equivalent (upper panel) and those who do not (lower panel). Coloured bars comprise the entire range of available model simulations. Horizontal lines provide the specific model simulations. Total sea level represents the sum of the different components assuming independence of the different contributions. Grey shaded bars exhibit the likely range for the 21st century projection from Figure 13.9 with the median as the horizontal line. [PLACEHOLDER FOR SECOND ORDER DRAFT: More simulations will be added including from the model intercomparison projects SeaRise and Ice2Sea.]

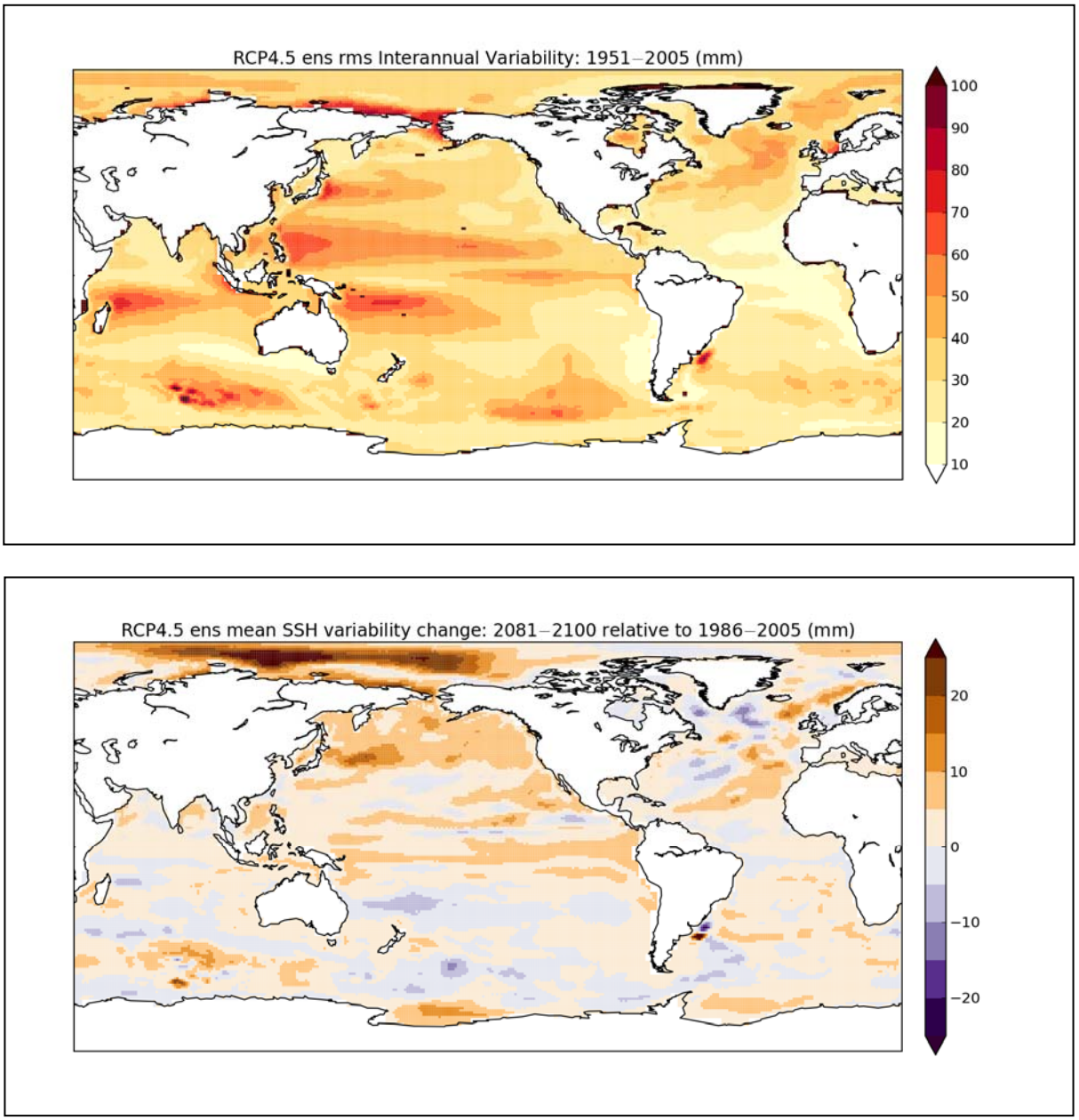

Figure 13.12: (a) RMS Interannual dynamic sea level variability (mm) in a CMIP5 multimodel ensemble (7 models total), built from the historically-forced experiments during the period 1951–2005; (b) Changes in the ensemble average inter-annual dynamic sea level variability (std. dev.; in mm) in 2081–2100 relative to 1986–2005. The projection data (2081-2100) is from the RCP4.5 experiment.

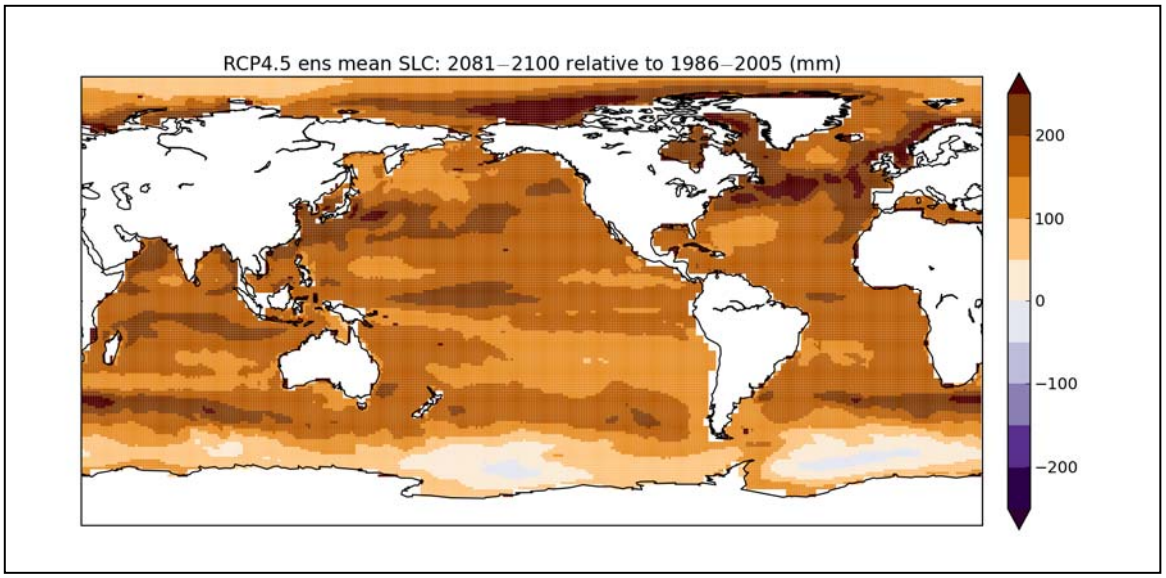

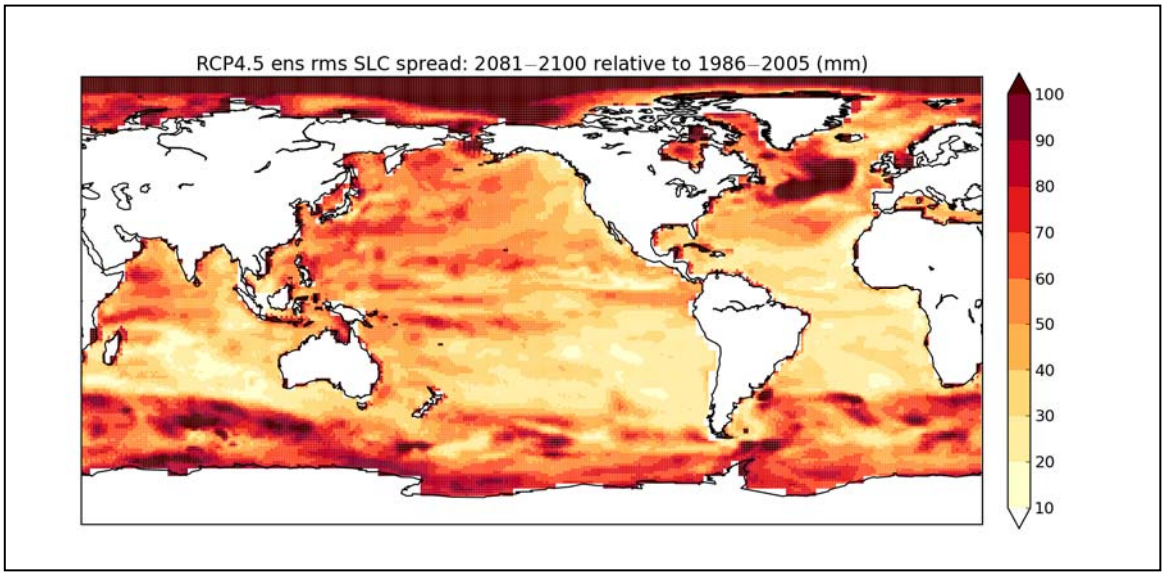

Figure 13.13: (a) CMIP5 ensemble mean projection of the steric sea level in 2081–2100 relative to 1986–2005 computed from 7 models (in mm), using the RCP4.5 experiment. The figure includes the globally averaged steric sea level increase. (b) RMS spread (deviation) of the ensemble mean (mm).

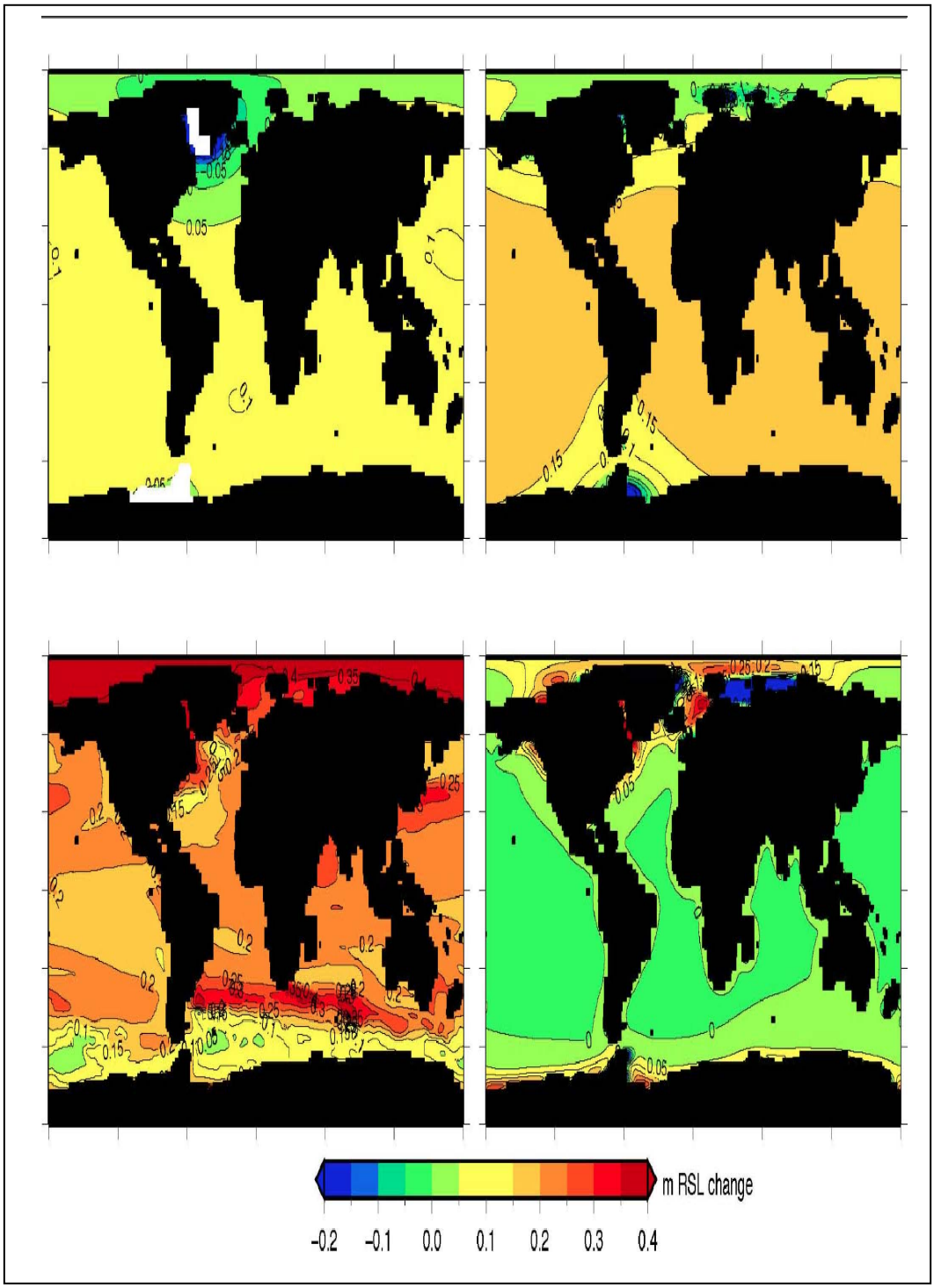

Figure 13.14: [PLACEHOLDER FOR SECOND ORDER DRAFT: CMPI5 results.] Ensemble mean RSL contribution (m) of ice sheets (upper left), glaciers (upper right), steric changes (lower left) and GIA (lower right) for scenario A1B between 1980–1999 and 2090–2099. White shading in upper left panel indicates the mass loss regions on AIS and GIS (from Slangen et al., 2011).

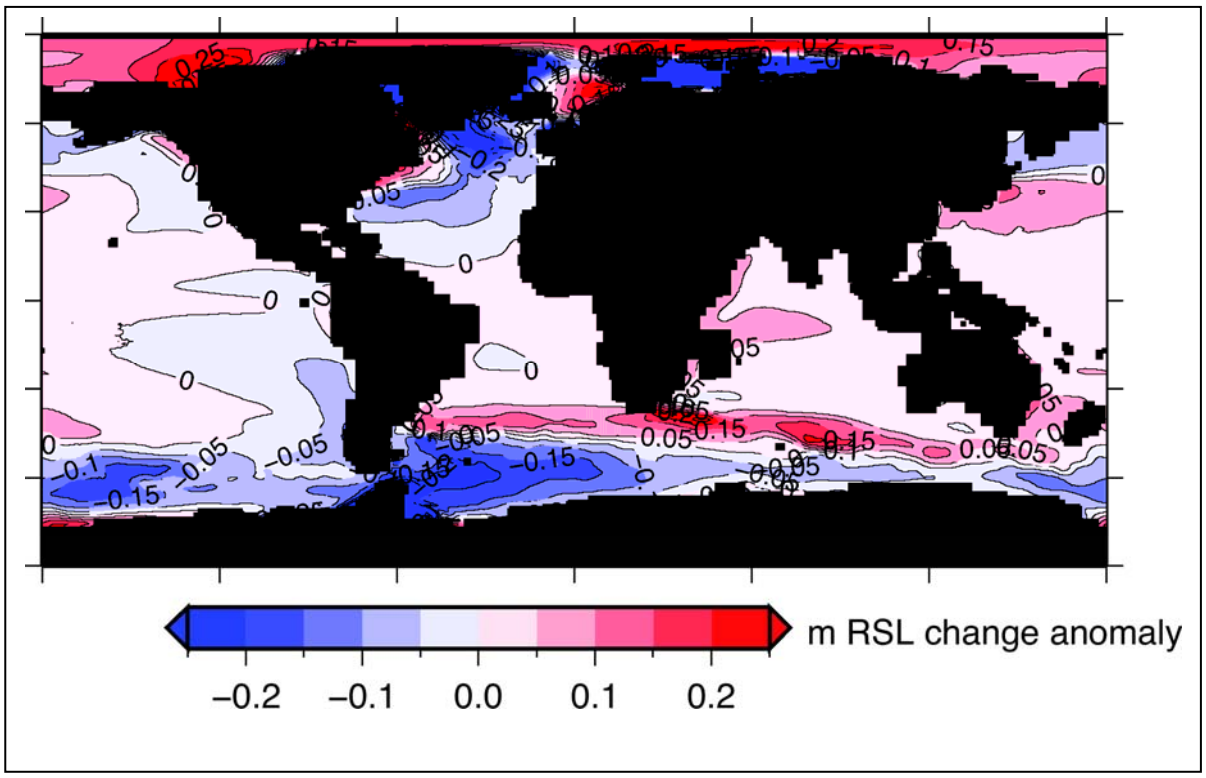

Figure 13.15: [PLACEHOLDER FOR SECOND ORDER DRAFT: CMPI5 results.] Ensemble mean sea level anomaly (m) with respect to global mean RSL change (0.47 m) for scenario A1B between 1980–1999 and 2090–2099 (from Slangen et al., 2011). Global mean = 0.47 m; range = –3.65 to +1.01 m.

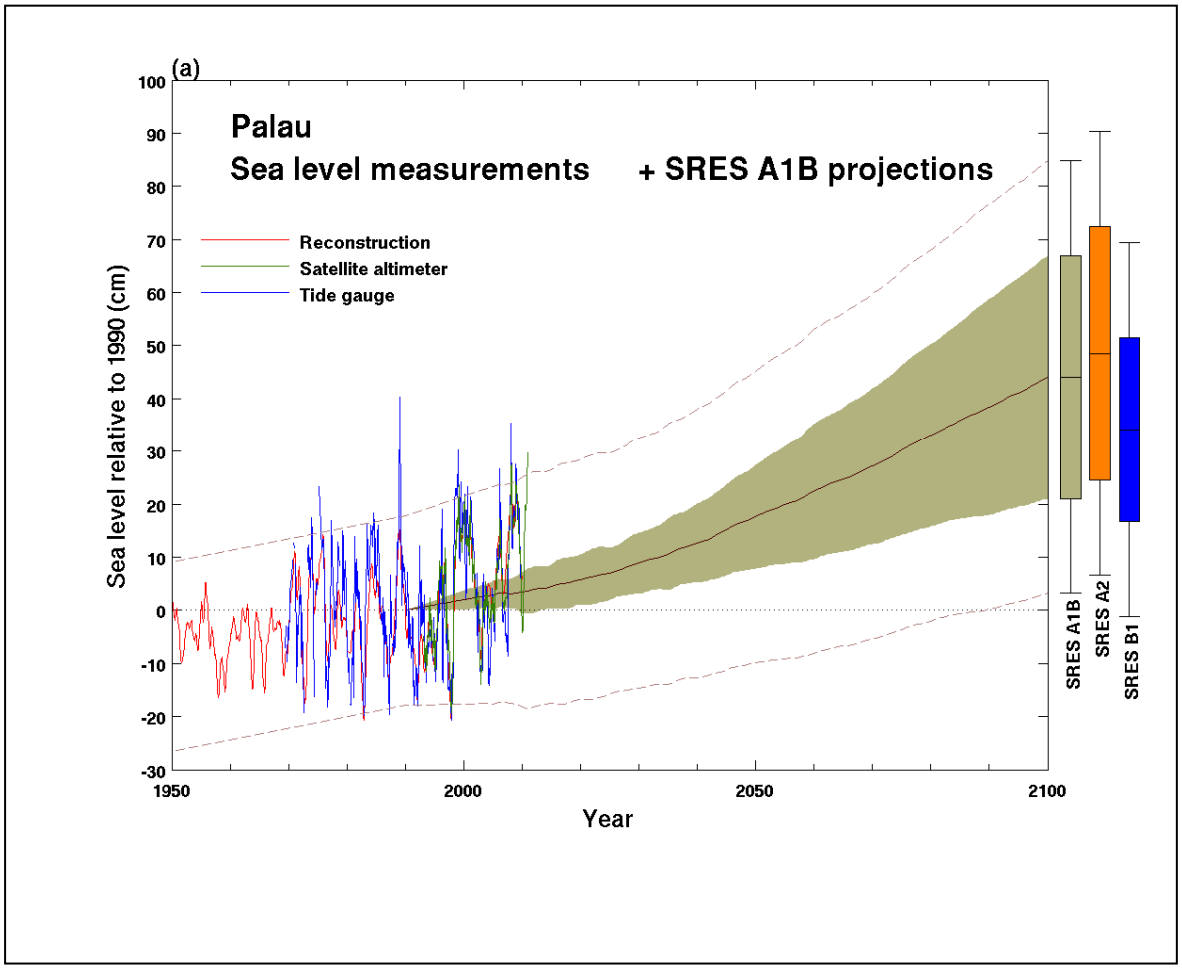

Figure 13.16: [PLACEHOLDER FOR SECOND ORDER DRAFT: CMPI5 results. To be expanded/updated f when CMIP projections are available – will show results for some key locations around the globe.] Observed and projected relative sea level change near Palau. The observed *in situ* relative sea level records (since the late 1970s) are indicated in blue, with the satellite record (since 1993) in green. The gridded sea level at Cook Islands (since 1950, from Church and White, 2011) is shown in red. The projections for the A1B scenario (5–95% uncertainty range) are shown by the shaded region from 1990–2100. The range of projections for the A1B, A2 and B1 scenarios by 2100 are also shown by the bars on the right. The dashed lines are an estimate of interannual variability in sea level (5–95% range about the long-term trends) and indicate that individual monthly averages of sea level can be above or below longer term averages.

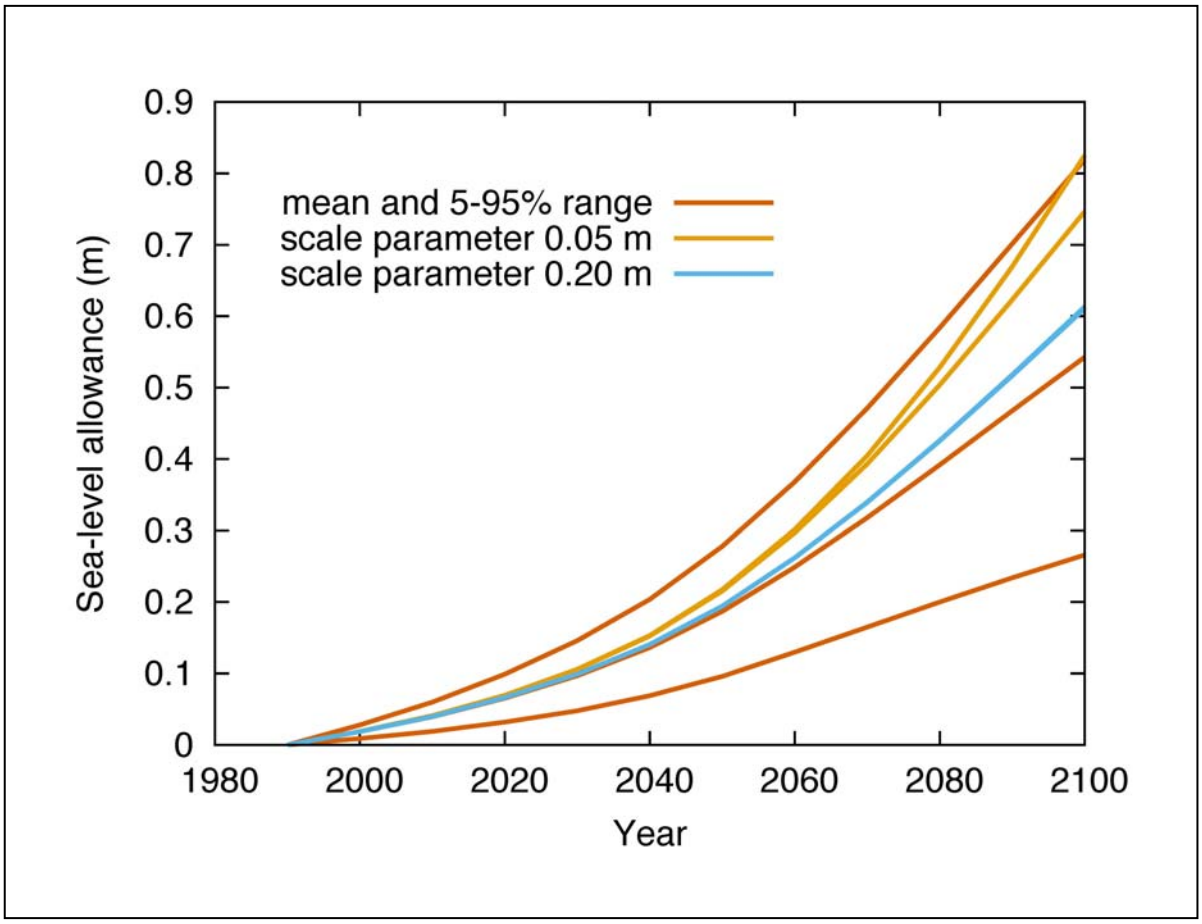

Figure 13.17: Sea level allowance based on scale parameters of 0.05 and 0.20 m (covering 90% of the global range) for the A1FI projections. For each scale parameter, there are two curves (for 0.20 m the two curves are not distinguishable): the upper one is based on fitting a normal uncertainty distribution to the 5 to 95-percentile limits, while the lower one is based on a raised-cosine distribution. Also shown are the mean and the 5 to 95-percentile range of projections based on the A1FI emission scenario and a combination of the results of the TAR and AR4.

Figure 13.18: [PLACEHOLDER FOR SECOND ORDER DRAFT: COWCLIP results - will present overview of wave projections based on studies to date, with indication of robustness between studies.]

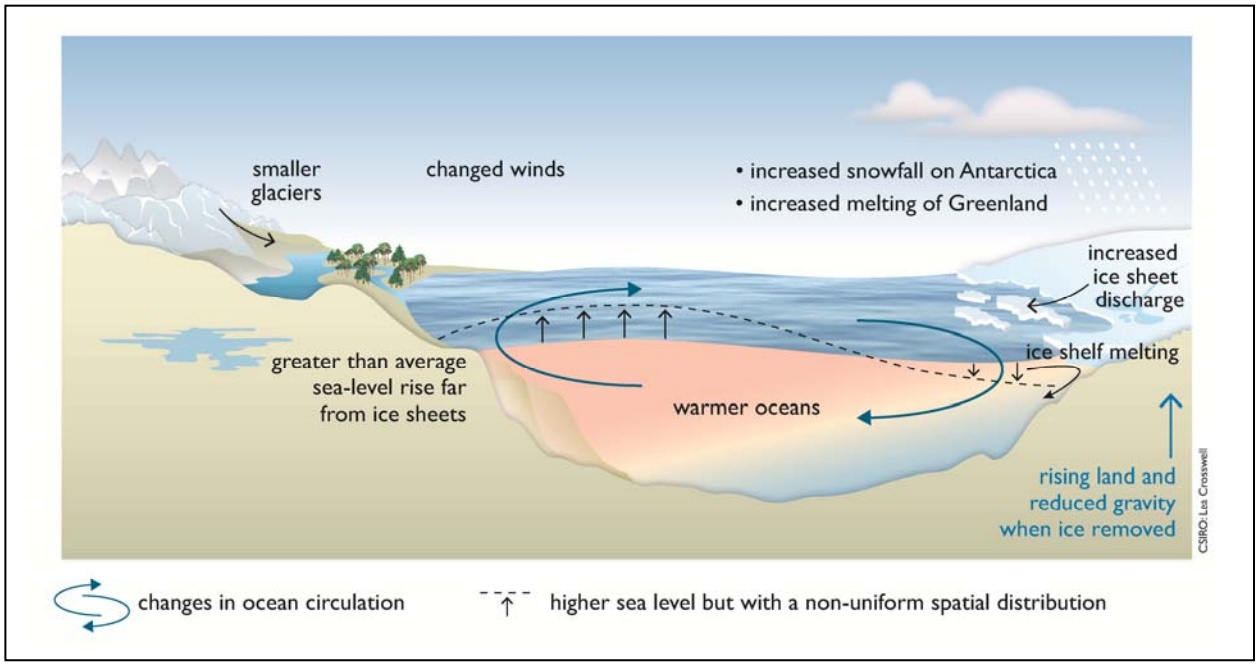

Figure 13.19: Schematic diagram of the major changes that influenced sea level during the 20th century and will potentially to drive sea level change during the 21st century and beyond.

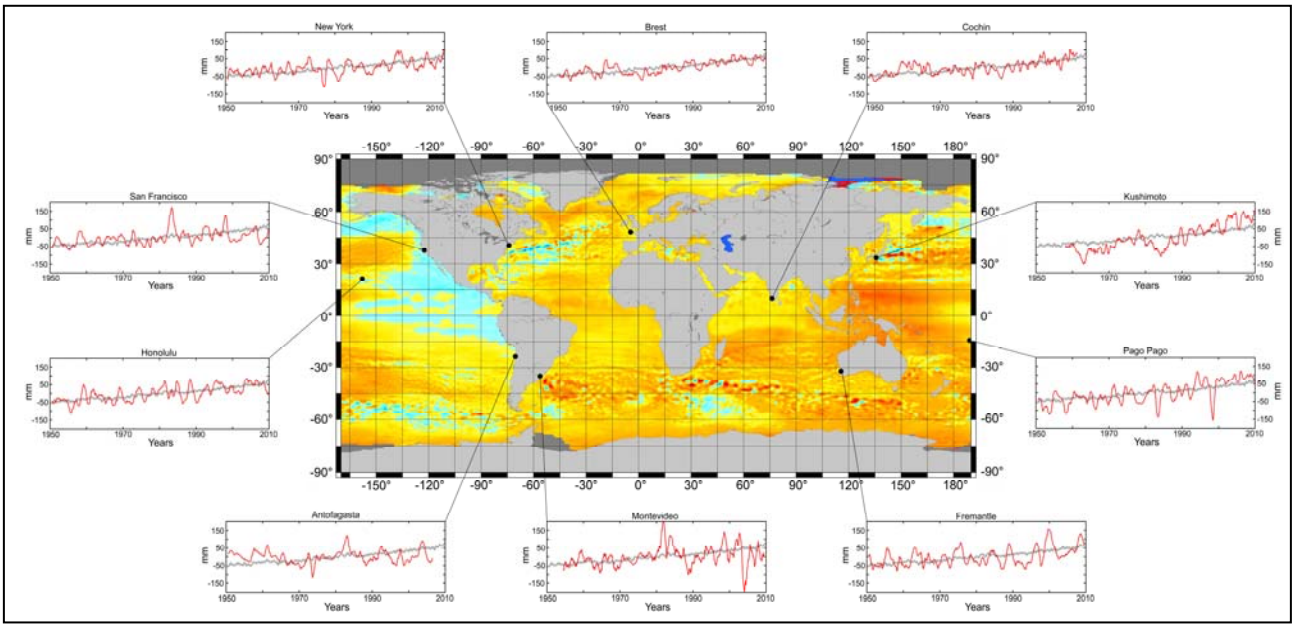
New York
Brest
Cochin
San Francisco
Kushimoto
Honolulu
Pago Pago
Antofagasta
Montevideo
Fremantle
mm
Years
1950
1970
1990
2010
-150°
-120°
-90°
-60°
-30°
0°
30°
60°
90°
120°
150°
180°

(a)

(b)

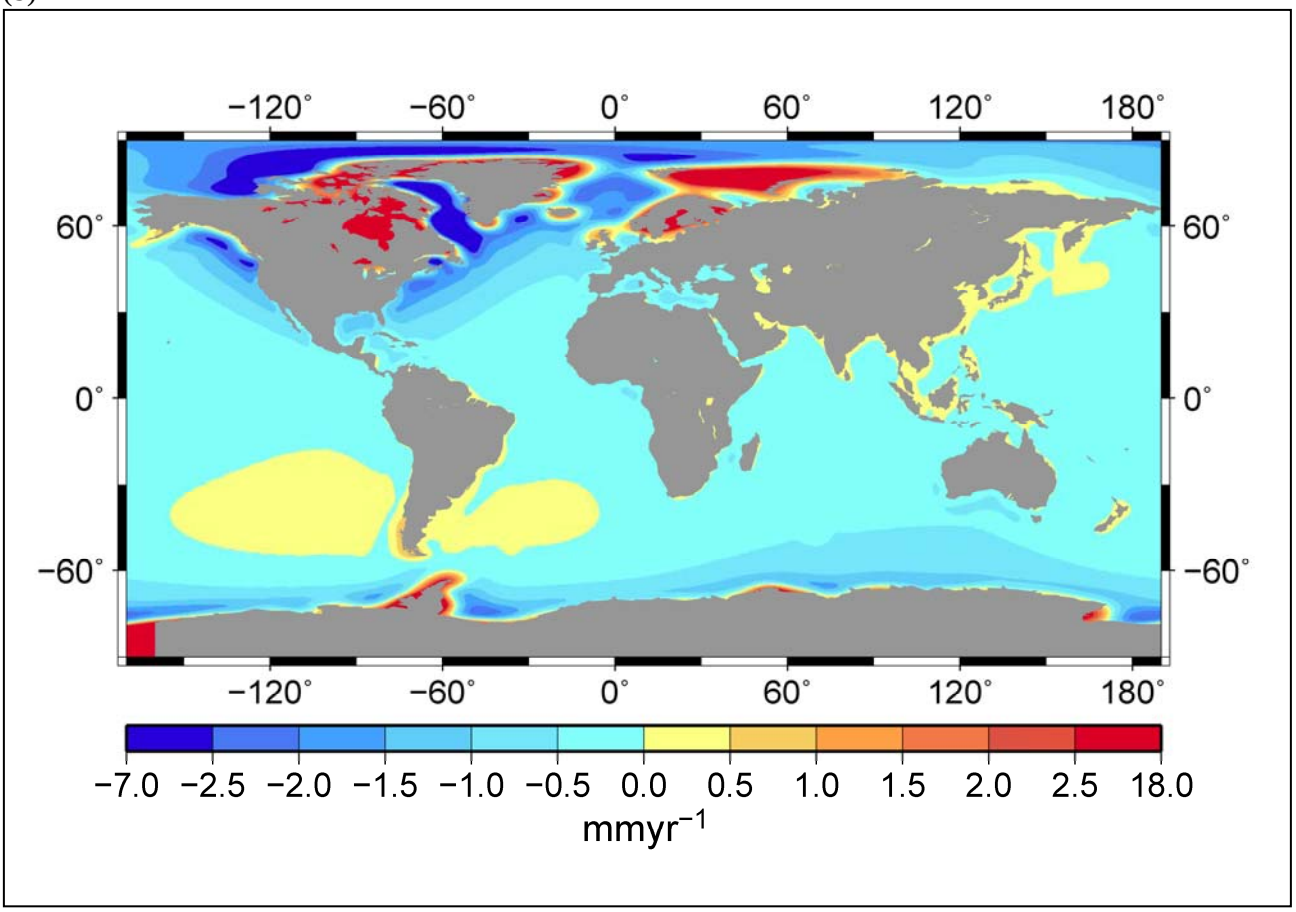
−120°
−60°
0°
60°
120°
180°
60°
0°
−60°
−7.0 −2.5 −2.0 −1.5 −1.0 −0.5 0.0 0.5 1.0 1.5 2.0 2.5 18.0
mmyr−1

(c)

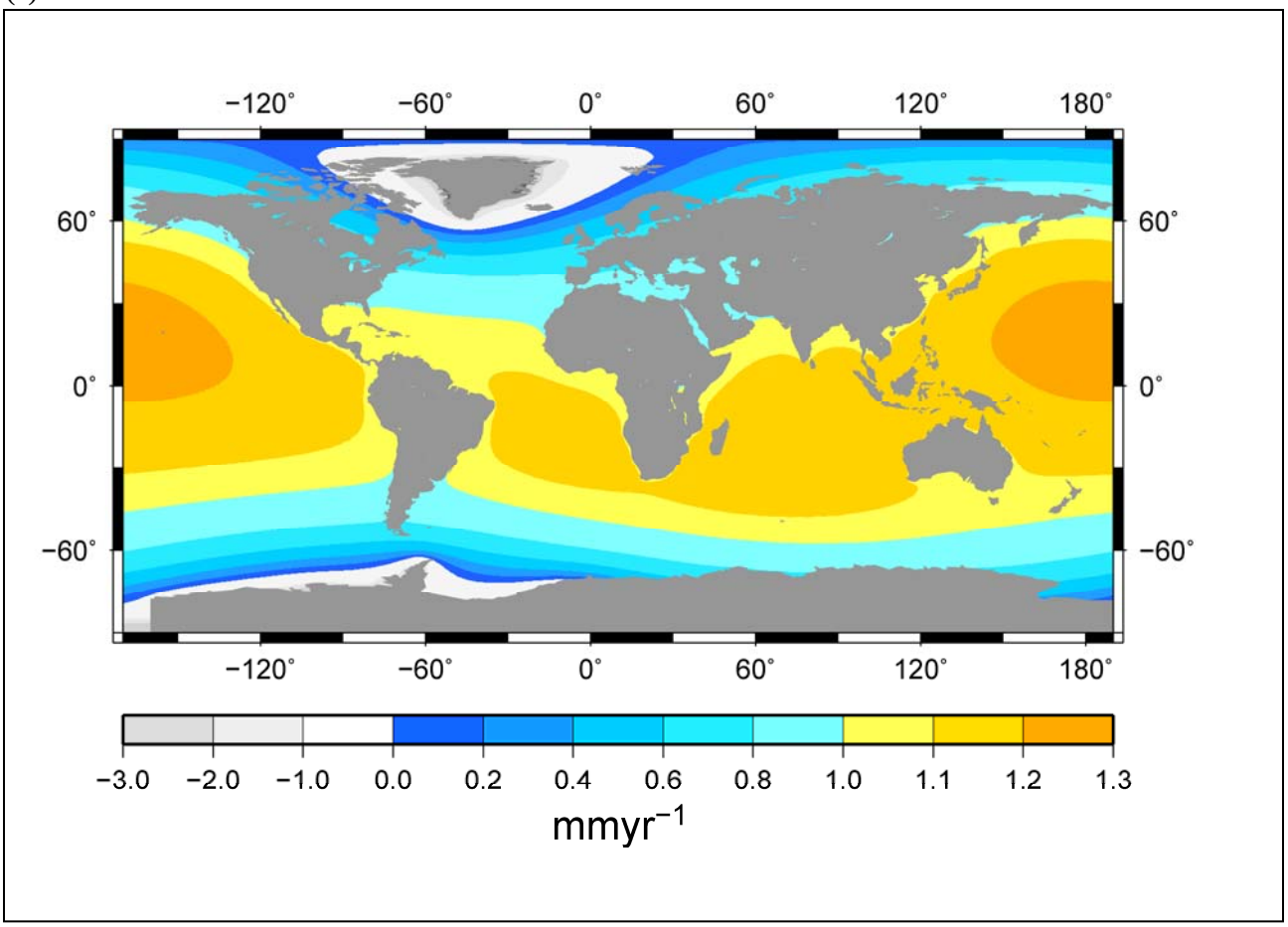

FAQ 13.1, Figure 1: (a) Sea-surface height (SSH) trends (in mm yr^{-1}) from October 1992 to December 2010 from satellite altimetry. Also shown are time series from selected tide gauge stations (red lines) for the period 1950 to 2010. Note that the tide gauge data have been corrected for vertical land motion due to glacial isostatic adjustment. For comparison, an estimate of global mean sea level change (and associated uncertainty) is also shown (black line) with each tide gauge time series. (b) A map of present-day vertical sea-floor motion associated with the on-going deformation of the solid Earth due to the large reduction in land-ice volume that occurred between about 20,000 and 6,000 years before present. Note that, this deformation influences the gravity field and thus also contributes to relative sea level through changes in SSH. (c) Model output showing relative sea level change due to melting of the Greenland ice sheet and the West Antarctic ice sheet at rates of 0.5 mm yr^{-1} each (giving a global mean value of 1 mm yr^{-1}). In this case, the spatial pattern reflects vertical changes in both SSH and the sea floor in response to the contemporary re-distribution of mass between the ice sheets and the oceans.

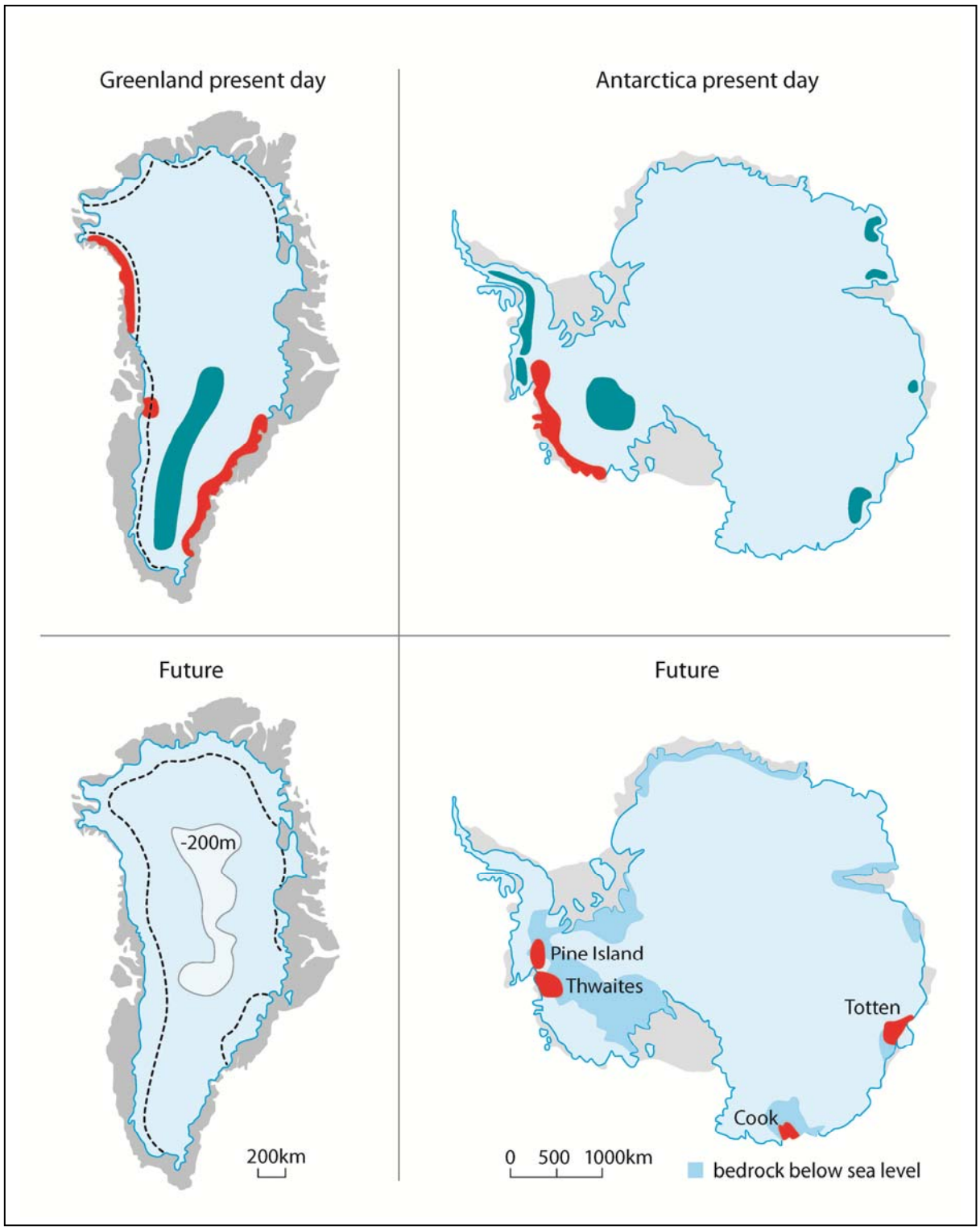

FAQ 13.2, Figure 1: Current and future (circa 2100) ice-sheet processes associated with sea level rise. (upper left) Greenland Ice Sheet during the last decade showing areas experiencing thinning more than 0.2 m yr^{-1} (red), thickening more than 0.2 m yr^{-1} (dark blue). Contemporary equilibrium line altitude (ELA) is shown as a dashed line. (lower left) Schematic illustration of Greenland projections for 2090–2099 showing ELA and area greater than 200 m below sea level, suggesting that future interaction with the oceans will be limited. (upper right) Antarctic ice sheets during the last decade indicating areas experiencing thinning and thickening (same colour scale). (lower right) Schematic illustration of Antarctic projections for 2090–2099 showing coincidence of areas currently experiencing thinning and areas grounded below sea level that are connected to the ocean.